Technical University of Denmark

DTU

Sedimentology, hydrogeology and hydrogeochemistry of Machile Basin, Zambia

Banda, Kawawa Eddy; Bauer-Gottwein, Peter; Larsen, Flemming; Jakobsen, Rasmus; A. Nyambe, Imasiku

Link back to DTU Orbit

DTU Library
Technical Information Center of Denmark

Sedimentology, hydrogeology and hydro-geochemistry of Machile Basin, Zambia

Kawawa E. Banda

Sedimentology, hydrogeology and hydro-geochemistry of Machile Basin, Zambia

Kawawa E. Banda

PhD Thesis
August 2015

Kawawa E. Banda

Sedimentology, hydrogeology and hydrogeochemistry of Machile Basin, Zambia

PhD Thesis, August 2015

The synopsis part of this thesis is available as a pdf-file for download from the DTU research database ORBIT: http://www.orbit.dtu.dk

Preface

The work presented in this PhD thesis, entitled "Sedimentology, hydrogeology and hydrogeochemistry of Machile Basin, Zambia", was conducted at the Department of Environmental Engineering of the Technical University of Denmark (DTU) under the supervision of Associate Professor Peter Bauer-Gottwein (DTU), Flemming Larsen and Rasmus Jakobsen (GEUS), and Imasiku Nyambe (UNZA-IWRM). The work was conducted in the period December 2011 to March 2015. The PhD project was funded by Danida, Danish Ministry of Foreign Affairs.

The PhD thesis is based on three scientific journal papers which were submitted to international, ISI-indexed scientific journals:

   I   Banda, K.E, Jakobsen R., Bauer-Gottwein P., Murray A.S., Nyambe I.A., Bender-Koche C., Larsen F. Palaeo-Lake Makgadikgadi: New perspectives and insights on its evolution from western Zambia. Journal of African Earth Sciences, under revision.

   II   Banda, K.E, Jakobsen R., Bauer-Gottwein P., Nyambe I.A., Laier T., Larsen F. Identification and evaluation of hydro-geochemical processes in the groundwater environment of Machile Basin, western Zambia. Journal of Applied Geochemistry, under review.

   III   Banda, K.E, Jakobsen R., Bauer-Gottwein P., Nyambe I.A., Larsen F. Hydrogeochemistry of the Palaeo-Lake Makgadikgadi: a review. Journal of Applied Geochemistry, submitted.

The papers are referred to by their roman numerals throughout the thesis (e.g. Paper I).

Acknowledgements

Abstract

An important environmental problem in arid to semi-arid regions of the world is salinisation of water resources. Moreover, most of these regions are inhabited by poor communities in developing countries, with limited or no financial resources to develop suitable alternatives to meet their basic water needs. With increasing world population and increasing effects of climate change, groundwater resources are seen as a suitable alternative. However, the exploitation of groundwater in these regions requires knowledge of aquifer structure and genesis, and mechanisms that control hydrochemistry. Water resources practioners in arid and semi-arid regions accept that future development of groundwater resources depends largely on the degree and rate of salinisation.

This PhD study focuses on investigating the sedimentological and hydro-geochemical conditions that have shaped the groundwater environment in Western Zambia to the present hydrogeology, in particular the origin and dynamics of groundwater salinity. The case study is the Machile Basin of south-western Zambia, a semi-arid region on the northern extension of a desiccated lake system – Palaeo-lake Makgadikgadi (PLM), southern Africa. PLM is a palaeo-mega endorheic lake system that was formed due to tectonic disruptions in the Early Pleistocene (speculated at c. 1.4 Ma). The lake has sustained several lake levels, with the highest level at ~995 m above mean sea level (amsl) and became largely desiccated in the Late Pleistocene (probably by c. 500 ka).

Methods used in the field and laboratory included: deep borehole drilling, geophysical borehole logging, groundwater table measurements, sediment dating (with optically stimulated luminescence - OSL), mineralogical analysis (XRD and SEM), groundwater tracers (^{18}O, ^{2}H, $^{3}H/^{3}He$, ^{14}C), hydrochemistry (including pore-water), cation exchange capacity and sediment dilution experiments. Unconsolidated sediment samples at intermittent depths up to 50 m below ground level (bgl) were retrieved from a 100 m bgl research borehole. Sediment XRD analysis shows that the sediment has predominantly silicate minerals (quartz and feldspars) with whitish nodule like structures detected to be bassanite (dehydrated gypsum), whereas carbonates (calcite and dolomite) were below detection by XRD; a simple acid test, however, validated the presence of carbonates. OSL dating showed that the sediments are old (> 300 ka) and cannot be accurately constrained as the quartz mineral grains are fully or nearly saturated. The

sediment pack shows conditions of palaeo-environmental changes of wet and dry conditions (based on microfossils and facies changes) depositing fluvio-lacustrine sediments (sand, silt and clay intercalations); geophysical logging delineated and resolved these sediments well, showing high salinity down to the basement rocks at 100 m bgl.

Within the Machile Basin, the groundwater table has a low hydraulic gradient in the central palaeo-lake sediment region, characterized by brackish-saline water, and higher gradients in the fresh water fringe region. The fresh water is typically Ca-Mg-HCO$_3$ and Na-HCO$_3$ dominated due to silicate weathering, whereas, the saline groundwater is Na-SO$_4$-Cl dominated, the result of sustained dedolomitization and ion exchange processes as modelled using the geochemical code PHREEQC. The groundwater ages along a flow line using ^{14}C and ^{3}H/^{3}He are < 10 ka and generally < 50 ka at a regional scale over the PLM, compared to very old sediments (> 300 ka), suggesting pluvial climatic recharge process during Late Pleistocene (> 30-20 ka) and Holocene (8-4.5 ka) that induced partial leaching of the sediments. Stable water isotopes (^{2}H and ^{18}O) data suggest that groundwater receives meteoric recharge; however most of this water is lost to evapo-transpiration rendering the saline environment a virtually stagnant groundwater zone without any through flow. Fresh groundwater is therefore hosted in the near-surface zone (such as river channels, palaeo drainages and alluvial deltaic features) within the PLM region.

This study supports a tectonically controlled evolution of PLM in which hydrological feedbacks were secondary processes during the PLM development; climatic variation during pluvial events was, however, critical in flushing the sediment. The present hydrogeology of the desiccated lake, includes, clay, silt and sand sediments that host almost stagnant saline water. Freshwater from the regional groundwater is generally lost to evapo-transpiration or superficial drainage. These findings suggest that the salinisation of the groundwater resources in this system is primarily the result of the palaeo processes that formed PLM in an arid climate leaving evaporitic minerals and high salinity in the sediments. Because of the generally arid climate since the formation, combined with low hydraulic conductivity the PLM sediments are still not flushed after c. 500 ka. This implies that investigations for fresh groundwater must be targeted at deeper aquifers or other technologies such as groundwater desalination and rain-water harvesting must be implemented.

Dansk sammenfatning

Et af de stor miljøproblemer i verdens aride og semi-aride områder verden er salinisering af vandressourcen. Tilmed er de fleste af disse områder befolket af fattige samfund i udviklingslande, med begrænsede eller ingen finansielle ressourcer til at udvikle alternativer til at opfylde det basale behov for vand. Med en voksende befolkning og tiltagende virkninger af klimaændringerne kan grundvandsressourcer være et muligt alternativ. Imidlertid kræver udnyttelsen af grundvandet i disse områder kendskab til grundvandssystemets struktur og tilblivelse og de mekanismer der styrer vandkemien. De, der arbejder med vandressourcer i aride og semi-aride områder, er enige om, at det fremtidige potentiale for udvikling af grundvandsressourcerne især afhænger af graden og hastigheden af saliniseringen.

Dette ph.d. arbejde fokuserer på de sedimentologiske og hydro-geokemiske forhold, der har formet grundvandsystemet i det vestlige Zambia til den nuværende hydrogeologi, med særligt fokus på oprindelsen af og dynamikken i grundvandets saltindhold. Det undersøgte område er Machile Bassinet i det sydvestlige Zambia, et semi-aridt område i den nordlige forlængelse af et udtørret søsystem – Palæo Makgadikgadi Søen (PMS) i det sydlige Afrika. PMS er en palæo-endorheisk megasø, dannet som følge af tektoniske hændelser i Tidlig Pleistocæn (anslået - ca. 1,4 Ma). Søoverfladen har siden dannelsen ligget i flere niveauer, med det højeste niveau på ~ 995 m over middel havniveau. Søen tørrede stort set ud i Sen Pleistocæn (sandsynligvis ca. 500 ka).

De anvendte felt-og laboratoriemetoder omfatter: boring til 100 m under terræn (mut), geofysisk borehulslogging, måling af grundvandsspejlets beliggenhed, datering af sediment (med optisk stimuleret luminescens - OSL), mineralogiske analyser (XRD), sporkomponenter i grundvandet (^{18}O, ^{2}H, ^{3}H / ^{3}He, ^{14}C), vandkemi (herunder pore-vand), kationbytningsevne og sediment udvaskningsforsøg. Der blev udtaget prøver fra de ukonsoliderede sedimenter ved flere dybder ned til 50 mut fra den 100 m dybe boring. XRD-analyse af sedimentet viser, at det overvejende består af silikat mineraler (kvarts og feldspater) med hvidlige noduler af bassanite (dehydreret gips), mens indholdet af karbonater (kalcit og dolomit) var under detektionsgrænsen for XRD; brusen ved syretilsætning viste dog et vist indhold af karbonater. OSL dateringen viste, at sedimenterne er gamle (> 300 ka), men alderen kan ikke bestemmes mere præcist, da kvartskornene er helt eller næsten mættet mht. det oplagrede strålingssignal. Sedimenterne viser at palæo-miljøet har være karakteriseret ved vekslende våde og tørre perioder (baseret på mikrofossiler og

facies ændringer), hvor der er afsat fluviatile og lacustrine sedimenter (sand, silt og ler aflejringer). De geofysiske logs formåede i høj grad at afgrænse den vertikale udstrækning af sedimenttyperne og påviste en høj saltholdighed ned til de underliggende basalter 100 mut.

Inden for Machile Bassinet, har grundvandsspejlet en lav hydraulisk gradient i de centrale del af området med palæo-søsedimenter, kendetegnet ved brak-vand-saltvand, og en stejlere gradient i det omkransende ferskvandsområde. Det ferske vand er typisk Ca-Mg-HCO$_3$ og Na-HCO$_3$ domineret, et resultat af silikatforvitring, mens det salte grundvand er Na-SO$_4$-Cl domineret, som føl-ge af en vedvarende dedolomitisering og ionbytning, modelleret ved hjælp af den geokemiske kode PHREEQC. Grundvandets aldre langs en strømnings-bane, bestemt ved hjælp af ^{14}C og ^{3}H/^{3}He er <10 ka og generelt <50 ka inden-for PMS regionen, og dermed betydeligt yngre end de meget gamle sedimen-ter (> 300 ka). Dette tyder på en høj infiltration under nedbørsrige perioder i Sen Pleistocæn (> 30-20 ka) og Holocæn (8-4,5 ka), der medførte en delvis udvaskning af sedimenterne. Stabile vandisotopdata (^{2}H og ^{18}O) data tyder på, at grundvandet modtager infiltration fra nedbør, men at det meste af dette vand fjernes ved evapo-transpiration og gør den salte del af systemet til en zone med næsten stillestående grundvand uden nogen gennemstrømning. Fersk grundvand befinder sig derfor i en zone nær overfladen (i f.eks flodløb, palæo dræneringer og alluviale deltaiske systemer) inden for PMS regionen.

Denne undersøgelse understøtter en tektonisk styret udvikling af PMS, hvor hydrologiske feedbacks var sekundære processer under PMS udviklingen. Klimatiske variationer med nedbørsrige perioder var imidlertid afgørende for udvaskningen af sedimentet. Den nuværende hydrogeologi i den udtørrede sø, omfatter, ler, silt og sandede sedimenter, som indeholder næsten stillestående saltvand. Ferskvand fra det regionale grundvand bliver generelt fjernet ved evapo-transpiration eller overfladisk dræning. Disse resultater tyder på, at tilsaltningen af grundvandsressourcerne i dette system primært er et resultat af de palæo processer, der dannede PLM i et aridt klima og efterlod evapo-ritmineraler og et højt saltindhold i sedimenterne. Det generelt tørre klima siden dannelsen, kombineret med lav hydraulisk ledningsevne indebærer, at PLM sedimenterne stadig ikke er skyllet fri for salte efter ca. 500 ka. Dette indebærer, at søgning efter fersk grundvand skal målrettes mod dybere grundvandsmagasiner, eller at andre teknologier såsom grundvand afsaltning og regnvandsopsamling må tages i brug.

Table of contents

x

1 Introduction

1.1 Background and motivation

Nearly one third of the world's population are inhabitants of arid to semi-arid regions, a large proportion of whom are among the poorest in the world especially in developing countries (MEA, 2005). Typically, these regions are characterised by variable and scarce precipitation, high potential evapotranspiration and high temperatures that lead to widespread salinisation problems.

Salinisation has negative global environmental impacts and contributes to loss of biodiversity, taxonomic replacement by halotolerant species (Williams, 1999), loss of fertile soil, collapse of agricultural and fishery industries, and severe health problems in Africa, China, and India (Weert et al., 2009). Salinisation problems will only exacerbate, given the increasing global population and climatic variability (Bates et al., 2008). There are two forms of Salinisation, differing in the mechanism by which they occur. Primary salinity is a natural phenomenon in arid to semi-arid environments and closed basins, with examples including Salt Lake in the USA, the Dead Sea in the Middle East, the dry valleys of the Antarctica, and the Lake Eyre in central Australia (Jankowski & Jacobson, 1989; Essington, 2004; Weert et al., 2009). Secondary salinity is instead caused by a human disturbance to the hydrological cycle such as irrigation of an aquifer system with limited groundwater discharge (Greenwood et al., 1992; Salama et al., 1999; Jasonsmith et al., 2011).

Salinisation of water resources is the most prominent incident of water quality degradation in arid to semi-arid regions (Vengosh, 2005). Both for the scientific community and the many practitioners, dealing with the challenges of groundwater management, the major challenge facing hydro-geochemical investigations of saline groundwater is the determination of the source of salt (e.g Hardie, 1968; Barica, 1972; Nordstrom et al., 1989; Marshall & Harmse, 1992; Yager et al., 2007) and mechanism(s) that redistribute the salt to other locations where it becomes a problem (e.g Gunn & Richardson, 1979; McCarthy et al., 1991; Jones et al., 2009). However, the validity of the potential explanation of such hydro-geochemical problems, must be underpinned by a well refined understanding of the geological processes and subsequent hydrogeology framework, which is crucial for model prediction (Sanford &

Wood, 1991; Yechieli & Wood, 2002) and remediation (Herczeg et al., 2001).

In this context, the PhD study was focused at alleviating the aforementioned problems in semi-arid regions through a case study in the Machile Basin, western Zambia, which hosts the northern most extension of the Palaeo-Lake Makgadikgadi - PLM (Thomas & Shaw, 1991a).

The main objectives of the research were:

- To improve the current understanding of the geological evolution and palaeo-environmental settings of PLM and the nature of groundwater formations (Paper I).

- Identify the hydro-geochemical processes and controls within the saline and fresh groundwater (Paper II).

- Review the current understanding of the PLM hydrogeochemistry and hydrogeology in relation to the current findings in the Machile Basin (Paper III).

This thesis provides a summary of the three papers submitted for publication as part of the PhD study, as well as an overview of the methods and the main findings of the investigation. It is structured as follow; Chapter 2 presents a literature review of the previous work on the research topic, chapter 3 presents the case study, chapter 4 presents the methods used for the study. The main results are summarised in chapter 5 and conclusions are presented in chapter 6. Finally the papers are presented in chapter 8. The results highlight the mechanism and controls of salinisation processes and the role of geological events.

2 Context

The first section of this chapter summarizes existing knowledge on the development of the PLM and the type of the sediments that were deposited. The last section discusses on the hydrochemistry and hydrogeology studies within PLM. The linkage of the PLM to similar basin systems of the world is also discussed.

2.1 Formation and evolution of PLM

PLM is a large endoheric basin in southern Africa, delineated by the present day 995 m amsl shoreline as the highest lake level stand (Cooke, 1979; Thomas & Shaw, 1991a; McFarlane & Eckardt, 2006; Burrough et al., 2009a). McFarlane & Eckardt (2006) based on observed shoreline data suggest the lake reached a maximum areal extent of 175,000 km^2 at ~995 m amsl referred to as the Palaeo-Lake Deception (PLD). PLM occupied predominately northern Botswana and centred on the modern day Makgadikgadi Pans; fluvial sediments in the basin, however, occupy an area in excess of 100,000 km^2 (Thomas & Shaw, 1991b) as shown in Fig. 1, referred to as the Makgadikgadi-Okavango-Zambezi Basin (MOZB) (Ringrose et al., 2005) . MOZB extent includes the Mababe Basin, Ngami Basin, the Okavango Graben and most of the upper part of the Zambezi trough as shown in Fig. 1. Today, these elements are tenuously connected via near-defunct river channels. This palaeo-lake is controlled by post-Gondwana faults, which continue to show seismic activity to the present (e.g. Hutchins & Reeves, 1980; Modisi et al., 2000).

It is believed that during the upper Jurassic to Cretaceous, the proto-Upper Zambezi, Okavango, and Cuando rivers found their way to the Indian Ocean via the Limpopo (Wellington, 1955; Moore & Larkin, 2001). During the Pliocene, however, there was a flexuring of the Okavango-Kalahari-Zimbabwe axis and further down-warping of the Kalahari Rift (Cooke, 1979; Thomas & Shaw, 1990), which interrupted these drainage flows towards the Limpopo. As a result, a huge basin of internal drainage, PLM fed predominantly by the Zambezi and Okavango rivers, was effectively created (Grey & Cooke, 1977; Cooke, 1979; Shaw & Thomas, 1992; Moore & Larkin, 2001; Moore et al., 2012). Subsequent neo-tectonics and the down warping along the Zambezi River (Cooke, 1979; Shaw & Thomas, 1992) greatly reduced the lake water budget. Increased aridity is assumed to have served as a final blow to the desiccation of the PLM, leaving behind the Makgadikgadi pans as remnants of this vast endorheic lake (Grey & Cooke, 1977; Cooke, 1979, 1980). The lake

system sustained five major lake stages including; ~995-1000 m amsl (PLD), 945 m amsl (PLM), 936 m amsl (Palaeo-lake Thamalakane - PLT), 920 m amsl and 912 m amsl before complete desiccation (Moore et al., 2012), with tectonic disruptions as the controlling mechanism in the various lake stages. This constitutes the tectonic model for evolution of PLM.
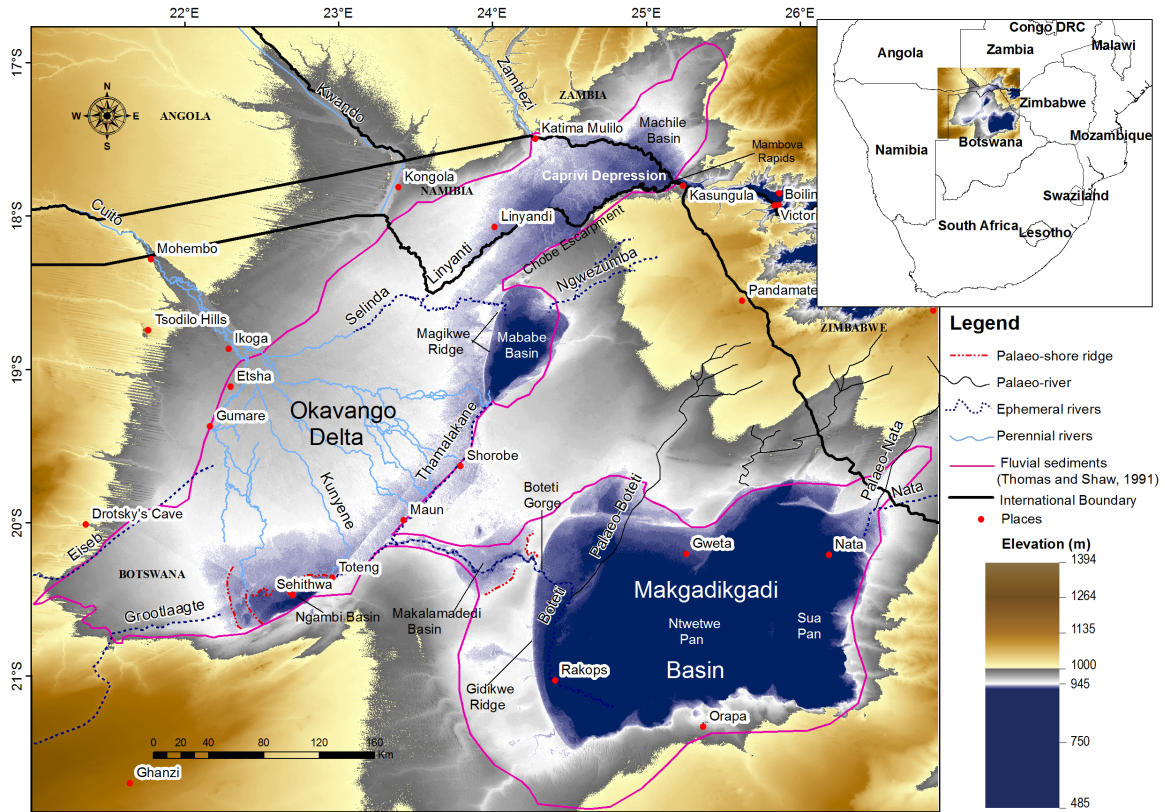
Fig. 1: SRTM-3 Digital Elevation Model exhibiting the structural depressions of the Northern and Middle Kalahari; with geographical references.

Several studies have identified the existence of this large Quaternary lacustrine system with several sub-basins using geomorphology and fossil evidence (Passarge, 1904; Grove, 1969; Ebert & Hitchcock, 1978; Cooke, 1979; Cooke & Verstappen, 1984; Lancaster, 1989; Thomas & Shaw, 1991a; 2002; Ringrose et al., 2005; White & Eckardt, 2006; Burrough et al., 2009a; Burrough et al., 2009b). According to Riedel et al. (2014), comprehensive geomorphology data exists to support Late Pleistocene to Holocene existence of the palaeo-lake. The assertion is underpinned by landforms (dunes and palaeo-shorelines) that invoke climatic controlled oscillations of the PLM lake stages during the late Pleistocene, as dated using Optically Stimulated Luminescence (OSL) (Stokes et al., 1997; O'Connor & Thomas, 1999; Thomas et al., 2000; Thomas et al., 2003; Ringrose et al., 2005; Burrough et

al., 2007; Burrough & Thomas, 2008, 2009; Burrough et al., 2009a). Early Pleistocene existence is considered to be highly speculative as the actual age of the lake is unknown. Moore et al. (2012) suggests on the basis of robust archaeological and other evidence that the lake system could have been initiated as early as 1.4 Ma, during the Early Pleistocene and retreated to progressively lower shorelines as a result of successive severance of the headwaters of the drainage network (Du Toit, 1927; Cooke, 1980; Thomas & Shaw, 1991a; Moore & Larkin, 2001; Haddon & McCarthy, 2005) and becoming largely desiccated prior to the end of the early stone age (i.e. prior to 500 ka). Moore et al. (2012), suggests that the order of magnitude mismatch identified between these evolution models could be due to the usage of OSL ages on the key Kalahari landforms. The method would require investigation in terms of suitability of use for the Kalahari and as well as possible influences in modification of geochronology such as bioturbation; OSL dating was implemented in this PhD research.

Similarly, in other continental endorheic basins above sea level such as the Lake Chad, Great Salt Lake and the Mono Lake, paleao-climatics, paleao-hydrology and tectonism have had a profound effect in the evolution and deposition of sediments. In the Lake Chad Basin, central Africa, higher palaeo-shorelines indicating periods of more intense surface drainage in the Late Quaternary (Leblanc et al., 2006) as well as a higher groundwater recharge rate of aquifers (Edmunds et al., 1999), has enabled the delineation of the extent of the Palaeo-Lake Chad. During the wet mid-Holocene, Palaeo-Lake Chad covered vast areas of central Africa in excess of 300,000 km^2 (Ghienne et al., 2002; Drake & Bristow, 2006; Leblanc et al., 2007). The Great Salt Lake in Utah, western US, also sustained lake level changes since the last 200 ka based on ^{87}Sr/^{86}Sr ratios and radiocarbon ages (Hart et al., 2004). Palaeo-Lake Bonneville was the predecessor of the present Great Salt Lake that span an area of 50,000 km^2 at its peak (Oviatt et al., 2005). In addition, the Mono Lake, California, USA is hosted within the Palaeo-Mono Basin. Since the late Quaternary, lake levels within the Mono Lake have dropped, based on shoreline elevation, due to climatics (Stine, 1990) and neotectonics (Reheis & Dixon, 1996). All the lakes are typical of a saline environment except for the Lake Chad. The location of major endorheic regions of the world is shown in Fig. 2.
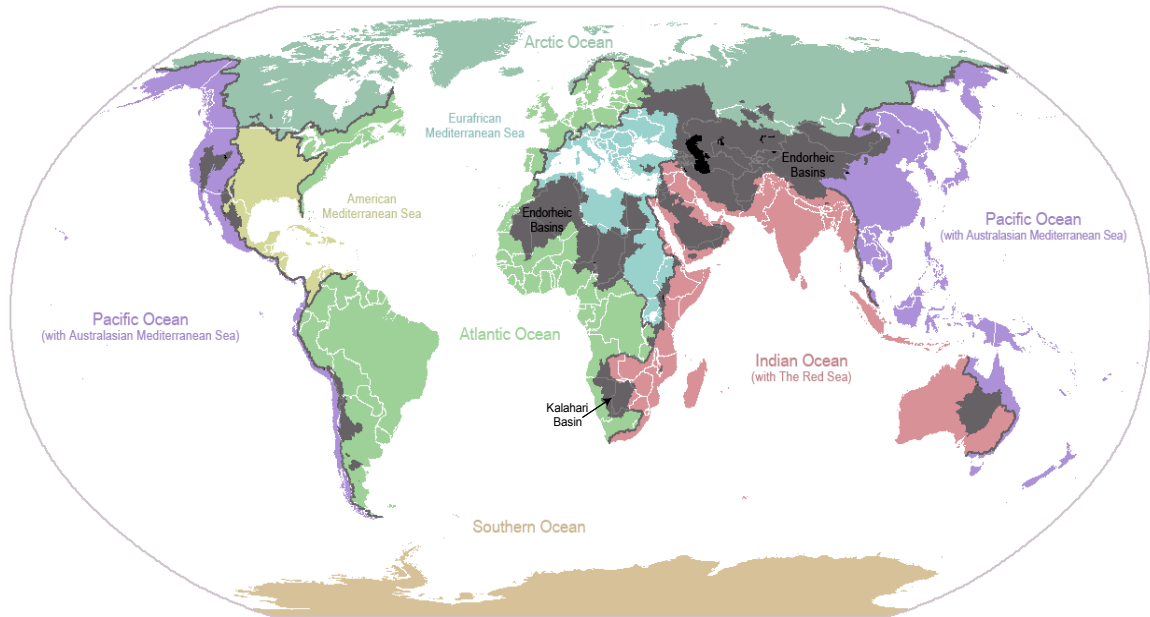
Fig. 2: Major endorheic basins of the world (Modified from Shiklomanov, 1998). Basins are shown in dark grey; major endorheic lakes are shown in black. Coloured regions represent the major drainage patterns of the continents to the oceans (non-endorheic). Continental divides are indicated by dark lines.

2.2 PLM Hydrochemistry and hydrogeology

Accumulation of solutes (mineralisation) under continental endorheic lake conditions balanced with evaporation are well documented in literature (Hardie & Eugster, 1970; Jones et al., 1977; Eugster & Hardie, 1978; Eugster & Jones, 1979; Spencer et al., 1985a; Jankowski & Jacobson, 1989; Wood & Sanford, 1990; Yechieli & Wood, 2002). Geochemical evolution is primarily controlled by inflow (surface/groundwater) composition, selective removal processes of dissolved species, and concentration processes operating within the lake basin (Yan et al., 2002). Fig. 3 shows the Hardie-Eugster evaporation model that suggests chemical evolution based on a chemical divide in which the least soluble solutes, carbonates, precipitate first and the most soluble, chlorides, precipitate last with progressive evaporation. In desiccated and buried continental systems which have undergone different phases of geological evolution and interactions with both surface and groundwater resources it is rather complex to account for sources and mineralisation processes.

Inflow

Na, Ca, Mg, HCO$_3$, SO$_4$, Cl

Calcite

Low Ca/SO$_4$ ratio,
Redissolution,
Sub-surface inflow

High Mg Calcite
& protodolomite

Path II

$2m_{Ca}^{2+} > $ Alk

Path I

Alk $> 2m_{Ca}^{2+}$
Mg $>>$ Ca

Na, Ca, Mg, SO$_4$, Cl

Gypsum

Na, Mg, CO$_3$, SO$_4$, Cl

Mg-clay Mirabilite

Na, CO$_3$, SO$_4$, Cl

Halite

Progressive Evaporation
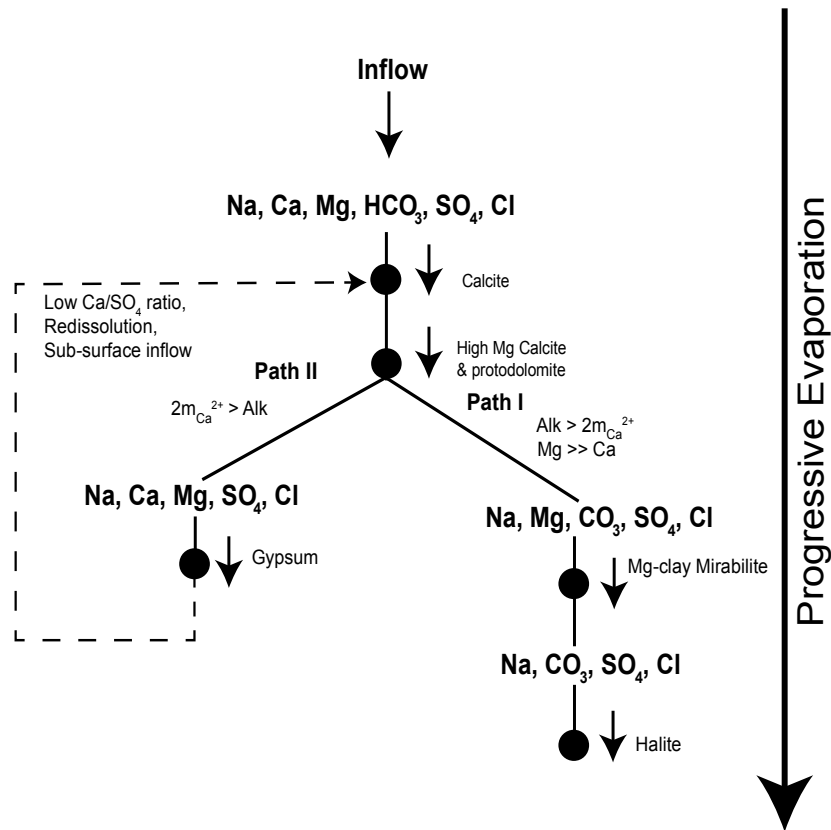
Fig. 3: Evaporation path of closed lake system of solutes with progressive evapo-concentration (adapted from Hardie & Eugster, 1970). Halite precipitation is typically at the last to form but the most soluble whereas, the least soluble, typical carbonates, will form first

In southern Africa, the sources of ions for inland salt waters has been considered to be leaching from the underlying Karoo Dwyka and Ecca shales that are widespread in the subcontinent (Seaman et al., 1991). Marine aerosols are also seen to have contributed to surface and groundwater by adding Na and Cl (Day, 1993). Both studies consider the source of solutes to be from atmospheric inputs and bedrock leaching.

Within the PLM region, large scale geophysical mapping has confirmed the occurrence of high salinity formations typically composed of intercalated clay and sand within the PLM (e.g. Sattel & Kgotlhang, 2004; Campbell et al., 2006). Eckardt et al. (2008) demonstrates that salinity of the water resources within the Sua Pans (part of the present day Makgadikgadi pans) has no marine inputs but are a result of evapo-concentration accumulations under closed basin conditions, and lithological inputs of undetermined origins. As there was no outlet identified for PLM coupled with aridity, it is generally assumed that a steady state was reached where inflow was balanced by evap-

oration precipitating evaporates (Hipondoka, 2005); upon desiccation, evaporates would potentially leach out of the sediments.

Groundwater chemistry studies within the PLM region have focused on mapping spatial and temporal variability of chemical composition (e.g. Mazor et al., 1980; McCarthy et al., 1991; Linn et al., 2003; Stadler et al., 2010) and determining recharge rates using tracers (e.g. Mazor et al., 1977; Beekman et al., 1999; De Vries et al., 2000; Brunner et al., 2004). Most of these studies have suggested water-rock interaction as a mechanism of mineralisation of groundwater. Verhagen (1995) suggests that mineralisation of groundwater in the PLM is constrained by the aquifer structure which also controls the build-up and/or flushing of the aquifer typically under *pluvial* climatic phases.

A lot of research has also been conducted within the Okavango Delta to explain hydrological processes, specifically, surface water-groundwater interactions and evapo-transpiration (e.g. McCarthy et al., 1991; McCarthy & Ellery, 1994; McCarthy & Ellery, 1998; Bauer et al., 2006a; Bauer et al., 2006b; Wolski & Savenije, 2006; Ramberg & Wolski, 2008; Milzow et al., 2009) However, mineralisation processes and controls are still poorly accounted for and only locally explained. No study has combined studies on hydrogeology and hydrochemistry within the PLM to provide not only a conceptual framework and explain mineralisation processes and controls but also the repercussions of such a hydrogeological system towards salinity build-up and/ or flushing within host formations.

Typically in other continental endorheic basin, above sea level, with a saline environment, a change in lake level (higher or lower) during evolution had an inverse relationship with the hydrochemistry, such as in the Great Salt Lake, Mono Lake and the Main Ethiopian Rift (MER) lakes. In the Great Salt Lake Basin, the total salinity of lake waters varies in time and space dependant on the balance between inflow and evaporation (Stephens, 1990). The lake water is typically a Na-chloride brine type with total salinity between 115-350 g/l (Kowalewska & Cohen, 1998). Based on palaeo and current geochemistry of the Great Salt Lake (Spencer et al., 1985a; Spencer et al., 1985b), it is suggested that groundwater salinity was due to evaporite dissolution and diffusion of solutes into the lake sediments. In the Mono Lake, total solid concentration of lake water is just in excess of 18,000 mg/L in most places with deposits of calcium carbonate tufa (Rogers & Dreiss, 1995b). High groundwater salinity (up to 100,000 mg/L) is attributed to high surficial evaporation, and upwelling of deep saline groundwater due to thermal effects (Rogers &

Dreiss, 1995b). Rogers & Dreiss (1995a), modelled the inter-relationship between the Mono Lake levels and the salinity of both lake water and the groundwater underneath. They conclude at low lake levels the high water salinity causes solute loss via diffusion into the sediments and via advection, through fractures and faults into the groundwater system. During higher lake levels, the shoreline discharge zone moves towards the basin edge and saline groundwater mass subsides drawing solutes from the lake into the basin sediments. In the MER lakes, hosted within the East African Rift valley, a geochemical zonation of groundwater exists, whereby the groundwater in highland areas is relatively fresh, Ca-Mg-bicarbonate type, saline, typically Na-bicarbonate in the low lying areas although locally enriched in sulphate and chloride (Ayenew, 2003; Kebede et al., 2008). The drop in lake levels due to evaporation is associated with high salinity build-up in lake water, which was advectively transported to the groundwater through the fault structure (Kafri & Yechieli, 2010). Regional groundwater flow in these endorheic systems is typically convergent and terminates within these regions.

3 Case Study

3.1 The Machile Basin

Machile Basin is located in the south-western part of Zambia, southern Africa. It lies between -15.98 S and -17.90 S decimal degrees latitude and 24.09 and 26.50 E decimal degrees longitude (Fig. 4). It covers an area of 26 088 km^2. It has a rural population density of 2-5 inhabitants/km^2 dependent on peasant farming and fishing (DFID, 2002). It hosts the northern extension of the PLM (Fig. 1) which has not been investigated in detail before. Water resources development in the region is typically groundwater dependant. However, an acute problem of widespread salinity has been observed in the basin rendering rural inhabitants to resort to hand dug wells in seasonal streams or walk long distances for clean water supply.
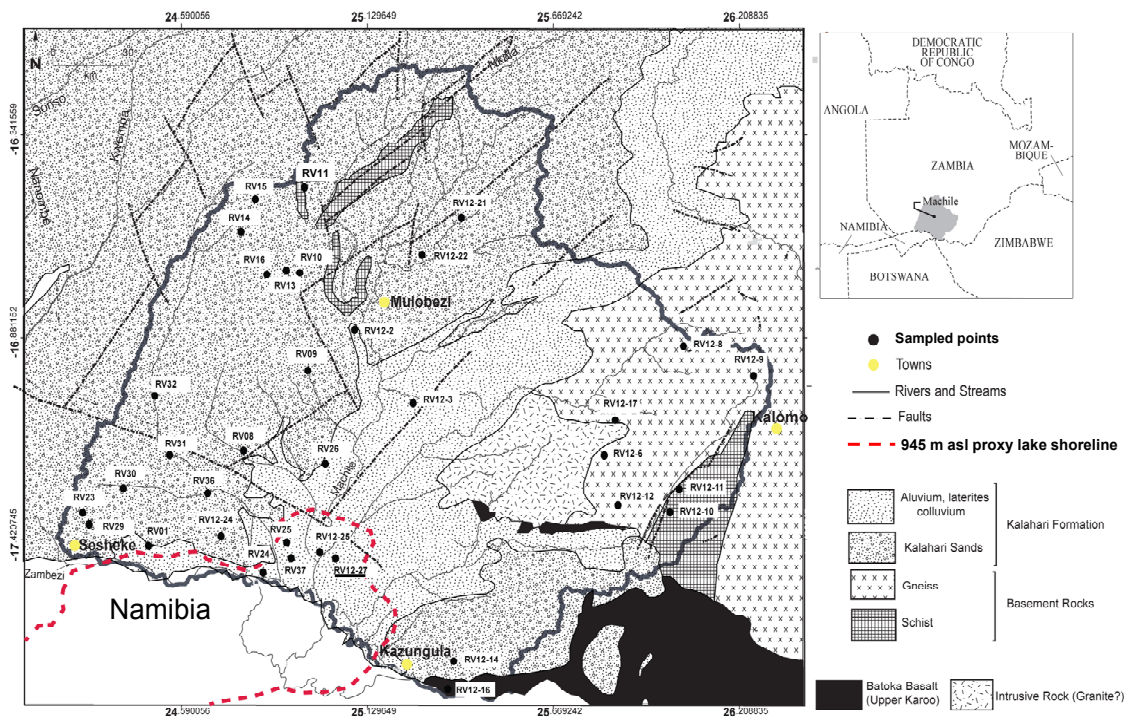
Fig. 4: Shows the surface geology of the Machile Basin (modified from Money, 1972; Yemane et al., 2002) and the sampled borehole. The basin is composed predominantly of loosely consolidated sediments of the Kalahari Group and hard rock in the western fringe, which affects the nature of water-rock interactions

It is typically a low gradient topography from 930 – 2000 m amsl sloping at an average gradient of 0.6% towards the south making it prone to extensive seasonal floods from the Zambezi in the wet season (YEC, 1995). Several

11

streams and rivers drain most of the basin and form seasonal tributaries of the perennial Zambezi River.

The climate of Machile Basin can be classified as semi-arid which is mainly dry except in rainy months (November to March), with annual rainfall of 900 mm, and characterised by hot-dry summer (April and May; August to October) and cold winter (June to August) (Fauchereau et al., 2003). Potential evapo-transpiration is estimated to be 1,600 mm/year (Beilfuss, 2012). Evapo-transpiration generally exceeds precipitation for most of the year with potential evaporation highest in the driest months. The area is covered with a Savannah type vegetation interrupted in places by deciduous broad leaf forest, dry land/cropland pasture and a cropland/woodland mosaic with a grassy understory (Heine, 1982). More recently, these forests have been diminished because of increased demand for timber.

Geologically (Fig. 4), the Machile Basin forms part of the Kalahari Group with sediments of Post-Cretaceous age (Money, 1972). The study area is covered by an alluvial complex of fluvio-lacustrine nature from erosion and sedimentation of Pre-Kalahari sediments of the Karoo and Basement rocks (Nugent, 1990; Thomas & Shaw, 1991; Moore & Larkin, 2001; Haddon & McCarthy, 2005; McCarthy, 2013); these formations form part of the Lower Kalahari Group and consist mainly of sandstones, quartzite, chert, conglomerates, clay, sand and silts deposited in the Miocene (Money, 1972). The Upper Kalahari Group is composed of aeolian sands formed from weathering of Karoo rocks, basement rocks and reworking of parts of the Lower Kalahari Group. The thickness of the Kalahari Group formations in Zambia typically ranges between 10 – 100 m (Haddon & McCarthy, 2005).

Groundwater development project boreholes, drilled to an average depth of 50 m, are well documented in the Machile Basin. The main aquifer units, in order of increasing importance as groundwater resources, are (1) the weathered and/or fractured basement rocks, (2) weathered basalts, (3) Karoo sedimentary rocks and (4) the unconsolidated alluvial deposits (YEC, 1995). The unconsolidated alluvial aquifer units, typically sand, gravel and sandstone with intervening clay layers of the Kalahari Group (YEC, 1995) are the main focus in this paper. These aquifers have an inter-granular sediment matrix with an average porosity of 30 % and a hydraulic conductivity between 1.50 x 10^{-7} and 1.25 x 10^{-4} m/s (YEC, 1995).

The first part of the study focused on drilling a deep research borehole to investigate in detail the nature of sediments and geochronology to cast new insights and perspectives on the evolution of PLM (Paper I). A basin scale study was undertaken to explain hydrochemistry and hydrogeology in relation to groundwater mineralisation processes (Paper II). Paper III focused on an assimilation/review of the hydrogeology and hydrochemistry of for the PLM in the wake of information obtain from the Machile Basin to draw inferences of a regional perspective from several isolated studies available.

4 Methods

4.1 Infield measurements

4.1.1 Location of boreholes and groundwater levels

Accurate elevation above mean sea level (amsl) and location coordinates of available boreholes were obtained with a differential Trimble [TM] R4-5800 system GPS (Fig. 5); borehole top of collar was used as a reference point for these measurements. Trimble Business Center 2.30 was used for post-processing these data. The results were used in Paper I and II.

Groundwater levels were then measured from the reference points using a dip meter to obtain hydraulic heads above mean sea level. The error budget was 2 mm on the GPS antenna levelling, 4 mm on the antenna height reading and 1 cm on the dip measurement. Water table data points were then interpolated using the kriging method (Alley, 1993) to produce a continuous water table surface (Paper II). The thickness of the unsaturated zone was then estimated by subtracting water table surface elevation from Shuttle Radar Topographic Mission (SRTM) data (Paper II).

Fig. 5: Typical differential GPS setup with receivers at the base station and borehole site of interest.

4.1.2 Physio-chemical and water sampling

To map spatial variation of groundwater quality, 34 water samples were collected from boreholes for chemical analysis (Paper II). Boreholes were purged by three well volumes before samples were collected. This was done to remove groundwater stored in the well and allow for fresh aquifer water to enter the borehole. In the field, physico-chemical analysis for pH, water electrical conductivity (EC), temperature was done with a WTW 350i Multimeter using pH-EC-DO probes (Fig. 6). Measurement of alkalinity, was conducted on site using the Gran titration (Gran, 1952). Polyethylene bottles (20 mls) were thoroughly washed three times with groundwater before sampling. Samples for cations were filtered with a 0.45 µm filter into the bottles and acidified to pH < 2 with nitric acid before storage in a cooler box for transportation to the laboratory. Samples for anions were neither acidified nor filtered after collection. In addition, water samples for stable isotopes (hydrogen and oxygen) were also collected using 20 mls polyethylene bottles.

Fig. 6: Infield measurement involved opening of the production wells, measuring the groundwater level, physico-chemical measurements (pH, EC, DO and temperature) and alkalinity using the gran titration

Based on the groundwater flow direction (section 4.1.1), selected boreholes (nine) were sampled for tritium-helium ($^3H/^3He$) and carbon-14 (C-14) (Paper II). $^3H/^3He$ were sampled using 40 mls copper tubes to prevent any atmospheric interaction. C-14 samples were collected in 50 mls polythene bottles with tight screw caps to prevent any atmospheric contamination.

4.1.3 Borehole logging

High resolution geophysical logging in a total of 20 boreholes was done to delineate the nature of sediments in the basin and outline the occurrence of high salinity formations (Paper I & II). Robertson Research Geologging equipment (Fig. 7) was used to log natural gamma radiation (NGR) and formation electrical conductivities. Units of NGR were in API (American Petroleum Institute). Formation electrical conductivities were measured from inside the PVC casings using a focused dual induction probe, which has a formation penetration depth of approximately 5 m and 2 m for the Long and Short Electrical Conductivity (LCON and SCON), respectively. The classification of formation electrical conductivity was based on 500-1,000 and 1,000-10,000 mS/m for fresh and saline water, respectively (Palacky, 1988).

Fig. 7: Geophysical borehole logging during a field campaign.

4.1.4 Sediment Cores

This work involved drilling a 100 m deep research borehole, designated RV 12-27 in Fig. 2, in the centre of the Zambian part of PLM (inferred from the 945 m amsl shoreline - (Cooke, 1979; Shaw & Thomas, 1996)) extent into the Machile Basin (Paper I). It was envisaged that the core would represent a complete sedimentation history of the lake at the drill site. The borehole (RV 12-27) was located at 24.9992 E, 17.5172 S decimal degrees with a surface elevation of 944.41 m amsl. It was cased with a 75 mm diameter Polyvinyl Chloride (PVC) plastic pipe and screened at the bottom 1 m. Sediment cores (Fig. 8) were collected from the borehole using a modified version of the Waterloo sampler (Zapico et al., 1987) at intermittent depths below the saturated zone. To ensure that we took samples with little or no disturbance from vege-

tation, large and small mammals, reptiles, insects, arachnids, termites and ants we started the sampling just below the water table. The sampling interval was on average every 2 m and dictated by lithology changes observed in borehole data drilled within close priority and mapped with geophysical borehole logging. Using a drilling rig, stainless steel core tubing (to avoid exposure to light) was pushed into the unconsolidated sediments to extract drill cores for Optically Stimulated Luminescence (OSL) and other measurements. Due to difficulty of sample collection and the nature of subsurface geology, the maximum sampling depth was 50 m below ground level (bgl). However, the borehole was drilled down to the bedrock (Batoka Basalt), which was intercepted at 100 m bgl to allow for borehole geophysical profiling. Calibration of the borehole logging profile was done after sediment core description. In addition, a recently deposited sediment sample from the riverbed of Zambezi River was collected for geo-chronology analysis.

Fig. 8: Borehole core drilling at the Kasaya site (RV 12-27, see Fig. 2 for location) for sediment characterisation and geochronology.

4.2 Laboratory analysis

4.2.1 Water chemistry

Chemical analysis of cations was done using the Perkin Elmer (Analyst 400) Atomic Absorption Spectrometry (AAS) and for anions using Metrohm Ion Chromatography (IC). Trace elements were analysed using Inductively Coupled Plasma Mass Spectrometry (ICP-MS) at the Geological Survey of Denmark and Greenland (GEUS). The quality of the chemical data was assessed using the ionic charge balance. The results have been used in Paper II.

4.2.2 Isotope Analysis

Stable isotope ratios of oxygen ($^{18}O/^{16}O$) and hydrogen ($^{2}H/^{1}H$) were measured relative to the Vienna Standard Mean Ocean Water (VSMOW) standard and analysed using the Picarro Cavity Ring – Down Spectrometer (PCRDS) equipped with an autosampler and a vaporizer at GEUS. The results were expressed as ‰ units using the δ (delta) notation (Einbond et al., 1996) with standard deviations not larger than ± 0.2 ‰ ($\delta^{18}O$) and ± 0.5 ‰ (δD), as calculated from four replicate injections into the vaporizer. Tritium (^{3}H) and helium (^{3}He) was measured at the University of Bremen, Germany, using the Bremen Mass Spectrometer System. ^{3}He was measured from radioactive decay of ^{3}H using an ingrowth method (Sültenfuß et al., 2009); samples are degassed, sealed and stored for 110 days to allow for formation of ^{3}He from the tritium decay. The ^{3}H results were expressed in Tritium Units (TU), whereas ^{3}He in cubic centimetres at standard temperature and pressure per kilogram water (cc STP/kg).

The proportion of young and old water was estimated by comparison of the measured ^{3}H concentration to the infiltrated ^{3}H content (from precipitation) in the last decades. ^{3}H datasets from the last decades (1960-2005) are obtainable from the WISER Database (IAEA & WMO, 2006), at the Ndola Station being the closet proxy to the study area. The tritium concentration in the long term record was corrected to account for radioactive decay scaled to 2014. We applied an approximate steady state decay correction factor of 0.08 (Kalinowski, 2004) to the tritium precipitation data at Ndola station hence a long term tritium average of 2 TU. Therefore you can derive, that water below 2 TU should be a mixture of older water which is free of tritium, (recharged before 1955). The ^{14}C activity and $\delta^{13}C$ in ‰ (versus V-PDB) were measured at Beta Analytic Limited, Florida by accelerator mass Spectrometry. Uncertainty for $\delta^{13}C$ is 0.15 ‰ and that for ^{14}C is 1 % of the measured

activity and expressed as percent of modern carbon (pmc). Isotope analysis results have been used in Paper II.

4.2.3 Optical Stimulated Luminescence (OSL)

Optical luminescence dating of quartz grains is based upon the response of light-exposed quartz grains to the cumulative effects of natural radiation on the grains during dark burial. Upon light exposure, quartz grain defects lose previously stored charge (in the form of trapped electrons at the defects) thereby zeroing the amount of luminescence that can be detected in a laboratory experiment. At the moment of burial the luminescence clock is therefore set to zero time. During burial in dark conditions, natural radioactivity in the form of alpha, beta, and gamma radiation associated with the decay of natural uranium, thorium and potassium will cause electrons to again be trapped in the defects.

In the laboratory, the electrons are untrapped emitting ultraviolet wavelength photons that are counted as the luminescence and whose intensity is proportional to the radiation dose acquired during burial in dark conditions. The recently deposited sample was used to determine if the sediment core material could be completely 'bleached'. Bleaching in this context means the potential for the sediment to lose its ionizing energy stored in its crystal lattice from the decay of radioactive species and their daughter products within and around the grains, which builds up over time following burial. The stages of OSL analysis are summarised in Fig. 9.

Analytical work, involved splitting the core and samples were taken under low-level red light conditions. Potentially mixed sediment adjacent to the core barrel walls was avoided. Chemical analysis and measurements were conducted at the Nordic Laboratory for Luminescence Dating, University of Aarhus at Risø. Each sample was treated with concentrated (36%) HCl to remove carbonates, H_2O_2 to remove organic matter and sieved to isolate the 180-250 μm sand fractions.
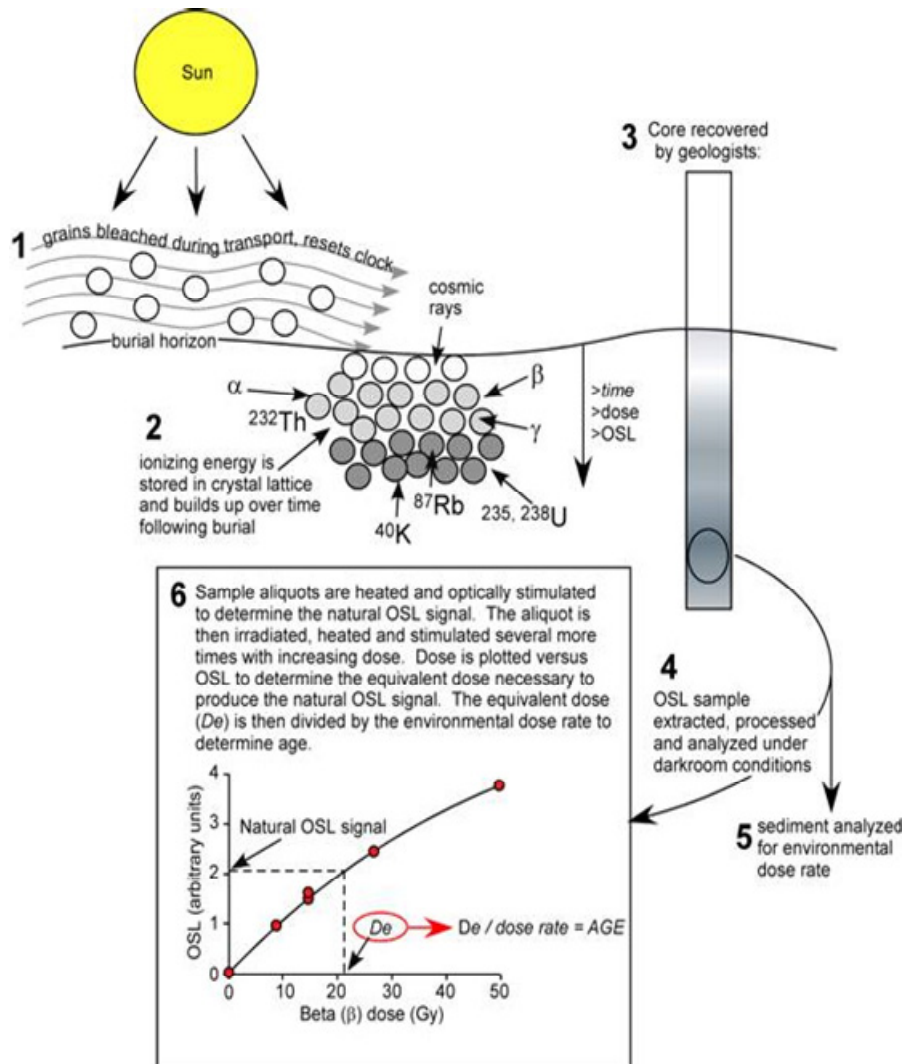
Fig. 9: Generalized processes that produce the luminescence signal (steps 1 and 2), and the sampling and analytical procedure to determine the age of deposition (steps 3 through 6). (Source: Mallinson, 2008).

The sand grains were placed in 1% HF for 50 minutes and then again treated with HCl to remove any fluoride precipitates, before using density separation (2.58 g cm^{-3} aqueous solution of sodium polytungstate) to separate quartz and other grains from a lighter K-rich feldspar extract. Finally, the quartz-rich extract was placed in 40% HF for 50 minutes and again treated with HCl to give the 'quartz-extract' from which all feldspar had been removed. Luminescence measurements were made on a Risø TL/OSL-DA-20 reader (DTU Nutech) with a bialkali PM tube (Thorn EMI 9635QB) and Hoya U-340 filters (290-370 nm). The built-in calibration using a ^{90}Sr/^{90}Y beta source gives a dose rate of ~0.1 Gy/s (typical uncertainty ~2.5%). Blue light-emitting diodes (LEDs) (~80 mW.cm^{-2}; 470 nm), and infra-red (IR) LEDs (~150

mW.cm^{-2}; 875 ± 80 nm) provided optical stimulation. The heating rate used was 5 °C/s. The luminescence purity of the quartz extracts were confirmed using IR stimulation (only feldspars have a significant IR stimulated signal; quartz is insensitive). The Single Aliquot Regenerative-dose (SAR) measurement procedure outlined by Murray & Wintle (2000) and Wintle & Murray (2006) was used to estimate quartz equivalent doses. In summary of the SAR method, each sample was irradiated with increasing radiation levels (beta), and re-exposed (stimulated) to determine the luminescence that occurs at each irradiation level. The equivalent dose was then determined by applying a regression to the data, and determining the radiation dose that corresponds to the initial luminescence signal. A pre-heat of 260°C for 10 seconds and a cut-heat of 220°C were employed, and optical stimulation was undertaken with a sample held at 125°C. A dose recovery test gave an average ratio of measured to given dose of 0.994 ± 0.004 (n = 18), demonstrating that our chosen protocol was able to accurately measure a known dose given to our samples before any prior treatment. Radionuclide concentrations were estimated using HRGS - High Resolution Gamma Spectrometry (Murray et al., 1987); these were converted to dose rates using the factors given by (Guérin et al., 2013). Cosmic ray dose rates are based on Prescott & Hutton (1994) and an average water content of 10% was assumed with an uncertainty of ± 4%. The time since burial is the ratio of the total dose divided by the annual radiation dose experienced at the burial position. A similar process was applied to river bed sediments from the Zambezi River (Fig. 2) for zero age determination. The results were used in Paper I.

4.2.4 XRD, SEM and microfossils

Samples were taken from the drilled borehole (section 4.1.4) at 14 m, 21 m, 23 m, 28 m, 35 m and 45 m bgl for X-Ray Diffraction (XRD) and microfossils. The purpose of these measurements was to understand the palaeo-environmental conditions of PLM preserved at deposition. For XRD analysis, bulk samples were crushed to powder form and oven-dried at 35 °C. Where appropriate, for diagnostic tests of the type of clay minerals, samples were heated to 550 °C and glycolation was applied. X-ray peak heights (intensity) were used as gross indicators of the relative proportions of minerals present using the standard mineralogy libraries. To validate the presence of carbonates, where indicative above background peaks were seen in the XRD measurements, sediment effervescence test upon the addition of hydrochloric acid (HCl) was conducted.

To visualise the mineral structure and support XRD analysis, representative samples (same depths as XRD) were analysed using a Philips XL 40 Scanning Electron Microscope (SEM) equipped with backscattered and secondary electron detectors coupled to an Energy Dispersive X-ray Spectrometry (EDS). Sample pre-treatment followed the standard method as described by Welton (1984).

Aiming at supporting the sedimentological interpretation of the depositional environment, microfossil samples were prepared for analysis according to the methods described by Renberg (1990) at GEUS. Identifications were carried out with an Olympus BX60 light microscope using phase-contrast illumination at 1000x magnification. It should be noted, however, that poor preservation of diatoms will occur due to high salinity trends (Ryves et al., 2006; Flower & Ryves, 2009); samples were selected on the basis of proxy high clay content as indicated by natural gamma radiation in the investigation borehole. Both XRD and Microfossil samples were used in Paper I.

4.2.5 Sediment dilution experiment

Approximately 20 g of sediment samples in nine batches from drill cores of varying depth (section 4.1.4) was collected in 50 mls centrifuge tubes and filled with deionised water; specific sample depths were at 14 m, 15 m, 17 m, 19 m, 23 m, 28 m, 30 m, 45 m and 50 m bgl. Centrifuge tubes were placed on a mechanical shaker to dissolve soluble mineral phases. The EC was measured at various time periods until a constant EC was observed to indicate equilibrium. To separate the aliquot from the sediment, it was centrifuged and water extracts were placed in a 1L polythene bottle. Fresh deionised water was then replaced in the centrifuge tube and the dilution process repeated several times until the EC was almost zero; indicative of complete dissolution of readily soluble mineral phases. Sediment dilution results have been used in Paper II.

4.2.6 Cation exchange capacity

Cation exchange capacity (CEC) measurements, modified after Appelo & Postma (2005) were carried out on sediment core (section 4.1.4); specific sample depths were at 14 m, 15 m, 17 m, 19 m, 23 m, 28 m, 30 m, 45 m and 50 m bgl. Adsorbed cations and total cation-exchange capacity (CEC) was based on using 1M NH_4Cl rather than NaCl to replace adsorbed cations enabling ICP-MS analysis of the desorbed cations. Adsorbed NH_4 was determined by replacing adsorbed NH_4 using a 1M NaCl solution. Total CEC was determined by replacing the adsorbed NH_4 from the first step with Na using 1

M NaCl. The pH of all solutions was kept close to 4.9. Ten grams of sediment core from each interval sampled were immersed in 1 M NH_4Cl in a 30 ml Teflon centrifuge tube for one hour. After centrifugation and decanting of the supernatant, the NH_4Cl saturation step was repeated twice more, for a total of three stages. The supernatant from each step was combined and analysed by ICP-MS for Na, K, Ca, Mg, Al and Fe. Alkalinity and SO_4 was measured on the first saturation step to enable correction for dissolved carbonate and gypsum, the effect turned out to be negligible. CEC results have been used in paper II.

4.2.7 Sediment Pore-water chemistry

Sediment drill core samples from the investigation borehole (section 4.1.4) were also subjected to pore-water analysis at varying depths (14 m, 15 m, 17 m, 19 m, 19.6 m, 21 m, 23.5 m, 28 m, 30 m, 35.2 m, 45 m and 50 m bgl.). Pore-water was extracted using centrifugation as described by Edmunds & Bath (1976). The resulting water sample (usually ~2 mls) was filtered through 0.45-µm membrane filters. A saturated paste method was used for the low yielding sediments. These Saturated Paste Extracts (SPEs), provide information on the chemistry of solutes in soil solution (Rhoades, 1982) and were prepared using the method described by the Non-affiliated Soil Analysis Work Committee - NASWC (1990). The samples were saturated with deionised water to create a saturated paste, and the water was extracted and filtered using centrifugation followed by filtering. The dilution factor introduced was computed by calculating the sum of the available soil water mass as aliquot (using the measured moisture content) added to the measured diluent (deionised water) mass divided by the aliquot mass. The measured concentrations were multiplied by the dilution factor to get actual pore-water concentrations. It is possible, however, that some reactions between the sediment and added water during the 'pasting' could changes the water chemistry. Pore-water chemical analysis for major cations and anions was done using the Perkin Elmer ICP-MS and Dionex IC, respectively. Physico-chemical measurements of electrical conductivity (EC) were made with a benchtop Hach Radiometer Analytical and CDC866T Conductivity Cell and pH was measured using a WTW 3310 IDS instrument and electrode. Alkalinity was determined by Gran titration (Gran, 1952). Pore-water chemistry has been used in paper II.

4.3 Modelling

4.3.1 PHREEQC, PMWIN and NETPATH

A steady state numerical groundwater flow model was set up along a groundwater flow line using the code MODFLOW (Harbaugh et al., 2000) in the graphic user interface PMWIN 8 (Chiang & Chiang, 2001) to understand the hydrological regime. To explain geochemical reactions and mineral equilibria, PHREEQC 3 (Parkhurst & Appelo, 1999), was used.

Traditionally well-known inorganic adjustment models (Ingerson & Pearson, 1964; Mook, 1972; Tamers, 1975; Fontes & Garnier, 1979; Eichinger, 1983) have been applied to Dissolved Inorganic Carbon (DIC) of water from a single well to estimate ^{14}C ages. This approach is well suited for geochemical systems undergoing simple water-rock reactions, such as carbonate mineral dissolution, gypsum dissolution, Ca/Na ionic exchange, CO_2 gas dissolution, and isotopic exchange between soil CO_2, calcite and DIC during recharge; some of these processes have been shown to occur within the Machile Basin.

NETPATH (Plummer et al., 1994) incorporates these traditional adjustment models and can be used for complex hydro-chemical systems. Typically in NETPATH, initial and final water compositions are defined separately. NETPATH can then be used to derive chemical reactions that reproduce the chemical and δ^{13}C isotopic composition of DIC in the final water. This in effect produces separate adjustment models for each water analysis. The modelling software (PHREEQC, PMWIN and NETPATH) have been used in paper II.

4.4 Assimilation of available hydrogeological data

Paper III, amalgamates geophysics, hydrochemistry and groundwater studies from local studies within the palaeo-lake basin, to draw convergence on the state of hydrogeological knowledge. ArcGIS^{TM} 10.X software was used for the quantitative data interpolations as well as map creation and detailing.

5 Results and discussion

In this chapter, the main results of the research will be highlighted. The first two sections present results on the sedimentological evolution of the PLM (Paper I), and physical processes and hydrogeological aspects (Paper II and Paper III). The third section focus on the hydrogeochemistry (Paper III).

5.1 Sedimentology

5.1.1 Drill core sediments and microfossils

The investigation borehole was drilled to 100 m bgl, and showed siliclastic sediments of fluvio-lacustrine origin composed of intercalations clay and sand. Further, evaporite minerals in a whitish vein-like nodule structures was observed (Fig. 10). XRD analysis reveals this as bassanite (dehydrated gypsum). Carbonate minerals were undetectable except under a simple acid test.
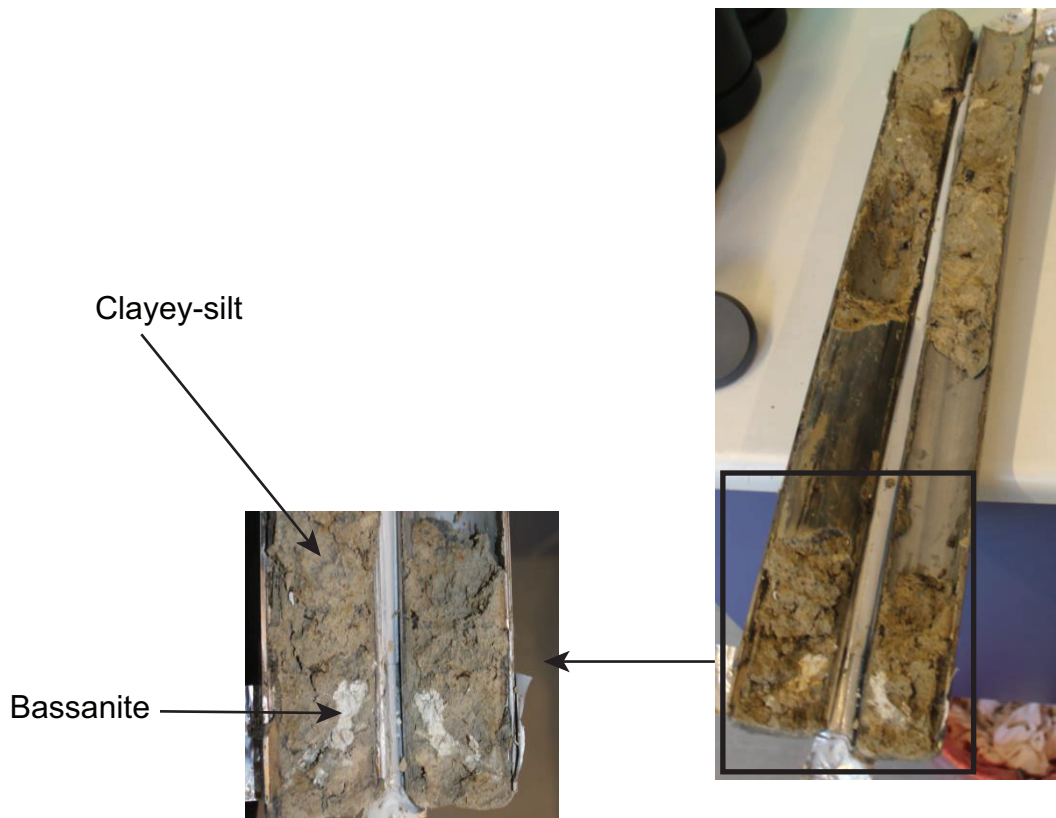
Fig. 10: Typical sediments (clayey-silt) and disseminated vein-like nodule structures of gypsum evaporites.

SEM (Fig. 11), showed both gypsum and calcite minerals supportive of the XRD analysis and simple acid test, respectively. Gypsum minerals outlined

its typical 'desert rose' morphology, whereas, the calcite in a rhombohedra form.
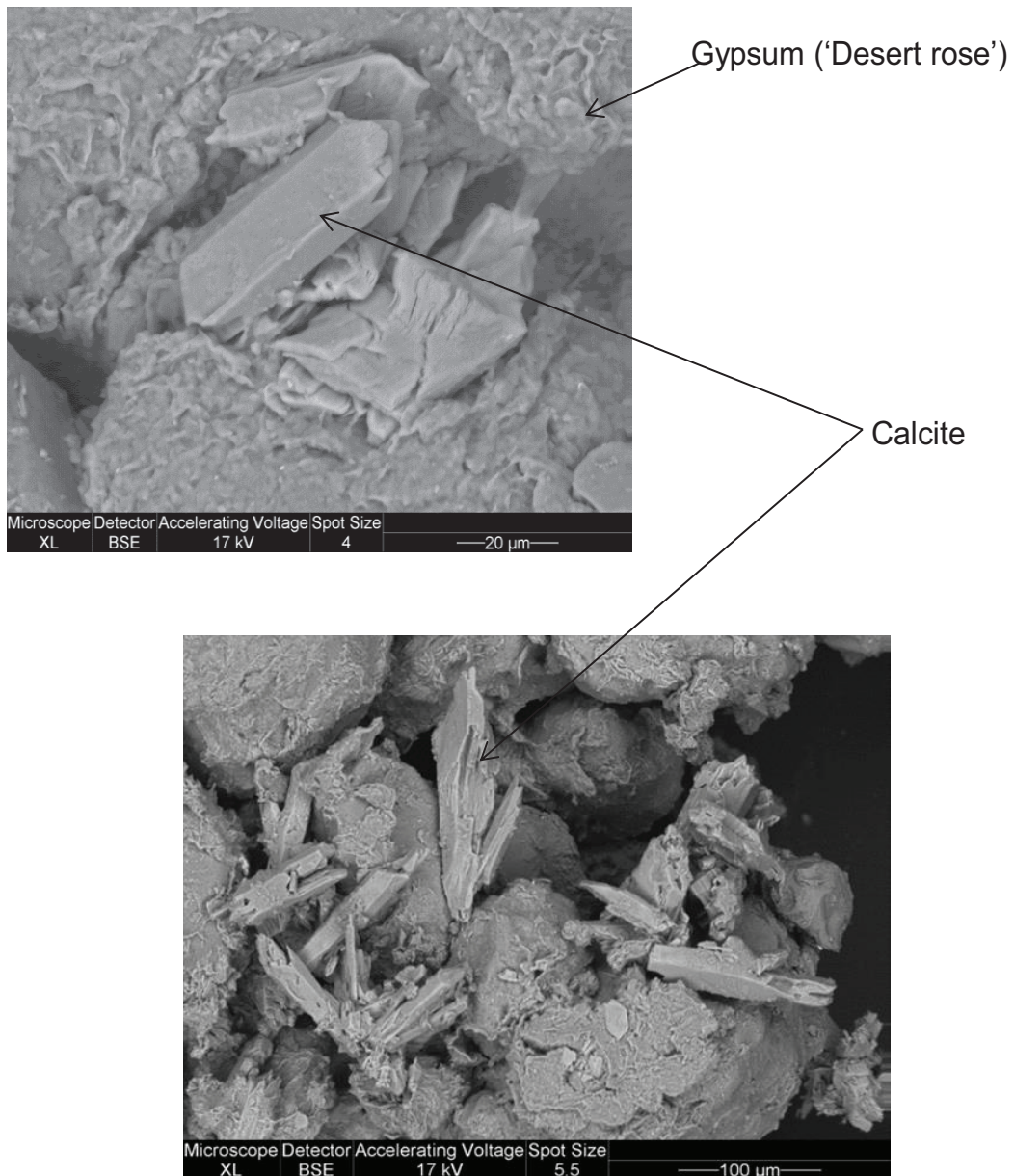
Fig. 11: SEM showing calcite and gypsum (bassanite) for sediments at 45 m below ground level. Calcite is identified with its crystalline and rhombohedra morphology whereas gypsum has its typical 'desert rose' structure.

The sediments also host mixed microfossil assemblages of pennate and centric diatoms, and sponge spicules; this is interpreted to be a result of changing paleao-environmental conditions as shown in Fig. 12; details in paper I.
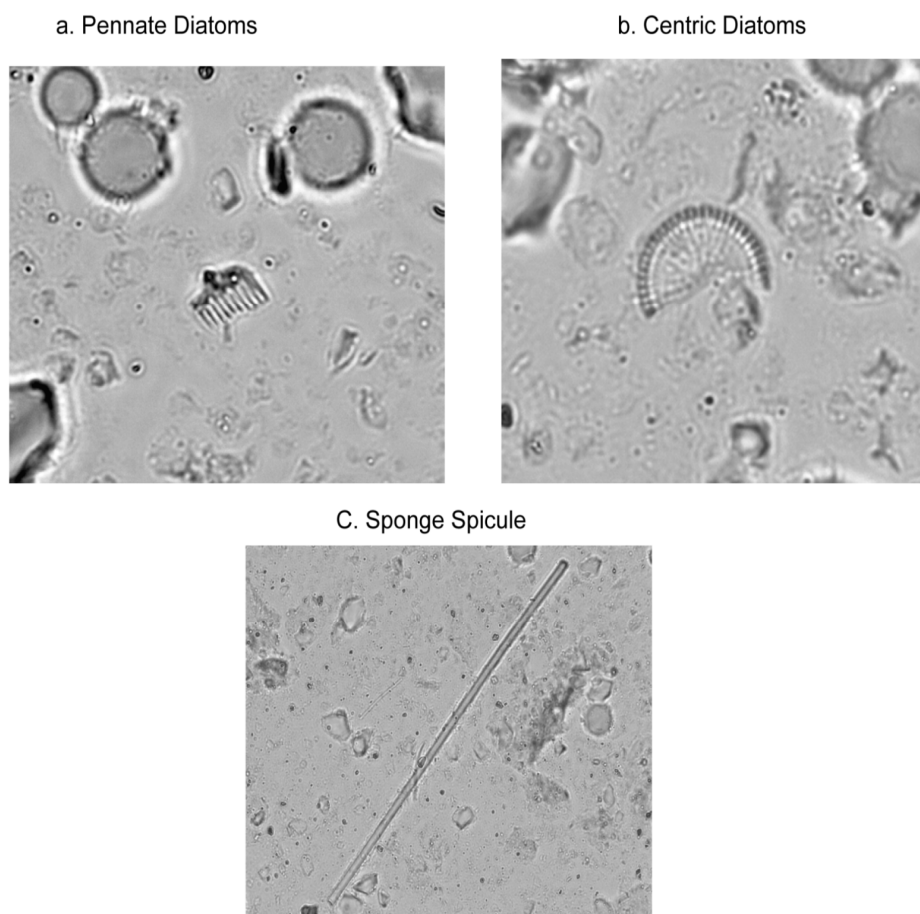
Fig. 12: Representative fossil (1000x magnification) from the sediment core at 21 m bgl (the region with most fragments).

The centric and pennate diatoms (Fig. 12) are likely of the genus Cyclotella and Nitzschia, respectively; of which we infer a mixed fossil assemblage of the palaeo-environmental condition during the existence of the PLM, ranging from weakly to strongly alkaline lake water conditions (Hecky & Kilham, 1973; Nyambe & Utting, 1997; Fritz et al., 1999; Smol & Stoermer, 2010). Geophysical logging of the deep borehole shows the high salinity formation continues down to the bed rock – basalt (Fig. 13a). The formation electrical conductivity varies between approximately 0 and 750 mS/m in the log profile. Low conductivities are observed between 944-933 m amsl ranging from 0-250 mS/m, whereas, >250 ms/m are observed below 933 m amsl with a peak as high as 750 mS/m at 874 m amsl. Three sequences (I, II, III) are mapped based on variation in sediments from clay to sand conditions indicative of lacustrine to fluvial environments, respectively as mapped using natural gamma spectrum; this corroborates with the diatoms used as a proxy lake sediment deposition mechanisms.
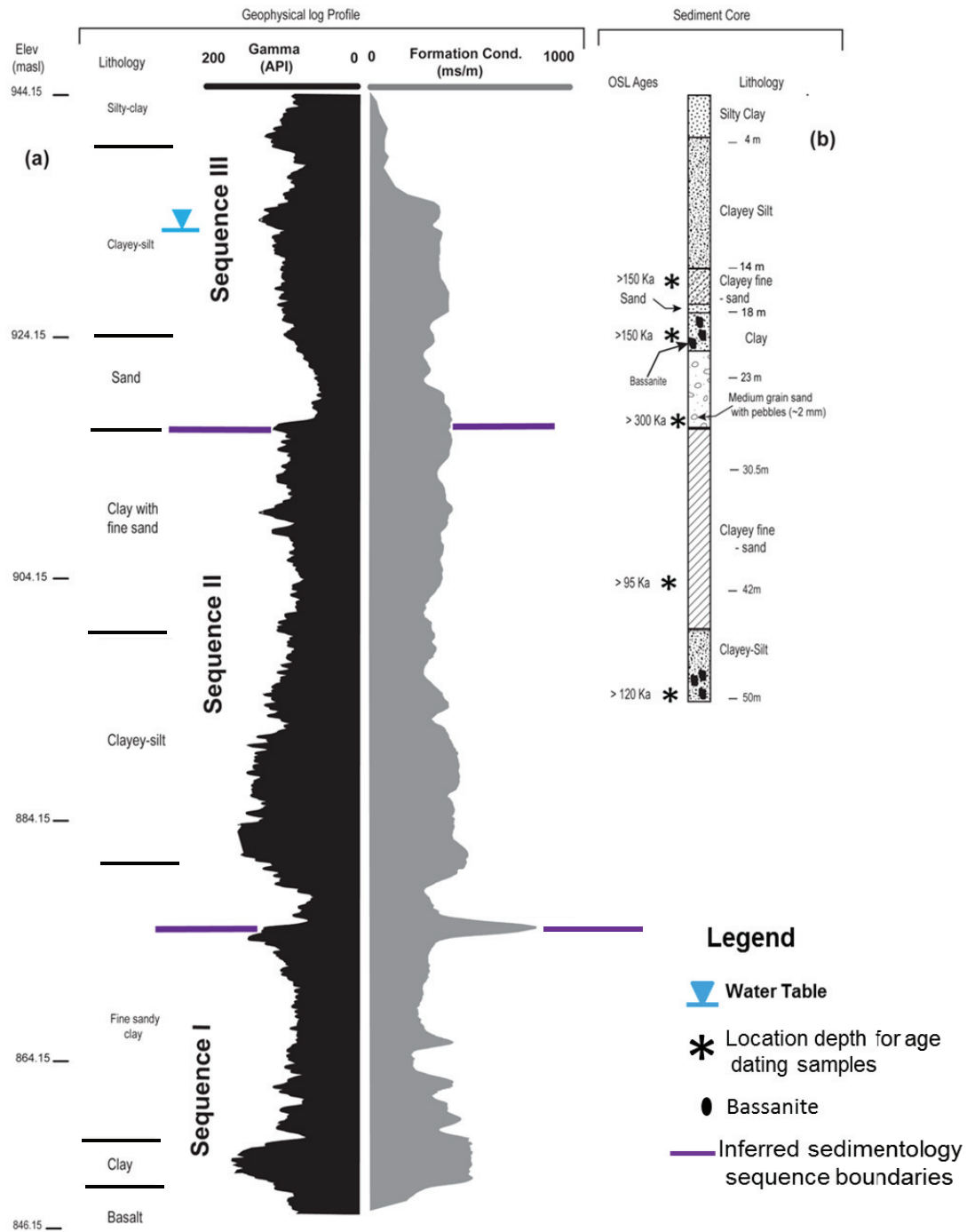
Fig. 13: (a) Shows the 100 m deep geophysical profile of natural gamma rays (NGR) and formation electrical conductivity (FEC) as sampled by logging from the investigative borehole RV 12-27 (for the location see Fig. 2.). FEC varies approximately between 0 and 750 mS/m indicative of hyper-saline pore-water. NGR outlines the lithological boundaries between the clay and sand fractions which enabled the mapping of three sequences suggestive of climatic changes in the basin. (b) Core litho-stratigraphy profile outlining the various lithologies intersected (predominately silt and clay or a combination of the two), age dating results specific to the sampled depth and the evaporite mineral basanite are shown.

5.1.2 OSL ages and chronostratigraphy

Chronostratigraphy of the sediments based on the OSL ages are shown in Fig. 13b (above) and Table 1. Dose rates were found to be relatively low (Table 1), ranging from total values of 0.71 ± 0.06 grays per thousand years (Gy/ka) in the coarser sediments and up to 2.16 ± 0.10 Gy/ka in the clay-silt sediments. The recently deposited superficial river bank sample (Table 1) had a dosage rate of 0.75 ± 0.04 Gy/ka comparable to the coarser sediments at depth. Given that the dose of the quartz grains in the sediments were above 200 GY, this suggests they are either nearly or fully saturated with radiation. The dose therefore is a minimum dose detectable using OSL. The calculated ages therefore represent minimum ages and not actual ages. Minimum ages between 14-28 m bgl, range from >150 to >300 ka, whereas, below 40-50 m bgl, range from >95 to >120 ka. Stratigraphically, we can only say both the upper (14-28 m bgl) and lower (40-50 m bgl) must be >300 ka in age. An accurate constraint on ages is not possible on these sediments due to radiation saturation. The river bed sediment (Table 1, 1.10 ± 0.14 ka in age) shows that it is possible to completely bleach the sediment cores.

Table 1: Optically Stimulated Luminescence (OSL) analysis results from the investigation borehole core showing the age (ka), dose (Gy), number of samples, dose rate (Gy/ka) and water content (%). Quartz dose (Gy) suggests the quartz is saturated by radiation to an extent we can only report the results are minimum ages (ka).

Lithology	Sample Depth m bgl (± 0.20 m)	Age, ka	Dose, Gy	Number of samples	Dose rate Gy/ka	Water Content %
Sand	Riverbed sample	1.10 ± 0.14	0.82 ± 0.10	27	0.75 ± 0.04	22
Clayey silt	14	> 150	> 280	24	1.95 ± 0.09	20
Silt-sand	19	> 150	> 260	17	1.73 ± 0.09	18
Sand	28	> 300	> 210	14	0.71 ± 0.06	16
Clay with fine sand	40	> 95	> 200	18	2.16 ± 0.10	13
Clayey silt	50	> 120	> 260	23	2.13 ± 0.11	17

Analysis over 50 m bgl of core, using OSL dating, for the first time within the PLM system, has shown that the quartz grains are nearly or fully saturated with radiation. The maximum measurable ages using OSL is 300 ka (Cordier et al., 2012). Based upon Early Stone Age tools McFarlane & Eckardt (2006) suggested a minimum age of the PLM lake floor of 500 ka. This is in line with the molecular dating of a Pleistocene cichlid fish radiation which emerged in PLM (Joyce et al., 2005) the oldest clade dated to c. 600 ka (Genner et al., 2007). OSL dating within the PLM can therefore not accurate-

ly constrain the formation of PLM. Our findings are in contradiction with Burrough et al. (2009a), who suggest a Late Pleistocene to Holocene existence of PLM based on OSL ages from palaeo-shorelines. They suggest a climatically controlled fluctuation of palaeo-shorelines during its existence. Within the Machile Basin, it is evident that sediments are old (>300 ka) and cannot be constrained using OSL, we support the tectonic evolution (Moore et al., 2012) of the lake system, specifically that the lake was formed much earlier (~1.4 Ma) and predominately desiccated by 500 ka; the tectonic evolution is discussed in chapter 2. Further details are discussed in paper I.

Due to increasingly arid conditions, evaporites of carbonates, sulphate and chlorides were formed, however, in the marginal areas (Machile), the evapo-concentration sequence based on Hardie-Eugster's model (Hardie & Eugster, 1970) did not continue beyond a gypsum forming stage based on the sediments analysed. More investigations are required for deeper sediments above 50 m bgl. The formation of bassanite evaporites which are intimately mixed with sediments supports deposition under high evaporation conditions; the timing of the event cannot be well constrained from our study but is probably in the period when profound desiccation of the lake commenced ~500 ka. Although the sediments host disseminated evaporates, we did not observe any thick beds of pure evaporate, which is indicative of the importance of surface water-groundwater interaction (Bowler, 1986; Sinha & Raymahashay, 2004). It is likely that the sediment interstitial water had a higher salinity than the overlying lake water during desiccation due to rapid exchange between the surface water and groundwater (Bowler, 1986). Evaporates within the PLM, possibly developed during high evaporation and groundwater inflow (Bowler, 1986; Rosen, 1991; Rosen, 1994); details of the conceptual model of formation are given in Paper III.

5.2 Hydrogeology

Results for the ^{3}H, ^{14}C and δ^{13}C isotopes along the flow line (high to low hydraulic gradient in Fig. 14) show ^{3}H results ranged from 0.03-0.94 TU in the fresh-transition zone and 0.00-0.71 TU within the brackish to saline zone this is indicative of generally old water (> 60 yrs) with some fraction of young water (Clark & Fritz, 1997).
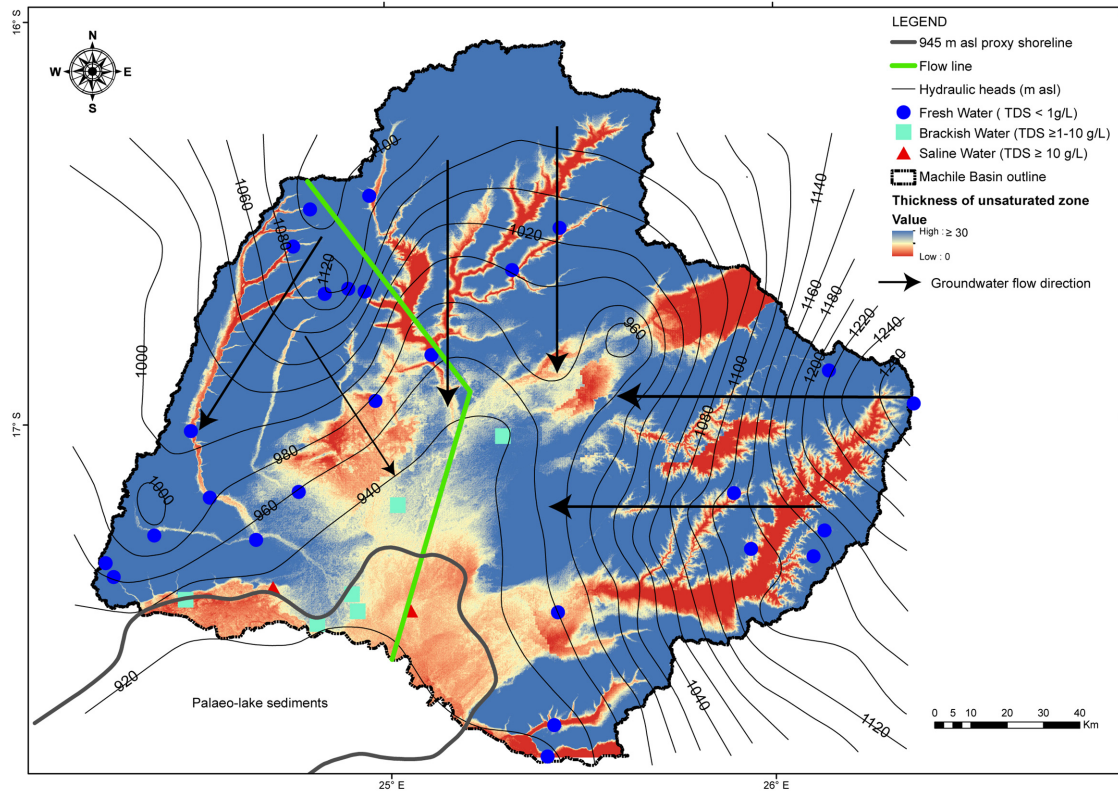
Fig. 14: Map of the thickness of the unsaturated zone showing a near surface water table within the topographic low region and the river channels suggesting groundwater loss through these channels and evaporation in the dry season period – August to November. The river channels and topographically low central area are discharge zones. The groundwater flow line (green line) was used to investigate groundwater processes within the region. Groundwater flow is convergent towards the central region

The ^{14}C activities in the fresh-transition zone were from 57.3-93.2 pmc (uncorrected), whereas in the brackish-saline zone values between 66.3 and 106.2 pmc were encountered (Table 2). Increase in the ^{14}C activity in the transition and within the saline region, is suggestive of an infiltrating water contribution with recent atmospheric-water interaction. Furthermore, δ^{13}C showed an increasing trend in the fresh-transition zone from -21.5 to -16 and -20.1 to -12.8 in the brackish-saline zone, suggestive of formation derived

dissolution of carbonate solutes, which increase along the groundwater flow line.

Table 2: Shows the isotopic chemistry and the proposition of old and young water along the flow line. The aquifer system is predominately old (> 60 years) based on the low tritium concentration; however, juvenile water is more prevalent in the transition zone (i.e. Lutaba).

Borehole name (Upland to topographic low)	Depth of Borehole (m)	Tritium [TU]	δ13C ‰	14C pmc (uncorrected)	Water Quality Zone
1. Sipula Village	25	0.03	-21.5	87.9	Fresh
2. Machile Basic School	60	0.29	-20.1	57.3	Fresh
3. Salumbwe Village	55	0.94	-19.5	93.2	Transition
4. Lutaba Basic School	45	0.43	-16.0	63.6	Transition
5. Adonsi Basic School	45	0.00	-20.1	67.8	brackish
6. Situlu Health Post	50	0.00	-13.7	66.3	brackish
7. Kasaya Basic School	25	0.05	-14.9	75.6	Saline
8. Makanga Village	40	0.03	-15.1	102.5	brackish
9. Mwandi Basic school	30	0.71	-12.8	106.2	Fresh in close proximity (<5 km) to Zambezi River

NETPATH uses inputs of both measured ^{14}C and δ^{13}C as inputs to generate several adjustment radioactive model results; typically the results from the Vogel (1970) model are acceptable as apparent ages for Kalahari groundwaters (Vogel & Van Urk, 1975; Selaolo, 1998; Stadler, 2005) with an assumption of 85 pmc as initial ^{14}C activity and a 15 % carbonate dilution effect. Typical ages within the fresh water zone range from 281-4,540 yrs, whereas, in the brackish-saline region 139-11,700 yrs (corrected ^{14}C ages). Details are discussed in Paper II. At a regional scale (Paper III), it is evident that the ages of sediments are much older (> 300 ka) compared to groundwater ages within 50 ka thus palaeo-recharge; groundwater age corroborates with pluvial climatic events in the Late Pleistocence and Holocene (> 30-20 and 8-4.5 ka, (De Vries et al., 2000)).

Groundwater flow within the Machile converges towards the central region of the Machile Basin with a higher hydraulic gradient of 0.002 in the fresh water zone compared to 3.08×10^{-4} in the saline zone (Fig. 14). These gradients suggest a net high groundwater flow within the freshwater fringe zone compared to a more or less stagnant saline central pool. The upland unsaturated zone is thicker (more than 30 m) and thins out towards the topographic low (central region), topographic depressions and in the river valleys; these regions are topographic groundwater discharge zones (Fig. 14). Evaporation and evapo-transpiration are potential groundwater sinks in these discharge zones. A conceptual model of the groundwater flow regime (Fig. 15) was also developed based on available literature and field experiences (Paper II). It is possible that fresh groundwater from the upstream regions is lost to evaporation/ evapo-transpiration or forced out through topographic depressions due to the hydraulic conductivity contrast between the fresh high permeable and low permeable saline region (mainly clay and silt). Local flow systems around the topographic depressions, dambos (small wetlands), deltaic alluvial features and rivers (i.e. Perennial Zambezi River and some of its tributaries) are present. Intermediate systems of groundwater flow could occur at the topographic depressions and at the interface between saline and fresh groundwater. Regional systems of groundwater flow would probably occur from the recharge area to the saline/fresh water interface. Infiltration of precipitation is probably the main source of groundwater replenishment generating a flow towards the saline low hydraulic conductivity region. Diminutive amounts of fresh groundwater may penetrate the saline zone; however, the majority is lost to evaporation.

To test the feasibility of the proposed conceptual model, a model was developed of the groundwater flow regime based on parameters, grid dimensions and assumptions given in Table 3. Given the heterogeneity of lithologies within the saline zone (intercalations of sand and clay) a net average hydraulic conductivity of 10^{-6} m/s is assumed, and 10^{-4} m/s for sand in the fresh water zone was used (Table 1). Recharge of 10 mm/yr (Wanke et al., 2008) was assumed for the entire transect with potential evapo-transpiration of 1500 mm and the depth to which the roots would reach the water table (extinction depth) of 10 m. The model simulates the topography of the transect line.
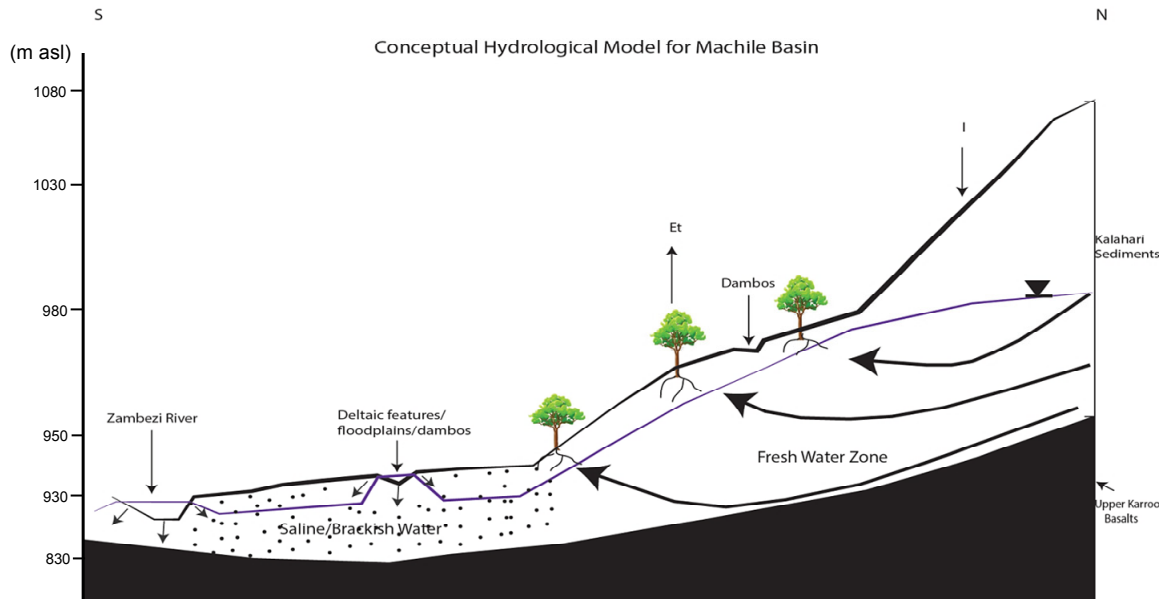
Fig. 15: Conceptual model of the Machile Basin, North to South following a streamline. Evapo-transpiration through the root zone and evaporation through the topographic are the main sinks for the groundwater. Flow through the saline zone is probably not present or at least very little given the hydraulic conductivity contrast. Lateral groundwater flows are probably possible via the dambos.

Table 3: Modelling parameters used to simulate the hydrological regime in the Machile Basin.

Parameters	Grid Dimensions
- Recharge on the entire transect 10 mm/yr - Potential Evaporation over the entire transect 1500mm/yr - Extinction depth 10 m - Horizontal Conductivity 10^{-6} m/s (clay in saline pool); 10^{-4} m/s (fresh water zone) - Vertical Conductivity 10% Horizontal - Wetting capability: -1	- 1 x 100 x 50 (Row x Columns x layers) - 150 Km transect N-S across the Machile, following a streamline - Width of each 1.5 km - follows the topographic surface

It is observed that fresh groundwater flows towards the saline pools, but due to the hydraulic conductivity contrast groundwater is forced out and lost to evaporation through river channels and dambos (wetlands) in the topographic depressions (Fig. 16). Particle tracking shows local flow systems are younger in age ranging from <500-2 000 yrs in the freshwater zone whereas these are

much older in the saline regions in excess of 50 000 yrs old. Intermediate and regional flow was focused in the freshwater zone with ages up to 5 000 and 10 000 yrs.
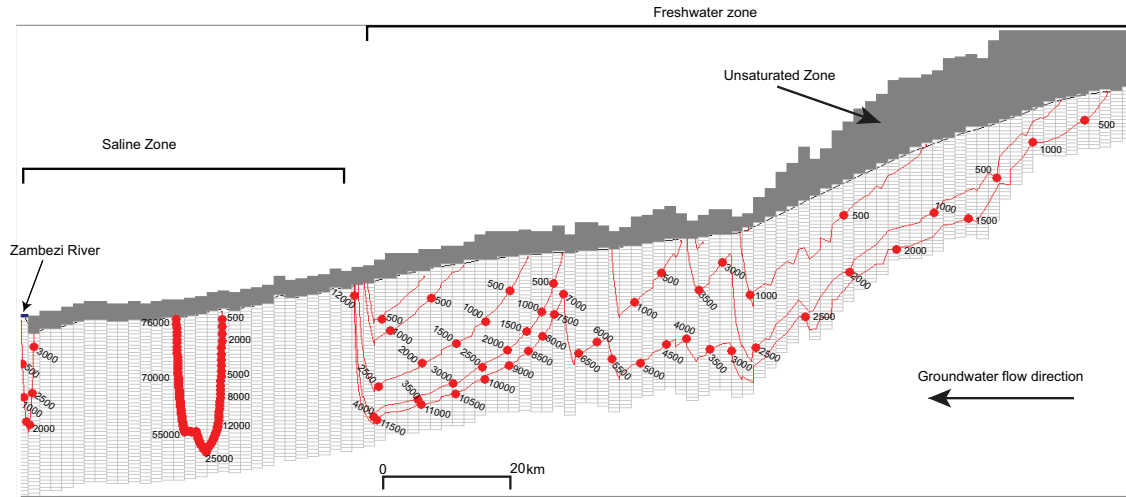
Fig. 16: Two-dimensional transect model showing groundwater flow within the fresh groundwater zone and particle tracking time stamps; each time stamp after the starting point is 500 years. Due to the conductivity contrast, most of the groundwater upstream is forced upwards at the interface and lost to evapo-transpiration in the unsaturated zone (shown in grey). Younger water occurs close to the water table in the fresh water zone and becomes older with depth compared to the saline zone with high residence time.

Evapo-transpiration effects are profound with the Okavango Delta at a regional scale in the MOZB at it does not interact with the regional groundwater (Fig. 17). In Paper III, stable isotope data in groundwater (including the Machile Basin), and surface water (Okavango) was compiled as shown in Fig. 16. Groundwater isotopes on the precipitation line have undergone evaporation under varied humidity conditions which influences precipitation variability. Gonfiantini (1986) suggests a gradient of 8 on a 2H-18O, represent a low relative humidity, > 95 %, indicative of potential evaporation effects. The evaporation slope (5) suggests a relative humidity of 75 % with higher evaporation. All the groundwater isotopes have thus sustained evaporation prior to infiltration.
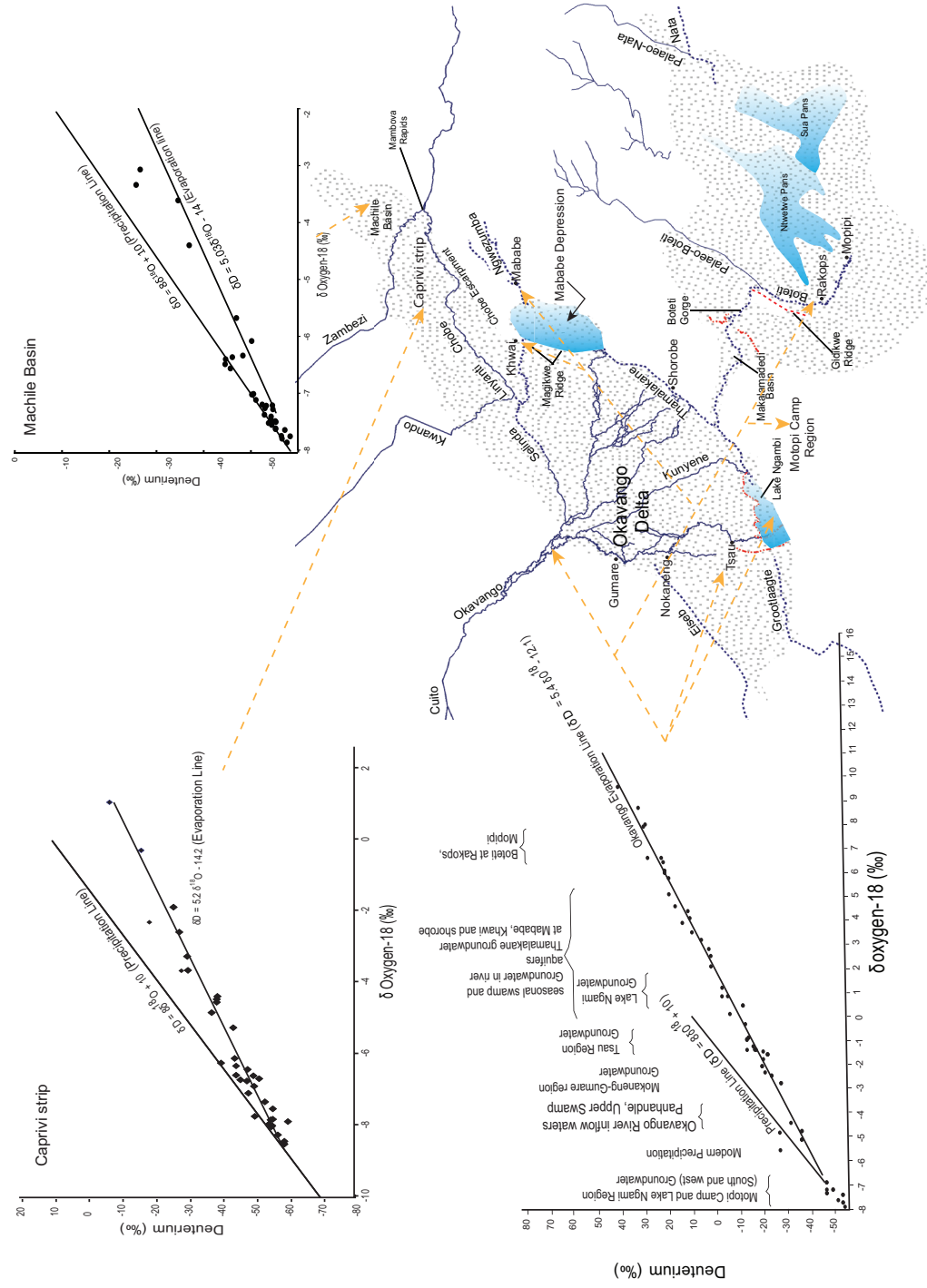
Fig. 17: A synthesis of stable isotope of Oxygen-18 and Deuterium (Paper III). Stable isotopes suggest all groundwater undergoes evaporation both on the precipitation and evaporation before infiltration.

38

Recharge studies over the basin (Jennings, 1974; Beekman et al., 1996; Beekman et al., 1997; Beekman et al., 1999; De Vries et al., 2000; Selaolo et al., 2003; Obakeng, 2007) suggest that recharge is typically lost through evapo-transpiration with barely 1 mm/yr as direct recharge and 6-7 mm/yr as indirect recharge (De Vries et al., 2000) getting to the groundwater, with losses to evapo-transpiration (details in Paper III). Consequently, the PLM sediments typically, host of stagnant saline groundwater with fresh water lost through evapo-transpiration.

Groundwater flow at a regional scale (Fig. 18) is endoheric and terminates at the MOZB. The modern day relicts of PLM, Makgadikgadi salt-pans seem to sit on top of a stagnant saline groundwater as the groundwater table is near-surface that is subjected to evapo-transpiration/evaporation effects as the water table is < 20 m (details in paper III).
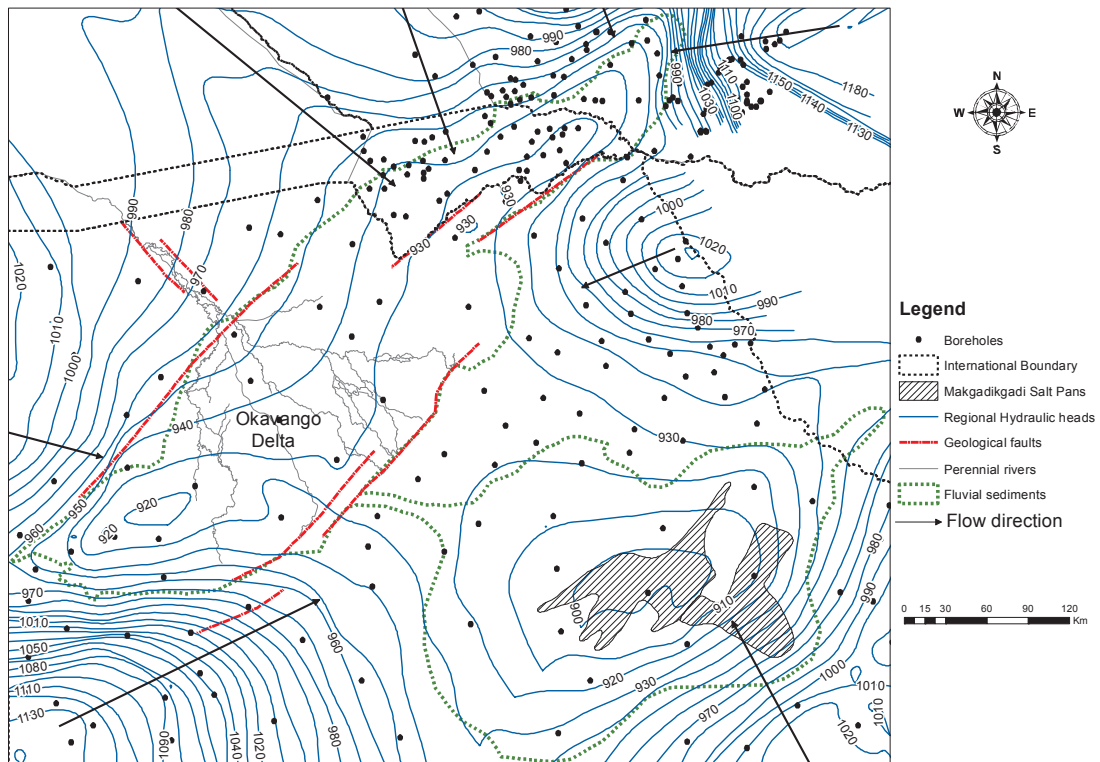
Fig. 18: Shows the groundwater flow regime over MOZB in which regional groundwater terminates at the MOZB. Groundwater is hosted within a closed basin system.

Under local conditions, localised groundwater movement would be present. A conceptual model of the current hydrogeological situation is shown in Fig. 19. Evaporites are formed in areas were the groundwater table is near-surface and subjected to continuous evapo-concentration within PLM. Based on the conceptual flow model in the Machile Basin (Fig. 14), fresh groundwater is lost through evapo-transpiration or depressions at the fringes of the PLM due to the hydraulic conductivity contrast. Fresh groundwater potential is in the river drainages/ palaeo drainage systems.
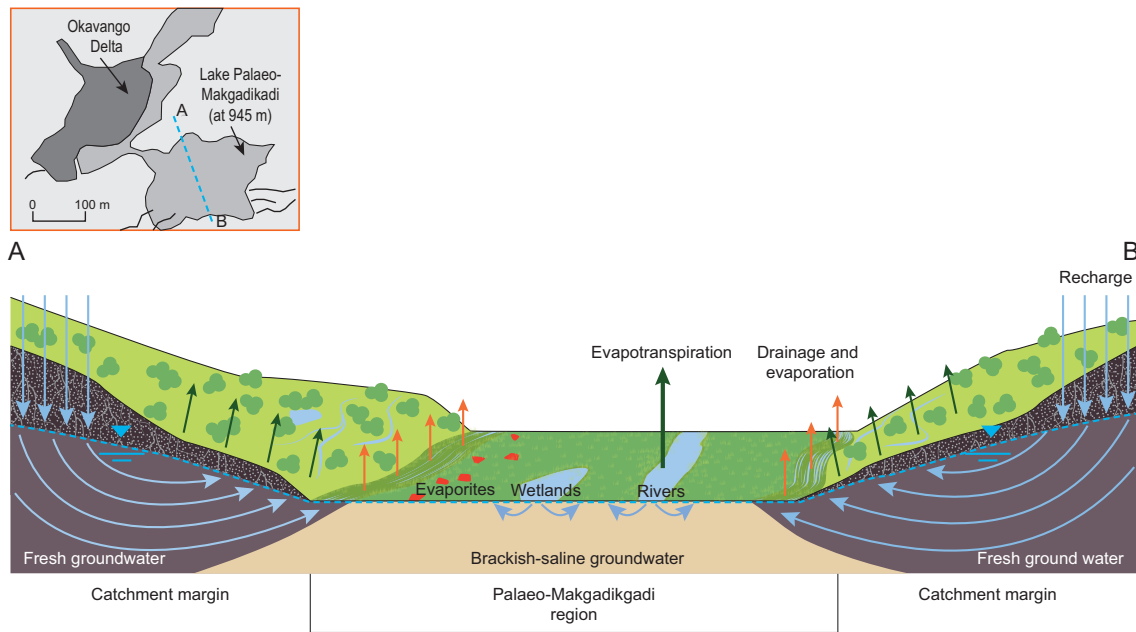
Fig. 19: Conceptual present groundwater flow regime of the PLM. Groundwater is typically lost through topographic depressions (dambos) and drains facilitated by evapo-transpiration; combined with the presence of lacustrine sediments (clays) groundwater flow is negligible within the PLM sediments although localised flow systems are present.

5.3 Hydrogeochemistry

Regional scale studies (Paper III), shows three water types, carbonates, sulphide and chlorides (Fig. 20a).
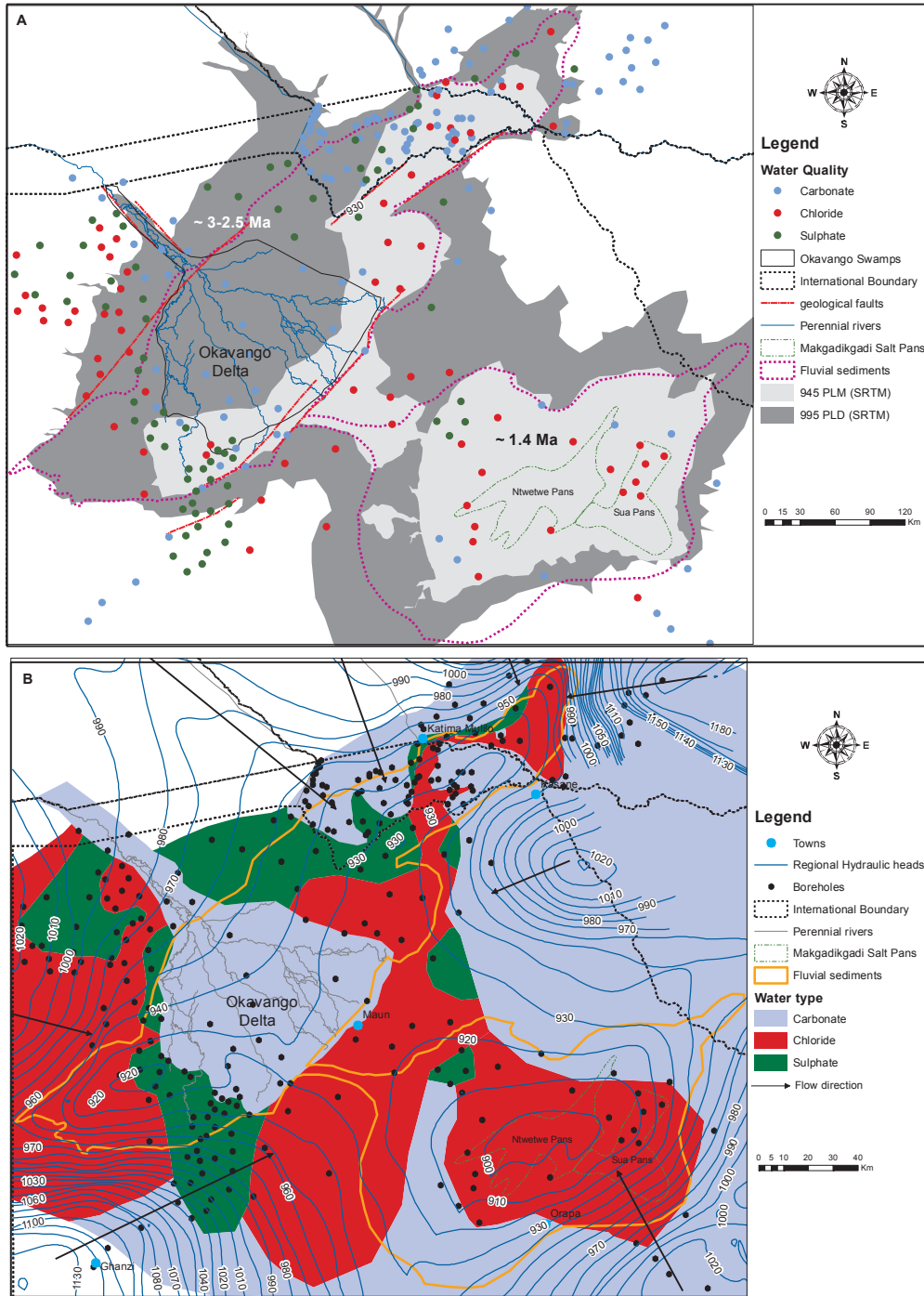
Fig. 20: (a) Synthesis of water quality facies (Paper III) and computed groundwater heads based on the digital elevation model (SRTM) from water level (shown in Fig. 2). (b) Interpolated water quality (carbonates, chlorides and sulphates) with the groundwater flow regime.

An interpolation of the water quality data (Fig. 20b), shows hydro-chemical zoning with the chloride in the central zone followed by pockets of sulphate. Carbonates occur in the fringes and the Okavango Delta. Detailed studies were carried out in the Machile Basin (Paper II). Groundwater spatial variation of the Machile Basin shows fresh (TDS < 1 g/L), brackish (TDS ≥ 1-10 g/L) and saline (TDS ≥ 10 g/L), water types (Fig. 12). Groundwater flows towards the saline zone with discharge through river channels and depression zones (Fig 14). The fresh water quality are typically Na-Mg-HCO$_3$, whereas, the brackish-saline groundwater was Na-Cl-SO$_4$ and Na-SO$_4$-Cl as shown Fig. 21 (details are shown in Paper II).
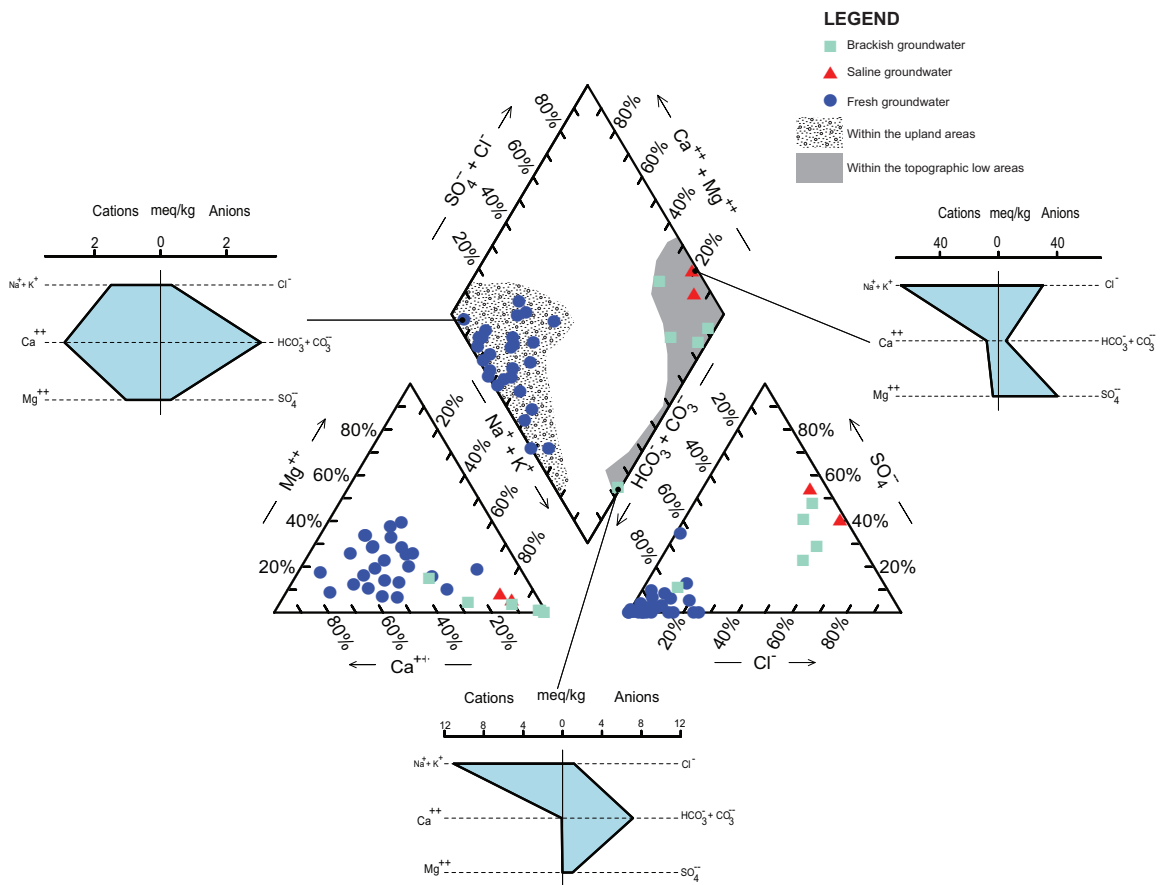
Fig. 21: Piper Diagram (Piper, 1944) and Stiff diagram (Stiff Jr, 1951) showing distinct groundwater types in the Machile River Basin (fresh Ca-Mg-HCO3- water type and saline Na-Cl-SO4/ Na-SO$_4$-Cl type) and the location within the basin.

To explain the observed water chemistry, it was modelled using PHREEQC using data from the groundwater flow-line in Fig. 14. The fresh groundwater is characterized by increasing dissolved carbonate and cations from weathering of silicate minerals (such as anorthite, albite, K-feldspars, hornblende,

42

olivines) presumably in equilibrium with secondary minerals, resulting in Ca-Mg-HCO_3 and Na-HCO_3 water. In the model description, along the advective flow path, irreversible dissolution of varying amounts of H_2CO_3 reacting with simplified alumino-silicate minerals was allowed: anorthite, albite, tremolite and K-feldspars, to supply Ca, Na, Mg and K cations that are assumed not to reprecipitate. Added amounts of reacting silicate minerals are anorthite (0.009-0.629 μmol/L/yr), albite (0.001-0.114 μmol/L/yr), tremolite (0.029-0.057 μmol/L/yr), K-feldspars (0.057-0.086 μmol/L/yr) and H_2CO_3 (0.014-1.143 μmol/L/yr). The source of H_2CO_3 is assumed to be degradation of organic matter in the system. The simple phases gibbsite and chalcedony were permitted to precipitate when oversaturated in order to control the Al and Si concentrations; the observed saturation index (SI) of 1.8 for chalcedony and 0.15 for gibbsite calculated from water chemistry measured at the downstream point (Machile) was used. Using the PHREEQC output and groundwater flow velocity, we calculate an approximate amount of formed gibbsite, 1.20-58.16 μmol/L/yr and chalcedony, 0-92.19 μmol/L/yr.

Fig. 22 a & b, shows the output of the simulation compared to the observed field results along the flow-line; Fig. 22a, shows the measured cations compared with modelled results whereas, Fig. 22b, shows simulation results with anions and pH. The model fits relatively well for pH and alkalinity, however, misfits can be seen especially for the Al and Si; this could be because of the actual reprecipitation of Al and Si comprises more complex silicate minerals such as Ca-montimorillonite, kaolinite, and illite. It was tested using Ca-montimorillonite and kaolinite equilibrium phases, however, this showed much higher concentrations of Al before precipitation initiates and a drastic drop after, and in addition it was difficult to get a good fit on the pH and alkalinity.

The presence of Ca and Mg is an indication the minerals reacting in the aquifers could be plagioclase, amphiboles, pyroxenes and/or olivines; this could not be distinguished through modelling. The model misfit could also be due to a more complex flow pattern e.g. mixing with CO_2 rich surface water or that the measured values represent different local flow lines. The ion ratios in the water from the downstream observation points (beyond 50 kms) indicate that the water chemistry is influenced by ion exchange which is not included in the model.

(a) Cations
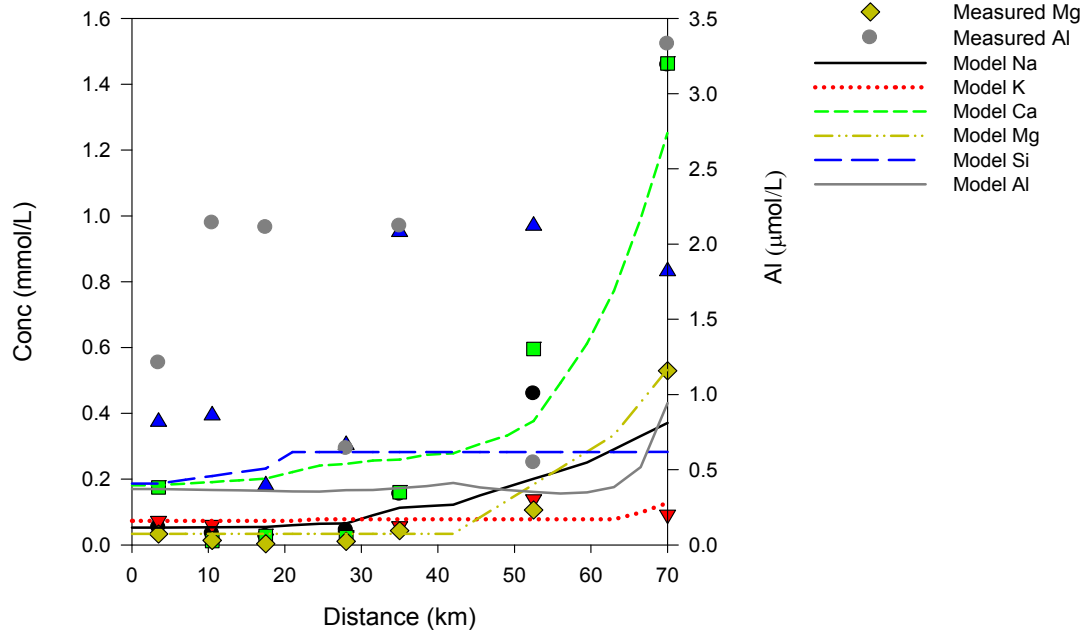
(b) Anions
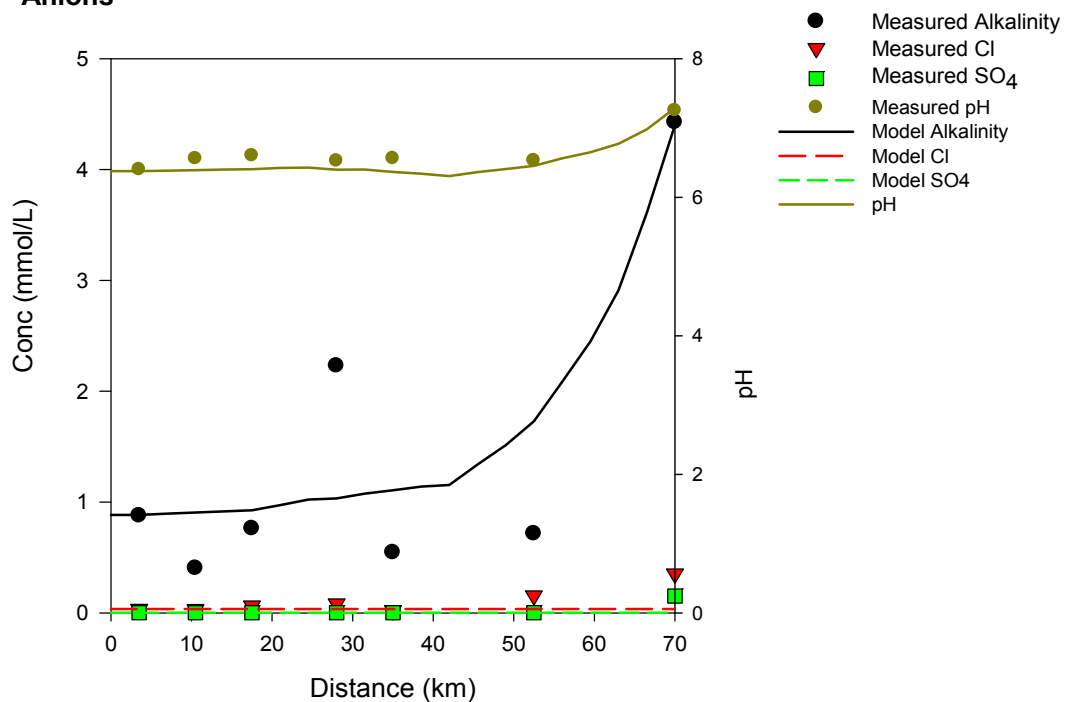
Fig. 22: (a) Observations and PHREEQC model of the 1D advection model with defined chemical reactions within the fresh groundwater zone of cations. Chemistry of the system is due to dissolution of varying amounts of silicate minerals (albite and anorthite). (b) Observations and simulation of anions and Al on the groundwater flow line in the 1D advection. The increase in alkalinity is due to carbonic acid promoting silicate weathering.

44

In addition, the last observed downstream point, which is at the transition zone between fresh and saline water, has a higher sulphate concentration in excess of 50 times more compared to the rest of the points on the flow line. This is an indication of a sulphate phase dissolving, coupled with ion exchange; this is discussed further for the saline groundwater as an extended dedolomitization process. In general, the silicate weathering reactions in the fresh groundwater zone, leads to HCO_3^- groundwater type enriched in Mg^{2+}, Na^+ and Ca^{2+} ions.

Sediment pore-water chemistry results from the research borehole (Paper II) were used to explain the processes of groundwater evolution in the saline zone. There is a strong correlation between the sulphate concentration and the sum of Ca, Mg and Na with an almost 1:1 relation (details in Paper II) indicative of ion exchange reactions (Fig 23a). The cation exchange capacity (CEC) of the sediments hosting high salinity showed species of Ca, Na and Mg are the dominating ions with values of 0.51-11.0, 0.16-7.03 and 0.10-3.60 meq/100g, respectively. The rest of the ionic species have low to negligible contribution on the sediments, K (0.05-0.48 meq/100g), Al (0.00-1.52) and NH_4 (0.00-0.20). CEC thus covers a wide range from 0.87-21.0 meq/100g, with an average of 12.4 meq/100g or ~1 eq/l pore-water if we assume a sediment porosity of 0.25 and bulk density of 1.86 g/cm^3 (details in Paper II). The ratio of Na : Cl in the pore-water suggests it's not a simple dissolution of halite as there is a poor correlation with chloride, with almost twice as much Na as expected (Fig. 23b) from halite dissolution.

Given the high amount of sulphate in the saline groundwater and high ion exchanger sediment, we suggest dedolomitization with ion exchange was the controlling process in producing the observed Na-Cl-SO_4 water. These reactions can be seen as a special type or extension of dedolomitization. The "simple" irreversible dedolomitization (Naus et al., 2001) reaction can be generalised as follows:

$$CaSO_{4\ (Gypsum)} + CaMg\ (CO_3)_{2\ (Dolomite)} \longrightarrow 2\ CaCO_{3\ (Calcite)} + Mg^{2+} + SO_4^{2-}$$

But in our case the presence of an exchanger filled with Na implies that instead of precipitating as calcite, the Ca exchanges with the Na:

$$Ca^{2+} + 2NaX \longrightarrow CaX_2 + 2Na^+$$
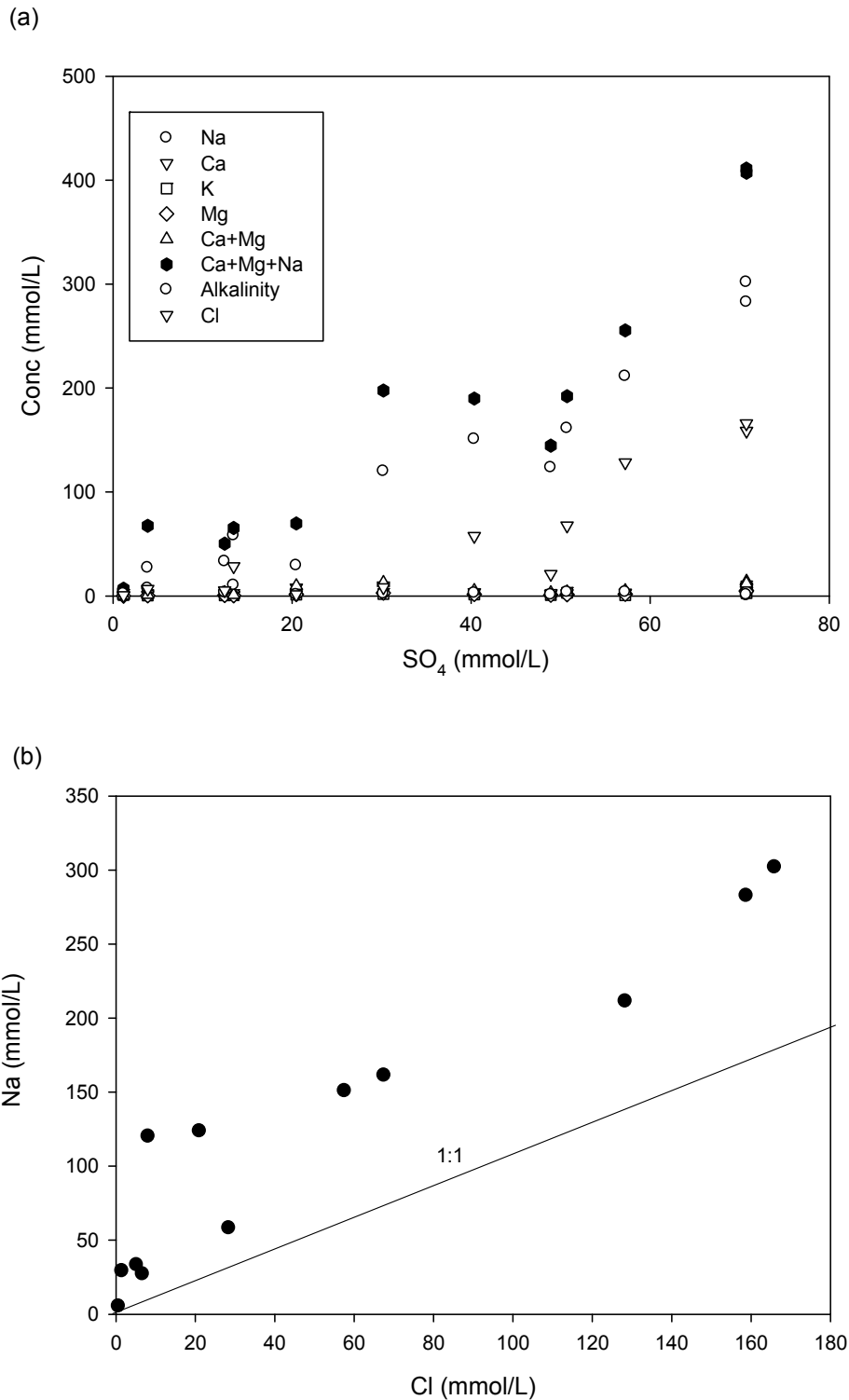
Fig. 23: (a): Plot of the major ions as a function of the sulphate concentration of pore-water samples. There is a strong linear relationship of pore-water sulphate with Ca+Mg+Na. Therefore pore-water chemistry can probably be explained by extended dedolomitization including ion exchange and carbonate equilibria (calcite and dolomite), (b) Pore-water 1:1 Na–Cl line shows a poor correlation hence halite dissolution is not probable. The current source of Na+ in the pore-water is therefore not halite.

Likewise, most of the Mg released is exchanged for Na+ on the exchanger hence Mg concentrations are low in the saline groundwater. Dedolomitization with ion exchange was modelled within the saline zone (Fig. 24a), which shows a relative good fit to the observed evolution in Ca and Mg with increasing sulphate dissolution, and concomitant ion exchange. The model misfit could be due to initially higher Ca and Mg ions contents on the exchanger as the extended dedolomitisation processes has probably been going on for a long time leading to increased Ca and Mg concentrations in the groundwater and on the exchanger. The effect is demonstrated by having an exchanger with a higher proportion of Ca on the exchanger, by defining Ca in the initial solution 1 to be in equilibrium with gypsum rather than calcite, (sulphate was also defined by equilibrium with gypsum) (output is shown in Fig. 24a). The modelled cation exchanger composition (with an initial high Na on the exchanger) was NaX, 522-647, CaX2, 243-301 and MgX2, 32.3-35.2 mmol/L, similar to measured cation distributions of NaX, 9.92-435, CaX2, 15.8-339 and MgX2, 3.10-111 mmol/L (Table 5; assuming a porosity of 30 % and bulk density, 1.86 g/cm^3). The wide range in measured distributions of exchangeable cations show that the groundwater samples are the result of different mixtures of saline and fresh pore-water and would be expected to give a range of Ca and Mg concentrations, but with similar geochemical pattern as simulated.

A misfit in the decrease of alkalinity with increasing sulphate (Fig. 24b) was also observed which would also be controlled by the initial composition on the exchanger; the model result for the Na and Ca dominated exchangers are shown in the Fig.. Higher PCO_2 conditions can also affect the alkalinity variations. Higher PCO_2 could be due to decomposition of organic matter and/or root respiration (vegetation) and redox processes such as bacterial sulphate reduction (Plummer et al., 1990). However, the pH variations were generally comparable to field results. The proposed extended dedolomitisation process appears to explain most of the features in the Na-Cl-SO_4 water type in the saline zone. Details of the inputs are discussed in Paper II.
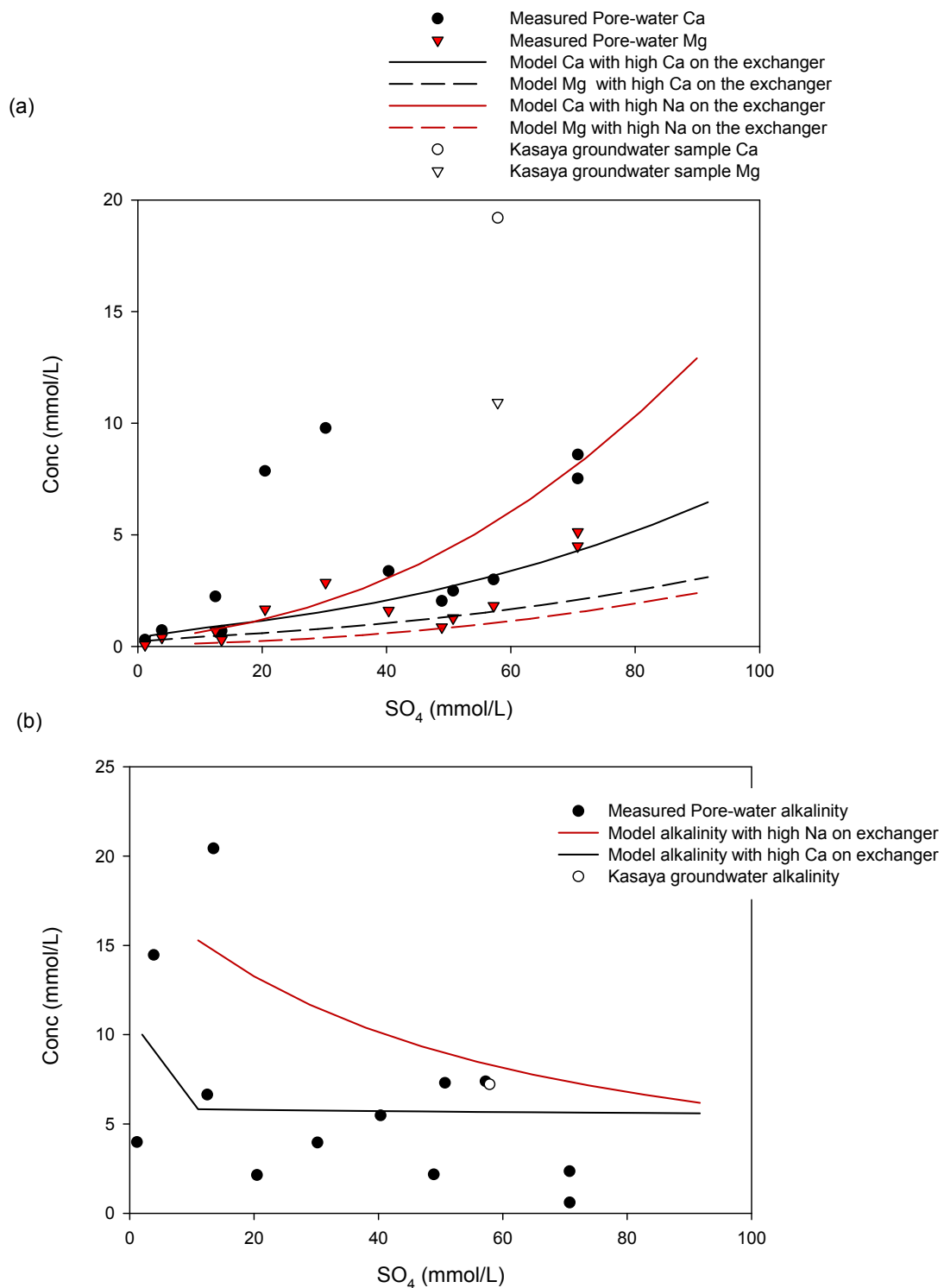
Fig. 24: (a) PHREEQC modelled Ca and Mg from the extended dedolomitization process including ion exchanges (Na and Ca dominated conditions) and observed Ca and Mg species in the saline groundwater. (b) PHREEQC modelled and observed alkalinity with Na and Ca exchanger as a function of sulphate concentration, showing that the modelled alkalinity is sensitivity to the initial composition on the exchanger.

5.3.1 Sediment dilution experiments

Sediment dilution experiments were conducted, to establish how much calcite and gypsum would be released from the sediment after correction with pore-water chemistry. Table 4, shows it is not possible to establish the exact amount of calcite or gypsum on the sediment by weight because the pore-water chemistry probably dissolved these salts hence negative numbers after the correction with pore-water chemistry (see Table 4). The sediments have a small amount of gypsum (< 0.03 % by weight) and calcite (< 0.2 % by weight) as seen in Table 2; however these numbers are just indicative. The dilution experiment (Fig. 25), with the addition of increasing pore-volumes, showed a rapid dissolution of gypsum and a slower dissolution of calcite; details are discussed in Paper II. It is evident, above 50 pore volumes would be flushed or diluted completely.
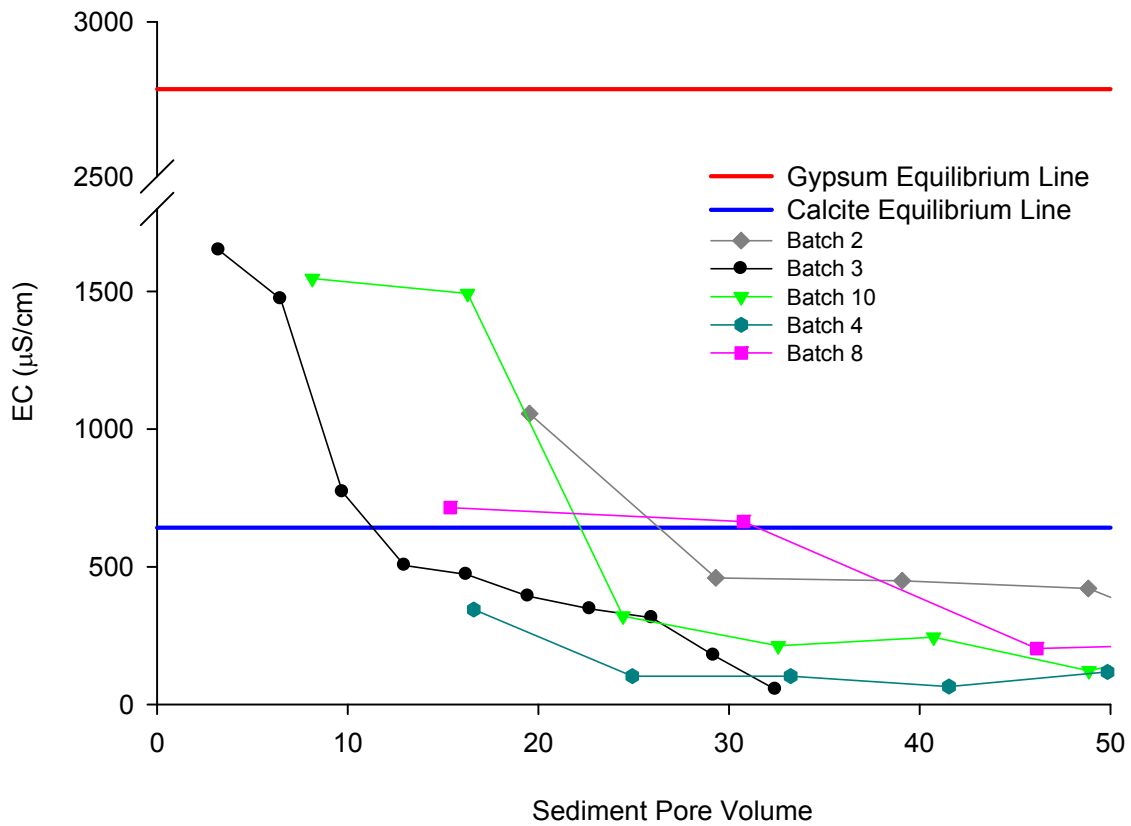
Fig. 25: Dilution experiment plot of five batches, indicating initial and rapid complete dissolution of gypsum followed by slow carbonate dissolution. Calculated EC at equilibrium for gypsum and calcite using PHREEQC are also shown. Results show that salinity within the saline groundwater would be flushed if there was through flow.

49

Table 4: Shows the sediment dilution experiment chemical analysis from the final pool volume with corrections for pore-water composition. Negative dissolved mineral amounts occur when solute contribution from the pore-water content appears higher than the sediment contribution. This is however an artefact occurring because gypsum is also dissolved during pore-water extraction by pasting, actually indicating that gypsum is present, but the amount is not known; based on samples where the pore-water was extracted by centrifugation, gypsum on the sediment is <0.03 %, whereas calcite is <0.20 %.

Batch	Final water pool concentration after dilution runs (mmol/L)		Volume of water used (L)	Mass released from sediment (mmol)		Sediment mass (g)	Pore-water concentration (mmol/L)		Amount released from the sediment (mmol)		assuming gypsum (g)	assuming Calcite (g)	Gypsum in sediment (%)	Calcite in sediment (%)
	SO$_4$	Alk/2		SO4	Alk		SO4	Alk	SO4	Alk	CaSO$_4$.2H$_2$O	CaCO$_3$		
1	0.547	0.486	0.348	0.190	0.079	37.9	0.268	0.012	-0.077	0.079	-0.013	0.008	-0.04%	0.02%
2	0.277	1.534	0.613	0.170	0.456	38.8	0.201	0.027	-0.032	0.456	-0.005	0.046	-0.01%	0.12%
3	1.204	0.244	0.303	0.365	0.036	41.1	0.334	0.003	0.031	0.036	0.005	0.004	0.01%	0.01%
4	0.237	1.101	0.681	0.162	0.370	41.4	0.098	0.010	0.064	0.370	0.011	0.037	0.03%	0.09%
5	0.049	2.508	0.313	0.015	0.349	39.1	0.024	0.088	-0.008	0.349	-0.001	0.035	0.00%	0.09%
6	0.008	0.112	0.329	0.003	0.009	29.9	0.005	0.018	-0.003	0.009	-0.001	0.001	0.00%	0.00%
7	0.263	2.525	0.702	0.185	0.728	49.7	0.209	0.317	-0.024	0.728	-0.004	0.073	-0.01%	0.15%
8	0.549	0.381	0.260	0.143	0.046	30.0	0.204	0.007	-0.061	0.046	-0.011	0.005	-0.04%	0.02%
9	0.522	2.053	0.773	0.403	0.771	44.1	0.339	0.045	0.064	0.771	0.011	0.077	0.02%	0.17%
10	0.546	3.012	0.395	0.216	0.574	44.4	0.293	0.042	-0.078	0.574	-0.013	0.057	-0.03%	0.13%
11	0.333	2.426	0.450	0.150	0.530	33.9	0.238	0.031	-0.089	0.530	-0.015	0.053	-0.05%	0.16%
12	0.175	2.232	0.274	0.048	0.280	48.7	0.097	0.052	-0.049	0.280	-0.008	0.028	-0.02%	0.06%

50

6 Conclusions

The objectives of this PhD study were to investigate sedimentological and hydro-geochemical processes shaping the groundwater environment to the present hydrogeology, in particular, to explain the origin and dynamics of groundwater salinity. We observe the following:

- The Machile Basin in western Zambia hosts lake sediments as relicts of the palaeo-lake Makgadikgadi typically as intercalations of silica bearing minerals in the clay-silt, clay-fine and sand fraction with incorporated evaporates of bassanite (dehydrated gypsum) and carbonates (calcite and dolomite).

- High salinity is widespread both vertically and horizontally as demonstrated by geophysical bore logging and other ground and air based studies within the palaeo-system.

- Observed evaporites are probably a result of continental evapo-concentration processes during long periods of the lake standing after tectonic disruptions and increasing aridity.

- The age of the system is still unknown although our OSL measurements indicate > 300 ka. Quartz grains are atleast nearly or fully saturated with radioactive which cannot be accurately measured with OSL.

- Sedimentological processes have resulted into a converging ground water flow system terminating at the fringes of the palaeo-lake system and lost through evapo-transpiration due to a hydraulic conductivity contrast instigated by the lake sediments; there is little or no interaction between the regional fresh groundwater flow and saline pool of the palaeo-lake system. Sediment dilution experiment confirms that if through flow was an active process, the sediments of the saline environment would have been completely flushed removing the high salinity after about 50 pore volumes.

- The hydrochemistry of the fresh groundwater is a result of water-rock interactions in which alumino-silicates such as plagioclase, K-feldspars and amphiboles/pyroxenes are dissolving and secondary phases such as gibbsite and chalcedony are precipitating. The water type is typically of Ca-Na-HCO_3.

- It is suggested that saline groundwater is stagnant and has a chemical composition which can be explained by an 'extended' dedolomitisation process; dedolomitisation driven by gypsum dissolution with ion exchange resulting in a Na-(Cl)-SO$_4$ water type.

- Radio-isotopic tracers (^{14}C) within the groundwater environment of Machile and regional studies, shows groundwater ages of less than 50 ka against an old sediment matrix (assumed to be almost 1.4 Ma), we suggest the observed salinity is of a palaeo-salinity induced during pluvial climatic events and was not deposited together with the sediment.

- This study supports a tectonic evolution of the palaeo-lake system in which sediment of the lake system, was formed in the early Pleistocence (speculated about 1.4 Ma), then completely desiccated by 500 ka based on archeological artefacts and followed by partial flushing during the various phases of pluvial climatic events hence the younger ages (< 50 ka) of the groundwater. Tectonics was the main control of sedimentological process and climatic events secondary.

- The findings shows there is a poor potential for fresh groundwater aquifers within the saline PLM and interventions must be focused at deeper strata or other sustainable technologies such as groundwater desalinisation or rain-harvesting.

7 References

Alley, W.M., 1993. Geostatistical Models. In: Alley, W.M. (ed.) Regional ground-water quality. John Wiley & Sons. pp. 87 - 108.

Appelo, C.A. & Postma, D., 2005. Geochemistry, groundwater and pollution. A.A. Balkema Publishers. 672 pp.

Ayenew, T., 2003. Environmental isotope-based integrated hydrogeological study of some Ethiopian rift lakes. Journal of Radioanalytical and Nuclear Chemistry, 257, 11-16.

Barica, J., 1972. Salinization of groundwater in arid zones. Water Research, 6, 925-933.

Bates, B., Kundzewicz, Z.W., Wu, S. & Palutikof, J., 2008. Climate change and water. Intergovernmental Panel on Climate Change (IPCC).

Bauer, P., Held, R.J., Zimmermann, S., Linn, F. & Kinzelbach, W., 2006a. Coupled flow and salinity transport modelling in semi-arid environments: The Shashe River Valley, Botswana. Journal of Hydrology, 316, 163-183.

Bauer, P., Supper, R., Zimmermann, S. & Kinzelbach, W., 2006b. Geoelectrical imaging of groundwater salinization in the Okavango Delta, Botswana. Journal of Applied Geophysics, 60, 126-141.

Beekman, H., Gieske, A. & Selaolo, E., 1996. GRES: Groundwater recharge studies in Botswana 1987-1996. Botswana J. Earth Sci, 3, 1-17.

Beekman, H., Selaolo, E., Van Elswijk, R., Lenderink, N. & Obakeng, O. 1997. Groundwater recharge and resources assessment in the Botswana Kalahari–chloride and isotope profiling studies in the Letlhakeng-Botlhapatlou area and the Central Kalahari: GRES 11 Technical Report. Gaborone.

Beekman, H., Selaolo, E.T. & De Vries, J., 1999. Groundwater Recharge and Resources Assessment in the Botswana Kalahari: Executive Summary GRES II. Geological Survey Department.

Beilfuss, R., 2012. A risky climate for southern African hydro: assessing hydrological risks and consequences for Zambezi River Basin dams. International Rivers.

Bowler, J.M., 1986. Spatial variability and hydrologic evolution of australian lake basins - analogue for pleistocene hydrologic change and evaporite formation. Palaeogeography Palaeoclimatology Palaeoecology, 54, 21-41.

Brunner, P., Bauer, P., Eugster, M. & Kinzelbach, W., 2004. Using remote sensing to regionalize local precipitation recharge rates obtained from the Chloride Method. Journal of Hydrology, 294, 241-250.

Burrough, S.L., Thomas, D.S., Shaw, P.A. & Bailey, R.M., 2007. Multiphase quaternary highstands at lake Ngami, Kalahari, northern Botswana. Palaeogeography, Palaeoclimatology, Palaeoecology, 253, 280-299.

Burrough, S.L. & Thomas, D.S.G., 2008. Late quaternary lake-level fluctuations in the Mababe Depression: Middle Kalahari palaeolakes and the role of Zambezi inflows. Quaternary Research, 69, 388-403.

Burrough, S.L. & Thomas, D.S.G., 2009. Geomorphological contributions to palaeolimnology on the African continent. Geomorphology, 103**,** 285-298.

Burrough, S.L., Thomas, D.S.G. & Bailey, R.M., 2009a. Mega-lake in the Kalahari: A late pleistocene record of the Palaeolake Makgadikgadi system. Quaternary Science Reviews, 28**,** 1392-1411.

Burrough, S.L., Thomas, D.S.G. & Singarayer, J.S., 2009b. Late Quaternary hydrological dynamics in the Middle Kalahari: Forcing and feedbacks. Earth-Science Reviews, 96**,** 313-326.

Campbell, G., Johnson, S., Bakaya, T., Kumar, H. & Nsatsi, J., 2006. Airborne geophysical mapping of aquifer water quality and structural controls in the Lower Okavango Delta, Botswana. South African Journal of Geology, 109**,** 475-494.

Chiang, W.-H. & Chiang, W., 2001. 3D-groundwater modeling with PMWIN. Springer.

Clark, I.D. & Fritz, P., 1997. Environmental isotopes in hydrogeology. CRC press.

Cooke, H., 1979. The origin of the Makgadikgadi Pans. Ministry of Mineral Resources and Water Affairs, Botswana notes and records No. 11, pp. 37-42.

Cooke, H., 1980. Landform evolution in the context of climatic change and neo-tectonism in the Middle Kalahari of north-central Botswana. Transactions of the Institute of British Geographers**,** 80-99.

Cooke, H. & Verstappen, H.T., 1984. The landforms of the western Makgadikgadi basin in northern Botswana, with a consideration of the chronology of the evolution of Lake Palaeo-Makgadikgadi. Zeitschrift fur Geomorphologie, 1**,** 1-19.

Cordier, S., Harmand, D., Lauer, T., Voinchet, P., Bahain, J.-J. & Frechen, M., 2012. Geochronological reconstruction of the Pleistocene evolution of the Sarre valley (France and Germany) using OSL and ESR dating techniques. Geomorphology, 165**,** 91-106.

Day, J., 1993. The major ion chemistry of some southern African saline systems. Hydrobiologia, 267**,** 37-59.

De Vries, J.J., Selaolo, E.T. & Beekman, H.E., 2000. Groundwater recharge in the Kalahari, with reference to paleo-hydrologic conditions. Journal of Hydrology, 238**,** 110-123.

DFID - Department for International Development, 2002. An assessment of trends in the Zambian Agriculture Sector, December, 2002. www.theIDLgroup.com.

Drake, N. & Bristow, C., 2006. Shorelines in the Sahara: geomorphological evidence for an enhanced monsoon from palaeolake Megachad. The Holocene, 16**,** 901-911.

Du Toit, A., 1927. The Kalahari and some of its problems. South African Journal of Science, 24**,** 88-101.

Ebert, J.I. & Hitchcock, R.K., 1978. Ancient Lake Makgadikgadi, Botswana: mapping, measurement and palaeoclimatic significance. Palaeoecology of Africa, 10**,** 47-56.

Eckardt, F.D., Bryant, R.G., McCulloch, G., Spiro, B. & Wood, W.W., 2008. The hydrochemistry of a semi-arid pan basin case study: Sua Pan, Makgadikgadi, Botswana. Applied Geochemistry, 23, 1563-1580.

Edmunds, W., Fellman, E. & Goni, I., 1999. Lakes, groundwater and palaeohydrology in the Sahel of NE Nigeria: evidence from hydrogeochemistry. Journal of the Geological Society, 156, 345-355.

Edmunds, W.M. & Bath, A.H., 1976. Centrifuge extraction and chemical analysis of interstitial waters. Environmental Science & Technology, 10, 467-472.

Eichinger, L., 1983. A Contribution to the Interpretation of C-14 Groundwater Ages Considering the Example of a Partially Confined Sandstone Aquifer. Radiocarbon, 25, 347-356.

Einbond, A., Sudol, M. & Coplen, T., 1996. New guidelines for reporting stable hydrogen, carbon, and oxygen isotope-ratio data. Geochimica Et Cosmochimica Acta, 60, 3359-3360.

Essington, M.E., 2004. Soil and water chemistry: An integrative approach. CRC press.

Eugster, H.P. & Hardie, L.A., 1978. Saline Lakes. In: Lerman, A. (ed.) Lakes. Springer, New York. pp. 237-293.

Eugster, H.P. & Jones, B.F., 1979. Behavior of major solutes during closed-basin brine evolution. American journal of science, 279, 609-631.

Fauchereau, N., Trzaska, S., Rouault, M. & Richard, Y., 2003. Rainfall variability and changes in southern Africa during the 20th century in the global warming context. Natural Hazards, 29, 139-154.

Flower, R.J. & Ryves, D.B., 2009. Diatom preservation: differential preservation of sedimentary diatoms in two saline lakes. Acta Botanica Croatica, 68, 381-399.

Fontes, J.C. & Garnier, J.M., 1979. Determination of the initial 14C activity of the total dissolved carbon: A review of the existing models and a new approach. Water Resources Research, 15, 399-413.

Fritz, S.C., Cumming, B., Gasse, F. & Laird, K.R., 1999. Diatoms as indicators of hydrologic and climatic change in saline lakes. In: Stoermer, E.F. & John, S.P. (eds.) The diatoms: applications for the environmental and earth sciences. Cambridge University Press, Cambridge. pp. 41-72.

Genner, M.J., Seehausen, O., Lunt, D.H., Joyce, D.A., Shaw, P.W., Carvalho, G.R. & Turner, G.F., 2007. Age of cichlids: new dates for ancient lake fish radiations. Molecular Biology and Evolution, 24, 1269-1282.

Ghienne, J.-F.o., Schuster, M., Bernard, A., Duringer, P. & Brunet, M., 2002. The Holocene giant Lake Chad revealed by digital elevation models. Quaternary International, 87, 81-85.

Gonfiantini, E., 1986. Environmental isotopes in lake studies. In: P.Fritz & J.-Ch.Fontes (eds.) Handbook of environmental isotope geochemistry. 2. Elsevier, Amsterdam, The Netherlands. pp. 113-168.

Gran, G., 1952. Determination of the equivalence point in potentiometric titrations (Part II). Analyst, 77, 661-671.

Greenwood, E., Milligan, A., Biddiscombe, E., Rogers, A., Beresford, J., Watson, G. & Wright, K., 1992. Hydrologic and salinity changes associated with tree plantations in a saline agricultural catchment in southwestern Australia. Agricultural Water Management, 22, 307-323.

Grey, D. & Cooke, H., 1977. Some problems in the Quaternary evolution of the landforms of northern Botswana. Catena, 4, 123-133.

Grove, A.T., 1969. Landforms and climatic change in the Kalahari and Ngamiland. Geographical Journal, 191-212.

Guérin, G., Murray, A.S., Jain, M., Thomsen, K.J. & Mercier, N., 2013. How confident are we in the chronology of the transition between Howieson's Poort and Still Bay. Journal of human evolution, 64, 314-317.

Gunn, R. & Richardson, D., 1979. The nature and possible origins of soluble salts in deeply weathered landscapes of eastern Australia. Soil Research, 17, 197-215.

Haddon, I.G. & McCarthy, T.S., 2005. The Mesozoic-Cenozoic interior sag basins of Central Africa: The Late-Cretaceous-Cenozoic Kalahari and Okavango basins. Journal of African Earth Sciences, 43, 316-333.

Harbaugh, A.W., Banta, E.R., Hill, M.C. & McDonald, M.G., 2000. MODFLOW-2000, the US Geological Survey modular ground-water model: User guide to modularization concepts and the ground-water flow process. US Geological Survey Reston, VA, USA.

Hardie, L.A., 1968. The origin of the Recent non-marine evaporite deposit of Saline Valley, Inyo County, California. Geochimica Et Cosmochimica Acta, 32, 1279-1301.

Hardie, L.A. & Eugster, H.P., 1970. The evolution of closed-basin brines. Mineral. Soc. Amer. Spec. Pap, 3, 273-290.

Hart, W.S., Quade, J., Madsen, D.B., Kaufman, D.S. & Oviatt, C.G., 2004. The 87Sr/86Sr ratios of lacustrine carbonates and lake-level history of the Bonneville paleolake system. Geological Society of America Bulletin, 116, 1107-1119.

Hecky, R.E. & Kilham, P., 1973. Diatoms in alkaline, saline lakes - ecology and geochemical implications. Limnology and oceanography, 18, 53-71.

Heine, K., 1982. The main stages of the late Quaternary evolution of the Kalahari region, southern Africa. Palaeoecology of Africa and the surrounding islands, 15, 53-76.

Herczeg, A., Dogramaci, S. & Leaney, F., 2001. Origin of dissolved salts in a large, semi-arid groundwater system: Murray Basin, Australia. Marine and Freshwater Research, 52, 41-52.

Hipondoka, M.H., 2005. The development and evolution of Etosha Pan, Namibia. Doctor rerum naturalium thesis, University of Würzburg, Germany, 152pp.

Hutchins, D.G. & Reeves, C.V., 1980. Regional geophysical exploration of the Kalahari in Botswana. Tectonophysics, 69, 201-220.

IAEA, W. & WMO, W., 2006. Global Network of Isotopes in Precipitation. The GNIP database.

Ingerson, E. & Pearson, F., 1964. Estimation of age and rate of motion of groundwater by the 14C-method. Recent Researches in the Fields of Atmosphere, Hydrosphere and Nuclear Geochemistry, 263-283.

Jankowski, J. & Jacobson, G., 1989. Hydrochemical evolution of regional groundwaters to playa brines in central Australia. Journal of Hydrology, 108, 123-173.

Jasonsmith, J.F., Macdonald, B.C.T., McPhail, D.C., Beavis, S., Norman, M., Roach, I.C., Harris, B., Isaacson, L., White, I. & Biswas, F., 2011. Salinisation processes in a sub-catchment of Wybong Creek, Hunter Valley, Australia. Australian Journal of Earth Sciences, 58, 177-193.

Jennings, C.M.H. 1974. The hydrogeology of Botswana. PhD Thesis, University of Natal, Pietermaritzburg, 850 pp.

Jones, B.F., Eugster, H.P. & Rettig, S.L., 1977. Hydrochemistry of the Lake Magadi basin, Kenya. Geochimica et Cosmochimica Acta, 41, 53-72.

Jones, B.F., Naftz, D.L., Spencer, R.J. & Oviatt, C.G., 2009. Geochemical Evolution of Great Salt Lake, Utah, USA. Aquatic Geochemistry, 15, 95-121.

Joyce, D.A., Lunt, D.H., Bills, R., Turner, G.F., Katongo, C., Duftner, N., Sturmbauer, C. & Seehausen, O., 2005. An extant cichlid fish radiation emerged in an extinct Pleistocene lake. Nature, 435, 90-95.

Kafri, U. & Yechieli, Y., 2010. Salinity, Salination and Freshening of the Different Base-Levels and Their Adjoining Groundwater Systems. Groundwater Base Level Changes and Adjoining Hydrological Systems. Springer Berlin Heidelberg. pp. 43-54.

Kalinowski, M.B., 2004. International Control of Tritium for Nuclear Nonproliferation and Disarmament. CRC Press.

Kebede, S., Travi, Y., Asrat, A., Alemayehu, T., Ayenew, T. & Tessema, Z., 2008. Groundwater origin and flow along selected transects in Ethiopian rift volcanic aquifers. Hydrogeology Journal, 16, 55-73.

Kowalewska, A. & Cohen, A.S., 1998. Reconstruction of paleoenvironments of the Great Salt Lake Basin during the late Cenozoic. Journal of Paleolimnology, 20, 381-407.

Lancaster, N., 1989. Late Quaternary paleoenvironments in the southwestern Kalahari. Palaeogeography, Palaeoclimatology, Palaeoecology, 70, 367-376.

Leblanc, M., Favreau, G., Maley, J., Nazoumou, Y., Leduc, C., Stagnitti, F., Van Oevelen, P.J., Delclaux, F. & Lemoalle, J., 2006. Reconstruction of Megalake Chad using shuttle radar topographic mission data. Palaeogeography, Palaeoclimatology, Palaeoecology, 239, 16-27.

Leblanc, M., Favreau, G., Tweed, S., Leduc, C., Razack, M. & Mofor, L., 2007. Remote sensing for groundwater modelling in large semiarid areas: Lake Chad Basin, Africa. Hydrogeology Journal, 15, 97-100.

Linn, F., Masie, M. & Rana, A., 2003. The impacts on groundwater development on shallow aquifers in the lower Okavango Delta, northwestern Botswana. Environmental Geology, 44**,** 112-118.

Mallinson, D., 2008. A Brief Description of Optically Stimulated Luminescence Dating, http://core.ecu.edu/geology/mallinsond/OSL.

Marshall, T.R. & Harmse, J.T., 1992. A review of the origin and propagation of pans. S. Afr. Geographer, 19**,** 9-21.

Mazor, E., Bielsky, M., Verhagen, B.T., Sellschop, J.P.F., Hutton, L. & Jones, M.T., 1980. Chemical composition of groundwaters in the vast Kalahari flatland. Journal of Hydrology, 48**,** 147-165.

Mazor, E., Verhagen, B.T., Sellschop, J.P.F., Jones, M.T., Robins, N.E., Hutton, L. & Jennings, C.M.H., 1977. Northern Kalahari groundwaters - hydrologic, isotopic and chemical studies at Orapa, Botswana. Journal of Hydrology, 34**,** 203-234.

McCarthy, T. & Ellery, W., 1998. The Okavango Delta. Transactions of the Royal Society of South Africa, 53**,** 157-182.

McCarthy, T.S. & Ellery, W.N., 1994. The effect of vegetation on soil and ground-water chemistry and hydrology of islands in the seasonal swamps of the Okavango-fan, Botswana. Journal of Hydrology, 154**,** 169-193.

McCarthy, T.S., McIver, J.R. & Verhagen, B.T., 1991. Groundwater evolution, chemical sedimentation and carbonate brine formation on an island in the Okavango Delta swamp, Botswana. Applied Geochemistry, 6**,** 577-595.

McFarlane, M. & Eckardt, F., 2006. Lake Deception: a new Makgadikgadi palaeolake. Botswana notes and records**,** 195-201.

MEA - Millennium Ecosystem Assessment, 2005. Ecosystems and Human Well-being: Synthesis. Island Press, Washington, DC.

Milzow, C., Kgotlhang, L., Bauer-Gottwein, P., Meier, P. & Kinzelbach, W., 2009. Regional review: the hydrology of the Okavango Delta, Botswana—processes, data and modelling. Hydrogeology Journal, 17**,** 1297-1328.

Modisi, M., Atekwana, E., Kampunzu, A. & Ngwisanyi, T., 2000. Rift kinematics during the incipient stages of continental extension: Evidence from the nascent Okavango rift basin, northwest Botswana. Geology, 28**,** 939-942.

Money, N.J., 1972. An outline of the Geology of western Zambia. Records of the Geological Survey, Republic of Zambia No. 12, pp. 103-123.

Mook, W., 1972. On the reconstruction of the initial 14 C content of groundwater from the chemical and isotopic composition. Proceedings of the 8th International Conference on Radiocarbon Dating. pp. 342–352.

Moore, A.E., Cotterill, F.P.D. & Eckardt, F.D., 2012. The evolution and ages of Makgadikgadi palaeo-lakes: consilient evidence from Kalahari drainage evolution. South African Journal of Geology.

Moore, A.E. & Larkin, P.A., 2001. Drainage evolution in south-central Africa since the breakup of Gondwana. South African Journal of Geology, 104**,** 47-68.

Murray, A., Marten, R., Johnston, A. & Martin, P., 1987. Analysis for naturally occuring radionuclides at environmental concentrations by gamma spectrometry. Journal of Radioanalytical and Nuclear Chemistry, 115**,** 263-288.

Murray, A.S. & Wintle, A.G., 2000. Luminescence dating of quartz using an improved single-aliquot regenerative-dose protocol. Radiation Measurements, 32**,** 57-73.

NASWC (Non-Affiliated Soil Analysis Work Committee), 1990. Handbook of standard soil testing methods for advisory purposes. Soil Science Society of South Africa, Pretoria.

Naus, C.A., Driscoll, D.G. & Carter, J.M., 2001. Geochemistry of the Madison and Minnelusa aquifers in the Black Hills area, South Dakota. Citeseer.

Nordstrom, D.K., Ball, J.W., Donahoe, R.J. & Whittemore, D., 1989. Groundwater chemistry and water-rock interactions at Stripa. Geochimica Et Cosmochimica Acta, 53**,** 1727-1740.

Nyambe, I.A. & Utting, J., 1997. Stratigraphy and palynostratigraphy, Karoo Supergroup (Permian and Triassic), mid-Zambezi Valley, southern Zambia. Journal of African Earth Sciences, 24**,** 563-583.

O'Connor, P.W. & Thomas, D.S.G., 1999. The timing and environmental significance of late quaternary linear dune development in western Zambia. Quaternary Research, 52**,** 44-55.

Obakeng, O.T. 2007. Soil moisture dynamics and evapotranspiration at the fringe of the Botswana Kalahari, with emphasis on deep rooting vegetation. M.Sc, ITC International Institute for Geo-Information science and earth observation, 225 pp.

Oviatt, C.G., Miller, D.M., McGeehin, J.P., Zachary, C. & Mahan, S., 2005. The younger Dryas phase of great salt Lake, Utah, USA. Palaeogeography, Palaeoclimatology, Palaeoecology, 219**,** 263-284.

Palacky, G., 1988. Resistivity characteristics of geologic targets. Electromagnetic methods in applied geophysics, 1**,** 53-129.

Parkhurst, D.L. & Appelo, C., 1999. Description of input and examples for Phreeqc (vers. 2) - a computer program for speciation, batch-reaction,one-dimensional transport, and inverse geochemical calculations. United States Geological Survey - water resources investigation report. pp 99 - 4259.

Passarge, S., 1904. Die Kalahari. Dietrich Reimer (Ernst Vohsen), Berlin.

Piper, A.M., 1944. A graphic procedure in the geochemical interpretation of water-analyses. Transactions, American Geophysical Union, 25**,** 914-928.

Plummer, L., Prestemon, E. & Parkhurst, D., 1994. An interactive code (NETPATH) for modeling net geochemical reactions along a flow path Version 2.0. USGS, Washingston, DC, Water-Resources Investigations Report 94-4169.

Plummer, L.N., Busby, J.F., Lee, R.W. & Hanshaw, B.B., 1990. Geochemical modeling of the Madison aquifer in parts of Montana, Wyoming, and South Dakota. Water Resources Research, 26, 1981-2014.

Prescott, J. & Hutton, J.T., 1994. Cosmic ray contributions to dose rates for luminescence and ESR dating: large depths and long-term time variations. Radiation Measurements, 23, 497-500.

Ramberg, L. & Wolski, P., 2008. Growing islands and sinking solutes: processes maintaining the endorheic Okavango Delta as a freshwater system. Plant Ecology, 196, 215-231.

Reheis, M.C. & Dixon, T.H., 1996. Kinematics of the eastern California shear zone: Evidence for slip transfer from Owens and Saline Valley fault zones to Fish Lake Valley fault zone. Geology, 24, 339-342.

Renberg, I., 1990. A procedure for preparing large sets of diatom slides from sediment cores. Journal of Paleolimnology, 4, 87-90.

Riedel, F., Henderson, A.C., Heußner, K.-U., Kaufmann, G., Kossler, A., Leipe, C., Shemang, E. & Taft, L., 2014. Dynamics of a Kalahari long-lived mega-lake system: hydromorphological and limnological changes in the Makgadikgadi Basin (Botswana) during the terminal 50 ka. Hydrobiologia, 1-29.

Ringrose, S., Huntsman-Mapila, P., Kampunzu, A.B., Downey, W., Coetzee, S., Vink, B., Matheson, W. & Vanderpost, C., 2005. Sedimentological and geochemical evidence for palaeo-environmental change in the Makgadikgadi subbasin, in relation to the MOZ rift depression, Botswana. Palaeogeography Palaeoclimatology Palaeoecology, 217, 265-287.

Rogers, D.B. & Dreiss, S.J., 1995a. Saline groundwater in Mono basin, California .2. Long-term control of lake salinity by groundwater. Water Resources Research, 31, 3151-3169.

Rogers, D.B. & Dreiss, S.J., 1995b. Saline groundwater in Mono Basin, California: 1. Distribution. Water Resources Research, 31, 3131-3150.

Rosen, M.R., 1991. Sedimentologic and geochemical constraints on the hydrologic evolution of Bristol Dry lake, California, USA. Palaeogeography Palaeoclimatology Palaeoecology, 84, 229-257.

Rosen, M.R., 1994. The importance of groundwater in playas: a review of playa classifications and the sedimentology and hydrology of playas. Geological Society of America Special Papers, 289, 1-18.

Ryves, D.B., Battarbee, R.W., Juggins, S., Fritz, S.C. & Anderson, N.J., 2006. Physical and chemical predictors of diatom dissolution in freshwater and saline lake sediments in North America and West Greenland. Limonology & Oceanography, 51, 1355-1368.

Salama, R.B., Otto, C.J. & Fitzpatrick, R.W., 1999. Contributions of groundwater conditions to soil and water salinization. Hydrogeology Journal, 7, 46-64.

Sanford, W.E. & Wood, W.W., 1991. Brine evolution and mineral deposition in hydrologically open evaporite basins. Am. J. Sci, 291, 687-710.

Sattel, D. & Kgotlhang, L., 2004. Groundwater exploration with AEM in the Boteti area, Botswana. Exploration Geophysics, 35, 147-156.

Seaman, M.T., Ashton, P.J. & Williams, W.D., 1991. Inland salt waters of southern Africa. Hydrobiologia, 210, 75-91.

Selaolo, E.D. 1998. Tracer studies and groundwater recharge assessment in the Eastern Fringe of the Botswana Kalahari. The Lethlakeng – Botlhapatlou Area. . Ph.D. thesis, Vrije Universiteit te Amsterdam, 228 pp.

Selaolo, E.T., Beekman, H.E., Gieske, A.S.M. & De Vries, J.J., 2003. Multiple tracer profiling in Bostwana - GRES findings. In: Xu, Y.P. & Beekman, H.E. (eds.) Groundwater recharge estimation in Southern Africa. UNESCO IHP Series No. 64, UNESCO Paris. pp. 33-49.

Shaw, P. & Thomas, D., 1992. Geomorphology, sedimentation, and tectonics in the Kalahari Rift. Israel journal of earth-sciences, 41, 87-94.

Shaw, P.A. & Thomas, D.S.G., 1996. The quaternary palaeoenvironmental history of the Kalahari, Southern Africa. Journal of Arid Environments, 32, 9-22.

Shiklomanov, I.A., 1998. World water resources. A new appraisal and assessment for the 21st century.

Sinha, R. & Raymahashay, B.C., 2004. Evaporite mineralogy and geochemical evolution of the Sambhar Salt Lake, Rajasthan, India. Sedimentary Geology, 166, 59-71.

Smol, J.P. & Stoermer, E.F. (eds.), 2010. The diatoms: applications for the environmental and earth sciences. Cambridge University Press, Cambridge. 466 pp

Spencer, R.J., Eugster, H.P. & Jones, B.F., 1985a. Geochemistry of great Salt Lake, Utah II: Pleistocene-Holocene evolution. Geochimica et Cosmochimica Acta, 49, 739-747.

Spencer, R.J., Eugster, H.P., Jones, B.F. & Rettig, S.L., 1985b. Geochemistry of Great Salt Lake, Utah I: Hydrochemistry since 1850. Geochimica Et Cosmochimica Acta, 49, 727-737.

Stadler, S. 2005. Investigation of natural processes leading to nitrate enrichment in aquifers of semi-arid regions. PhD thesis, Karlsruhe University, Germany, 262 pp.

Stadler, S., Osenbruck, K., Suckow, A.O., Himmelsbach, T. & Hotzl, H., 2010. Groundwater flow regime, recharge and regional-scale solute transport in the semi-arid Kalahari of Botswana derived from isotope hydrology and hydrochemistry. Journal of Hydrology, 388, 291-303.

Stephens, D.W., 1990. Changes in lake levels, salinity and the biological community of Great Salt Lake (Utah, USA), 1847–1987. Saline Lakes. Springer. pp. 139-146.

Stiff Jr, H.A., 1951. The interpretation of chemical water analysis by means of patterns. Journal of Petroleum Technology, 3, 15-3.

Stine, S., 1990. Past climate at mono lake. Nature, 345, 391.

Stokes, S., Thomas, D.S.G. & Shaw, P.A., 1997. New chronological evidence for the nature and timing of linear dune development in the southwest Kalahari Desert. Geomorphology, 20, 81-93.

Sültenfuß, J., Roether, W. & Rhein, M., 2009. The Bremen mass spectrometric facility for the measurement of helium isotopes, neon, and tritium in water†. Isotopes in environmental and health studies, 45, 83-95.

Tamers, M., 1975. Validity of radiocarbon dates on ground water. Geophysical surveys, 2, 217-239.

Thomas, D. & Shaw, P., 1990. The deposition and development of the Kalahari Group sediments, central southern Africa. Journal of African Earth Sciences (and the Middle East), 10, 187-197.

Thomas, D. & Shaw, P., 1991a. The deposition and development of the Kalahari Group sediments, central southern Africa. Journal of African Earth Sciences (and the Middle East), 10, 187-197.

Thomas, D.S. & Shaw, P.A., 1991b. The Kalahari Environment. Cambridge University Press.

Thomas, D.S.G., Brook, G., Shaw, P., Bateman, M., Appleton, C., Nash, D., McLaren, S. & Davies, F., 2003. Late Pleistocene wetting and drying in the NW Kalahari: an integrated study from the Tsodilo Hills, Botswana. Quaternary International, 104, 53-67.

Thomas, D.S.G., O'Connor, P.W., Bateman, M.D., Shaw, P.A., Stokes, S. & Nash, D.J., 2000. Dune activity as a record of late Quaternary aridity in the Northern Kalahari: new evidence from northern Namibia interpreted in the context of regional arid and humid chronologies. Palaeogeography Palaeoclimatology Palaeoecology, 156, 243-259.

Thomas, D.S.G. & Shaw, P.A., 2002. Late Quaternary environmental change in central southern Africa: new data, synthesis, issues and prospects. Quaternary Science Reviews, 21, 783-797.

Vengosh, A., 2005. Salinisation and saline environments. In: Sherwood Lollar, B., Holland, H.D. & Turekian, K.K. (eds.) Treatise on geochemistry: Environmental Geochemistry. 9. Elsevier. pp. 168-333.

Verhagen, B.T., 1995. Semiarid zone groundwater mineralization processes as revealed by environmental isotope studies. In: Adar, E.M. & Leibundgut, C. (eds.) Application of Tracers in Arid Zone Hydrology. International Association Hydrological Sciences, Volume 232, Wallingford. pp. 245-266.

Vogel, J., 1970. Carbon-14 dating of groundwater. Isotope hydrology, 1970, 225-239.

Vogel, J.C. & Van Urk, H., 1975. Isotopic composition of groundwater in semi-arid regions of southern Africa. Journal of Hydrology, 25, 23-36.

Wanke, H., Dunkeloh, A. & Udluft, P., 2008. Groundwater recharge assessment for the Kalahari catchment of north-eastern Namibia and north-western Botswana with a regional-scale water balance model. Water Resources Management, 22, 1143-1158.

Weert, F.V., Gun, J.V.D. & Reckman, J., 2009. Global Overview of Saline Groundwater Occurrence and Genesis, GP 2009-1. International Groundwater Resources Assessment Centre, Utrecht, 105 pp.

Wellington, J.H. 1955. Southern Africa - A Geographic Study. Vol.1, Physical Geography. Cambridge University Press,Cambridge.

Welton, J.E., 1984. SEM petrology atlas. American Association of Petroleum Geologists.

White, K. & Eckardt, F., 2006. Geochemical mapping of carbonate sediments in the Makgadikgadi basin, Botswana using moderate resolution remote sensing data. Earth Surface Processes and Landforms, 31, 665-681.

Williams, W.D., 1999. Salinisation: A major threat to water resources in the arid and semi‐arid regions of the world. Lakes & Reservoirs: Research & Management, 4, 85-91.

Wintle, A.G. & Murray, A.S., 2006. A review of quartz optically stimulated luminescence characteristics and their relevance in single-aliquot regeneration dating protocols. Radiation Measurements, 41, 369-391.

Wolski, P. & Savenije, H., 2006. Dynamics of floodplain-island groundwater flow in the Okavango Delta, Botswana. Journal of Hydrology, 320, 283-301.

Wood, W.W. & Sanford, W.E., 1990. Ground-water control of evaporite deposition. Economic Geology, 85, 1226-1235.

Yager, R.M., Kappel, W.M. & Plummer, L.N., 2007. Origin of halite brine in the Onondaga Trough near Syracuse, New York state, USA: modeling geochemistry and variable-density flow. Hydrogeology Journal, 15, 1321-1339.

Yan, J.P., Hinderer, M. & Einsele, G., 2002. Geochemical evolution of closed-basin lakes: general model and application to Lakes Qinghai and Turkana. Sedimentary Geology, 148, 105-122.

YEC (Yachiyo Engineering Company), 1995. The Study on the National Water Resources Master Plan in the Republic of Zambia. Japan International Cooperation Agency & Ministry of Energy and Water Development, Republic of Zambia. Final Report – Hydrogeology, 128 pp.

Yechieli, Y. & Wood, W.W., 2002. Hydrogeologic processes in saline systems: playas, sabkhas, and saline lakes. Earth-Science Reviews, 58, 343-365.

Yemane, K., D, G. & Nyambe, I., 2002. Paleohydrological signatures and rift tectonics in the interior of Gondwana documented from Upper Permian lake deposits, the mid-Zambezi Rift basin, Zambia. In SEPM Special Publication No. 73 on Sedimentation in Continental Rifts, SEPM (Society for Sedimentary Geology), ISBN 1-56576-082-4, pp. 143-162.

Zapico, M.M., Vales, S. & Cherry, J.A., 1987. A wireline piston core barrel for sampling cohesionless sand and gravel below the water table. Ground Water Monitoring & Remediation, 7, 74-82.

8 Papers

I Banda, K.E, Jakobsen R., Bauer-Gottwein P., Murray A.S., Nyambe I.A., Bender-Koche C., Larsen F. Palaeo-Lake Makgadikgadi: New perspectives and insights on its evolution from western Zambia. Journal of African Earth Sciences, under revision

II Banda, K.E, Jakobsen R., Bauer-Gottwein P., Nyambe I.A., Laier T., Larsen F. Identification and evaluation of hydro-geochemical processes in the groundwater environment of Machile Basin, western Zambia. Journal of Applied Geochemistry, under review.

III Banda, K.E, Jakobsen R., Bauer-Gottwein P., Nyambe I.A., Larsen F. Hydrogeochemistry of the Palaeo-Lake Makgadikgadi: a review. Journal of Applied Geochemistry, submitted.

I

Palaeo-Lake Makgadikgadi: New perspectives and insights on its evolution from western Zambia

Kawawa E. Banda, Rasmus Jakobsen, Peter Bauer-Gottwein, Andrew Sean Murray, Imasiku A. Nyambe, Christian Bender Koch, Flemming Larsen

Palaeo-Lake Makgadikgadi: New perspectives and insights on its evolution from western Zambia.

Kawawa E. Banda[a,b*], Rasmus Jakobsen[c], Peter Bauer-Gottwein[a], Andrew Sean Murray[d], Imasiku A. Nyambe[b], Christian Bender Koch[e], Flemming Larsen[c]

[a] Department of Environment, *Technical University of Denmark*, DK-2800 Kgs Lyngby, Denmark.

[b] Department of Geology, *University of Zambia - Integrated Water Resources Management Centre*, C/O School of Mines, Lusaka, Zambia.

[c] Department of Geochemistry, *Geological Survey of Denmark and Greenland (GEUS)*, 10, Øster Voldgade, DK-1350 Copenhagen K, Denmark.

[d] Department of Earth Sciences, *The Nordic Laboratory for Luminescence Dating*, *University of Aarhus*, Risø Campus, DK-4000 Roskilde, Denmark.

[e] Department of Chemistry, *University of Copenhagen*, 5Universitetsparken, DK-2100Copenhagen Ø, Denmark.

Abstract

The Machile Basin is a semi-arid region in western Zambia, which hosts the northern marginal extension of the Palaeo-Lake Makgadikgadi (PLM), has not been studied sedimentilogically in details before. We drilled a 100 m deep borebole through the Quarternary sediments, into the underlying Batoka basalt, and cored the upper 50 m of the sediments. The sediments was investigated mineralogically, diatoms in the sediments were examined, and also dated using the optical stimulated luminescence (OSL) technique. The regonal extension of the PLM sediments in the Machile basin was examined by geophysical borehole logging in 20 boreholes. Results suggest a fluvio-lacustrine depocenter with a sediment load that deposited intercalated beddings of clayey-silts and sands, through a 100 m bgl thick profile of high salinity sediments on top of the underlying basalt. Palaeontological examination of diatoms and sponge spicule support a fluvio-lacustrine environment that sustained mesic climatic changes. We observe OSL minimum ages of 300 ka over the 50 m drilled sediments, which can be devided into three lithostratigraphic sequences. This is the first time OSL ages are taken over a much longer section than from earlier studies of OSL ages on PLM shorelines (generally < 10 m bgl). Two contrasting models exists to explain the evolution of PLM, (1) a climate variability approach that invokes Late Pleistocene to Holocene ages for fossil shorelines and linear dunes based on OSL ages mostly from northern Botswana, and (2) a tectonic drainage evolution model based on archaeological and fossil ages for the formation and final desiccation of PLM. We conclude that collectively, our datasets support the tectonic disruptions as the primary control of PLM evolution and that climatic variability, especially during high lake stands, was ancillary. OSL ages do not appear to provide accurate constraints on the time of formation for deeper sediments within PLM.

1 Introduction

One of the major tectonic events in southern Africa during the break-up of Gondwana was the formation of a passive continental margin along the Atlantic Ocean coastal region and a gently down warped interior basin (Ollier, 1985; Thomas & Shaw, 1991). Offshore sedimentary data along the southern African west coast (Dingle et al., 1983) suggests the Orange River drained the interior of southern Africa at the time or atleast shortly after the breakup

of the Gondwana in the Lower Cretaceous. Landscape evolution may have been rejuvenated by subsequent flexures along the Etosha-Griqualand-Transvaal (EGT) axis (mid-upper Cretaceous) and the Late Neogene Okavango-Kalahari-Zimbabwe (OKZ) axes (Moore, 1999; Moore et al., 2009), see insert in Fig. 1.
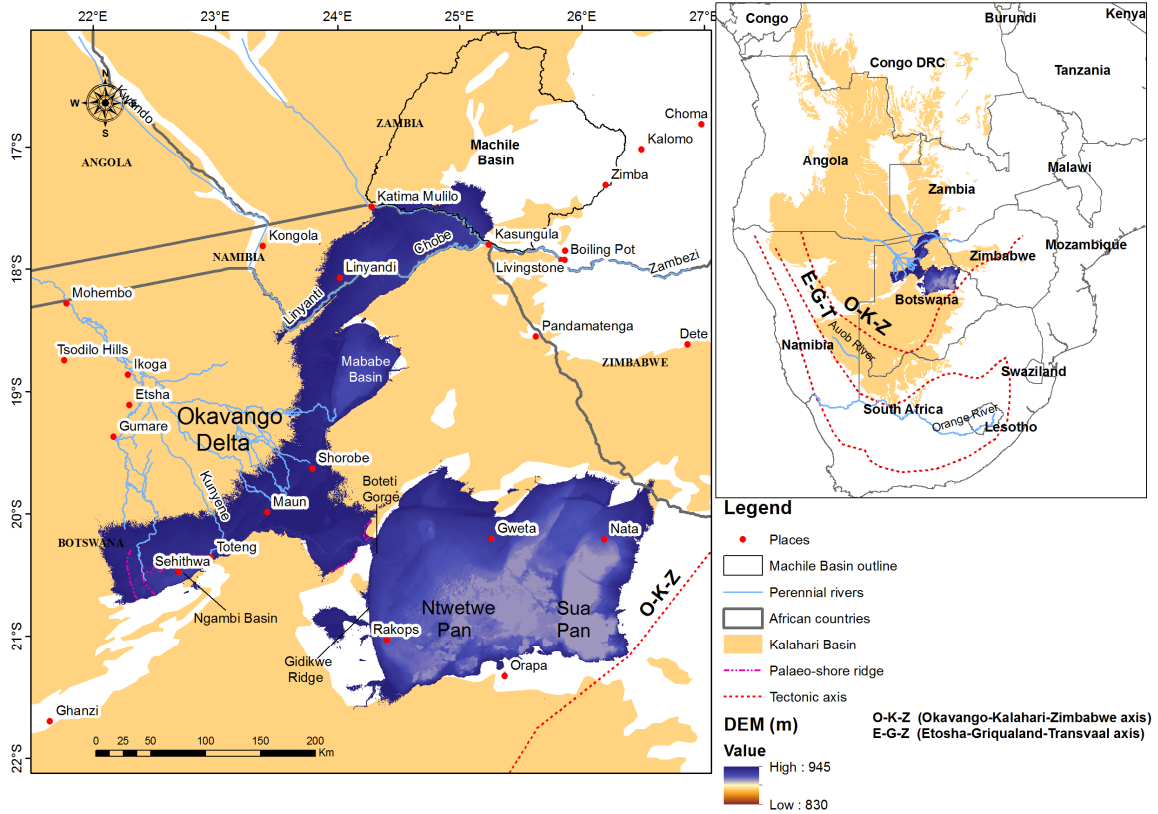
Fig.1: The Lake Palaeo-Makgadikgadi areal coverage (inferred from the 945m amsl contour) extending into the southern part of the Machile Basin. Inset illustrates the extent of the Kalahari Basin over southern Africa (Modified from:Thomas & Shaw, 1991; Haddon & McCarthy, 2005).

The Paleao-Lake Makgadikgadi (PLM) formation, and consequent desiccation, is suggested to be closely associated to tectonic disruptions along the OKZ axes and increasing dry climate, respectively (McCarthy, 2013). The mega-lake had sustained five major lake stage phases with the highest level at approximately 995 m above mean sea level - amsl (e.g. Thomas & Shaw, 1990; McFarlane & Eckardt, 2006; Burrough et al., 2009; Moore et al., 2012). Lake stage include, 995 m amsl (Paleao-Lake Deception (PLD)), 945 m amsl (PLM), 936 m amsl (Palaeo-Lake Thamalakane), 920 m amsl and 912 m amsl (Moore et al., 2012). However, the 945 m amsl phase was the longest and profound in the evolution of the lake, estimated to have existed between

1.5-0.5 Ma (Moore et al., 2012). Although the geomorphological data on the Late Pleistocene to Holocene development of the lake system are comprehensive (Riedel et al., 2014), Early to Middle Pleistocene history is still speculative, and the age of the lake system is still uncertain. Studies based on published optically stimulated luminescence (OSL) dating (Stokes et al., 1997; O'Connor & Thomas, 1999; Thomas et al., 2000; Thomas et al., 2003; Ringrose et al., 2005; Burrough et al., 2007; Burrough & Thomas, 2008, 2009; Burrough et al., 2009) invoke a Late-Middle to Late Pleistocene age for the lake with climatically controlled palaeo-shoreline oscillations. In contrast, based upon Early Stone Age (ESA) tools, McFarlane & Eckardt (2006) suggested a minimum age of the lake floor of 500 ka. This is in line with the molecular dating of a Pleistocene cichlid fish radiation which emerged in lake system (Joyce et al., 2005), the oldest clade dated to *c*. 600 ka (Genner et al., 2007). Recently, Moore et al. (2012) suggests on the basis of robust archaeological and other evidence that the lake system could have been initiated as early as 1.4 Ma during the Early Pleistocene and retreated to progressively lower shorelines as a result of successive severance of the headwaters of the drainage network (Du Toit, 1927; Cooke, 1980; Thomas & Shaw, 1991; Moore & Larkin, 2001; Haddon & McCarthy, 2005). According to this model, the PLM was desiccated prior to the end of the ESA (i.e. prior to 500 ka). OSL has several advantages, the most important of which is the ability to obtain dates from strata that lack associated, datable carbon. Like the development of radiocarbon dating, as OSL use becomes more widespread, the factors that can affect the association of ages and the strata of interest need to be fully explored. Moore et al. (2012) in their synthesis paper suggests that the order of magnitude mismatch identified between luminescence dates of quartz grains versus age constraints on key Kalahari landforms provided by archaeological evidence highlights questions about the role and extent of bioturbation in modifying Kalahari sediments.

This paper examines the types and nature of deep sediment cores in detail within the Zambian annex of PLM for the first time. OSL ages of sediment cores are collected to examine the role or extent of factors influencing age chronologies on deep in-situ PLM strata if any. The palaeo-environmental and depositional implications facies are also discussed. This study will contribute to refining of the current understanding on the evolution of the PLM system.

1.1 Study area

The Machile Basin is located in the semi-arid environment of south-western Zambia between latitudes 15.9809 S and 17.9044 S and longitudes 24.0997 E and 26.5065 E decimal degrees (Fig. 2). The area in this basin is typically a low gradient topography from 930 – 2000 m amsl sloping at an average gradient of 0.6 % making it prone to extensive seasonal floods from the Zambezi River in the wet season (YEC, 1995). Several streams and rivers drain most of the basin and form seasonal tributaries of the perennial Zambezi River.
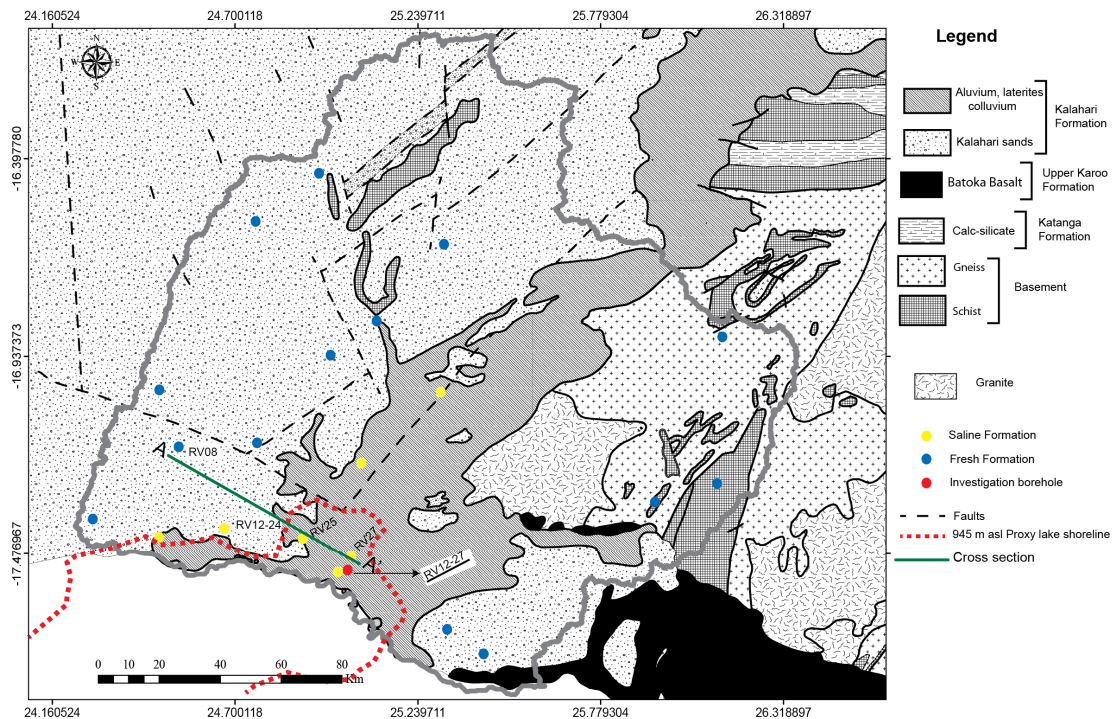
Fig. 2: Geology of the Machile Basin, showing the major geological formations (Yemane et al., 2002) and locations of fresh and saline formation electrical conductivities. High salinity is concentrated within the Kalahari Formation rather than confined to the extents of the 945m amsl proxy lake shoreline.

Rainfall is restricted to periods between September to April with an average of 500 mm/yr (New et al., 2002; Beilfuss, 2012). The lowest temperatures are observed at the start of the dry season between mid-May and the end of July, with an average temperature of 10°C in July (Wang et al., 2007). The months of October and November are the hottest with a daily maximum average of 28°C. Potential evapo-transpiration is estimated to be 1,600 mm/year (Beilfuss, 2012). Evapo-transpiration generally exceeds precipitation for most of the year with potential evaporation highest in the driest months. The area

is covered with a Savannah type vegetation interrupted in places by deciduous broad leaf forest, dry land/cropland pasture and a cropland/woodland mosaic with a grassy understory. More recently, these forests have been diminished because of increased demand for timber.

The geology of western Zambia and the studied Machile Basin, was first described by Money (1972). It is predominantly made up of a surficial wind-blown desert sand cover (the Kalahari sands) considered to represent the end of the Neogene erosion surface (Money, 1972; Haddon & McCarthy, 2005) on the west and south-east as shown in Fig. 2. These aeolian sands have a predominant grain size of 0.2 mm and are well sorted (Thomas & Shaw, 1993). Sandstone with clays, gravels and fine sands typically occur in deeper Kalahari beds. Alluvium, laterite and colluvium sediments are found in the more central region within river systems or terraces; these second order landforms are due to post-Neogene cycles of erosion and deposition, most of which were probably initiated by a series of down-warps and alternating upwarps (Haddon & McCarthy, 2005). The described strata constitute the Kalahari Group formations that varies in depth and may reach up to 450 m at its thickest but is more typically 10–100 m thick (Haddon & McCarthy, 2005). Surface outcrops of Basement and Karoo rocks are infrequent and almost invariably restricted to the basin margins in the east and north-west as shown in Fig. 2.

2 Materials and Methods

2.1 Borehole investigation in the Machile Basin

High resolution geophysical logging in a total of 20 boreholes was done to delineate the nature of sediments in the basin and outline the occurrence of high salinity formations; earlier studies had reported wide spread high salinity assumed to be confined to the PLM region (Chongo et al., 2011). Robertson Research Geologging equipment was used to log natural gamma radiation (NGR) with units in American Petroleum Institute (API) and formation electrical conductivities. Formation electrical conductivities were measured from inside PVC casings using a focused dual induction probe, which has a formation penetration depth of approximately 5 m and 2m for the Long and Short Electrical Conductivity (LCON and SCON), respectively. The location of the logged boreholes and the inferred formation salinity (fresh or saline) is shown in Fig. 2; the classification of formation electrical conductivity was

based on 500-1,000 and 1,000-10,000 mS/m hosting fresh and saline pore-water, respectively (Palacky, 1988).

2.1.1 Sample collection

This work involved drilling a 100 m deep research borehole, designated RV 12-27 (underlined in Fig 2), in the centre of the Zambian part of PLM (inferred from the 945m amsl shoreline - (Cooke, 1979; Shaw & Thomas, 1996; Gumbricht et al., 2001; McCarthy, 2013)) extent into the Machile Basin. Accurate elevation (m amsl) and location co-ordinates of available boreholes were obtained using a differential Trimble (TM) R4-5800 system GPS; borehole top of collar was used as a reference point for the measurements with an elevation error of ± 0.01 m amsl. Trimble Business Center 2.30 was used for post-processing. It was envisaged that the core would represent a complete sedimentation history of the lake at the drill site. The borehole (RV 12-27) was located at 24.9992 E, 17.5172 S with a surface elevation of 944.41 m amsl (Fig. 2). It was cased with a 75 mm diameter PVC pipe and screened for 1 metre at the bottom. Sediment cores were collected from the borehole using a modified version of the Waterloo Sampler (Zapico et al., 1987) at intermittent depths within the saturated zone. The sampling interval was on average every 2 m and dictated by lithology changes observed in the borehole data drilled within close proximity and mapped with geophysical borehole logging. Using a drilling rig, stainless steel core tubing (to avoid exposure to light) was pushed into the unconsolidated sediments to extract drill cores for OSL and other measurements. Due to difficulty of sample collection and the nature of subsurface geology, the maximum sampling depth was 50 m bgl. This 50 m section is much longer than those sampled for OSL ages in the shoreline studies (Burrough et al., 2009), and other coring activities within PLM (Holmgren & Shaw, 1997; Huntsman-Mapila et al., 2006; Teter, 2007), which were generally < 10 m bgl. The borehole was drilled down to the bedrock (Batoka basalt), which was intercepted at 100 m bgl to allow for borehole geophysical profiling. Calibration of the borehole logging profile was done after sediment core description. In addition, a recently deposited sediment sample from the riverbed of Zambezi River was collected for geochronology analysis.

OSL dating of quartz grains is based upon the response of light-exposed quartz grains to the cumulative effects of natural radiation on the grains during dark burial. Upon light exposure, quartz grain defects lose previously stored charge (in the form of trapped electrons at the defects) thereby zeroing the amount of luminescence that can be detected in a laboratory experiment.

At the moment of burial the luminescence clock is therefore set to zero time. During burial in dark conditions, natural radioactivity in the form of alpha, beta and gamma radiation associated with the decay of natural uranium, thorium and potassium will cause electrons to again be trapped in the defects. In the laboratory, the electrons are released emitting ultraviolet wavelength photons that are counted as the luminescence and whose intensity is proportional to the radiation dose acquired during burial in dark conditions. The recently deposited Zambezi sample was used to determine if the sediment core material could be completely 'bleached'. Bleaching in this context means the potential for the sediment to lose its ionizing energy stored in its crystal lattice from the decay of radioactive species and their daughter products within and around the grains, which builds up over time following burial.

2.2 Measurements and Sample analysis

2.2.1 OSL dating

In the laboratory, the core was split and samples taken under low-level red light conditions. Potentially mixed sediment adjacent to the core barrel walls was avoided. Chemical analysis and measurements were conducted at the Nordic Laboratory for Luminescence Dating, University of Aarhus in Risø. Each sample was treated with concentrated (36%) HCl to remove carbonates, H_2O_2 to remove organic matter and sieved to isolate the 180-250 μm sand fractions. The sand grains were placed in 1%HF for 50 minutes and then again treated with HCl to remove any fluoride precipitates before using density separation (2.58 g cm-3 aqueous solution of sodium polytungstate) to separate quartz and other grains from a lighter K-rich feldspars extract. Finally, the quartz-rich extract was placed in 40% HF for 50 minutes and again treated with HCl to recover the 'quartz-extract' from which all feldspar had been removed. Luminescence measurements were made on a Risø TL/OSL-DA-20 reader (DTU Nutech) with a bialkali PM tube (Thorn EMI 9635QB) and Hoya U-340 filters (290-370 nm). The built-in calibration of 90Sr/90Y beta source gives a dose rate of ~0.1 grays per second (Gy/s) with a typical uncertainty ~2.5%. Blue light-emitting diodes (LEDs) (~80 mW.cm-2; 470 nm), and infra-red (IR) LEDs (~150 mW. cm-2; 875 ± 80 nm) provided optical stimulation. The heating rate used was 5 °C/s. The luminescence purity of the quartz extracts were confirmed using IR stimulation (only feldspars have a significant IR stimulated signal; quartz is insensitive). The Single Aliquot Regenerative-dose (SAR) measurement procedure outlined by Murray & Wintle (2000) and Wintle & Murray (2006) was used to estimate quartz

equivalent doses. In summary of the SAR method, each sample was irradiated with increasing radiation levels (beta), and re-exposed (stimulated) to determine the luminescence that occurs at each irradiation level (referred to as dose rate). The equivalent dose was then determined by applying a regression to the data, and determining the radiation dose that corresponds to the initial luminescence signal. A pre-heat of 260°C for 10 seconds and a cut-heat of 220°C was employed and optical stimulation was undertaken with a sample held at 125°C. A dose recovery test gave an average ratio of measured to given dose of 0.994 ± 0.004 (n = 18), demonstrating that our chosen protocol was able to accurately measure a known dose given to our samples before any prior treatment. Radionuclide concentrations were estimated using HRGS - High Resolution Gamma Spectrometry (Murray et al., 1987); these were converted to dose rates using the factors given by Guérin et al. (2013). Cosmic ray dose rates are based on Prescott & Hutton (1994) and an average water content of 10% was assumed with an uncertainty of $\pm$ 4%. The time since burial is the ratio of the total dose divided by the annual radiation dose experienced at the burial position. To get the OSL age, the quartz equivalent dose is divided by the dose rate.

2.2.2 XRD and microfossils

Samples were taken from 14 m, 21 m, 23 m, 28 m, 35 m and 45 m bgl for X-Ray Diffraction (XRD) and microfossils. The purpose of these measurements was to understand the palaeo-environmental conditions of PLM preserved at deposition. For XRD analysis, bulk samples were crushed to powder form and oven-dried at 35 °C. Where appropriate, for diagnostic tests of the type of clay minerals, samples were heated to 550 °C and glycolation was applied. X-ray peak heights (intensity) were used as gross indicators of the relative proportions of minerals present using the standard mineralogy libraries. To validate the presence of carbonates, where indicative peaks stood out from the background in from the XRD peaks, a simple effervescence test by addition of Hydrochloric acid (HCl) was conducted.

Microfossil samples were prepared for analysis according to the methods described by Renberg (1990) at GEUS. Identifications were carried out with an Olympus BX60 light microscope using phase-contrast illumination at 1000x magnification. It should be noted, however, that poor preservation of diatoms will occur due to high salinity trends (Ryves et al., 2006; Flower & Ryves, 2009); samples were selected from core segments with proxy high clay content as indicated by natural gamma radiation in the investigation borehole.

3 Results

3.1 Geophysical logging and lithostratigraphy

Geophysical logging shows that the occurrence of high salinity formations seems to be confined to the south central regions of the Machile Basin in close proximity to the 945 m amsl proxy lake shoreline as shown in Fig. 2. The cross-section (AA') of selected boreholes given in Fig 3, indicates that sediments within the proximity of the 945 m amsl proxy shoreline are typically composed of clay and sands/sandstones (fluvio-lacustrine sediments).
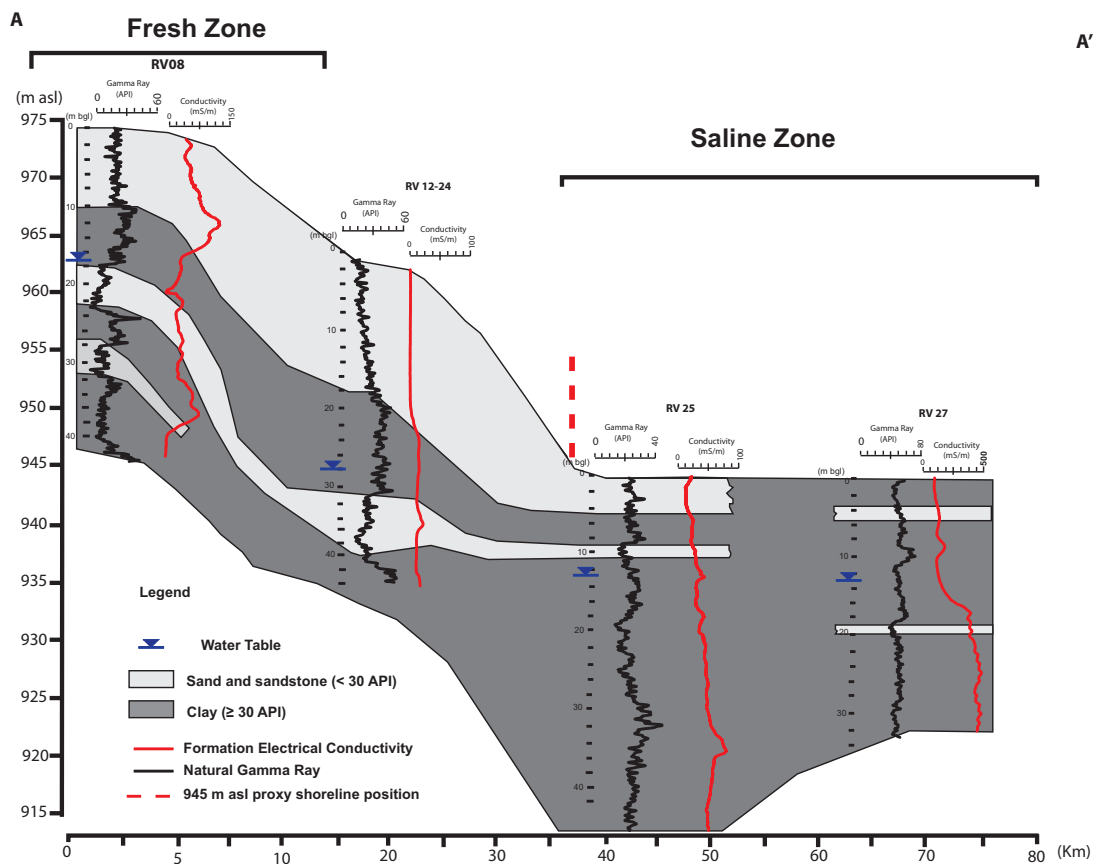
Fig. 3: Transect based on geophysical borehole logging of some of the production boreholes. The measured natural gamma radiation (NGR) and formation electrical conductivity (FEC) data are shown in red and black, respectively. For the location of the four boreholes (RV 08, RV 12-24, RV 26 and RV 27) see Fig. 2. NGR and FEC suggests that a clay formation hosts high salinity although spreads beyond the saline zone.

Natural gamma radiation (NGR) and formation electrical conductivity (FEC) further shows that clay sediments are more widespread and not limited to the immediate proximity of PLM shoreline position but spread towards the fringe

of the basin (shown by borehole RV 8 on which Fig. 3) with intercalations of sand lens.

Deep borehole geophysical logging in the investigation borehole, after calibration with core sediments, enabled lithological mapping between the intermittent core samples and lithological characterisation down to 100 m to the Batoka basalt. The natural gamma radiation log clearly delineates lithological variation and boundaries (Fig. 4a).
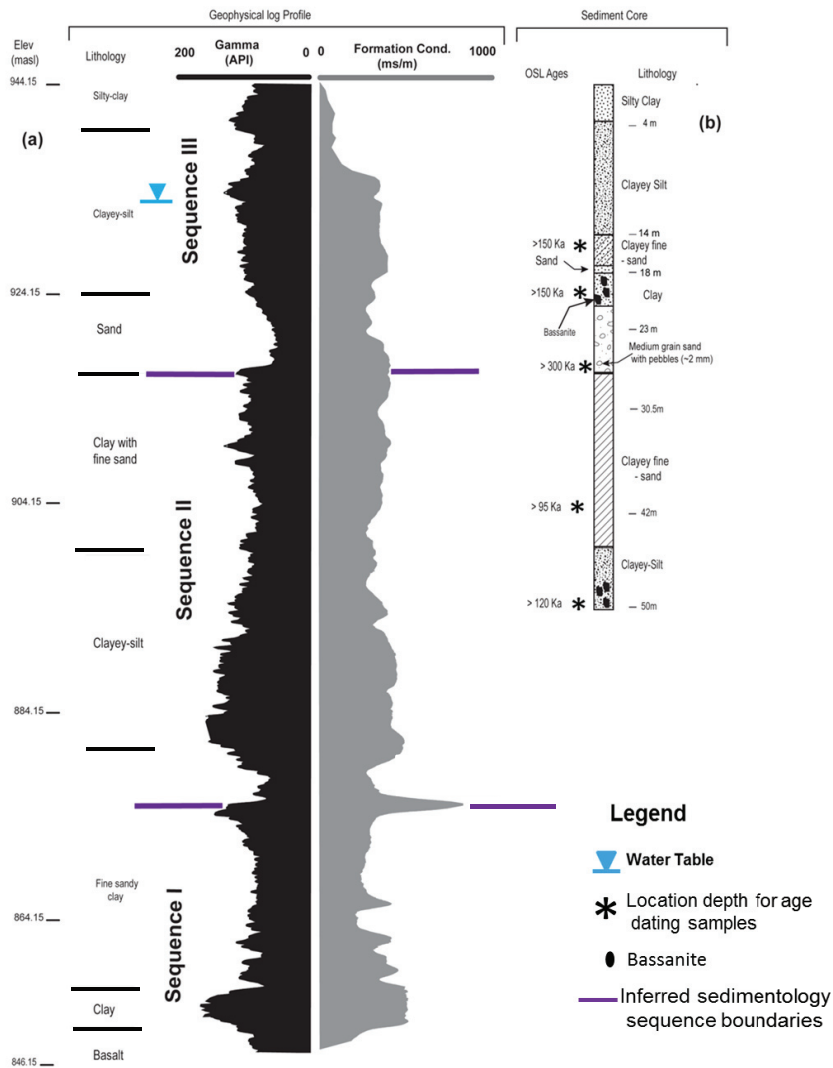
Fig. 4: (a) Shows the 100 m deep geophysical profile of natural gamma rays (NGR) and formation electrical conductivity (FEC) as sampled from investigative borehole RV 12-27 (for the location see Fig. 2.). FEC varies approximately between 0 and 750 mS/m indicative of hyper-saline pore-water. NGR outlines the lithological boundaries between the clay and sand fractions which enables us to define three sequences suggestive of climatic changes in the basin. (b) Core lithostratigraphy profile outlining the various lithologies intersected (predominately silt and clay or a combination of the two).

Natural gamma values > 30 API was observed at elevations, 944-924 m, 914-884 m and 894-846 m amsl indicative of clayey horizons, whereas, sands lens were seen at elevations 924-914 and 879-874 m amsl. The clayey horizons are typically silty-clay, clayey-silt and clay with fine sands. Sediments of the entire profile is interpreted to be fluvio-lacustrine in nature. Three lithostratigraphical sequences are outlined based on the facies heterogeneity and natural gamma radiation response (Fig. 4a). These are sequence I (874-846 m amsl), II (914-874 m amsl) and III (874-846 m amsl).

The FEC varies between approximately 0 and 750 mS/m in the log profile. Low conductivities are observed between 944-933 m amsl ranging from 0-250 mS/m, whereas, >250 ms/m are observed below 933 m amsl with a peak as high as 750 mS/m at 874 m amsl. The profile generally hosts high salinity within both clayey and sand sediments except for the upper part of approximately 10 m bgl.

3.2 Drill core mineralogy and palaeontology

The sediment drill core (Fig. 4b) is composed of fine- to medium-grained intercalated layers of clayey-silt, clay and sands hosting both clastic and evaporite minerals. XRD analysis shows the clastic fraction of the sediments consists of quartz, alkali feldspar (albite) and occasionally K-feldspars. Evaporite minerals, visible in hand-specimen (Fig. 5), occur as whitish, fine-grained, vein-like clasts (approximately 1 cm thick) of bassanite ($CaSO_4.\frac{1}{2}H_2O$).
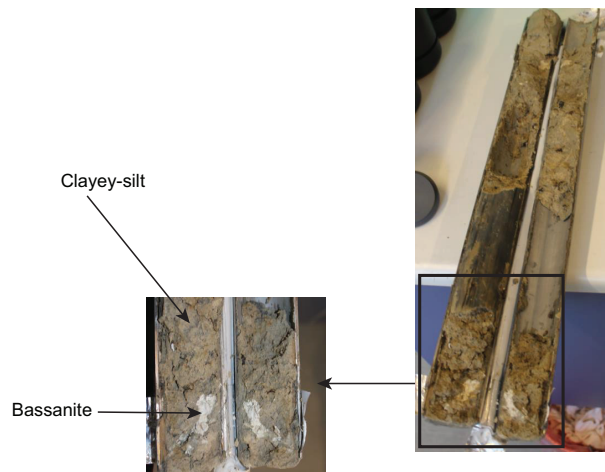
Fig. 5: Core profile from depth 18 to 19.5 m bgl showing whitish, fine-grained, vein-like shaped bassanite mineral lumps hosted in clayey-silt sediments. We suggest the bassanite was recrystallized at high temperature to attain the structural orientation and texture observed.

Although we drilled through 100 m of Kalahari sediments, and cored several intervals within the upper 50 m, we did not find pure evaporite mineral layers, except for clasts of bassanite in some sections of the sediments at depths 18 to 20 and 48 to 50 m bgl (Fig. 4b). XRD shows a dominant quartz peak and background peaks of carbonate minerals (indicative of calcite and dolomite) and bassanite in all the sediments. Effervescence after the addition of hydrochloric acid was seen as indicative of carbonate presence at a microcrystalline scale. Smectite clay type (13 – 14 angstrom (Å)) was identified in the lithologies as shown in the coupled diffractometry plot of samples at depths 15 and 28 m bgl (Fig. 6).
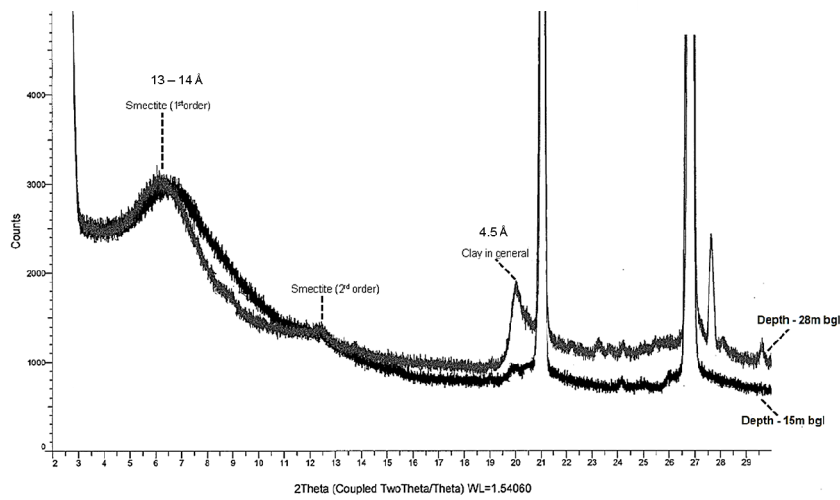
Fig. 6: X-Ray diffractometry plot of coupled samples taken from depths 15 and 28 m bgl from the investigation borehole. The plot outlines smectite clay peaks (13 – 14 Å) through the entire profile and shows higher general clay (4.5 Å) peak with increasing depth. We suggest the smectite is neoformed as a result of crystallisation from a high salinity solution.

Micro-palaeontological investigations of the sediments showed diatoms in varying amounts of preservation and abundance. These diatoms are diagnostic of both fluvial and lacustrine environments (Moos et al., 2005; Rioual et al., 2007; Heinsalu et al., 2008; Wolin & Stone, 2010). The siliceous fossil assemblage is seen most clearly at 21 m bgl depth; here centric (bottom-dwelling) and pennate (free-floating) diatoms, and skeletal remains (spicules of sponge) dominated as shown in Fig. 7.
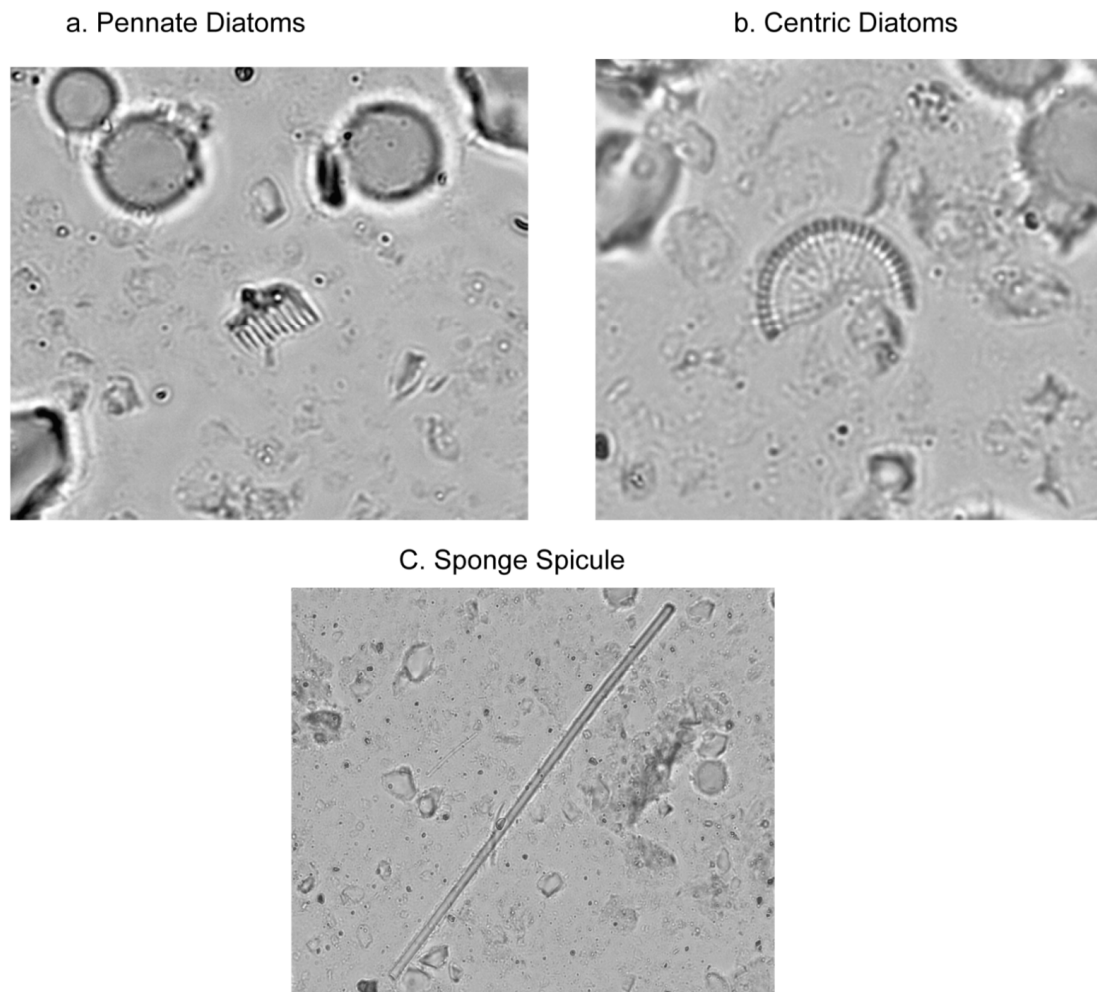
Fig. 7: Representative fossil (1000x magnification) from the sediment core at 21 m bgl (the region with most fragments). The presence of diatoms (pennate and centric) and sponge spicule are indicative of palaeo-environmental changes under a lacustrine system.

3.3 Chronostratigraphy

Equivalent doses in the drilled core sediments are > 200 Gy (Table 1), for which are considered to be close to or fully saturated with radioactive species. The actual dose experienced by the quartz grains can not be determined – only a minimum dose. The calculated sediment ages (Table 1) are therefore not actual ages and but minimum ages limited by the maximum dose that can be stored by the quartz grains. If the dose rate is high, minimum ages will be lower than if the dose rate is low. Dose rates were found to be relatively low (Table 1), ranging from total values of 0.71 ± 0.06 grays per thousand years

(Gy/ka) in the coarser sediments (28 ± 0.20 m bgl) and up to 2.16 ± 0.10 Gy/ka in the clay-silt sediments (40 ± 0.20 m bgl).

Table 1: Optically Stimulated Luminescence (OSL) analysis results from the investigation borehole core showing the age (ka), dose (Gy), number of samples, dose rate (Gy/ka) and water content (%). Quartz dose (Gy) suggests the quartz is saturated with radionuclides to an extent we can only report the results are minimum ages (ka).

Lithology	Sample Depth m bgl (± 0.20 m)	Age, ka	Dose, Gy	Number of samples	Dose rate Gy/ka	Water Content %
Sand	Riverbed sample	1.10 ± 0.14	0.82 ± 0.10	27	0.75 ± 0.04	22
Clayey silt	14	> 150	> 280	24	1.95 ± 0.09	20
Silt-sand	19	> 150	> 260	17	1.73 ± 0.09	18
Sand	28	> 300	> 210	14	0.71 ± 0.06	16
Clay with fine sand	40	> 95	> 200	18	2.16 ± 0.10	13
Clayey silt	50	> 120	> 260	23	2.13 ± 0.11	17

Stratigraphically, the minimum OSL ages (Fig. 4b and Table 1), show ages from > 95 ka, at 40 ± 0.20 m bgl and to > 300 ka, at 28 ± 0.20 m bgl. Since the upper section has older minimum ages ranging from 150 to 300 ka, and the bottom from > 95 to > 120 ka, we can only say both top and bottom sediments must be > 300 ka in age. The actual age of the sediments is still not known. The Zambezi River bed sediment (Table 1, 1.10 ± 0.14 ka in age) shows that it is possible to completely bleach the sediment cores.

4 Discussion

4.1 Depositional environment

The cored sediments from the 100 m deep boreholes, drilled through the Quaternary sediments in the Machile Basin, show clay and silt rich sediments with sandy intercalations. We suggest the sediments represent a deltaic feature, possibly linked to the former abandoned course of the Kafue River with sands and clay units simply reflecting differing sedimentary facies in a deltaic sedimentary package. Based on geophysical logging results, three sedimentary sequences can be identified as shown in Fig. 4.

Results from the geophysical logging also show saline pore water in the sediments from about 5 m below surface to the underlying basalt. Both airbourne and ground based geophysical mapping within the Machile Basin

(Chongo et al., 2011; Chongo et al., 2014) has shown high salinity sediments confined within the PLM shorelines. These, and other observations, indicate that the cored sediment package was deposition in a lake environment with high salinity. The basanite in the sediments were probably formed after gypsum ($CaSO_4.2H_2O$) dehydration under hyper-arid climate with progressive evaporation (Prasad et al., 2001; Peckmann et al., 2003; Harrison, 2012). The clay mineralogy (smectite) in the basin suggests *in-situ* neo-formation attained by direct crystallisation from high salinity solution rather than a modification of existing clay minerals (Singer, 2008); more investigations on the structure of the clay are required to further validate this assertion. Furthermore, the clay has no trace of amorphous or poorly crystalline iron-rich alumino-silicates that represent transitional precursors to support formation by replacement (Tazaki & Fyfe, 1985). Halite, and other highly soluble salts was not observed in the sediments, but are most likely present in deeper horizons, as this has been observed in sediments from other sub-basins in the PLM (Eckardt et al., 2008). The bassanite evaporites are intimately mixed with the sediments in vein-like structures. We suggest the displacive nature of the evaporites highlights that groundwater played an important role in transportation of high salinity solutes within the sediments upon primary evapoconcentration at the surface (Spencer et al., 1985; Rosen, 1994; Sinha & Raymahashay, 2004).

The presence of diatoms (pennate and centric) and sponge spicule further support the interpretation of a lacustrine system as the palaeo-environment (Smol & Stoermer, 2010). The centric and pennate diatoms are likely of the genus *Cyclotella* and *Nitzschia,* respectively; of which we infer a mixed fossil assemblage of the palaeo-environmental condition during the existence of the PLM, ranging from weakly to strongly alkaline lake water conditions (Hecky & Kilham, 1973; Nyambe & Utting, 1997; Fritz et al., 1999; Smol & Stoermer, 2010).

4.2 The age of the Quaternary sediments in the Machile Basin

Our analysis of 50 m of sediment core in the Machile Basin, using OSL for the first time, has shown that the quartz grains are nearly or fully saturated with radioactivity. The maximum measurable ages using OSL is 300 ka (Cordier et al., 2012). Based upon Early Stone Age tools McFarlane & Eckardt (2006) suggested a minimum age of the PLM lake floor of 500 ka. This is in line with the molecular dating of a Pleistocene cichlid fish radiation

which emerged in Lake Palaeo-Makgadikgadi (Joyce et al., 2005) the oldest clade dated to c. 600 ka (Genner et al., 2007). OSL dating within the PLM can therefore not accurately constrain the formation of PLM. In addition, one of the OSL ages from Burrough et al. (2009), dates 288 ± 25 ka which is at the limit of the OSL method.

Our OSL ages from the drilled borehole sediments indicate the sediments are old (> 300 ka) and deposited in a lake system most likely during Late Pleistocence. This is contrary to Burrough et al. (2009), who suggests, using palaeo-shorelines (generally < 10 m), a Late Pleistocence to Holocene existence of the mega-lake system (PLM). As the uncertainty from bioturbation on palaeo-shorelines sediments, which could result in younger ages using OSL, can not be excluded (Burrough et al., 2009), there is need for further investigation on its potential effects. Diamond exploration within the Kalahari sediments has shown that termites can carry sand grains upwards by as much as 70 m (Lock, 1985; Baumgartner & Neuhoff, 1998) exposing sediments to sunlight which induce a bleaching effect. Bateman et al. (2007) ascribed large palaeo-dose in samples (causing inconsistent chronology) from Tsodilo Hills in Botswana, studied by Thomas et al. (2003), was due to disturbances by bioturbation. Miller (2014) argues that the Late Pleistocene/Holocene OSL ages for dunes deposits in SW Botswana/SE Namibia conflict with the presence of early stone age lithic artefacts (i.e.> 500 ka in age), on the terraces of the Auob River, which had incised across the dunes – i.e. the river post-dates the dunes which it cuts; luminescence ages are interpreted as a consequence of periodic aeolian and biological reworking. However, there is still need to establish what geological process palaeo-shorelines represent if not the formation of the mega-lake PLM.

4.3 Implication on the evolution history of PLM.

Moore et al. (2012) suggests on the basis of archaeological and other evidence that the PLM system could have been initiated as early as 1.4 Ma, during the Early Pleistocene and retreated to progressively lower shorelines as a result of successive severance of the headwaters of the drainage network (Du Toit, 1927; Cooke, 1980; Thomas & Shaw, 1991; Moore & Larkin, 2001; Haddon & McCarthy, 2005) and becoming largely desiccated prior to the end of the ESA (i.e. prior to 500 ka). Lake water level in this model varies more than 50 m, and compared to climatic induced water level change of few meters in other African lake systems such as the Lake Victoria (Yin & Nicholson, 1998), it is suggested, that tectonic is the major controlling process for

changing catchment size to th PLM (Moore et al., 2012). In adition, water budgets required to sustain the various lake level phases cannot be in balance to 10-15 % increase in rainfall proposed by Burrough et al. (2009) rendering the climatic evolution model rather inadequent.

In the Machile basin, the old sediments (> 300 ka) show three sequences (I, II, and III in Fig. 4a) suggestive of changes in the climatic patterns from humid, depositing fluvial sediments (sands and silts) and arid periods, depositing lacustrine sediments of clays. The exact timing cannot be constrained by our ages; however, we suggest events must have occurred before the Late-Pleistocene. Various phases of glacial activity has been observed in the southern hemisphere in the Pleistocene which probably corresponds to these humid and drier periods (Martinson et al., 1987).

As the climatic model on the evolution of PLM is underpinned on OSL ages (from shorelines generally < 10 m bgl) which does not represent the formation of PLM and other evidence discussed, we support tectonics as primary control of lake stages and climatics was ancillary.

5 Conclusions

The study set out to establish the nature and type of sediments in the Zambian part of the Makgadikgadi, which has not before been studied in details. Insights and perspective were used to refine the understanding of the evolution of the Palaeo-Lake Makgadikgadi system. The following are our findings:

- In the Machile Basin, Kalahari sediments are 95 m bgl thick consisting of intercalations of clayey silt and sand in a deltaic nature overlying the Batoka basalt bedrock.

- Contributed, for the first time, within PLM, Optical Stimulated Luminescence (OSL) ages over 50 m bgl of core compared to variours research workers with OSL ages from palaeo-shorelines (generally < 10 m bgl). These ages vary from > 95 ka to > 300 ka through the sediments.

- OSL dating over the 50 m core stratigraphically suggests the sediments are generally old (> 300 ka). OSL dating within the Kalahari sediments therefore does not date the formation of landforms but other processes which must be investigated further.

- Three sediment sequences deposited under variable climatic conditions have been identified as evidenced from fossils, evaporite mineralogy and lithostratigraphy. These are sequence I (874-846 m amsl), II (914-874 m amsl), III (944-914 m amsl). These facies, fossils and evaporites changes are probably linked to mesic climatic changes during existence of the PLM system before the Late Pleistocence.

- The vein-like structure (displacive nature) of the bassanite evaporites supports an active role of groundwater in transportation of high salinity solutes.

- The sediment package of the palaeolake system hosts high salinity formations within a deltaic alternation of sediments typically of clay and sand. Evaporates of bassanite and the presence of smecite clays suggest insitu high evaporation effects after deposition of the sediments.

- Collectively, the findings of this study supports the tectonic evolution of the PLM rather than a more variable climate evolution to desiccation and is substantiated with robust archaeological and fossil evidence within the PLM system as well as the Kalahari as a whole.

References

Bateman, M.D., Boulter, C.H., Carr, A.S., Frederick, C.D., Peter, D. & Wilder, M., 2007. Preserving the palaeoenvironmental record in drylands: Bioturbation and its significance for luminescence-derived chronologies. Sedimentary Geology, 195, 5-19.

Baumgartner, M.C. & Neuhoff, I., 1998. The vertical distribution of indicator minerals within Kalahari cover overlying a kimberlite pipe. 7th International Kimberlite Conference, Department of Earth Science, University of Cape Town, Cape Town. pp. 55–57.

Beilfuss, R., 2012. A risky climate for southern African hydro: assessing hydrological risks and consequences for Zambezi River Basin dams. International Rivers.

Burrough, S.L., Thomas, D.S., Shaw, P.A. & Bailey, R.M., 2007. Multiphase quaternary highstands at lake Ngami, Kalahari, northern Botswana. Palaeogeography, Palaeoclimatology, Palaeoecology, 253, 280-299.

Burrough, S.L. & Thomas, D.S.G., 2008. Late quaternary lake-level fluctuations in the Mababe Depression: Middle Kalahari palaeolakes and the role of Zambezi inflows. Quaternary Research, 69, 388-403.

Burrough, S.L. & Thomas, D.S.G., 2009. Geomorphological contributions to palaeolimnology on the African continent. Geomorphology, 103, 285-298.

Burrough, S.L., Thomas, D.S.G. & Bailey, R.M., 2009. Mega-lake in the Kalahari: A late pleistocene record of the Palaeolake Makgadikgadi system. Quaternary Science Reviews, 28**,** 1392-1411.

Chongo, M., christiansen, A.V., Tembo, A., Nyambe, I., Larsen, F. & Bauer-Gottwein, P., 2014. Airborne and Ground based Transient Electromagnetic Mapping of Groundwater Salinity in the Machile-Zambezi Basin, South-western Zambia. . submitted to Hydrogeology Journal.

Chongo, M., Wibroe, J., Staal-Thomsen, K., Moses, M., Nyambe, I., Larsen, F. & Bauer-Gottwein, P., 2011. The use of Time Domain Electromagnetic method and Continuous Vertical Electrical Sounding to map groundwater salinity in the Barotse sub-basin, Zambia. Physics and Chemistry of the Earth, Parts A/B/C, 36**,** 798-805.

Cooke, H., 1979. The origin of the Makgadikgadi Pans. Ministry of Mineral Resources and Water Affairs, Botswana notes and records No. 11, pp. 37-42.

Cooke, H., 1980. Landform evolution in the context of climatic change and neo-tectonism in the Middle Kalahari of north-central Botswana. Transactions of the Institute of British Geographers**,** 80-99.

Cordier, S., Harmand, D., Lauer, T., Voinchet, P., Bahain, J.-J. & Frechen, M., 2012. Geochronological reconstruction of the Pleistocene evolution of the Sarre valley (France and Germany) using OSL and ESR dating techniques. Geomorphology, 165**,** 91-106.

Dingle, R., Siesser, W.G. & Newton, A., 1983. Mesozoic and Tertiary geology of southern Africa. A.A. Balkema, Rotterdam.

Du Toit, A., 1927. The Kalahari and some of its problems. South African Journal of Science, 24**,** 88-101.

Eckardt, F.D., Bryant, R.G., McCulloch, G., Spiro, B. & Wood, W.W., 2008. The hydrochemistry of a semi-arid pan basin case study: Sua Pan, Makgadikgadi, Botswana. Applied Geochemistry, 23**,** 1563-1580.

Flower, R.J. & Ryves, D.B., 2009. Diatom preservation: differential preservation of sedimentary diatoms in two saline lakes. Acta Botanica Croatica, 68**,** 381-399.

Fritz, S.C., Cumming, B., Gasse, F. & Laird, K.R., 1999. Diatoms as indicators of hydrologic and climatic change in saline lakes. In: Stoermer, E.F. & John, S.P. (eds.) The diatoms: applications for the environmental and earth sciences. Cambridge University Press, Cambridge. pp. 41-72.

Genner, M.J., Seehausen, O., Lunt, D.H., Joyce, D.A., Shaw, P.W., Carvalho, G.R. & Turner, G.F., 2007. Age of cichlids: new dates for ancient lake fish radiations. Molecular Biology and Evolution, 24**,** 1269-1282.

Guérin, G., Murray, A.S., Jain, M., Thomsen, K.J. & Mercier, N., 2013. How confident are we in the chronology of the transition between Howieson's Poort and Still Bay. Journal of human evolution, 64**,** 314-317.

Gumbricht, T., McCarthy, T.S. & Merry, C.L., 2001. The topography of the Okavango Delta, Botswana, and its tectonic and sedimentological implications. South African Journal of Geology, 104, 243-264.

Haddon, I.G. & McCarthy, T.S., 2005. The Mesozoic-Cenozoic interior sag basins of Central Africa: The Late-Cretaceous-Cenozoic Kalahari and Okavango basins. Journal of African Earth Sciences, 43, 316-333.

Harrison, T.N., 2012. Experimental VNIR reflectance spectroscopy of gypsum dehydration: Investigating the gypsum to bassanite transition. American Mineralogist, 97, 598-609.

Hecky, R.E. & Kilham, P., 1973. Diatoms in alkaline, saline lakes - ecology and geochemical implications. Limnology and oceanography, 18, 53-71.

Heinsalu, A., Luup, H., Alliksaar, T., Nõges, P. & Nõges, T., 2008. Water level changes in a large shallow lake as reflected by the plankton: periphyton-ratio of sedimentary diatoms. Hydrobiologia, 599, 23-30.

Holmgren, K. & Shaw, P., 1997. Palaeoenvironmental Reconstruction from Near-Surface Pan Sediments: An Example from Lebatse Pan, Southeast Kalahari, Botswana. Geografiska Annaler: Series A, Physical Geography, 79, 83-93.

Huntsman-Mapila, P., Ringrose, S., Mackay, A.W., Downey, W.S., Modisi, M., Coetzee, S.H., Tiercelin, J.J., Kampunzu, A.B. & Vanderpost, C., 2006. Use of the geochemical and biological sedimentary record in establishing palaeo-environments and climate change in the Lake Ngami basin, NW Botswana. Quaternary International, 148, 51-64.

Joyce, D.A., Lunt, D.H., Bills, R., Turner, G.F., Katongo, C., Duftner, N., Sturmbauer, C. & Seehausen, O., 2005. An extant cichlid fish radiation emerged in an extinct Pleistocene lake. Nature, 435, 90-95.

Lock, N., 1985. Kimberlite exploration in the Kalahari region of southern Botswana with emphasis on the Jwaneng kimberlite province. International Conference on Prospecting in Areas of Desert Terrain, Rabat, Morocco. London: Institution of Mining and Metallurgy. pp. 183-190.

Martinson, D.G., Pisias, N.G., Hays, J.D., Imbrie, J., Moore Jr, T.C. & Shackleton, N.J., 1987. Age dating and the orbital theory of the ice ages: development of a high-resolution 0 to 300,000-year chronostratigraphy. Quaternary Research, 27, 1-29.

McCarthy, T., 2013. The Okavango Delta and its place in the geomorphological evolution of southern africa. South African Journal of Geology, 116, 1-54.

McFarlane, M. & Eckardt, F., 2006. Lake Deception: a new Makgadikgadi palaeolake. Botswana notes and records, 195-201.

Miller, R.M., 2014. Evidence for the evolution of the Kalahari dunes from the Auob River, southeastern Namibia. Transactions of the Royal Society of South Africa, 69, 195-204.

Money, N.J., 1972. An outline of the Geology of western Zambia. Records of the Geological Survey, Republic of Zambia No. 12, pp. 103-123.

Moore, A., 1999. A reappraisal of epeirogenic flexure axes in southern Africa. South African Journal of Geology, 102**,** 363-376.

Moore, A., Blenkinsop, T. & Cotterill, F.W., 2009. Southern African topography and erosion history: plumes or plate tectonics? Terra Nova, 21**,** 310-315.

Moore, A.E., Cotterill, F.P.D. & Eckardt, F.D., 2012. The evolution and ages of Makgadikgadi palaeo-lakes: consilient evidence from Kalahari drainage evolution. South African Journal of Geology.

Moore, A.E. & Larkin, P.A., 2001. Drainage evolution in south-central Africa since the breakup of Gondwana. South African Journal of Geology, 104**,** 47-68.

Moos, M.T., Laird, K.R. & Cumming, B.F., 2005. Diatom assemblages and water depth in Lake 239 (Experimental Lakes Area, Ontario): implications for paleoclimatic studies. Journal of Paleolimnology, 34**,** 217-227.

Murray, A., Marten, R., Johnston, A. & Martin, P., 1987. Analysis for naturally occuring radionuclides at environmental concentrations by gamma spectrometry. Journal of Radioanalytical and Nuclear Chemistry, 115**,** 263-288.

Murray, A.S. & Wintle, A.G., 2000. Luminescence dating of quartz using an improved single-aliquot regenerative-dose protocol. Radiation Measurements, 32**,** 57-73.

New, M., Lister, D., Hulme, M. & Makin, I., 2002. A high-resolution data set of surface climate over global land areas. Climate Research, 21**,** 1-25.

Nyambe, I.A. & Utting, J., 1997. Stratigraphy and palynostratigraphy, Karoo Supergroup (Permian and Triassic), mid-Zambezi Valley, southern Zambia. Journal of African Earth Sciences, 24**,** 563-583.

O'Connor, P.W. & Thomas, D.S.G., 1999. The timing and environmental significance of late quaternary linear dune development in western Zambia. Quaternary Research, 52**,** 44-55.

Ollier, C.D., 1985. Morphotectonics of continental margins with great escarpments. In: Morisawa, M. & Hack, J.T. (eds.) Tectonic geomorphology. George Allen & Unwin, London. pp. 3-25.

Palacky, G., 1988. Resistivity characteristics of geologic targets. Electromagnetic methods in applied geophysics, 1**,** 53-129.

Peckmann, J., Goedert, J.L., Heinrichs, T., Hoefs, J. & Reitner, J., 2003. The Late Eocene 'Whiskey Creek' methane-seep deposit (western Washington State). Facies, 48**,** 241-253.

Prasad, P., Pradhan, A. & Gowd, T., 2001. In situ micro-Raman investigation of dehydration mechanism in natural gypsum. Current science - Bangalore, 80**,** 1203-1207.

Prescott, J. & Hutton, J.T., 1994. Cosmic ray contributions to dose rates for luminescence and ESR dating: large depths and long-term time variations. Radiation Measurements, 23**,** 497-500.

Renberg, I., 1990. A procedure for preparing large sets of diatom slides from sediment cores. Journal of Paleolimnology, 4**,** 87-90.

Riedel, F., Henderson, A.C., Heußner, K.-U., Kaufmann, G., Kossler, A., Leipe, C., Shemang, E. & Taft, L., 2014. Dynamics of a Kalahari long-lived mega-lake system: hydromorphological and limnological changes in the Makgadikgadi Basin (Botswana) during the terminal 50 ka. Hydrobiologia**,** 1-29.

Ringrose, S., Huntsman-Mapila, P., Kampunzu, A.B., Downey, W., Coetzee, S., Vink, B., Matheson, W. & Vanderpost, C., 2005. Sedimentological and geochemical evidence for palaeo-environmental change in the Makgadikgadi subbasin, in relation to the MOZ rift depression, Botswana. Palaeogeography Palaeoclimatology Palaeoecology, 217**,** 265-287.

Rioual, P., Andrieu-Ponel, V., de Beaulieu, J.-L., Reille, M., Svobodova, H. & Battarbee, R.W., 2007. Diatom responses to limnological and climatic changes at Ribains Maar (French Massif Central) during the Eemian and Early Würm. Quaternary Science Reviews, 26**,** 1557-1609.

Rosen, M.R., 1994. The importance of groundwater in playas: a review of playa classifications and the sedimentology and hydrology of playas. Geological Society of America Special Papers, 289**,** 1-18.

Ryves, D.B., Battarbee, R.W., Juggins, S., Fritz, S.C. & Anderson, N.J., 2006. Physical and chemical predictors of diatom dissolution in freshwater and saline lake sediments in North America and West Greenland. Limonology & Oceanography, 51**,** 1355-1368.

Shaw, P.A. & Thomas, D.S.G., 1996. The quaternary palaeoenvironmental history of the Kalahari, Southern Africa. Journal of Arid Environments, 32**,** 9-22.

Singer, A., 2008. Clay Mineral Formation. In: Chesworth, W. (ed.) Encyclopedia of Soil Science. Springer Netherlands. pp. 135-141.

Sinha, R. & Raymahashay, B.C., 2004. Evaporite mineralogy and geochemical evolution of the Sambhar Salt Lake, Rajasthan, India. Sedimentary Geology, 166**,** 59-71.

Smol, J.P. & Stoermer, E.F. (eds.), 2010. The diatoms: applications for the environmental and earth sciences. Cambridge University Press, Cambridge. 466 pp

Spencer, R.J., Eugster, H.P., Jones, B.F. & Rettig, S.L., 1985. Geochemistry of Great Salt Lake, Utah I: Hydrochemistry since 1850. Geochimica Et Cosmochimica Acta, 49**,** 727-737.

Stokes, S., Thomas, D.S.G. & Shaw, P.A., 1997. New chronological evidence for the nature and timing of linear dune development in the southwest Kalahari Desert. Geomorphology, 20**,** 81-93.

Tazaki, K. & Fyfe, W., 1985. Formation of primitive clay precursors on K-feldspar under extreme leaching conditions. Proceedings of the International Clay Conference. pp. 53- 58.

Teter, K.L. 2007. Paleoenvironmental reconstruction of Paleolake Mababe, northwestern Botswana from sediment chemistry and biological productivity data. Msc Thesis Oklahoma State University, 78 pp.

Thomas, D. & Shaw, P., 1990. The deposition and development of the Kalahari Group sediments, central southern Africa. Journal of African Earth Sciences (and the Middle East), 10, 187-197.

Thomas, D. & Shaw, P., 1991. The deposition and development of the Kalahari Group sediments, central southern Africa. Journal of African Earth Sciences (and the Middle East), 10, 187-197.

Thomas, D.S.G., Brook, G., Shaw, P., Bateman, M., Appleton, C., Nash, D., McLaren, S. & Davies, F., 2003. Late Pleistocene wetting and drying in the NW Kalahari: an integrated study from the Tsodilo Hills, Botswana. Quaternary International, 104, 53-67.

Thomas, D.S.G., O'Connor, P.W., Bateman, M.D., Shaw, P.A., Stokes, S. & Nash, D.J., 2000. Dune activity as a record of late Quaternary aridity in the Northern Kalahari: new evidence from northern Namibia interpreted in the context of regional arid and humid chronologies. Palaeogeography Palaeoclimatology Palaeoecology, 156, 243-259.

Thomas, D.S.G. & Shaw, P.A., 1993. The evolution and characteristics of the Kalahari, southern Africa. Journal of Arid Environments, 25, 97-108.

Wang, L., D'Odorico, P., Ringrose, S., Coetzee, S. & Macka, S.A., 2007. Biogeochemistry of Kalahari sands. Journal of Arid Environments, 71, 259-279.

Wintle, A.G. & Murray, A.S., 2006. A review of quartz optically stimulated luminescence characteristics and their relevance in single-aliquot regeneration dating protocols. Radiation Measurements, 41, 369-391.

Wolin, J.A. & Stone, J.R., 2010. Diatoms as indicators of water-level change in freshwater lakes. The diatoms: applications for the environmental and earth sciences, 174-185.

YEC (Yachiyo Engineering Company), 1995. The Study on the National Water Resources Master Plan in the Republic of Zambia. Japan International Cooperation Agency & Ministry of Energy and Water Development, Republic of Zambia. Final Report – Hydrogeology, 128 pp.

Yemane, K., D, G. & Nyambe, I., 2002. Paleohydrological signatures and rift tectonics in the interior of Gondwana documented from Upper Permian lake deposits, the mid-Zambezi Rift basin, Zambia. In SEPM Special Publication No. 73 on Sedimentation in Continental Rifts, SEPM (Society for Sedimentary Geology), ISBN 1-56576-082-4, pp. 143-162.

Yin, X. & Nicholson, S.E., 1998. The water balance of Lake Victoria. Hydrological Sciences Journal, 43**,** 789-811.

Zapico, M.M., Vales, S. & Cherry, J.A., 1987. A wireline piston core barrel for sampling cohesionless sand and gravel below the water table. Ground Water Monitoring & Remediation, 7**,** 74-82.

II

Identification and evaluation of hydro-geochemical processes in the groundwater environment of Machile Basin, western Zambia

Kawawa E. Banda, Rasmus Jakobsen, Peter Bauer- Gottwein, Imasiku Nyambe, Troels Laier, Flemming Larsen

Submitted

Identification and evaluation of hydro-geochemical processes in the groundwater environment of Machile Basin, western Zambia

Kawawa E. Banda [a,b*], Rasmus Jakobsen[c], Peter Bauer- Gottwein[a], Imasiku Nyambe[b], Troels Laier[C] Flemming Larsen[c]

[a] Department of Environment, *Technical University of Denmark*, 2500kgs-Lynby, Denmark

[b] Department of Geology, *University of Zambia - Integrated Water Resources Management Centre*, C/O School of Mines, Lusaka, Zambia.

[c] Department of Geochemistry, *Geological Survey of Denmark and Greenland (GEUS)*, 10, Øster Voldgade, DK-1350 Copenhagen K, Denmark.

Abstract

Salinity mechanisms and controls in groundwater are poorly accounted for in arid and semi-arid areas. We investigate the chemical and physical processes that control salinity of the groundwater in the semi-arid Machile Basin, western Zambia. Various methods were used including groundwater chemistry analysis, environmental isotopes, geochemical (using PHREEQC) and physical (with PMWIN) groundwater modelling. Fresh groundwater in the basin, with a Ca-Mg-HCO$_3$ /Na-HCO$_3$ composition, and saline groundwater with a Na-Cl-SO$_4$ composition has apparent ages of < 10 ka attributed to recharge during *pluvia*l climatic events in the Holocene. We model fresh water quality to be a result of silicate weathering, whereas, saline water is affected by dedolomitization and ionic exchange. Salinity in the groundwater flow system is therefore a result of mineral dissolution and precipitation, and evaporation effects. We further demonstrate that due to the hydraulic conductivity contrast in the host lithologies, fresh water in the basin is forced out through the topographic depressions and consumed by evapotranspiration with little or no interaction with the saline pool except in the transition zone. We conclude that the saline pool has only been flushed during *pluvial* periods and currently hosts stagnant groundwater.

1 Introduction

The United Nations Millennium goal to ensure adequate and potable water supply to all has necessitated the exploitation of groundwater resources for rural water supply in most developing countries (Monjerezi et al., 2011). Groundwater with high salinity attributed to dissolution of evaporites from the Lake Palaeo-Makgadikgadi, as found in Machile Basin, western Zambia (Banda et al., 2015; Chongo et al., 2014b), is a major groundwater quality problem. Accordingly, improved knowledge on the hydrological interaction between the fresh and saline water is critical in this basin. Boreholes delivering saline water are usually abandoned by communities, resorting to open water holes dug out in dry river beds or surface water resources, where these are available. An understanding of hydro-geochemical processes affecting water quality in these aquifers and the residence time is essential in order to assess potential effects of changes in environmental pressures and identify necessary abatement actions to sustain usable water supplies. In addition, sustainable exploitation of available groundwater resources is almost impossible

without adequate knowledge of the spatial distribution of fresh and saline groundwater and understanding of the processes that determine spatial variations of salinity (Bouchaou et al., 2008).

The interaction of groundwater with minerals in the aquifer through which the groundwater flows greatly controls the groundwater chemistry (Kumar et al., 2009; Ravikumar et al., 2011). Currently, groundwater mineralisation processes are often poorly described in arid and semi-arid regions (Verhagen, 1995; Wheater et al., 2010). A non-significant diffuse recharge in these regions, typically between <1 and 20 mm/yr (Wanke et al., 2008), will have an impact on the overall groundwater chemistry due to low water-rock ratios and larger residence times, leading to somewhat higher salinities and more evolved hydro-geochemistry (Wheater et al., 2010). Typically, spatial-temporal variations in groundwater chemistry depend on the quality of recharge water, and the processes affecting the water chemistry as it flows through the aquifer systems. However, the palaeo-environmental processes, tectonics and sedimentology have an impact particularly on the development of continental saline aquifers (Verhagen, 1995; Ringrose et al., 2005; Lindenmaier et al., 2014). These processes are a function of the general geology, degree of chemical weathering of the various rocks and inputs from other sources other than water-rock interactions (Domenico, 1972; Hem, 1985); such factors and their interaction consequences may convey complex groundwater quality.

In the semi-arid Kalahari Region, water quality studies have been used as a diagnostic tool to understand occurrence and evolution of groundwater (e.g. Mazor et al., 1980; McCarthy et al., 1991; Linn et al., 2003; Eckardt et al., 2008) and determining recharge rates (e.g. Mazor et al., 1977; De Vries et al., 2000; Brunner et al., 2004; Wanke et al., 2008; Stadler et al., 2010). However, the lithological, stratigraphic and structural controls of geology coupled to groundwater residence time on groundwater quality have been inadequately recognized. Knowledge of residence time is key to establishing if the water quality issue is due to water-rock interactions, mixing or contamination (Darling et al., 2012). Verhagen (1995) suggests that mineralisation of groundwater in the Kalahari Basin is constrained by the aquifer structure which also controls the build-up and/or flushing of the aquifer typically under *pluvial* climatic phases. We investigate the physical and chemical processes that are responsible for the present mineralisation and hydro-chemical evolution of the groundwater regime. It is envisaged that improved understanding of the hydro-chemical system can contribute to effective management and

utilisation of the groundwater resources by clarifying the relations among groundwater quality, aquifer geology and recharge type.

2 Study area

Machile Basin is located in the south-western part of Zambia, southern Africa. It lies between -15.98 S and 17.90 S decimal degrees latitude and 24.09 and 26.50 E decimal degrees longitude (Fig. 1). It covers an area of 26 088 Km^2. The climate of Machile Basin can be classified as semi-arid which is mainly dry except in rainy months (November to March) and characterised by hot-dry summer (April and May; August to October) and cold winter (June to August). The mean annual rainfall in the area is 500 mm (Beilfuss, 2012) and mean recharge has been estimated to 10 mm (Wanke et al., 2008).
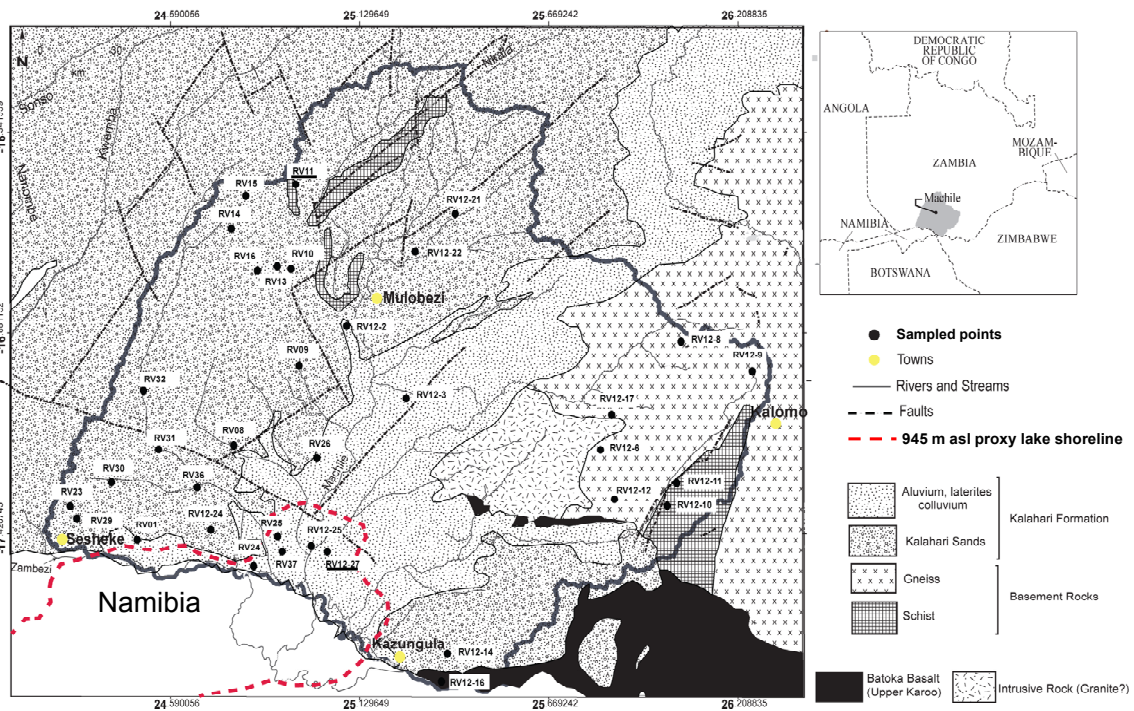
Fig. 1: Surface geology of the Machile Basin (modified fromYemane et al., 2002) and the sampled sites. The basin is composed predominantly of loosely consolidated sediments of the Kalahari formation and hard rock in the western fringe which affects the nature of water-rock interactions. Water chemistry within the 945 m asl proxy shoreline has saline groundwater according to Banda et. al, (2014).

Geologically, the Machile Basin forms part of the Kalahari Group formations with sediments of Post-Cretaceous age (Money, 1972). The study area is cov-

ered by an alluvial complex of fluvio-lacustrine nature from erosion and sedimentation of Pre-Kalahari sediments of the Karoo and Basement rocks (Nugent, 1990; Thomas & Shaw, 1991; Moore & Larkin, 2001; Haddon & McCarthy, 2005; McCarthy, 2013); these formations form part of the Lower Kalahari Group and consist mainly of sandstones, quartzite, chert, conglomerates, clay, sand and silts deposited in the Miocene (Money, 1972). The Upper Kalahari Group is composed of aeolian sands formed from weathering of Karoo rocks, basement rocks and reworking of parts of the Lower Kalahari Group. The thickness of the Kalahari Group formations in Zambia typically range between 10 – 100 m (Haddon & McCarthy, 2005). Tectonic activity along the marginal axes of the Kalahari Rift and the Linyanti-Chobe fault system in the Pliocene (Moore & Larkin, 2001) formed the Lake Palaeo-Makgadikgadi with its northern extension extending into the Machile Basin. Lacustrine sediments of the lake system in the basin have been scrutinized sedimentologically and fossil evidence provided to support its existence (Banda et al., 2015). The palaeo-lake sediments have been mapped to be hosted in the central topographic low of the basin (Chongo et al., 2014b). Mineralogically, alluvial sediments are dominated by quartz and feldspars (Banda et al., 2015) whereas as the basalt rock is composed of pyroxene, Ca-feldspars, volcanic glass and olivine in the Kalahari Basin (Mazor et al., 1980).

2.1 Hydrogeology

Groundwater development project boreholes, drilled to an average depth of 50 m, are the most well documented in the Machile Basin. The main aquifer units, in order of increasing importance as groundwater resources, are (1) the weathered and/or fractured basement rocks, (2) weathered basalts, (3) Karoo sedimentary rocks and (4) the unconsolidated alluvial deposits (YEC, 1995). The unconsolidated alluvial aquifer units, typically sand, gravel and sandstone with intervening clay layers of the Kalahari Group (YEC, 1995) are the main focus in this paper. These aquifers have a granular matrix with an average porosity of 30 % and a hydraulic conductivity between 1.50×10^{-7} and 1.25×10^{-4} m/s (YEC, 1995).

In the study area, depth to the water table in boreholes spread over the entire basin varies on average between 2 and 15 m in the wet season and between 5 and 27 m in the dry season. Piezometeric contours indicate a regime of groundwater flow towards the central axis hosting high salinity groundwater (Fig. 2). Saline groundwater is hosted in the silt-clay rich parts of the for-

mation (Banda et al., 2015) with a measured hydraulic conductivity around 10^{-12} m/s (Margane et al., 2005). Groundwater salinity is hypothesised to be due to dissolution of Lake Palaeo-Makgadigadi evaporites (Banda et al., 2015). It is inferred from previous work in the Kalahari Basin that groundwater recharge, transmission and discharge of the basin are probably controlled by the basin geomorphology, topography, sedimentology and geological structural patterns of the region (Verhagen, 1992; Verhagen, 1995).
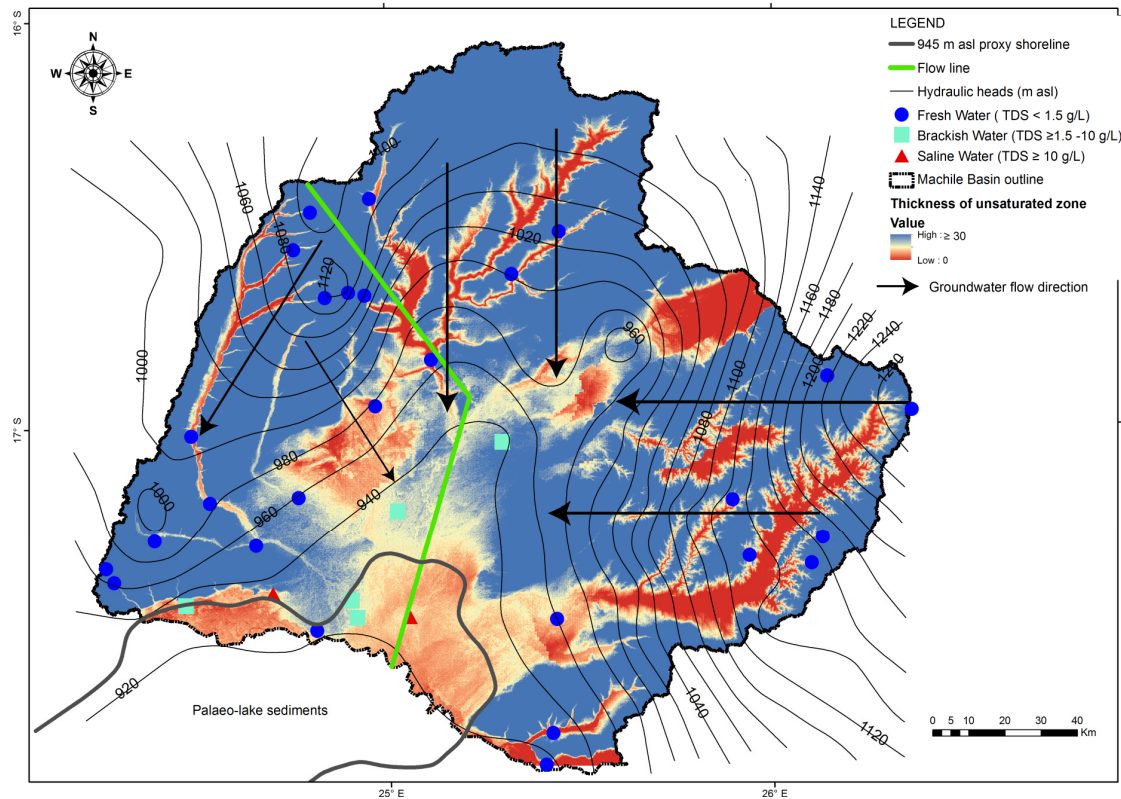
Fig. 2: Thickness of the unsaturated zone distribution map showing a surficial water table within the topographic low region and the river channels suggesting groundwater loss through these channels and evaporation in the dry season period – August to November. The river channels and central topographically low are discharge zones. The groundwater flow line (green line) was used to investigate groundwater processes within the region. Groundwater flow is convergent towards the central region.

3 Materials and methods

3.1 Field measurements

3.1.1 Water level measurements

Accurate elevation above mean sea level (amsl) and location coordinates of available boreholes were obtained with a differential Trimble [TM] R4-5800 system GPS; borehole top of collar was used as a reference point for these measurements. Trimble Business Center 2.30 was used for post-processing these data. Groundwater levels were then measured from the reference points using a dip meter to obtain hydraulic heads above mean sea level. The error budget was 2 mm on the GPS antenna levelling, 4 mm on the antenna height reading and 1 cm on the dip measurement. The locations of the GPS surveyed boreholes and groundwater flow direction with the associated water types are shown in Fig. 2. Water table data points were then interpolated using the kriging method (Alley, 1993) to produce a continuous water table surface. The thickness of the unsaturated zone was then estimated by subtracting surface water table elevation from Shuttle Radar Topographic Mission (SRTM) data.

3.1.2 Borehole logging

Geophysical (borehole) logging was done to delineate the occurrence of fresh and saline formation zones in the basin. Robinson Research Ltd equipment was used for the geophysical logging of the sediments for natural gamma radiation and formation electrical conductivities. Formation electrical conductivities were measured inside the PVC casings using a focused dual induction probe, which has a formation penetration depth of around 5 m and 2 m for the long and Short conductivity (LCON and SCON) respectively. Formation electrical resistivity from the logging was expressed as mS/m and natural gamma in American Petroleum Institute (API) units.

3.1.3 Water sampling

To map spatial variation of groundwater quality, 34 water samples were collected from boreholes for chemical analysis as shown in Fig. 1. Boreholes were purged by three well volumes before samples were collected. This was done to remove groundwater stored in the well and allow for fresh aquifer water to enter the borehole. Physio-chemical analysis for pH, water electrical conductivity (EC), temperature was done with a WTW 350i Multimeter using pH-EC-DO probes. Measurement of alkalinity, was conducted on site using

the Gran titration (Gran, 1952). Polyethylene bottles (20 mls) were thoroughly washed three times with groundwater before sampling. Samples for cations were filtered with a 0.45 µm filter into the bottles and acidified to pH < 2 with nitric acid before storage in a cooler box for transportation to the laboratory. Samples for anions were neither acidified nor filtered after collection. In addition, water samples for stable isotopes (hydrogen and oxygen) were also collected using 20 mls polyethylene bottles.

Based on the groundwater flow direction (section 3.1.1), selected boreholes (nine) were sampled for tritium-helium ($^3H/^3He$) and carbon-14 (C-14) along a flow line. $^3H/^3He$ were sampled using 40 mls copper tubes to prevent any atmospheric interaction. C-14 samples were collected in 50 mls polythene bottles with tight screw caps to prevent any atmospheric interaction.

3.2 Laboratory analysis

3.2.1 Hydrochemistry

Chemical analysis of cations was done using the Perkin Elmer (Analyst 400) Atomic Absorption Spectrometry (AAS) and for anions using Metrohm Ion Chromatography (IC). Trace elements were analysed using Inductively Coupled Plasma Mass Spectrometry (ICP-MS) at the Geological Survey of Denmark and Greenland (GEUS), Department of Geochemistry, Denmark. The quality of the chemical data was assessed using the ionic charge balance.

3.2.2 Isotope analytical methods

Stable isotope ratios of oxygen ($^{18}O/^{16}O$) and hydrogen ($^2H/^1H$) were measured relative to the Vienna Standard Mean Ocean Water (VSMOW) standard and analysed using the Picarro Cavity Ring – Down Spectrometer (PCRDS) equipped with an autosampler and a vaporiser at GEUS. The results were expressed as ‰ units using the δ (delta) notation (Einbond et al., 1996) with standard deviations not larger than ± 0.2 ‰ ($\delta^{18}O$) and ± 0.5 ‰ (δD), as calculated from four replicate injections into the vaporiser.

Tritium (^3H) and helium (^3He) was measured at the University of Bremen, Germany, using the Bremen Mass Spectrometer System. ^3He was measured from radioactive decay of ^3H using an ingrowth method (Sültenfuß et al., 2009); samples are degassed, sealed and stored for 110 days to allow for electrolytic enrichment of ^3He from the tritium decay. The ^3H results were expressed in Unity Tritium (TU), whereas ^3He in cubic centimetres standard temperature and pressure per kilogram (cc STP/kg).

We then estimated the proportion of young and old water by comparison of the measured ^{3}H concentration to the infiltrated ^{3}H content (from precipitation) in the last decades. ^{3}H datasets from the last decades (1960-2005) are obtainable from the WISER Database (IAEA & WMO, 2006), at the Ndola Station being the closet proxy to the study area. The tritium concentration in the long term record was corrected to account for radioactive decay scaled to 2014; We applied an approximate steady state decay correction factor of 0.08 (Kalinowski, 2004) to the tritium precipitation data at Ndola station hence a long term tritium average of 2 TU. Therefore you can derive, that water below 2 TU should be a mixture of older water which is free of tritium, (recharged before 1955). The ^{14}C activity and δ^{13}C versus ‰ (versus V-PDB) were measured at Beta Analytic Limited, Florida by accelerator mass Spectrometry. Uncertainty for δ^{13}C is 0.15 ‰ and that for ^{14}C is 1 % of the measured activity and expressed as percent of modern carbon (pmc).

3.2.3 Cation Exchange Capacity

Cation exchange capacity (CEC) measurements were carried out on sediment core from RV12-27 (shown in Fig. 1) after the work by Banda et al. (2015); specific sample depths were at 14, 15, 17, 19, 23, 28, 30, 45 and 50 m bgl. Adsorbed cations and total cation-exchange capacity (CEC) was based on Appelo & Postma (2005), using 1M NH_4Cl rather than NaCl to replace adsorbed cations enabling ICP-MS analysis of the desorbed cations. Adsorbed NH_4 was determined by replacing adsorbed NH_4 using a 1M NaCl solution. Total CEC was determined by replacing the adsorbed NH_4 from the first step with Na using 1 M NaCl. The pH of all solutions was kept close to 4.9. Ten grams of sediment core from each interval sampled were immersed in 1 M NH_4Cl in a 30 ml Teflon centrifuge tube for one hour. After centrifugation and decanting of the supernatant, the NH_4Cl saturation step was repeated twice more, for a total of three stages. The supernatant from each step was combined and analysed by ICP-MS for Na, K, Ca, Mg, Al and Fe. Alkalinity and SO_4 was measured on the first saturation step to enable correction for dissolved carbonate and gypsum, the effect turned out to be negligible.

3.2.4 Sediment pore-water analysis

Sediment drill core samples from the investigation borehole (RV 12-27) were also subjected to pore-water analysis at varying depths (14, 15, 17, 19, 19.6, 21, 23.5, 28, 30, 35.2, 45 and 50 m bgl.)

Pore-water was extracted using centrifugation as described by Edmunds & Bath (1976) (note that some of the sediment yielded little or no water). The

resulting water sample (usually ~2 mls) was filtered through 0.45-μm membrane filters. A saturated paste method was used for the low yielding sediments. These Saturated Paste Extracts (SPEs), provide information on the chemistry of solutes in soil solution (Rhoades, 1982) and were prepared using the method described by the Non-affiliated Soil Analysis Work Committee - NASWC (1990). The samples were saturated with deionised water to create a saturated paste, and the water was extracted and filtered using centrifugation followed by filtering. The dilution factor introduced was computed by calculating the sum of the available soil water mass as aliquot (using the measured moisture content) added to the measured diluent (deionised water) mass divided by the aliquot mass. The measured concentrations were multiplied by the dilution factor to get actual pore-water concentrations. It is possible however, that some reactions between the sediment and added water during the 'pasting' could changes the water chemistry. Pore-water chemical analysis for major cations and anions was done using the Perkin Elmer ICP-MS and Dionex IC, respectively. Physio-chemical measurements of electrical conductivity (EC) were made with a benchtop Hach Radiometer Analytical and CDC866T Conductivity Cell and pH was measured using a WTW 3310 IDS instrument and electrode. Alkalinity was determined by Gran titration (Gran, 1952).

3.2.5 Sediment dilution experiment

Approximately 20 g of sediment samples in 9 batches from drill cores of varying depth [Borehole RV 12-27, shown in Fig.1, sampled by Banda et. al, (2014)] was collected in 50 mls centrifuge tubes and filled with deionised water; specific sample depths were at 14, 15, 17, 17.5, 19, 23, 23.5, 28, 30, 45 and 50 m bgl in 12 batches. Centrifuge tubes were placed on a mechanical shaker to dissolve soluble mineral phases. The EC was measured at various time periods until a constant EC was observed to indicate equilibrium. To separate the aliquot from the sediment, it was centrifuged and water extracts were placed in a 1L polythene bottle. Fresh deionised water was then replaced in the centrifuge tube and the dilution process repeated several times until the EC was almost zero; indicative of complete dissolution of readily soluble mineral phases.

3.3 Modelling

3.3.1 Groundwater flow and geochemistry

A steady state numerical groundwater flow model was set up along a groundwater flow line using the code MODFLOW (Harbaugh et al., 2000) in

the graphic user interface PMWIN 8 (Chiang & Chiang, 2001) to understand the hydrological regime. To explain geochemical reactions and mineral equilibrium, PHREEQC 3 (Parkhurst & Appelo, 1999), was used.

3.3.2 Adjustment of Radiocarbon ages

Traditional well known inorganic adjustment models (Ingerson & Pearson, 1964; Mook, 1972; Tamers, 1975; Fontes & Garnier, 1979; Eichinger, 1983) have been applied to Dissolved Inorganic Carbon (DIC) of water from a single well to estimate ^{14}C ages. This approach is well suited for geochemical systems undergoing simple water-rock reactions, such as carbonate mineral dissolution, gypsum dissolution, Ca/Na ionic exchange, CO_2 gas dissolution, and isotopic exchange between soil CO_2, calcite and DIC during recharge. NETPATH (Plummer et al., 1994) was used in this paper, as it incorporates traditional models and can be used for complex hydro-chemical systems. Typically in NETPATH, the initial and final waters are defined separately. NETPATH is then used to describe chemical reactions that reproduce the chemical and δ^{13}C isotopic composition of DIC in the final water. This in effect produces separate adjustment models for each water analysis. The adjustment is applied to the initial ^{14}C to compute the ^{14}C expected in DIC at the final water as if there was no radioactive decay. The adjusted ^{14}C with no-decay is then used with the measured ^{14}C activity to compute travel time from the initial point to the final point. Details on radiocarbon adjustment with NETPATH are given in Plummer et al. (1994). The modelling uncertainty for δ^{13}C and ^{14}C activities is dependent on the inherent assumptions from the adjustment models.

4 Results

4.1 Physical processes (and groundwater flow modelling)

Groundwater flow converges towards the central region of the Machile Basin with a higher hydraulic gradient of 0.002 in the fresh water zone compared to 3.08×10^{-4} in the saline zone (Fig. 2). These gradients suggest a net high groundwater flow within the freshwater fringe zone compared to a more or less stagnant saline central pool. The upland unsaturated zone is thicker (more than 30 m) and thins out towards the topographic low (central region), topographic depressions and in the river valleys; these regions are topographic groundwater discharge zones (Fig. 2). Evaporation and evapo-transpiration are potential groundwater sinks in these discharge zones.

Generally, the geology is homogenous within individual fresh and saline areas of the basin; example logs are shown in Fig. 3. The long and short induction geophysical logs were exactly the same hence only one is shown. The fresh groundwater borehole was composed of unconsolidated sand and sandstone with natural gamma of 5-30 API and formation electrical conductivity between 0-5 mS/m. On the other hand, the saline borehole was intercalated sandy-clay, clayey-silt and sand with a natural gamma of 6-36 API and formation electrical conductivity 30-300 mS/m.

It is apparent from the hydro-stratigraphy and hydraulic gradients that two formations of contrasting hydraulic conductivities is present in the Machile Basin. A conceptual model of the groundwater flow regime (Fig. 4) was also developed based on available literature on the basin (YEC, 1995; Chongo et al., 2011; Banda et al., 2015; Chongo et al., 2014b) and field experiences. We infer that fresh groundwater from the upstream regions is lost to evaporation/ evapo-transpiration or forced out through topographic depressions due to the hydraulic conductivity contrast between the fresh and saline region.
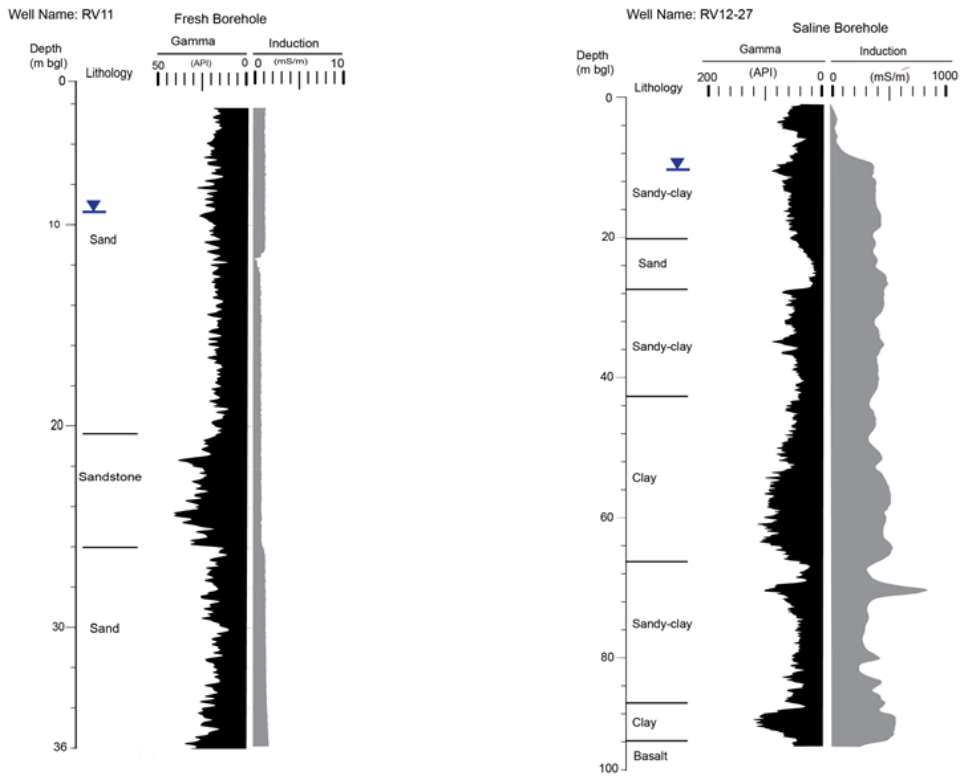
Fig. 3: Example borehole geophysical profile from the fresh and saline regions. Fresh groundwater boreholes are generally composed of unconsolidated sands compared to inter-calations of clayey silt and sands in the saline part
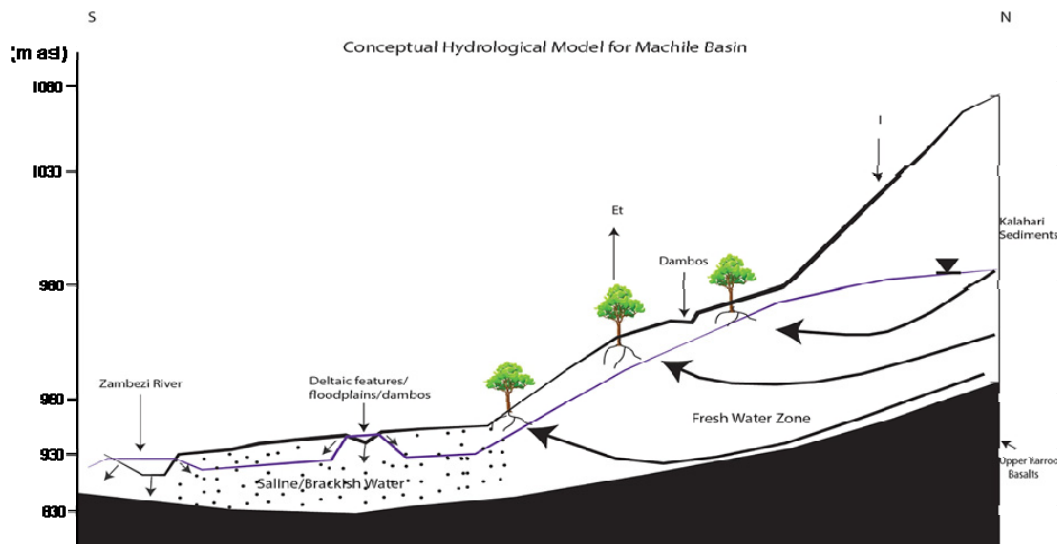
Fig. 4: Conceptual model of the Machile Basin, North to South following a streamline. Evapo-transpiration through the root zone and evaporation through the topographic are the main sinks for the groundwater. Flow through the saline zone is probably not present or at least very little given the hydraulic conductivity contrast. Lateral groundwater flows are probably possible via the dambos.

Local flow systems around the topographic depressions, dambos (small wetlands), deltaic alluvial features and rivers (i.e. Perennial Zambezi River and some of its tributaries) are present. Intermediate systems of groundwater flow could occur at the topographic depressions and at the interface between saline and fresh groundwater. Regional systems of groundwater flow would probably occur from the recharge area to the saline/fresh water interface. Infiltration of precipitation is probably the main source of groundwater replenishment generating a flow towards the saline low hydraulic conductivity region. Diminutive amounts of fresh groundwater may penetrate the saline zone; however, the majority is lost to evaporation.

To test the feasibility of the proposed conceptual model, we model the groundwater flow regime based on parameters, grid dimensions and assumptions given in Table 1. Given the heterogeneity of lithologies within the saline zone (intercalations of sand and clay) a net average hydraulic conductivity of 10^{-6} m/s is assumed. 10^{-4} m/s for sand in the fresh water zone was used (Table 1). Recharge of 10 mm/yr (Wanke et al., 2008) was assumed for the entire transect with potential evapo-transpiration of 1500 mm and the depth to which the roots would reach the water table (extinction depth) of 10 m. The model simulates the topography of the transect line.

Table 1: Modelling parameters used to simulate the hydrological regime in the Machile Basin. We assume a homogenous hydraulic conductivity of 10^{-4} for the fresh zone and 10^{-6} m/s for the saline zone.

Parameters	Grid Dimensions
- Recharge on the entire transect 10 mm/yr	- 1 x 100 x 50 (Row x Columns x layers)
- Potential Evaporation over the entire transect 1500mm/yr	- 150 Km transect N-S across the Machile, following a streamline
- Extinction depth 10 m	- Width of each 1.5 km
- Horizontal Conductivity 10^{-6} m/s (clay in saline pool); 10^{-4} m/s (fresh water zone)	- follows the topographic surface
- Vertical Conductivity 10% Horizontal	
- Wetting capability: -1	

We observe that fresh groundwater flows towards the saline pools, but due to the hydraulic conductivity contrast groundwater is forced out and lost to evaporation through river channels and dambos (wetlands) in the topographic

depressions (Fig. 5). Particle tracking shows local flow systems are younger in age ranging from <500-2 000 yrs in the freshwater zone whereas these are much older in the saline regions in excess of 50 000 yrs old. Intermediate and regional flow was focused in the freshwater zone with ages up to 5 000 and 10 000 yrs. The Zambezi River seems to be a losing river at least within 3 kms (Chongo et al., 2014a) probably during drier periods of the year. Leaching or weathering processes are thus probably more active in the freshwater zone given the high hydraulic permeability aquifer units. The consequential hydro-chemical regime is investigated in the proceeding sections.
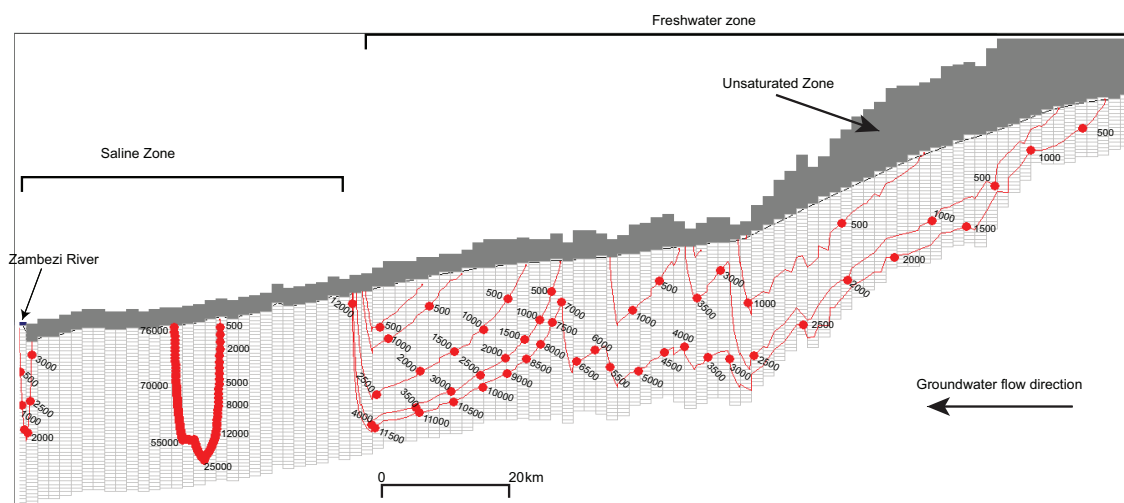
Fig. 5: Two-dimensional transect model showing groundwater flow within the fresh groundwater zone and particle tracking time stamps; each time stamp after the starting point is 500 years. Due to the conductivity contrast, most of the groundwater upstream is forced upwards at the interface and lost to evapotranspiration in the unsaturated zone (shown in grey). Younger water occurs close to the water table in the fresh water zone and becomes older with depth compared to the saline zone with high residence time. The Zambezi River is losing groundwater towards the saline pool at least within 3 km of the transect.

4.2 Hydrogeochemistry and isotopes

4.2.1 Hydrochemistry

Groundwater samples have been classified into three clusters based on water quality (fresh – Total Dissolved Solids (TDS) < 1.3 g/L, brackish – 1.3 to 10 g/L or saline, > 10 g/L) and spatial position within the basin as shown in Fig. 2. The results of field measurements and chemical analyses in the study area are shown in Table 2.

Table 2: Hydrochemistry results over the sampled boreholes in the Machile Basin highlighting low (fresh) salinity (brackish and saline) and high salinity water.

ID	Site	Stable Isotopes δD	δO^{18}	Temp °C	DO mg/L	pH	EC µS/cm	Na mg/L	K mg/L	Ca mg/L	Al mg/L	Si mg/L	Mg mg/L	HCO3 mg/L	Cl mg/L	SO$_4$ mg/L	Percent Error	Cal.	Gyp.	Dol.
Fresh groundwater																				
RV12-2	Machile Basic School	-49.9	-7.52	24.4	1.7	7.4	482	32.8	3.60	59.1	0.09	23.4	12.9	270	12.4	14.6	4%	-0.2	-2.5	-0.6
RV12-6	Nyawa Village	-41.6	-6.56	23.1	5.9	6.8	462	44.9	2.78	41.7	0.06	25.6	12.5	240	15.6	10.8	2%	-0.8	-2.7	-1.7
RV12-8	Sichifulo School	-46.8	7.12	27.6	4.3	6.9	425	29.1	2.93	41.0	0.04	19.5	20.3	290	2.45	1.20	4%	-0.4	-3.7	-0.8
RV12-9	Simuluwe Village	-48.5	-7.38	23.3	6	7.1	389	17.2	3.58	49.8	0.04	22.8	20.6	280	1.89	0.51	5%	-0.5	-3.9	-0.9
RV12-12	Malimba Village	-46.3	-7.01	25.7	6.8	7.3	558	51.6	1.48	49.7	0.05	18.3	20.0	300	9.36	5.43	5%	-0.1	-3	-0.3
RV12-16	Katombora Village	-44.3	-6.34	25.3	4.8	6.7	459	24.0	0.60	48.1	0.06	45.1	16.7	143	17.0	19.6	8%	-0.9	-2.4	-2
RV12-17	Kachabula Village	-40.9	-6.40	21.8	5.2	7.2	191	15.7	0.41	16.6	0.04	23.5	7.35	120	0.00	0.81	4%	-1.1	-4.1	-2.2
RV12-21	Mabwae Village	-49.8	-7.41	26.1	1.8	6.5	190	10.3	5.41	24.1	0.01	27.2	2.58	116	5.46	0.00	-0.3%	-1.8	-4.6	-4.2
RV12-22	Moomba Primary	-48.0	-7.20	25.9	4.2	6.8	64	2.13	5.15	7.02	0.03	14.8	0.52	24.2	2.50	0.00	10%	-3.4	-5.1	-7.7
RV10	Mulundano Village	-42.2	-6.37	24.5	6	5.3	16.4	1.01	1.02	0.96	0.02	8.52	0.27	1.67	2.96	0.00	12%	-3.8	-5.9	-8
RV11	Bwina RHC	-50.6	-7.49	12.8	7.1	6.9	56.4	1.20	2.86	7.06	0.03	10.5	0.82	53.5	1.24	0.00	4%	-2.3	-5	-5.5
RV13	Sipula Village	-49.3	-7.52	27.6	4.7	6.4	67.2	3.47	2.21	6.48	0.06	26.7	1.06	33.3	0.77	0.00	6%	-2.5	-5.1	-5.5
RV14	Sisibi Basic School	-51.8	-7.75	22.6	7.6	6.6	16.8	0.77	2.39	0.47	0.06	11.1	0.33	24.7	1.17	0.00	-3%	-3.7	-6.2	-7.3
RV15	Kabula Village	-49.7	-7.46	22.9	8.7	6.9	12.8	0.60	0.75	1.11	0.06	5.1	0.09	46.5	2.29	0.00	1%	-2.9	-5.8	-6.7
RV16	Sianga Village	-48.6	-7.26	23.7	2.6	6.4	18.6	0.64	2.75	1.06	0.04	11.1	0.20	17.1	0.00	0.00	3%	-3.6	-5.8	-7.8
RV23	Namatwi Village	-53.4	-7.76	26.7	6.1	7.4	566	31.9	5.04	68.3	0.04	30.1	24.3	405	1.76	0.79	2%	0.2	-3.7	0.5
RV29	Mapilelo Village	-51.9	-7.80	27	5	7.5	432	29.5	5.64	35.5	0.04	24.8	25.3	318	0.00	0.48	1%	-0.1	-4.1	0.1
RV30	Chisu Village	-50.6	-7.63	23	5.6	6.7	82.6	3.84	1.68	10.0	0.02	11.9	1.68	50	6.39	0.00	-1%	-2.2	-3	-4.9
RV31	Lusinina Village	-52.8	-7.87	21.1	5.3	7.4	327	12.0	2.80	55.5	0.04	17.2	3.94	200	6.11	3.82	2%	-0.1	-3	-1.1
RV32	Mushukula Village	-49.9	-7.56	17.6	4.2	6	28	0.52	1.72	2.21	0.07	8.4	0.63	15.3	1.04	0.00	1%	-4	-5.5	-8.4

ID	Site																		
RV09	Salumbwe Village	-50.7	-7.50	27.7	5.7	6.8	308	11.1	3.20	34.3	0.03	18.9	14.0	158	5.11	0.38	3%	-0.9	-4.2	-1.9
RV36	Lipumpu Village	-24.3	-3.07	24.1	5.9	7.2	563	6.9	4.44	105	0.05	42.7	13.5	398	3.00	3.45	0%	0.1	-2.8	-0.3
RV24	Mwandi Mission	-23.5	-3.34	24.6	7.5	6.8	580	13.7	1.52	9.20	0.03	17.3	2.29	65.7	2.68	1.27	5%	-1.7	-4.1	-3.7
RV08	Lutaba Basic School	-50.1	-7.28	26.6	6.6	7.3	519	16.4	7.07	69.9	0.03	38.5	18.7	320	3.91	3.20	2%	-0.1	-3.1	-0.2
RV12-10	Siamulunga Village	-48.8	-7.02	26.1	5.1	7	1156	71.1	2.99	102	0.09	16.8	57.3	532	38.8	17.2	3%	-0.1	-2.4	-0.1
RV25	Situlu Health Post	-31.7	-3.61	18.9	8.3	7.6	1017	256	3.00	1.85	4.10	54.6	0.26	505	42.1	49.1	4%	-1.1	-3.4	-2.9
RV12-11	Sijabala Village	-40.8	-6.49	25.6	6.7	7.2	825	60.7	3.66	55.6	0.04	12.2	24.1	0.58	14.2	7.74	8%	-0.1	-2.8	-0.2
RV12-14	Nachilinda School	-48.8	-7.22	27.5	2.4	6.9	946	24.6	1.65	27.0	0.03	18.9	4.56	85	2.11	57.1	4%	-0.9	-2.1	-2.2
Brackish groundwater																				
RV01	Katongo Basic	-46.0	6.08	25.5	6.1	7.9	1060	200	2.70	22.1	0.02	16.0	4.61	135	168	99.1	6%	-0.1	-2.1	-0.6
RV37	Makanga Village	-33.9	-4.40	22.6	6.1	6.9	2540	564	6.00	12.4	0.02	42.1	2.56	225	366	458.0	4%	-1.4	-1.9	-3.1
RV26	Adonsi Basic School	-52.4	-7.65	28.2	4.2	8.3	4710	1068	5.50	15.4	0.07	12.1	6.45	256	740	1097.3	0%	0.1	-1.6	0.2
RV12-3	Katemwa Village	-50.6	-7.62	27.8	5	7.1	2200	365	13.7	124.9	0.01	22.0	12.5	396	360	260.0	2%	-0.2	-1.2	-1
Saline groundwater																				
RV12-27	Kasaya Basic School	-46.0	-5.68	26.4	2.3	6.8	23300	5279	16.5	770	0.01	31.5	265.5	440	5904	5560.0	0%	0.2	0.1	0.3
RV12-24	Simungoma Basic	-50.0	-7.21	28.2	6	7.5	7210	1548	9.70	164	0.15	36.1	46.8	317	1092	1969.0	1%	0.4	-0.6	0.5

Temperature ranged from 12.8 to 28.2 °C with an average of 24.5 °C. The pH values ranged from 5.3 to 8.3 with most values near neutral (7). Water electrical conductivity (EC) ranged from 12.8 to 23 300 µS/cm and increases towards the centre of the basin following total dissolved solids (TDS) shown in Fig. 2.

The concentration of major cations decreased in the orders Na > Ca > Mg > K and of anions Cl > SO_4 > HCO_3 > NO_3. Cation concentrations are characterised with Na, 0.52-5,300 mg/L, Ca, 0.50-770 mg/L, Mg, 0.10-265 mg/L and K, 0.41-16.5 mg/L. Anions are typically of Cl, 0-5,900 mg/L, SO_4, 0-5,570 and HCO_3, 0-533 mg/L. Typically, the concentrations vary depending on salinity (Table. 2). A Piper plot (Piper, 1944) combined with stiff diagrams differentiates three types of geochemical types of groundwaters (Fig. 6); fresh groundwater was characterized by a Ca-(Na)-HCO_3^- water type, whereas the brackish and saline groundwaters characterised typically by Na-Cl-SO_4 (Na-SO_4-Cl in some places) and Na-HCO_3^- water type. Mineral saturation of calcite was observed in the majority of the of the groundwater types. In addition the saline water was saturated or close to saturation for gypsum and dolomite (Table 2).

4.2.2 Stable isotopes

Stable isotope results from the regional groundwater samples (Fig. 7) shows the fresh groundwater outside the topographic depression is on the precipitation line whereas the saline and brackish groundwater within the topographic low region are clustered on or between the evaporation ($\delta D = 5.03\delta^{18}O - 14$) and precipitation ($\delta D = 8.13\delta^{18}O + 10.8$) lines. The precipitation line was based on average stable isotope records (1968-2009), from the Ndola global monitoring station which was analogous to the global meteoric water line; $\delta^{18}O$ and δD range from -9.07 to -3.03 and -60.5 to -9.6 respectively. The majority of fresh groundwater samples are in receipt of rapid recharge with little or no evaporation before infiltration; evapotranspiration would potentially be a more important process.
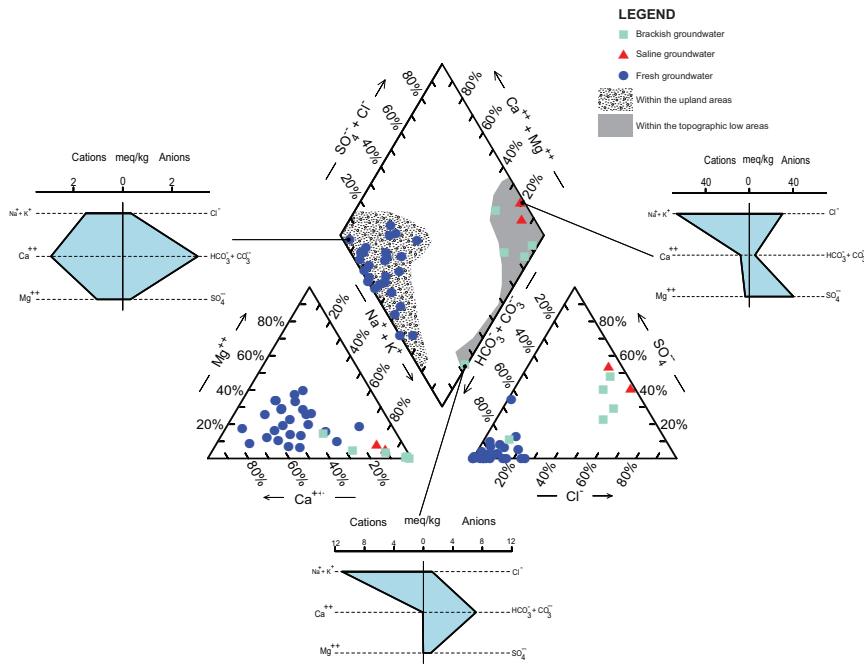
Fig. 6: Piper Diagram (Piper, 1944) and Stiff diagram (Stiff Jr, 1951) showing distinct groundwater types in the Machile River Basin (fresh Ca-Mg-HCO$_3^-$ water type and saline Na-Cl-SO$_4$ type) and the location within the basin.
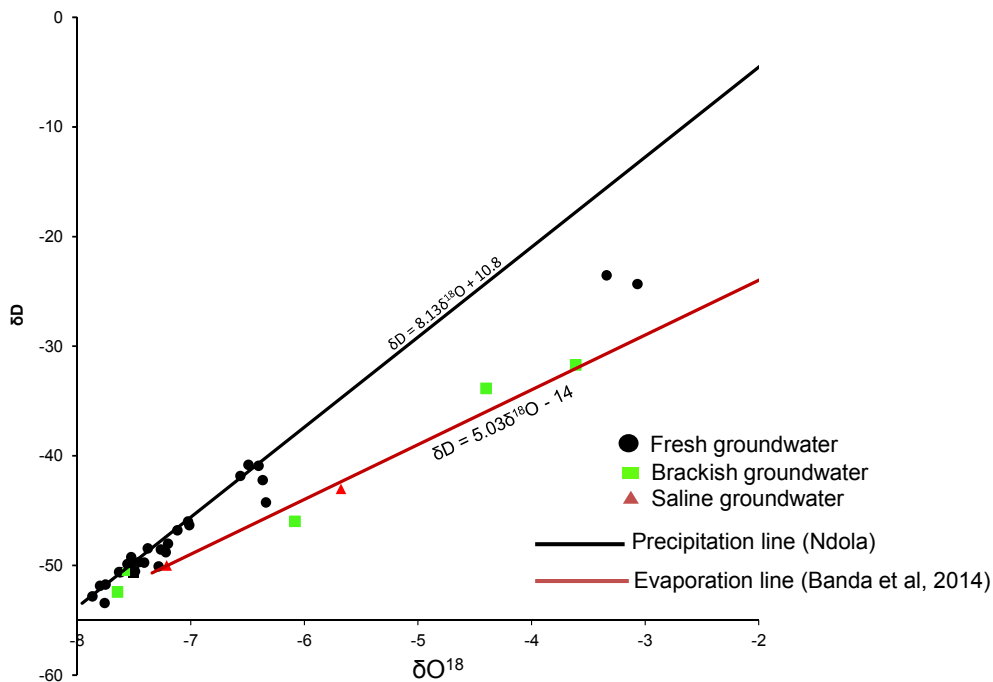
Fig. 7: A plot of stable isotope (δD and δ^{18}O) showing that the fresh groundwater and some brackish samples in the fringes of the Machile Basin plot on the precipitation line whereas saline-brackish samples within the palaeo-lake sediments plot on the evaporation and precipitation line. The saline-brackish samples are therefore a result of fresh water recharge and evapotranspiration.

However, highly fractioned fresh groundwater samples are also observed probably due to infiltration after surface evaporation from ponding within shallow depressions (dambos) which characterise the area. Stable isotopes of $\delta^{18}O$ and δD are -8 to -2 and -55 to -20 ‰, respectively, within the freshwater zone. Brackish groundwater was split between the precipitation and evaporation line suggestive of both evapotranspiration for those on the precipitation line and evaporation. Brackish samples have a δO^{18} ranging from -8 to -3 ‰ and δD between -55 to -30 ‰. Saline groundwater was on the evaporation line with a slope (5) suggestive of humidity 75 % assuming constant air speed, temperature before infiltration (Gonfiantini, 1986). Saline groundwater isotopes suggest a high degree of evaporation before infiltration giving an isotopic signature for δO^{18}, -8 to -5 ‰, and δD, -55 to -40 ‰.

4.2.3 Radioactive Isotopes and Modflow ages

Results for the ^3H, ^{14}C and $\delta^{13}C$ isotopes along the flow line (high to low hydraulic gradient in Fig. 2) are summarized in Table 3. ^3H results ranged from 0.03-0.94 TU in the fresh-transition zone and 0.00-0.71 TU within the brackish to saline zone; this is indicative of generally old water (> 60 yrs) with some fraction of young water. The fraction of the young groundwater component was between 15-40 % within the transition zone area and near the perennial Zambezi River.

Table 3: Shows the isotopic chemistry and the proposition of old and young water along the flow line. The aquifer system is predominately old (> 60 years) based on the low tritium concentration; however, juvenile water is more prevalent in the transition zone (i.e. Lutaba).

Borehole name (Upland to topographic low)	Depth of Borehole (m)	Tritium [TU]	Estimated portion of old water (> 60 years)	δ13C ‰	^{14}C pmc (uncorrected)	Water Quality Zone
1. Sipula Village	25	0.03	99%	-21.5	87.9	Fresh
2. Machile Basic School	60	0.29	90%	-20.1	57.3	Fresh
3. Salumbwe Village	55	0.94	60%	-19.5	93.2	Transition
4. Lutaba Basic School	45	0.43	85%	-16.0	63.6	Transition
5. Adonsi Basic School	45	0.00	100%	-20.1	67.8	Saline
6. Situlu Health Post	50	0.00	100%	-13.7	66.3	Saline
7. Kasaya Basic School	25	0.05	98%	-14.9	75.6	Saline
8. Makanga Village	40	0.03	99%	-15.1	102.5	Saline
9. Mwandi Basic school	30	0.71	75%	-12.8	106.2	Fresh in close proximity (<5 km) to Zambezi River

^{14}C activity in the fresh-transition zone was 57.3-93.2 pmc (uncorrected), whereas in the brackish-saline zone 66.3-106.2 pmc; increase in the ^{14}C activity in the transition and within the saline region are suggestive of infiltrating water contribution with recent atmospheric-water interaction. Furthermore, δ^{13}C showed an increasing trend in the fresh-transition zone from -21.5 to -16 and -20.1 to -12.8 in the brackish-saline zone, suggestive of formation derived dissolution of carbonate solutes, which increase along the groundwater flow line.

NETPATH uses inputs of both measured ^{14}C and δ^{13}C as inputs to generate several adjustment radioactive model results; typically the results from the Vogel (1970) model are acceptable as apparent ages for Kalahari groundwaters (Vogel & Van Urk, 1975; Selaolo, 1998; Stadler, 2005) with an assumption of 85 pmc as initial ^{14}C activity and a 15 % carbonate dilution effect. The Vogel model, however, overestimated the apparent ages for some stations along the flow line probably due to unaccounted for dissolved inorganic carbon (DIC). The Fontes & Garnier (1979) and Mass balance approach models then performed better in such cases (Table 4). Fontes & Garnier (1979) considers a two stage evolution of recharge water, accounting for dissolution and isotopic exchange with carbonate minerals: it assumes an initial ^{14}C of 50.7 pmc. The Mass balance model considers carbonate dissolution, soil gas CO_2 dissolution and gypsum dissolution; it was applied for the Kasaya station. Furthermore, we used a user defined model for the Mwandi station which was seemingly in receipt of fresh groundwater from the Zambezi River; an initial value for ^{14}C of 104.3 pmc (Clark & Fritz, 1997) was assumed. Typical ages within the fresh water zone range from 281-4,540, whereas, in the brackish-saline region 139-11,700 (corrected ^{14}C ages (Table 4)).

Table 4: Corrected Carbon-14 apparent ages, adjustment models and model ages for groundwater samples along the flow line. Different adjustment models were used for the correction which gave comparable ages to what has been reported in the Kalahari waters.

Well name & Water Quality	DIC (mmol/L)	Modflow ages (yrs.)	^{14}C apparent ages (Uncorrected)	^{14}C apparent ages (Corrected)	Adjustment model
Sipula Village (Fresh water- fringe Zone)	0.99	600	1040 +/- 30 BP	281	Fontes and Garnier
Machile Basic School (Fresh – fringe zone)	3.41	3600	106 +/- 30 BP	4 544	Vogel
Salumbwe Village (Freshwater – transition zone)	2.83	1000	570 +/- 30 BP	196	Vogel
Lutaba Basic School (Freshwater – transition zone)	3.56	2500	3640 +/- 30 BP	2 757	Vogel
Adonsi Basic School (Saline – central zone)	4.08	4000	3250 +/- 30 BP	1 869	Vogel
Situlu Health Post (Saline – central zone)	6.92	6000	3300 +/- 30 BP	2 054	Vogel
Kasaya Basic School (Saline – central zone)	8.80	10000	10210 +/- 40 BP	11 694	Mass Balance
Makanga Village (Saline – central zone)	4.62	2000	2250 +/- 30 BP	969	Vogel
Mwandi Basic school (Near the Zambezi River)	1.41	500	4470 +/- 30 BP	139	User defined

4.3 CEC

Table 5, shows the exchangeable cations (Ca, Mg, Na, K, Al, Fe, NH$_4$) on the sediments, and the total Cation Exchange Capacity given as the sum in meq/100g dry sediment. Ca, Na and Mg are the dominating ions with 0.51-11.0, 0.16-7.03 and 0.10-3.60 meq/100g respectively. The rest of the ionic species have low to negligible contribution on the sediments; Fe (0 meq/100g), K (0.05-0.48 meq/100g), Al (0.00-1.52) and NH$_4$ (0.00-0.20). CEC thus covers a wide range from 0.87-21.0 meq/100g, with an average of 12.4 meq/100g or ~1 eq/l pore-water if we assume a porosity of 0.25 of the sediments. The implications of these measurements on the resulting ground-water chemistry are discussed in section 5.

Table 5: Cation Exchange Capacity (CEC) of samples from the investigation borehole (RV 12-27) at sampled depths.

Depth m bgl	CaX2 meq/100g	NaX meq/100g	FeX2 meq/100g	MgX2 meq/100g	AlX3 meq/100g	KX meq/100g	NH4X meq/100g	EC (sum), meq/100g
14	5.80	2.22	0.00	3.09	1.52	0.27	0.02	12.9
15	10.95	2.31	0.00	2.78	0.00	0.28	0.12	16.5
17	7.29	2.42	0.00	1.22	0.00	0.17	0.20	11.3
19	9.75	2.70	0.00	2.70	0.00	0.23	0.01	15.4
23	8.11	0.53	0.00	0.43	0.00	0.05	0.00	9.13
28	5.36	1.33	0.00	0.59	0.00	0.05	0.18	7.52
30	0.51	0.16	0.00	0.10	0.02	0.06	0.00	0.87
45	9.66	3.42	0.00	3.60	0.00	0.37	0.08	17.1
50	10.90	7.03	0.00	2.51	0.00	0.48	0.09	21.0

4.4 Sediment pore-water analysis

Pore-water hydrochemistry results are shown in Table 6; the majority of analyses have an associated electrical balance charge error of < 10%. Hydrochemistry results indicate that cation dominance is Na >> Ca > Mg > K, whereas anion dominance was SO_4 > Cl > HCO_3 >> Br. Na concentrations range from 121 to 6,938 mg/L whereas Ca was 12.4 to 347 mg/L. Sulphate results range from 112 to 6,798 mg/L compared to chloride with a range of 24 to 5,883 mg/L. Pore-water electrical conductivity (EC) ranges from 648 to almost 30,000 µS/cm, corresponding to a range from fresh to saline water.

Table 6: Pore-water composition of the sediment core samples from the investigation borehole (RV 12-27). SPE refers to saturated paste extraction where centrifugation yielded little or no pore-water.

Depth m bgl	Method	pH	Alkalinity as HCO3 (mg/L)	Cl mg/L	SO$_4$ mg/L	Na mg/L	K mg/L	Ca mg/L	Mg mg/L	Mn mg/L	CBE (%)	EC µS/cm
14	SPE	6.2	133	747	4697	2840	10.7	82.4	21.0	0.22	3.7%	9766
15	SPE	6.5	242	290	2902	2759	23.4	395.4	69.4	7.66	34.3%	5919
17		7.9	405	185	1199	763	7.3	90.5	17.1	0.34	3.8%	2860
19	SPE	6.2	446	2395	4872	3704	36.5	100.8	31.0	0.02	1.3%	15179
21		5.7	37	5631	6798	6497	33.2	347.3	124.6	0.90	2.0%	25675
23		6.9	131	54	1966	670	16.1	317.9	40.6	0.20	5.4%	3670
28		8.6	882	238	373	622	5.7	29.6	9.8	0.07	2.5%	2389
30		7.5	243	24	113	122	11.8	12.4	1.7	1.17	0.7%	648
35	SPE	6.2	334	2043	3876	3465	18.7	136.4	39.1	0.00	6.1%	13560
45	SPE	6.2	144	5884	6795	6938	111.7	304.1	109.2	0.20	4.0%	29686
50	SPE	6.6	1246	1010	1295	1335	10.2	28.2	7.3	0.00	10.9%	5895

4.5 Sediment dilution experiment

Fig. 8 shows five representative batches of the sediment dilution experiment; maximum EC was 1600 µS/cm over several sediment pore volumes; maximum pore volumes were up to 300, but only data up to 50 pore volumes are shown for clarity. The calculated EC at equilibrium for calcite and gypsum (using PHREEQC) are also shown; the ECs are 642 and 2782 µS/cm respectively. The representative plot (Fig. 8) shows that initially gypsum is completely and relatively rapidly dissolved before calcite dissolves at a slower rate. Depending on evaporite sediment concentrations the sediment samples were leached completely of readily soluble phases after 10-60 days on the mechanical shaker.

We assume the amount of gypsum and calcite leached from the sediment could be derived from the SO$_4$, and measured alkalinity assumed to be HCO$_3^-$

concentrations in the final pool volume respectively; final pool volume represents the total volume of water used in each dilution batch experiment run.
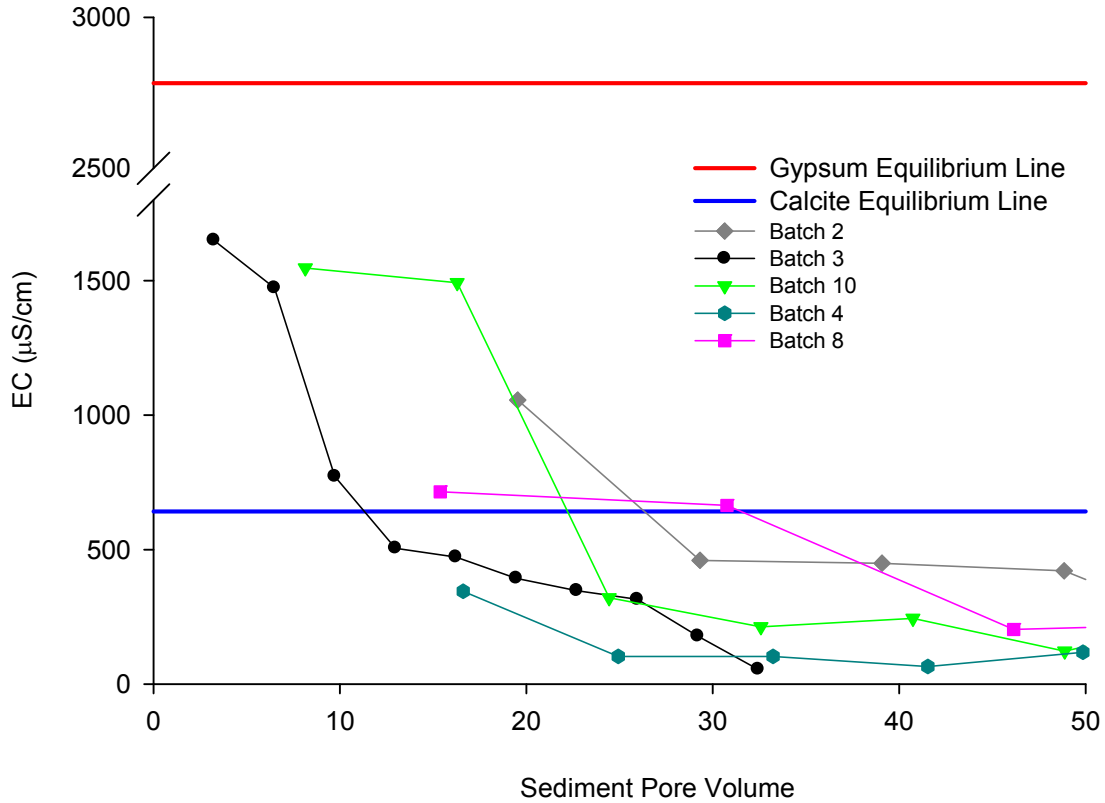
Fig. 8: Dilution experiment plot of five batches, indicating initial and rapid complete dissolution of gypsum followed by slow carbonate dissolution. Calculated EC at equilibrium line for gypsum and calcite using PHREEQC are also shown. Results show that salinity within the saline groundwater would be flushed if there was through flow.

We corrected the SO_4 and HCO_3 (assuming half of the measured concentration is from dissolving inorganic carbon) for the content in the pore-water (Table 6), to establish the contribution from the sediment. Less than 0.03% gypsum and <0.2 % calcite by weight of dried sediment, was computed as leached. The ratios of Ca/SO_4 and Ca/total inorganic carbon were meaningless probably because of substantial ion exchange, used to explain the observed pore-water chemistry in the following. Based on the results from the dilution experiment this is an ongoing process.

5 Discussion

5.1 Identification of hydro-geochemical processes along the flow line

Minerals which are probably controlling the fresh groundwater quality in the fringes of the Machile Basin are alumino-slicates that include plagioclase such as anorthite, albite, hornblende, K-feldspars, pyroxene, olivines and amphiboles. Lithologies in the fringes include sand, sandstone, schists and basalts. Reactions releasing Na^+ and Ca^{2+} are exemplified in these two reactions (Appelo & Postma, 2005); these reactions also result in an increase in alkalinity.

Albite	Kaolinite

$$2\,Na\,(AlSi_3)O_8 + 2H_2CO_3 + 3H_2O \longrightarrow Al_2Si_2O_5\,(OH)_4 + 2Na^+ + 4H_4SiO_4$$

$$+\,2HCO_3^-$$

Anorthite	Kaolinite

$$Ca\,(Al_2Si_2)O_8 + 2H_2CO_3 + H_2O \longrightarrow Al_2Si_2O_5\,(OH)_4 + Ca^{2+} + 2HCO_3^-$$
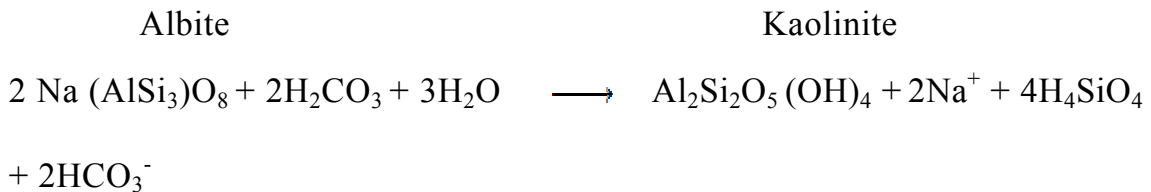
To get an idea on the amount of silicate minerals dissolving and precipitating we have used a constrained mass balance approach. Using PHREEQC (Parkhurst & Appelo, 1999), we assume fresh groundwater flows advectively from the head waters region with an initial chemistry similar to RV11 - Bwina RHC (slightly lower pH was used as we assume the recharge water acquires CO_2 from organic matter as it inflitrates (see Table 7)) along the flowline up to RV12-2 - Machile (Fig. 3),where it is lost to evaporation. The model setup is a 1D advective flow model with 20 cells each representing 3.5 km. Flow is modeled by shifting water forward so that at each shift water from each cell is transferred into the downstream cell; a total of 40 shifts each representing 350 years based on the flow rate of 10 m/year are simulated to ensure flushing of the system. Defined reactions representing irreversible dissolution occur at each shift and the water entering a given cell is equilibrated with the mineral phases defined to be present thereby constraining the model in the fitting to the observations.

Table 7: PHREEQC 1D advection model showing the composition of the flushing and initial solution of the 20 cells. Chemical additions and formations in each reaction cell given as amounts pr. year assuming a groundwater flowrate od 10 m/year and a cell length of 3500 m. Initial water composition is from Bwina site – RV11 (see Table 2 and Fig. 1) but with a slightly lower pH of 6.37, at the start of the flow line.

	Cell number	Amounts reacted (µmoles/L/yr)					Amount formed (µmoles/L/yr)	
		Anorthite	Albite	H_2CO_3	Tremolite	K-feldspar	Gibbsite	Chalcedony
HCO_3 0.510 Cl 0.264 SO_4 0.002 Na 0.052 K 0.073 Ca 0.177 Mg 0.034 Mn 0.001 Si 0.376 Al 3.72e-5 pH 6.37	1	0.014	0.001	0.014				
	2	0.014	0.001	0.014				
	3	0.014	0.001	0.014				0.032
	4	0.014	0.001	0.014				0.032
	5	0.014	0.001	0.014				0.030
	6	0.057	0.014	0.143				0.030
	7	0.057	0.014	0.257				0.030
	8	0.014	0.001	0.257				0.030
	9	0.029	0.071	0.257			0.015	0.129
	10	0.009	0.066	0.429			0.200	0.143
	11	0.042	0.013	0.429			0.033	0.030
	12	0.013	0.013	0.429			0.271	0.129
	13	0.023	0.081	0.571	0.029		0.214	0.083
	14	0.015	0.072	0.571	0.029		0.123	0.097
	15	0.071	0.071	0.714	0.029		0.066	0.039
	16	0.271	0.071	0.714	0.029		0.517	0.128
	17	0.286	0.071	0.857	0.029		0.474	0.102
	18	0.400	0.114	0.857	0.029		0.586	0.214
	19	0.514	0.114	1.14	0.057	0.057	0.986	0.614
	20	0.629	0.114	1.14	0.057	0.086	1.014	0.643

Along the advective flow path, we allow for the irreversible dissolution of varying amounts of H_2CO_3 reacting with simplified alumino-silicate minerals: anorthite, albite, tremolite and K-feldspars, to supply Ca, Na, Mg and K cations that are assumed not to reprecipitate. Added amounts of reacting silicate minerals are anorthite (0.009-0.629 µmol/L/yr), albite (0.001-0.114 µmol/L/yr), tremolite (0.029-0.057 µmol/L/yr), K-feldspars (0.057-0.086 µmol/L/yr) and H_2CO_3 (0.014-1.143 µmol/L/yr) as shown in Table 7. The source of H_2CO_3 is assumed to be degradation of organic matter in the system. The simple phases gibbsite and chalcedony were permitted to precipitate when oversaturated in order to control the Al and Si concentrations; we use the observed saturation index (SI) of 1.8 for chalcedony and 0.15 for gibbsite calculated from water chemistry measured at the downstream point (Machile). Using the PHREEQC output and groundwater flow velocity, we calculate an approximate amount of formed gibbsite, 1.20-58.16 µmol/L/yr and chalcedony, 0-92.19 µmol/L/yr (Table 7). Fig. 9a & b, shows the output of the simulation compared to the observed field results along the flow-line; Fig. 9a, shows the measured cations compared with modelled results whereas, Fig. 9b, shows simulation results with anions and pH. The model fits relatively well for pH and alkalinity, however, misfits can be seen especially for the Al and Si; this could be because of the actual reprecipitation of Al and Si comprises more complex silicate minerals such as Ca-montimorillonite, kaolinite and illite. We tested this assertion using Ca-montimorillonite, and kaolinite equilibrium phases that showed much higher concentrations of Al before precipitation initiates and a drastic drop after and in addition it was difficult to get a good fit on the pH and alkalinity. The presence of Ca and Mg is an indication that the minerals reacting could be plagioclase, amphiboles, pyroxenes and/or olivines; this could not be distinguished through modelling. The model misfit could also be due to a more complex flowpattern e.g. mixing with CO_2 rich surface water or that the measured values represent different local flow lines. The ion ratios in the water from the downstream observation points (beyond 50 kms) indicate that the water chemistry is influenced by ion exchange which is not included in the model. In addition, the last observed downstream point, which is at the transition zone between fresh and saline water, has a higher sulphate concentration in excess of 50 times more compared to the rest of the points on the flow line.
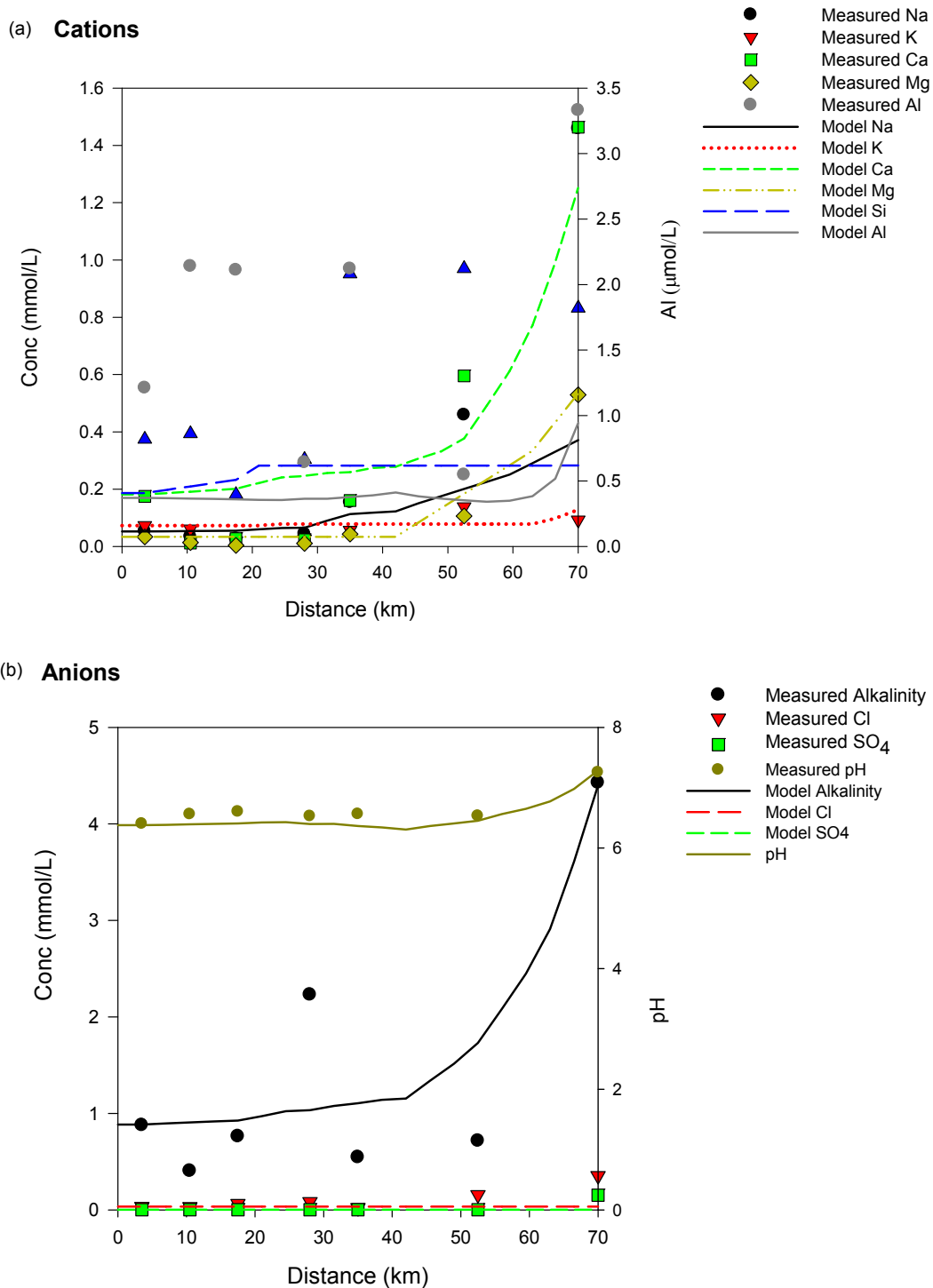
Fig. 9: (a) Observed and modelled cations from samples and a 1D advective PHREEQC model with defined chemical reactions adding carbonic acid and simple primary silicates (albite. anorthite, K-feldspar, tremolite) within the fresh groundwater zone (b) Observations and simulation of anions and Al on the groundwater flow line in the 1D advection. The increase in alkalinity is a product of the reaction between the added carbonic acid and silicate minerals.

This is an indication of a sulphate phase dissolving, coupled with ion exchange; this is disscussed further for the saline groundwater as an extended dedolomitization process. In general, the silicate weathering reactions in the fresh groundwater zone, leads to HCO_3^- groundwater type enriched in Mg^{2+}, Na^+ and Ca^{2+} ions.

In the saline region, we assume the saline evaporites were formed syndepositionally during sedimentation (Banda et al., 2015). The sediment dilution experiment (Fig. 8), hydrochemistry and mineral phases suggests the saline groundwater evolves chemically by three main processes: 1) dissolution of gypsum; 2) dissolution of calcite and dolomite to produce Ca-Mg-HCO_3, and 3) ion exchange with a Na-rich exchanger leading to formation of Na-Cl-SO_4 waters. These reactions can be seen as a special type or extension of dedolomitization. The "simple" irreversible dedolomitization (Naus et al., 2001) reaction can be generalised as follows:

$$CaSO_4 + CaMg(CO_3)_2 \longrightarrow 2CaCO_3 + Mg^{2+} + SO_4^{2-}$$

(Gypsum)   (Dolomite)   (Calcite)
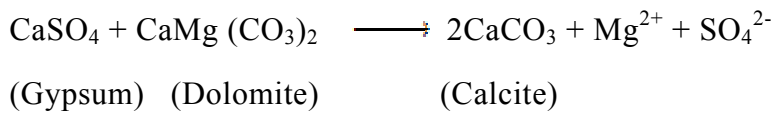
But in our case the presence of an exchanger filled with Na implies that instead of precipitating as calcite, the Ca exchanges with the Na:

$$Ca^{2+} + 2NaX \longrightarrow CaX_2 + 2Na^+$$

Likewise, most of the Mg released is exchanged for Na+ on the exchanger. This reaction results in a Na and SO_4 rich groundwater type; this is supported by CEC results as shown in Table 5 and by the very low Ca/SO_4 ratios found in the dilution experiments. Fig. 10a shows a plot of pore-water sulphate and Ca, Mg and Na solutes from the in-situ sediment core samples (Table 6). It is clear the correlation that would be expected for simple dedolomitization is completely absent, but there is a clear correlation between sulphate and the sum of Ca+Mg+Na; this provides a rationale to include ionic-exchange to remove Ca to simulate the observed water quality (Na-Cl-SO_4). Furthermore, Fig. 10b, illustrates that the Na in the pore-water is not simply a result of dissolution of halite as there is a poor correlation with chloride, with almost twice as much Na as expected.

The extended dedolomitization process was modelled by modifying the groundwater composition underlying Kasaya (see Table 2), with an initial solution 1 that is in equilibrium with gypsum, dolomite and calcite and with an exchanger with a total cation exchange capacity of 1.2 eq/L as shown in Table 8.

Table 8: PHREEQC input for the dedolomitization reaction, with the initial water composition (solution 1) and the CEC of the exchanger; which is equilibrated with the water in equilibrium with dolomite, calcite and a PCO2 of 10-1.89 resulting in high Na concentration on the clay. Solution 2 then replaces solution 1, modelling incoming water subsaturated for gypsum in the presence of calcite and dolomite. A range of extents in dedolomitization is generated by addition of 0.09 moles of gypsum in 10 steps.

Initial Water (Solution 1)	CEC (eq/L)	SI of Equilibrium Phases (used with initial water)			Initial composition (Solution 2)	Equilibrium Phases (saturation index)	
		Dolomite	Calcite	CO_2		Dolomite	Calcite
		0	0	-1.82		0	0
pH 7 units: mmol/L HCO₃ 10 Ca 5 SO₄ 2 Na 200 Cl 200 Mg 2	1.2				pH 6 units: mmol/L HCO₃ 3 Ca 1.5 SO₄ 0.2 Na 20 Cl 20 Mg 0.2		

The Ca (initially 5 mmol/L) and Mg (initially 2 mmol/L) was calculated from equilibrium with calcite and dolomite resulting in initial Ca and Mg concentrations of 4.19 mmol/L and 2.24 mmol/L respectively. Equilibration of this system yields an exchanger with Na (767 mmol/L), Ca (162 mmol/L) and Mg (54.4 mmol/L) thus a clearly Na dominated exchanger. Solution 1 physically represents the condition when the palaeo-lake system had desiccated precipitating evaporates of sulphates and carbonates (Banda et al., 2015). Solution 2 (Table 8) then replaces solution 1, representing the infiltration of fresh water into the sediments. We assume this water has partially dissolved evaporates in the system - Na and Cl ions are typically the first to dissolve. We assume a lower pH of 6 as this recharge water probably interacted with some organic matter as this is typical of a lake ecosystem. Dedolomitization was then driven by reacting 0.09 moles of gypsum in 10 reaction steps, representing different degrees of the extended dedolomitization. The defined mineral equilibrium phases calcite, and dolomite were the source of Ca and Mg in the system; the system was in equilibrium with a PCO_2 between $10^{-1.89}$ and $10^{-1.36}$ atm after addition of gypsum.

(a)

(b)
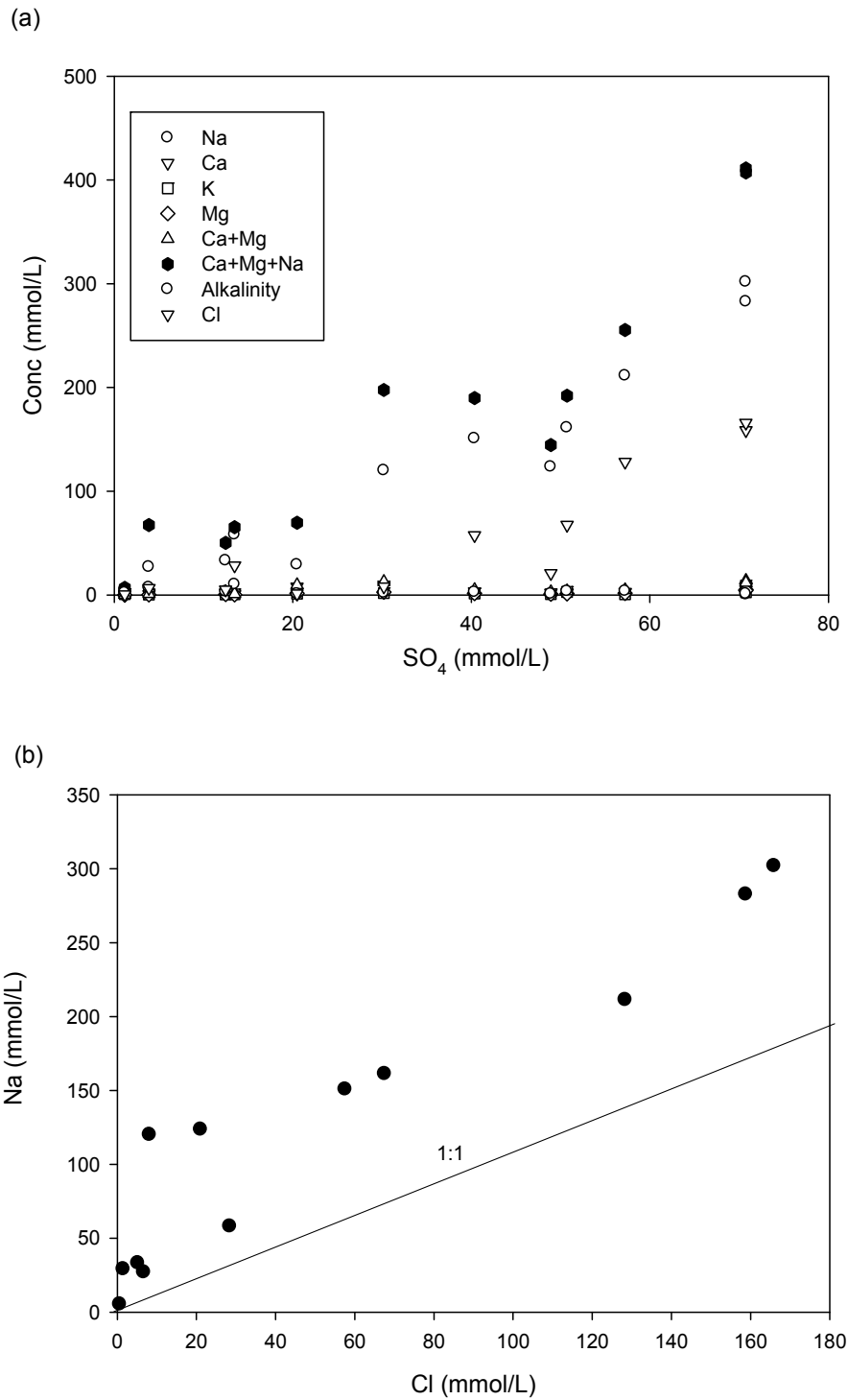
Fig. 10 (a): Plot of the major ions as a function of the sulphate concentration of pore-water samples. There is a strong linear relationship of pore-water sulphate with Ca+Mg+Na. Therefore pore-water chemistry can probably be explained by extended dedolomitization including ion exchange and carbonate equilibria (calcite and dolomite), (b) Pore-water 1:1 Na–Cl line shows a poor correlation hence halite dissolution is not probable. The current source of Na^+ in the pore-water is therefore not halite.

Results of the modelled and observed pore-water data are shown in Fig 11a & 11b; observation data is from the pore-water analysis (Table 6) and ground-water water sample at Kasaya site (Table 2). Fig. 11a, demonstrates a reasonable model fit to the observed evolution in Ca and Mg with increasing sulphate dissolution, and concomitant ion exchange. The model misfit could be due to initially higher Ca and Mg ions contents on the exchanger as the extended dedolomitisation processes has probably been going on for a long time leading to increased Ca and Mg concentrations in the groundwater and on the exchanger. The effect is demonstrated by having an exchanger with a higher proportion of Ca on the exchanger, by defining Ca in the initial solution 1 to be in equilibrium with gypsum rather than calcite, SO_4 was also defined by equilibrium with gypsum (output is shown in Fig. 11a). The modelled cation exchanger composition (with an initial high Na on the exchanger) was NaX, 522-647, CaX2, 243-301 and MgX2, 32.3-35.2 mmol/L, similar to measured cation distributions of NaX, 9.92-435, CaX2, 15.8-339 and MgX2, 3.10-111 mmol/L (Table 5; assuming a porosity of 30 % and bulk density, 1.86 g/cm^3). The wide range in measured distributions of exchangeable cations show that the groundwater samples are the result of different mixtures of saline and fresh pore-water and would be expected to give a range of Ca and Mg concentrations, but with similar geochemical pattern as simulated.

We also observed a misfit in the decrease of alkalinity with increasing sulphate (Fig. 11b) which is would also be controlled by the initial composition on the exchanger; the model result for the Na and Ca dominated exchangers are shown in the Fig.. Higher PCO_2 conditions can also affect the alkalinity variations. Higher PCO_2 could be due to decomposition of organic matter and/or root respiration (vegetation) and redox processes such as bacterial sulphate reduction (Plummer et al., 1990). However, the pH variations were generally comparable to field results. The proposed extended dedolomitisation process appears to explain most of the features in the Na-Cl-SO_4 water type in the saline zone.
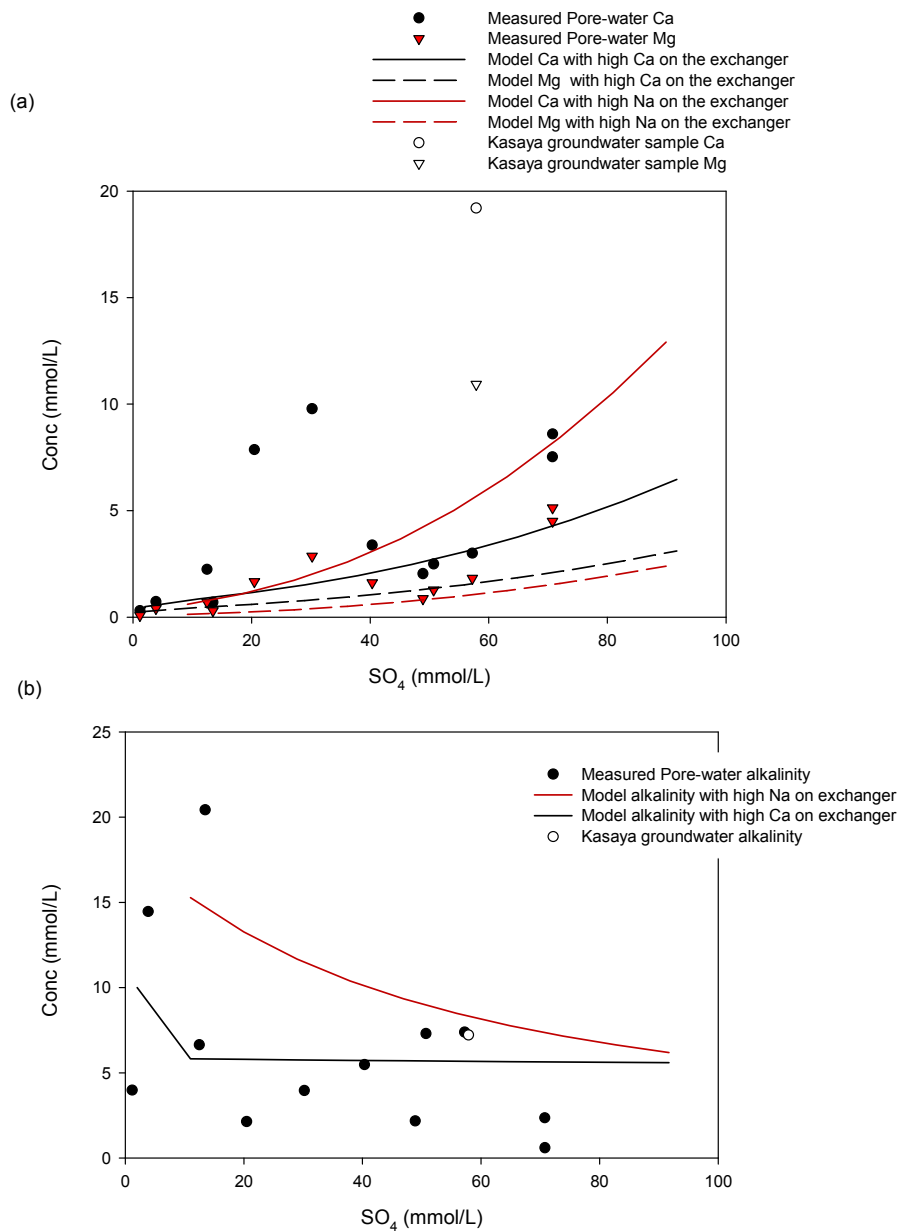
Fig. 11: (a) PHREEQC modelled Ca and Mg from the extended dedolomitization process including ion exchanges (Na and Ca dominated conditions) and observed Ca and Mg species in the saline groundwater. (b) PHREEQC modelled and observed alkalinity with Na and Ca exchanger as a function of sulphate concentration, showing that the modelled alkalinity is sensitivity to the initial composition on the exchanger.

5.2 Physical processes and hydrochemistry

In this study, we suggest the high salinity in the topographic low region (Lake Palaeo-Makgadikgadi sediments) represents palaeo-salinity with very limited groundwater through flow as demonstrated by groundwater flow

modelling and environmental isotopes. The saline zone hosts stagnant pore-water water that was introduced during *pluvial* climatic events which partially dissolved evaporites as demonstrated by the sediment dilution experiment. Possible chronologies for the most recent *pluvial* episodes in the Kalahari are 8-4.5 and 30-11 thousand years (ka) before present - B.P (Grey & Cooke, 1977; Heine, 1992; Shaw & Thomas, 1996; Stute & Talma, 1998; De Vries et al., 2000; Kulongoski et al., 2004; Riedel et al., 2014); these periods corroborates well with both modelled and ^{14}C apparent ages of < 10 ka in our flow system. Earlier studies by Banda et al, (2014) showed the sediments in the saline zone are old (> 300 ka) suggestive of an earlier phase of evaporite formation before dissolution by infiltrating groundwater. This agrees with earlier work by Verhagen (1995) who postulated that mineralisation of Kalahari groundwater was controlled by the aquifer structure and the build-up in salinity could have fully or partially flushed during *pluvial* climatic events. However, the sediment dilution experiment demonstrates that if through flow was an active process, salinity within the brackish-saline zone would have been washed out. In addition, recharge studies (De Vries et al., 2000; Brunner et al., 2004; Wanke et al., 2008) within the Kalahari region suggest current infiltration from precipitation is less than 10 mm/yr, most of which is later lost to evapo-transpiration, and thus has insignificant impact on the groundwater. De Vries (1984) considered the regional lateral flow through the larger Kalahari Basin, on the basis of hydraulic gradient and transmissivity and concluded a flux of less than 1 mm yr^{-1} which for steady state conditions would mean an overall recharge of the same order; the groundwater system in general is thus not actively recharged and probably was infiltrated during humid periods of quaternary period (Heine, 1992) in southern Africa.

The discussed physical processes have also had a corresponding chemical effect as a result of water-rock interactions. PHREEQC modelling has demonstrated that the freshwater zone has undergone weathering of alumino-silicates (mostly Ca-rich such as plagioclase) by CO_2-rich groundwater releasing varying amounts Ca, Na and K; small amounts of Mg probably from amphibole, pyroxene or olivine are also released. The high alkalinity in the transition zone is an additional effect from evapo-concentration; this has been corroborated by the stable isotopes. The PHREEQC simulation is in agreement with the processes suggested by Mazor et al. (1980) controlling the chemical composition in the Kalahari groundwaters. The composition of the saline groundwater appears to be is a result of an extended dedolomitization including ion exchange with an exchanger dominated by Na, as demonstrated

by PHREEQC modelling; this is, to our knowledge, the first time these two processes have been described as acting together to explain chemical evolution at the field scale. Groundwater chemical evolution by dedolomitization has been well described in other systems such as the Madison Aquifer, Canada (Back et al., 1983; Plummer et al., 1990; Naus et al., 2001).

6 Conclusions

Physical and hydro-chemical processes were assessed in the Machile Basin, south-western Zambia to explain the spatial groundwater chemistry. Groundwater in the region can be characterised as fresh water, Ca-Mg-(Na)-HCO$_3$ and Na-HCO$_3$ type, and saline water of Na-Cl-SO$_4$.

The following was observed;

- Groundwater flow modelling along a 2D transect demonstrates that physically, there is little or no interaction between the freshwater in the fringe zone and saline pool in the centre; fresh water is forced out through topographic depressions, rivers, creeks and dambos (wetlands) and lost to evapo-transpiration. Within the saline pool, localised fresh-water lateral flow is very limited judging from the rather flat slope of the groundwater heads.

- The lithological hydraulic conductivity contrast is the foremost control of flow and distribution of water types; the saline pool is stagnant and hosts palaeo-salinity from dissolution of evaporites (gypsum and carbonate minerals).

- Apparent groundwater ages along the flow line are < 10 ka in old sediments of more than 300 ka suggestive of pluvial climatic recharge that induced partial flushing. Pluvial climatic phases in the region were >30-11 ka and 8-4.5 ka.

- Fresh groundwater in the fringe zone is dorminated by slow silicate weathering due to the absence of more reactive minerals, leading to low salinities. The minerals weathering are most probably calcic plagioclases, olivine, pyroxenes and amphiboles present in the rocks. PHREEQC modelling of the system demonstrates that weathering of these minerals releasing the observed cations can produce the observed associated effects on alkalinity and pH.

- The saline pool is undergoing an extended dedolomitization reaction including ion exchange hence exhibiting a Na-Cl-SO$_4$ as the Ca is exchanged for Na on the clay minerals in the formation. This is the first time dedolomitization with ion exchange is documented at a field scale.

7 References

Alley, W.M., 1993. Geostatistical Models. In: Alley, W.M. (ed.) Regional ground-water quality. John Wiley & Sons. pp. 87 - 108.

Appelo, C.A. & Postma, D., 2005. Geochemistry, groundwater and pollution. A.A. Balkema Publishers.

Back, W., Hanshaw, B.B., Plummer, L.N., Rahn, P.H., Rightmire, C.T. & Rubin, M., 1983. Process and rate of dedolomitization: mass transfer and 14C dating in a regional carbonate aquifer. Geological Society of America Bulletin, 94, 1415-1429.

Banda, K., Jakobsen, R., Bauer-Gottwein, P., Murray, A.S., Nyambe, I. & Larsen, F., 2015. Palaeo-Lake Makgadikgadi: New perspectives and insights of its evolution from western Zambia. In preparation.

Beilfuss, R., 2012. A risky climate for southern African hydro: assessing hydrological risks and consequences for Zambezi River Basin dams. International Rivers.

Bouchaou, L., Michelot, J., Vengosh, A., Hsissou, Y., Qurtobi, M., Gaye, C., Bullen, T. & Zuppi, G., 2008. Application of multiple isotopic and geochemical tracers for investigation of recharge, salinization, and residence time of water in the Souss–Massa aquifer, southwest of Morocco. Journal of Hydrology, 352, 267-287.

Brunner, P., Bauer, P., Eugster, M. & Kinzelbach, W., 2004. Using remote sensing to regionalize local precipitation recharge rates obtained from the Chloride Method. Journal of Hydrology, 294, 241-250.

Chiang, W.-H. & Chiang, W., 2001. 3D-groundwater modeling with PMWIN. Springer.

Chongo, M., Christiansen, A.V., Fiandaca, G., Nyambe, I.A., Larsen, F. & Bauer-Gottwein, P., 2014a. Mapping localized freshwater anomalies in the brackish Paleo-Lake sediments of the Machile-Zambezi Basin with transient electromagnetic sounding, geoelectrical imaging and induced polarization. In preparation.

Chongo, M., christiansen, A.V., Tembo, A., Nyambe, I., Larsen, F. & Bauer-Gottwein, P., 2014b. Airborne and Ground based Transient Electromagnetic Mapping of Groundwater Salinity in the Machile-Zambezi Basin, South-western Zambia. . submitted to Hydrogeology Journal.

Chongo, M., Wibroe, J., Staal-Thomsen, K., Moses, M., Nyambe, I., Larsen, F. & Bauer-Gottwein, P., 2011. The use of Time Domain Electromagnetic method and Continuous Vertical Electrical Sounding to map groundwater salinity in the Barotse sub-basin, Zambia. Physics and Chemistry of the Earth, Parts A/B/C, 36, 798-805.

Clark, I.D. & Fritz, P., 1997. Environmental isotopes in hydrogeology. CRC press.

Darling, W., Gooddy, D., MacDonald, A. & Morris, B., 2012. The practicalities of using CFCs and SF6 for groundwater dating and tracing. Applied Geochemistry, 27, 1688-1697.

De Vries, J.J., 1984. Holocene depletion and active recharge of the Kalahari groundwaters — A review and an indicative model. Journal of Hydrology, 70, 221-232.

De Vries, J.J., Selaolo, E.T. & Beekman, H.E., 2000. Groundwater recharge in the Kalahari, with reference to paleo-hydrologic conditions. Journal of Hydrology, 238, 110-123.

Domenico, P.A., 1972. Concepts and models in groundwater hydrology. McGraw-Hill Inc.

Eckardt, F.D., Bryant, R.G., McCulloch, G., Spiro, B. & Wood, W.W., 2008. The hydrochemistry of a semi-arid pan basin case study: Sua Pan, Makgadikgadi, Botswana. Applied Geochemistry, 23, 1563-1580.

Edmunds, W.M. & Bath, A.H., 1976. Centrifuge extraction and chemical analysis of interstitial waters. Environmental Science & Technology, 10, 467-472.

Eichinger, L., 1983. A Contribution to the Interpretation of C-14 Groundwater Ages Considering the Example of a Partially Confined Sandstone Aquifer. Radiocarbon, 25, 347-356.

Einbond, A., Sudol, M. & Coplen, T., 1996. New guidelines for reporting stable hydrogen, carbon, and oxygen isotope-ratio data. Geochimica Et Cosmochimica Acta, 60, 3359-3360.

Fontes, J.C. & Garnier, J.M., 1979. Determination of the initial 14C activity of the total dissolved carbon: A review of the existing models and a new approach. Water Resources Research, 15, 399-413.

Gonfiantini, E., 1986. Environmental isotopes in lake studies. In: P.Fritz & J.-Ch.Fontes (eds.) Handbook of environmental isotope geochemistry. 2. Elsevier, Amsterdam, The Netherlands. pp. 113-168.

Gran, G., 1952. Determination of the equivalence point in potentiometric titrations (Part II). Analyst, 77, 661-671.

Grey, D. & Cooke, H., 1977. Some problems in the Quaternary evolution of the landforms of northern Botswana. Catena, 4, 123-133.

Haddon, I.G. & McCarthy, T.S., 2005. The Mesozoic-Cenozoic interior sag basins of Central Africa: The Late-Cretaceous-Cenozoic Kalahari and Okavango basins. Journal of African Earth Sciences, 43, 316-333.

Harbaugh, A.W., Banta, E.R., Hill, M.C. & McDonald, M.G., 2000. MODFLOW-2000, the US Geological Survey modular ground-water model: User guide to modularization concepts and the ground-water flow process. US Geological Survey Reston, VA, USA.

Heine, K., 1992. On the ages of humid Late Quaternary phases in southern African arid areas (Namibia, Botswana). In: Heine, K. (ed.) Palaeoecology of Africa and the surrounding islands. 23. Balkema A.A., Netherlands. pp. 149-164.

Hem, J.D., 1985. Study and interpretation of the chemical characteristics of natural water. Department of the Interior, United States Geological Survey water- supply paper No. 2254, 263 pp.

IAEA, W. & WMO, W., 2006. Global Network of Isotopes in Precipitation. The GNIP database.

Ingerson, E. & Pearson, F., 1964. Estimation of age and rate of motion of groundwater by the 14C-method. Recent Researches in the Fields of Atmosphere, Hydrosphere and Nuclear Geochemistry, 263-283.

Kalinowski, M.B., 2004. International Control of Tritium for Nuclear Nonproliferation and Disarmament. CRC Press.

Kulongoski, J.T., Hilton, D.R. & Selaolo, E.T., 2004. Climate variability in the Botswana Kalahari from the late Pleistocene to the present day. Geophysical Research Letters, 31.

Kumar, M., Kumari, K., Singh, U.K. & Ramanathan, A.L., 2009. Hydrogeochemical processes in the groundwater environment of Muktsar, Punjab: conventional graphical and multivariate statistical approach. Environmental Geology, 57, 873-884.

Lindenmaier, F., Miller, R., Fenner, J., Christelis, G., Dill, H.G., Himmelsbach, T., Kaufhold, S., Lohe, C., Quinger, M., Schildknecht, F., Symons, G., Walzer, A. & van Wyk, B., 2014. Structure and genesis of the Cubango Megafan in northern Namibia: implications for its hydrogeology. Hydrogeology Journal, 22, 1307-1328.

Linn, F., Masie, M. & Rana, A., 2003. The impacts on groundwater development on shallow aquifers in the lower Okavango Delta, northwestern Botswana. Environmental Geology, 44, 112-118.

Margane, A., Baeumle, R., Schildknecht, F. & Wierenga, A., 2005. Groundwater investigation in the Eastern Caprivi Region - Main Hydrogeological Report. Department of Water Affairs (Namibia) and Federal Institute of Geosciences and Natural Resources (Hannover). 164pp.

Mazor, E., Bielsky, M., Verhagen, B.T., Sellschop, J.P.F., Hutton, L. & Jones, M.T., 1980. Chemical composition of groundwaters in the vast Kalahari flatland. Journal of Hydrology, 48, 147-165.

Mazor, E., Verhagen, B.T., Sellschop, J.P.F., Jones, M.T., Robins, N.E., Hutton, L. & Jennings, C.M.H., 1977. Northern Kalahari groundwaters - hydrologic, isotopic and chemical studies at Orapa, Botswana. Journal of Hydrology, 34, 203-234.

McCarthy, T., 2013. The Okavango Delta and its place in the geomorphological evolution of southern africa. South African Journal of Geology, 116, 1-54.

McCarthy, T.S., McIver, J.R. & Verhagen, B.T., 1991. Groundwater evolution, chemical sedimentation and carbonate brine formation on an island in the Okavango Delta swamp, Botswana. Applied Geochemistry, 6, 577-595.

Money, N.J., 1972. An outline of the Geology of western Zambia. Records of the Geological Survey, Republic of Zambia No. 12, pp. 103-123.

Monjerezi, M., Vogt, R.D., Aagaard, P., Gebru, A.G. & Saka, J.D.K., 2011. Using Sr-87/Sr-86, delta O-18 and delta H-2 isotopes along with major chemical composition to assess groundwater salinization in lower Shire valley, Malawi. Applied Geochemistry, 26, 2201-2214.

Mook, W., 1972. On the reconstruction of the initial 14 C content of groundwater from the chemical and isotopic composition. Proceedings of the 8th International Conference on Radiocarbon Dating. pp. 342–352.

Moore, A.E. & Larkin, P.A., 2001. Drainage evolution in south-central Africa since the breakup of Gondwana. South African Journal of Geology, 104, 47-68.

NASWC (Non-Affiliated Soil Analysis Work Committee), 1990. Handbook of standard soil testing methods for advisory purposes. Soil Science Society of South Africa, Pretoria.

Naus, C.A., Driscoll, D.G. & Carter, J.M., 2001. Geochemistry of the Madison and Minnelusa aquifers in the Black Hills area, South Dakota. Citeseer.

Nugent, C., 1990. The Zambezi River - Tectonism, climatic-change and drainage evolution. Palaeogeography Palaeoclimatology Palaeoecology, 78, 55-69.

Parkhurst, D.L. & Appelo, C., 1999. Description of input and examples for Phreeqc (vers. 2) - a computer program for speciation, batch-reaction,one-dimensional transport, and inverse geochemical calculations. United States Geological Survey - water resources investigation report. pp 99 - 4259.

Piper, A.M., 1944. A graphic procedure in the geochemical interpretation of water-analyses. Transactions, American Geophysical Union, 25, 914-928.

Plummer, L., Prestemon, E. & Parkhurst, D., 1994. An interactive code (NETPATH) for modeling net geochemical reactions along a flow path Version 2.0. USGS, Washingston, DC, Water-Resources Investigations Report 94-4169.

Plummer, L.N., Busby, J.F., Lee, R.W. & Hanshaw, B.B., 1990. Geochemical modeling of the Madison aquifer in parts of Montana, Wyoming, and South Dakota. Water Resources Research, 26, 1981-2014.

Ravikumar, P., Venkatesharaju, K., Prakash, K.L. & Somashekar, R.K., 2011. Geochemistry of groundwater and groundwater prospects evaluation, Anekal Taluk, Bangalore Urban District, Karnataka, India. Environmental Monitoring and Assessment, 179, 93-112.

Riedel, F., Henderson, A.C., Heußner, K.-U., Kaufmann, G., Kossler, A., Leipe, C., Shemang, E. & Taft, L., 2014. Dynamics of a Kalahari long-lived mega-lake system: hydromorphological and limnological changes in the Makgadikgadi Basin (Botswana) during the terminal 50 ka. Hydrobiologia, 1-29.

Ringrose, S., Huntsman-Mapila, P., Kampunzu, A.B., Downey, W., Coetzee, S., Vink, B., Matheson, W. & Vanderpost, C., 2005. Sedimentological and geochemical evidence for palaeo-environmental change in the Makgadikgadi subbasin, in relation to the MOZ rift depression, Botswana. Palaeogeography Palaeoclimatology Palaeoecology, 217, 265-287.

Selaolo, E.D. 1998. Tracer studies and groundwater recharge assessment in the Eastern Fringe of the Botswana Kalahari. The Lethlakeng – Botlhapatlou Area. . Ph.D. thesis, Vrije Universiteit te Amsterdam, 228 pp.

Shaw, P.A. & Thomas, D.S.G., 1996. The quaternary palaeoenvironmental history of the Kalahari, Southern Africa. Journal of Arid Environments, 32, 9-22.

Stadler, S. 2005. Investigation of natural processes leading to nitrate enrichment in aquifers of semi-arid regions. PhD thesis, Karlsruhe University, Germany, 262 pp.

Stadler, S., Osenbruck, K., Suckow, A.O., Himmelsbach, T. & Hotzl, H., 2010. Groundwater flow regime, recharge and regional-scale solute transport in the semi-arid Kalahari of Botswana derived from isotope hydrology and hydrochemistry. Journal of Hydrology, 388, 291-303.

Stiff Jr, H.A., 1951. The interpretation of chemical water analysis by means of patterns. Journal of Petroleum Technology, 3, 15-3.

Stute, M. & Talma, A.S., 1998. Glacial temperatures and moisture transport regimes reconstructed from noble gases and O-18, Stampriet aquifer, Namibia. -In: Isotope Techniques in the Study of Environmental Change. pp. 307–318.

Sültenfuß, J., Roether, W. & Rhein, M., 2009. The Bremen mass spectrometric facility for the measurement of helium isotopes, neon, and tritium in water†. Isotopes in environmental and health studies, 45, 83-95.

Tamers, M., 1975. Validity of radiocarbon dates on ground water. Geophysical surveys, 2, 217-239.

Thomas, D. & Shaw, P., 1991. The deposition and development of the Kalahari Group sediments, central southern Africa. Journal of African Earth Sciences (and the Middle East), 10, 187-197.

Verhagen, B.T., 1992. Detailed geohydrology with environmental isotopes. A case study at Serowe, Botswana. -in: Isotope Techniques in Water Resources Development. pp. 345-362.

Verhagen, B.T., 1995. Semiarid zone groundwater mineralization processes as revealed by environmental isotope studies. In: Adar, E.M. & Leibundgut, C. (eds.) Application of Tracers in Arid Zone Hydrology. International Association Hydrological Sciences, Volume 232, Wallingford. pp. 245-266.

Vogel, J., 1970. Carbon-14 dating of groundwater. Isotope hydrology, 1970, 225-239.

Vogel, J.C. & Van Urk, H., 1975. Isotopic composition of groundwater in semi-arid regions of southern Africa. Journal of Hydrology, 25, 23-36.

Wanke, H., Dunkeloh, A. & Udluft, P., 2008. Groundwater recharge assessment for the Kalahari catchment of north-eastern Namibia and north-western Botswana with a regional-scale water balance model. Water Resources Management, 22, 1143-1158.

Wheater, H.S., Mathias, S.A. & Li, X., 2010. Groundwater Modelling in Arid and Semi-Arid Areas. Cambridge University Press.

YEC (Yachiyo Engineering Company), 1995. The Study on the National Water Resources Master Plan in the Republic of Zambia. Japan International Cooperation Agency & Ministry of Energy and Water Development, Republic of Zambia. Final Report – Hydrogeology, 128 pp.

Yemane, K., D, G. & Nyambe, I., 2002. Paleohydrological signatures and rift tectonics in the interior of Gondwana documented from Upper Permian lake deposits, the mid-Zambezi Rift basin, Zambia. In SEPM Special Publication No. 73 on Sedimentation in Continental Rifts, SEPM (Society for Sedimentary Geology), ISBN 1-56576-082-4, pp. 143-162.

III

Hydrogeochemistry of the Palaeo-Lake Makgadikgadi – a review

Kawawa E. Banda, Peter Bauer- Gottwein, Rasmus Jakobsen,
Imasiku Nyambe, Flemming Larsen

Submitted

Hydrogeochemistry of the Palaeo-Lake Makgadikgadi – a review

Kawawa E. Banda [a,b*], Peter Bauer- Gottwein[a], Rasmus Jakobsen[c], Imasiku Nyambe[b], Flemming Larsen[c]

[a] Department of Environment, *Technical University of Denmark*, DK-2800 Kgs Lyngby, Denmark.

[b] Department of Geology, *University of Zambia - Integrated Water Resources Management Centre*, C/O School of Mines, Lusaka, Zambia.

[c] Department of Geochemistry, *Geological Survey of Denmark and Greenland (GEUS)*, 10, Øster Voldgade, DK-1350 Copenhagen K, Denmark.

Abstract

Palaeo-lake Makgadikgadi (PLM) in southern Africa is comprehensively understood in terms of geomorphological events through Pleistocene and Holocene times. However, hydrological dynamics and feedbacks within the same time period, with a direct impact on the present day hydrogeology, are still a contentious issue. This paper synthesises the existing state of knowledge within and around the PLM to develop a coherent understanding of the present hydrogeology and groundwater geochemistry. The PLM was predominantly desiccated by 500 ka initial evaporates of carbonates (calcite and dolomite), later of gypsum and progressive evaporation led to precipitation of chloride or several chloride minerals in the central region of the basin. Water types affected by evaporites are surrounded by carbonate groundwater, which represent recent recharge into the Makgadikgadi-Okavango-Zambezi Basin. Pluvial climatic phases (>30-20 Ka and 8-4.5 Ka) have recharged the groundwater system resulting in younger ages of groundwater compared to sediments ages, which are more than 300 ka. The observed groundwater salinity today is therefore not from the Palaeo-lake but from other processes that include evapotranspiration and mineral dissolution. Hydrogeophysics has resolved and delineated lithologies into saline/clay (< 3 Ωm), brackish/clayey sand (3-10 Ωm) and sand or Basement rocks (fresh/weathered) with a potential of fresh water (10-100 Ωm). The saline-brackish water is typically chloride and/or sulphate water type. We conclude that the present day PLM system hosts stagnant brackish to saline groundwater and fresh groundwater is lost to evapotranspiration.

1 Introduction

Upon traversing the Kalahari (Fig. 1) in the 19th century, David Livingstone recognised a wide distribution of fossil shells, which he interpreted to have lived in a vast freshwater lake. He postulated that the vanishing of the lake was due to climate and tectonic events that changed the course of the Zambezi River and created an outflow at the Victoria Falls (Fig. 1), which subsequently drained the lake (Livingstone, 1857). Since then, several studies have identified the existence of a large Quaternary lacustrine system with several sub-basins (Passarge, 1904; Grove, 1969; Ebert & Hitchcock, 1978; Cooke, 1979; Cooke & Verstappen, 1984; Lancaster, 1989; Thomas & Shaw, 1991a; Moore, 1999; Moore & Larkin, 2001; 2002; Ringrose et al., 2005; McFarlane

& Eckardt, 2006; White & Eckardt, 2006; Burrough et al., 2009a; Burrough et al., 2009b; Moore et al., 2012). This large lacustrine system was termed Lake Palaeo-Makgadikgadi by Grey & Cooke (1977) but commonly referred to as the Palaeo-Lake Makgadikgadi (PLM). PLM sustained several lake stages, the highest ~995-1,000 m above mean sea level (amsl), spanning an area in excess of 175,000 km^2 referred to as the Palaeo-Lake Deception - PLD (McFarlane & Eckardt, 2006; Moore et al., 2012).
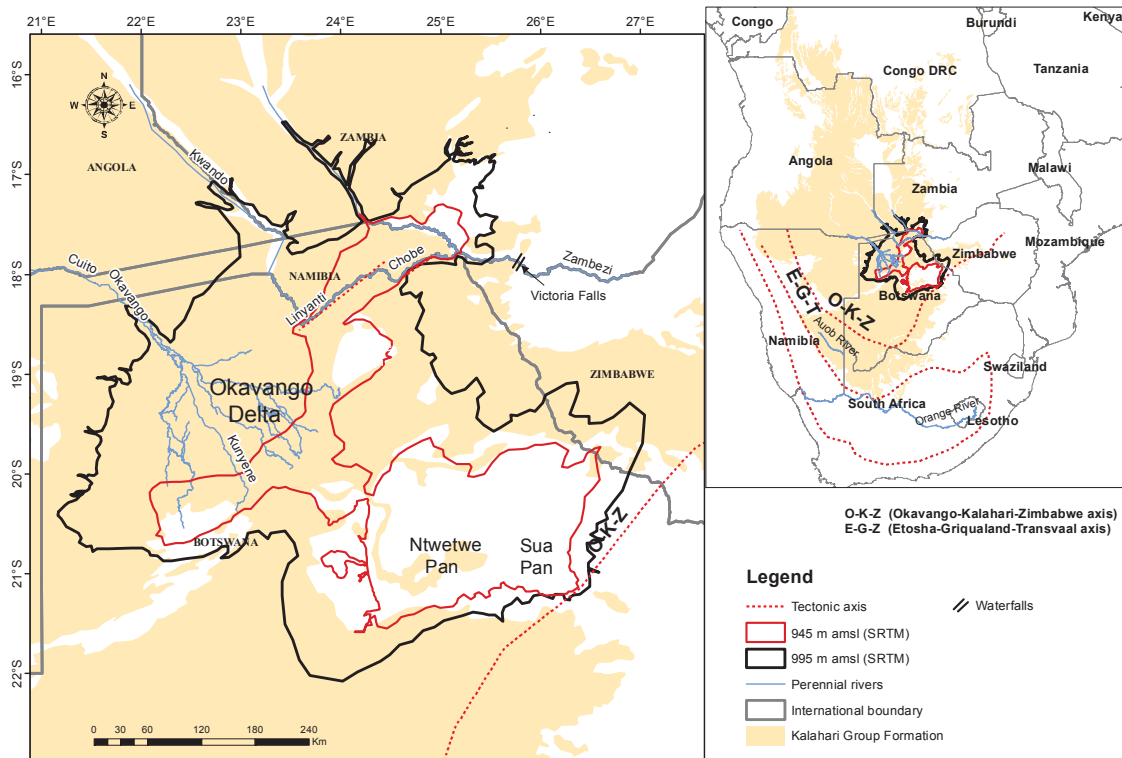
Fig. 1: Shows the outline of the Palaeo-Lake Deception (995 m amsl) and Palaeo-Lake Makgadikgadi (945 m amsl), extracted from the digital elevation model (Shuttle Radar Topographic Mission- SRTM) within the Kalahari Group Formation. Insert Fig. shows the coverage of the Kalahari Basin over Southern Africa and the tectonic axes of deposit (EGT - Etosha-Griqualand-Transvaal and OKZ – Okavango-Kalahari-Zimbabwe)

The actual age of the lake system is unknown. *In-situ*-sediments (Banda et al., submitted 2015a) and palaeo-shoreline sediments (Burrough & Thomas, 2009) indicate minimum ages of *c*. 300 kilo-annus (ka). Early stone artefacts (McFarlane & Eckardt, 2006) and molecular dating of cichlid fish (Joyce et al., 2005) found at the basin floor of PLM, suggest that by *c*. 500 ka the mega-lake was predominantly desiccated. More recently, Moore et al. (2012) speculates the lake was initiated as early as 1.4 Ma (Early Pleistocene). Geo-

logical data suggests that Neogene drainage flowing west towards the Limpopo River was disrupted between the Early to Late Pleistocene by the uplift of epeirogenetic axes (Linyanti-Chobe faults, Fig 1) resulting in the creation of a huge internal drainage basin - PLM (Du Toit, 1927; Cooke, 1980; Moore & Larkin, 2001; Haddon & McCarthy, 2005).

While it can only be speculated on the events between the Early to Middle Pleistocene, probably due to masking or obliteration of the evidence by subsequent events (Thomas & Shaw, 1991b), geomorphological data used to explain lake evolution events in Late Pleistocene to Holocene are considered comprehensive (Riedel et al., 2014). However, hydrological dynamics (forcing and feedbacks) is a contentious issue (Street & Grove, 1976; Butzer et al., 1978; Heine, 1978; Street & Grove, 1979; Heine, 1982, 1992; Lancaster, 1979; Thomas & Shaw, 1991b; Burrough et al., 2009b; Riedel et al., 2009; Riedel et al., 2012; Riedel et al., 2014) specifically, the paleao-hydrology induced by climatics of PLM before and after the Last Glacial Maximum (LGM; *c.* 23-18 ka (Gasse, 2000)) to indicate if surface water contributions were predominantly in high lake level at 945 m amsl of PLM or not. Heine (1982) demonstrated that results from different palaeo-climatic indicators (geomorphological, sedimentological, palaeo-botanical, palaeontological and archaeological) would have different time-stratigraphic periods for the Late Quaternary over the PLM Basin; strong winds movements are suggested to control the pluvial climatic phases [>30-20 ka and 8-4.5 ka (De Vries et al., 2000)] over southern Africa. However, lake systems from about 20-15 ka, such as Lake Victoria in East Africa (largest lake in Africa) and many others, are considered to have been completely desiccated (Johnson et al., 1996; Gasse, 2000; Kafri & Yechieli, 2010). Consequently, the influence of groundwater relative to surface water inflow between humid to arid, must have increased progressively to exert a controlling influence on the arid environment, impacting geochemical, sedimentological and morphological evolution as observed in other regions such as Australia (Bowler, 1986).

The influence of Pleistocene hydrologic changes on the spatial variability, hydrological configuration and evaporite formation has been shown in other closed basins such as the Lake Chad (Edmunds et al., 1999; Edmunds et al., 2002), Great Artesian Lake (Bowler, 1986) and the Great Salt Lake (Spencer et al., 1985a). In the light of these studies, we compile numerous studies that have focused on sedimentology, palaeontology, hydrochemistry, hydrogeophysics, stable and radiogenic isotopes in the PLM to draw insights on the influence of the Pleistocence environmental changes and how they have

shaped the groundwater environment of this mega-lake system. The review paper aims to improve the overall understanding of the hydrogeological and groundwater geochemical features of the PLM system and highlight aspects where further research is required in this field.

2 Regional Setting and basin development

After the break-up of Gondwana, Southern Africa formed a passive continental margin along the Atlantic coastal margins, and a gently down warped interior basin (Ollier, 1985; Thomas & Shaw, 1991a). Offshore sedimentary data along the southern African west coast (Dingle et al., 1983; Moore & Larkin, 2001; McCarthy, 2013) suggests that the Orange River in South Africa (Fig. 1) drained the interior of Southern Africa to the west at the time or at least shortly after the breakup of Gondwana in the Late Jurassic-Cretaceous. Sedimentation consequently may not have been initiated by the escarpment flexure at the time of break-up, but rather linked to the later Etosha-Griqualand-Transvaal (EGT) axis (Mid-Upper Cretaceous) and the Late Neogene Okavango-Kalahari-Zimbabwe (OKZ) axes (Moore, 1999; Moore et al., 2009); these tectonic axes are shown in Fig. 1. The formation of the OKZ and EGT is attributed to the propagation of the east African rift system into Southern Africa (McCarthy, 2013). The formation of EGT and later OKZ created a closed basin system with active sedimentation depositing weathered sediments from the underlying Karoo Formation depositing mostly fluvio-lacustrine sediments today referred to as the Kalahari Basin (Thomas & Shaw, 1991a). The Kalahari covers seven countries of Southern Africa including Angola, Congo DRC, Zambia, Zimbabwe, Namibia, Botswana and South Africa (Fig. 1).

The restricted drainage within the OKZ formed a mega-lake system referred to as the Palaeo-Lake Deception (PLD) reaching a shoreline elevation 995-1000 m amsl; this is assumed to have been in the Pliocene, 3-2.5 Ma (McFarlane & Eckardt, 2006; Moore et al., 2012). Digital elevation data from Shuttle Radar Topographic Mission (SRTM) showing the 995 m amsl is shown in Fig. 1. Tectonic disruption along the Linyanti-Chobe faults formed the PLM (Fig. 1) probably around 1.4 Ma (Moore et al., 2012); it captured the Cubango-Cuito-Okavango, Kwando-Linyanti-Chobe and Zambezi River (Du Toit, 1927; Cooke, 1980; Nugent, 1990; Moore & Larkin, 2001; Moore et al.,

2012). Other prominent lake stages of the PLM are 936 m amsl (Palaeo-lake Thamalakane (PLT), 920 and 912 m amsl (Moore & Larkin, 2001; Moore et al., 2012). At 936 m amsl, river contributions to the lake include, the Zambezi, Cuando and Okavango rivers, whereas, at 920 m amsl, it was sustained by reduced inputs from the Zambezi, Cuando and Okavango. Finally at 912 m amsl, the lake was sustained by the Okavango and Cuando rivers; tectonic activities between 100 ka to present, led to formation of a full graben structure after down throw (400-700 m) bound by the Gumare and Thamalakane faults (Modisi et al., 2000; Kinabo et al., 2007; Kinabo et al., 2008; Milzow et al., 2009; Bufford et al., 2012) forming the Okavango Delta and Boteti River (Fig. 2). Progressive desiccation of the Makgadikgadi Pans (Sua and Ntwetwe saltpans) was the result. PLM is composed of several sub-basins hosted in a fluvial-lacustrine depression (Thomas & Shaw, 1991a) known as the Makgadikgadi-Okavango-Zambezi Basin - MOZB (Ringrose et al., 2005) as outlined in Fig. 2.
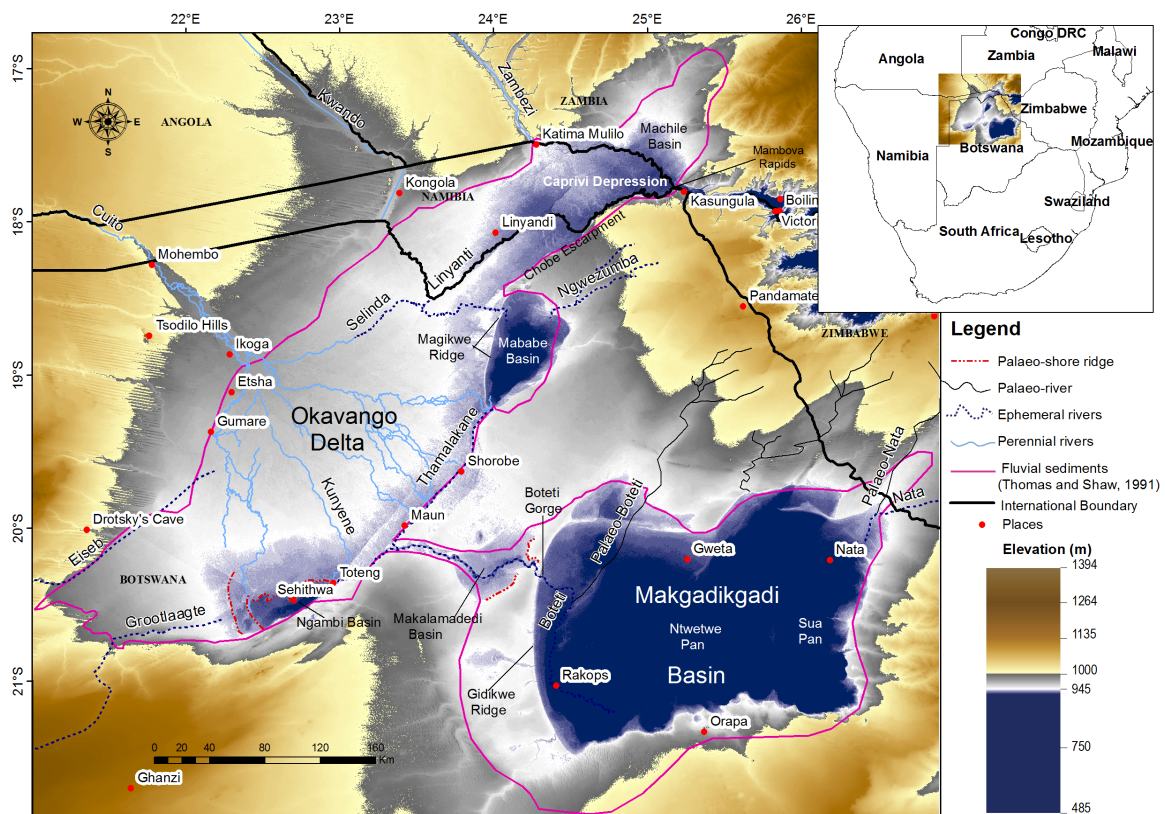
Fig. 2: Digital elevation model (Shuttle Radar Topographic Mission- SRTM) exhibiting structural depressions of the northern and central Kalahari with geographic references. Fluvial-lacustrine sediments (Pink outline) known as the Makgadikgadi-Okavango-Zambezi Basin – MOZB (Ringrose et al., 2005) host the palaeo-lakes.

3 Geology and Geochronology

Surficial geology within the MOZB is mainly composed of the Kalahari Group formations and outcrops of Karoo (Stromberg basalts) and Basement formations (Purdy & MacGregor, 2003) as shown in Fig. 3.
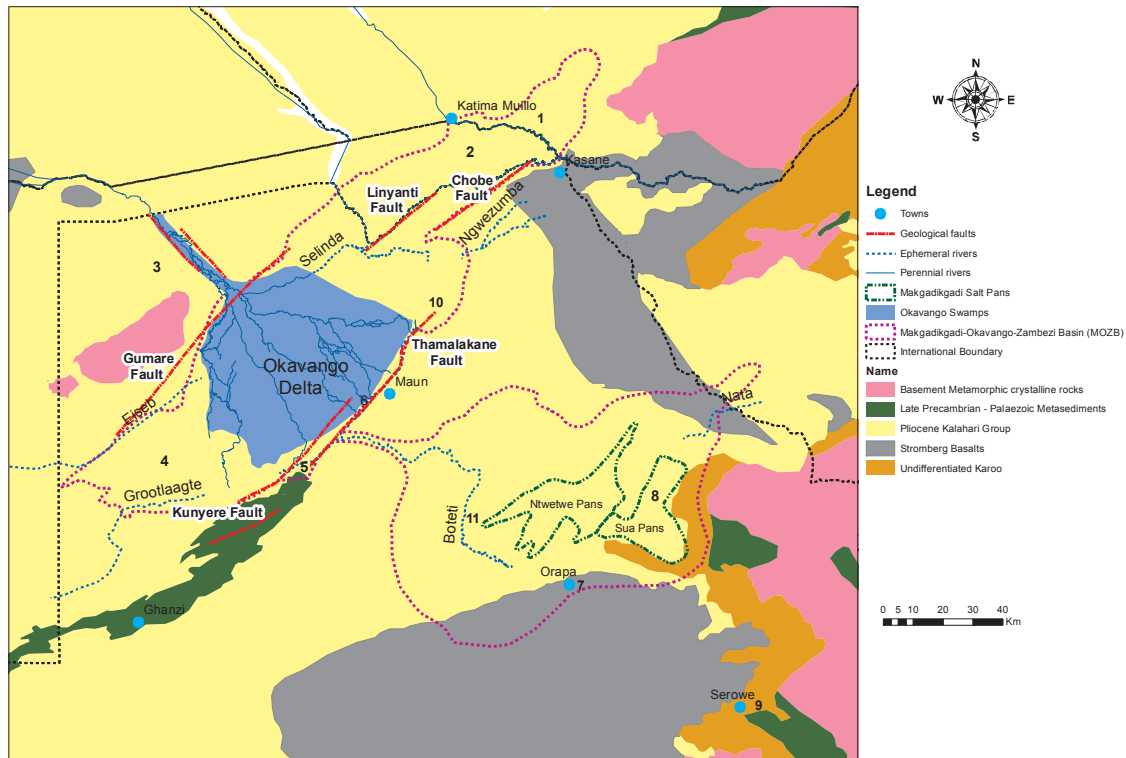
Fig. 3: Shows the surficial geology over the Makgadikgadi-Okavango-Zambezi Basin (adapted from Purdy & MacGregor, 2003) and the main structural fault systems. Typically, the basin is covered by Pliocene Kalahari Group formations within outcrops of Stromberg basalts and undifferentiated Karoo in the fringe region (Kasane and Orapa regions). The number references are used in Table 1.

Due to the lack of exposed outcrops and consistently datable fossils or mineralogical records in the Kalahari Group formations, a lithological approach is recognised for defining hydrogeological units (Thomas & Shaw, 1991b). Lower Kalahari Group units include; conglomerates and gravel units which sporadically occur at the base of the Lower Kalahari Group and occasionally within the units; pink to red, fine-grained, homogenous marls/clays; varicoloured, sandstones; calcretes, silcretes and other duricrusts. The Upper Kalahari Group is composed mainly of aeolian sands, colluvium, alluvial/deltaic sands, interbedded alluvium, sand, silt and clay (Thomas & Shaw, 1991b).

Table 1: A synthesis table of sediment and groundwater ages within MOZB. Groundwater ages are younger (< 50 ka) compared to the sediment suggestive of groundwater infiltration after sediment deposition.

Site (location in Fig. 2)	Sediment					Groundwater		References
	Material	Location Coordinates	Sampling Depth	Methods	Age	Method	Age	
Machile Basin (1)	Fluvial sediments	25.043 E -17.4899 S	~50 m	OSL	> 300 ka [1]	^{14}C	C.12-1.5 Ka [2]	[1] Banda et al. (submitted 2015a) [2] Banda et al. (submitted 2015b)
Caprivi strip (2)	Shell (spp Lymnaeae)/Calcretes	24.4008 E -17.7393 S	~1.5 m to the surface	^{14}C	15.4-11.5 Ka BP [1]	^{14}C	C.15-3 Ka BP [2]	[1] Shaw & Cooke (1986), Shaw & Thomas (1988), Thomas & Shaw (2002). [2] Margane et al. (2005)
Okavango Pan region (3)	Fluvial sediments	21.815 E -18.6656 S	~6 m to the surface	^{14}C	17-15 Ka BP [1]	^{14}C	C.15-1.7 Ka BP [2]	[1] Nash et al. (1997) Thomas et al. (2003) [2] Vogel & Van Urk (1975)
Drotskys' Cave (4)	Stalagmites (Sinister developments)	21.917 E -20.2818 S	Cave in-growth	^{14}C and Th/U	50-43 ka, 38-35 ka, 31-29 ka, 26-21 ka, 19-14 ka, 12.5-11 ka, 6.9-2.6 ka, 1.6-0.5 ka [1]	^{14}C	C.16-1.6 Ka BP [2]	[1] Cooke & Verhagen (1977), Cooke (1984), Shaw & Cooke (1986), Thomas & Shaw (2002), [2] Cooke (1975)
Lake Ngami Basin (5)	Calcretes [1] Palaeo-shorelines [1b]	22.9858 E -20.4604 S	~3.5 m to the surface	^{14}C [1] OSL [1b]	23.9-1.5 ka BP [1] 140-3 ka BP [1b]			[1a] Shaw (1985a) [1b] Shaw et al. (2003) Burrough & Thomas (2009)
Okavango Delta (6)	Fluvial sediments	23.5348 E -19.8315 S		Sedimentation Rates	146-15.5 Ka BP [1]	Groundwater Modelling	C.36-8.6 Ka BP [2]	[1] Heine (1978) McCarthy et al. (2012) [2] McCarthy & Metcalfe (1990), Langer & Heusser (2004)

Region	Material	Coordinates	Depth	Method	Age	Method	Age	References
Orapa Region (7)	Stromberg basaltic minerals	25.2632 E -21.3341 S	Outcrops	^{40}Ar/^{39}Ar	180.9-178.3 Ma [1]	^{14}C	C.30-2 Ka BP [2]	[1] Duncan et al. (1997), Le Gall et al. (2002), Jourdan et al. (2004), Jourdan et al. (2005). [2] Stadler (2005), Foster et al. (1982), Mazor et al. (1977)
Makgadikgadi Salt Pans (Sua Pans) (8)	Calcrete and shells [1] Fluvial sediments [1b]	25.9548 E -20.5632 S	~2.5 m to the surface	^{14}C [1] OSL and TL [1b]	40.8-21.9 ka BP[1] 288-8 ka BP [1b]			[1] Heine (1978), Cooke & Verstappen (1984), Riedel et al. (2012), Riedel et al. (2014) [1b] Ringrose et al. (2005), Burrough et al. (2009a)
Serowe region (9)	Karoo Sediments	26.6854 E -22.3734 S	~40 m	U-Pb	305-283 Ma [1]	^{14}C Argon-38	C.40-0.5 Ka BP [2]	[1] Bangert et al. (1999) [2] Selaolo (1998) Kulongoski et al. (2004)
Mababe Basin (10)	Calcrete and shells [1] Fluvial sediments [1b]	26.6854 E -22.3734 S	~7 m to the surface	^{14}C [1] OSL [1b]	25-13 ka BP [1] 35.6-5 ka BP [1b]			[1] Shaw (1985b), Shaw & Cooke (1986) Thomas & Shaw (1991b) [1b] Teter (2007), Burrough & Thomas (2008), Burrough & Thomas (2009)
Boteti region (11)	Calcrete and shells [1] Fluvial sediments [1b]	24.4286 E -20.8373 S	~6 m to the surface	^{14}C [1] OSL [1b]	42-12 ka BP [1] 109-8 ka BP [1b]	Ground-water modelling	C.12-7.5 Ka BP[2]	[1] Heine (1978), Cooke & Verstappen (1984), Thomas & Shaw (1991b), Shaw et al. (1992), Shaw et al. (1997), Burrough et al. (2009a), Riedel et al.(2009),Riedel et al. (2014) [2] De Vries (1984)

Given that much of the Kalahari Group occurrence is less than 100 m thick within MOZB (Haddon & McCarthy, 2005), the lithological classification rather than lithostratigraphy has been widely applied to hydrogeological investigations, where the focus has largely been on recharge studies (we discuss this later in the paper).

Sediment ages have been measured using various materials (fluvial sediments, calcretes and fossils) with ages such as 15.4-11.5 ka BP (using shells, see Table 1 for references) at Caprivi Strip, fluvial sediments at Okavango Delta (146-15.5 ka BP, references in Table 1), and Mababe Basin with calcretes of ages 25-13 ka BP. Interpretation of sediment age has to be done with caution as the dating material including calcretes, fossils (typically shells) and speleothems represent different phases of hydrological regimes with varying palaeo-environmental conditions (Thomas & Shaw, 1991b). Stromberg Basalt and Karoo at Orapa and Serowe (further than MOZB) have ages 180-178 Ma and 305-283 Ma, respectively (Table 1). Geochronology in the MOZB has been determined using radiocarbon and Optically Stimulated Luminescence (OSL) dating on sediments, fossils and sinter formations (such as speleothems). The oldest dated sediments in the basin are from the Machile Basin (up to 50 m bgl) and Palaeo-Shoreline sediments (< 2.5 m bgl) of Makgadikgadi Salt Pans (Sua Pans), using OSL, not younger than *C.* 300 Ka; this is the age limit of OSL method (Cordier et al., 2012) and hence sediments may be much older and speculated to be 1.4 Ma (Moore et al., 2012).

4 Hydrogeology

4.1 Thickness of the unsaturated zone and groundwater flow

The thickness of the unsaturated zone (or depth to the groundwater table) using data from various works within and around MOZB (YEC, 1995; Klock, 2001; Mendelsohn & El Obeid, 2004; Margane et al., 2005; GRB, 2006; Bäumle et al., 2007; Banda et al., submitted 2015b) was plotted with the thickness of the Kalahari Group formations (adapted from Thomas & Shaw, 1991b; Haddon & McCarthy, 2005) as shown in Fig. 4. On average, groundwater sits between 10-20 m below ground level - bgl and relatively shallow in the central regions of MOZB compared to the north-east and south-west por-

tions (> 60 m bgl), which is below the Kalahari Group (Karoo) where the phreatic surface is much deeper (Fig. 4).
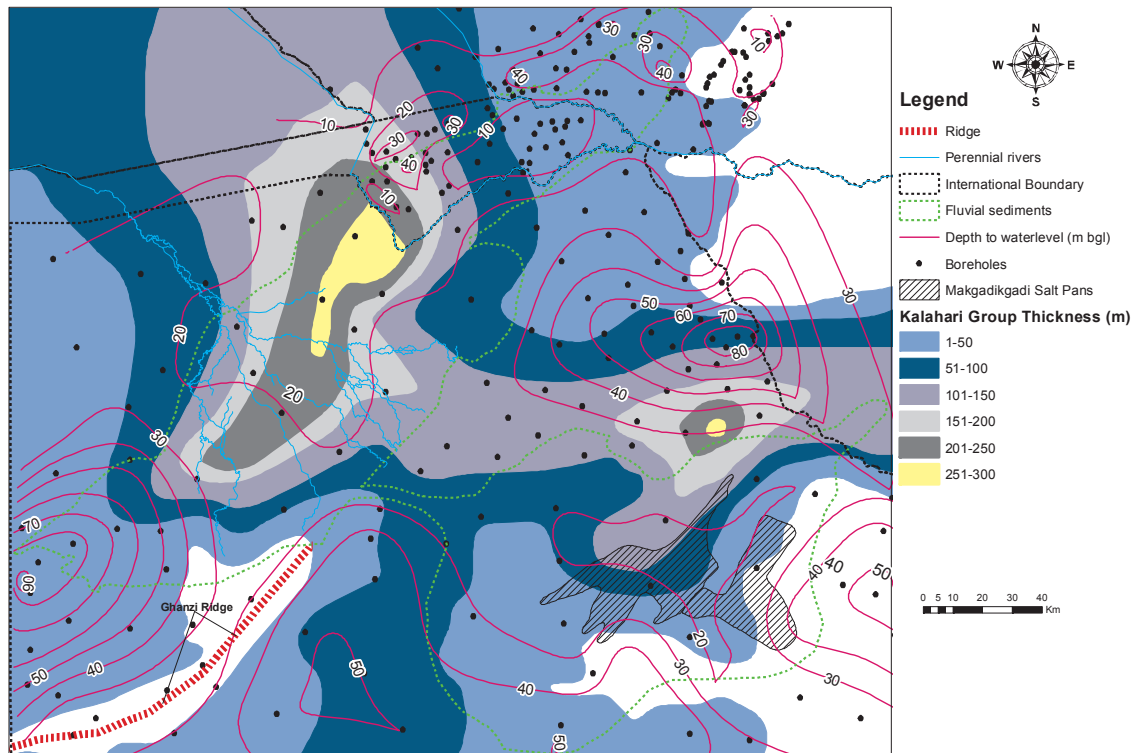
Fig. 4: A synthesis of interpolated Kalahari thickness (adapted from Haddon & McCarthy, 2005) and an extract of contoured depth to the saturated zone (m bgl) (De Vries et al., 2000; Klock, 2001; Margane et al., 2005; GRB, 2006; Bäumle et al., 2007; Banda et al., submitted 2015b). Groundwater sits in the Kalahari Group and characterised by near surface water table (10-20 m bgl) susceptible to evapo-transpiration loss.

Groundwater is at or near the surface around and inside the Makgadikgadi salt-pans. The broad range of depths to the groundwater table probably mirrors the potential recharge under current climatic conditions; areas with groundwater level less than 40 m bgl points to potential aquifer recharge through groundwater circulation. In addition, areas with groundwater levels more than 60 m bgl, under current climatic conditions most likely receive little or no recharge. De Vries (1984) modelled the regional flow through the central Kalahari sediments from southwest to northeast, on the basis of hydraulic conductivity (2 m/day) and transmissivity (150 m^2/day) and concluded an existence of a flux of less than 1 mm/yr, which for steady-state conditions would mean an overall recharge of the same order. He argued however, that the present gradient could also be a residual from a previous wet period,

which would mean an even lower recharge. Starting from a wet period with the groundwater table close to the surface, it would, according to his calculations, take more than 10,000 yrs of depletion by discharge to reach the present groundwater table. The present hydraulic head could thus equally be explained as a residual of a previous wet pluvial period.

Groundwater flow (Fig. 5) towards MOZB, shows a closed basin flow regime terminating within MOZB. The hydraulic gradient with MOZB, however, appears rather horizontal with values in the order of 0.0004. We suggest the geological faults (Thamalakane and Kunyere) form a first order hydrogeological division in which groundwater from the Okavango Region does not interact with the surrounding groundwater from other parts of MOZB.
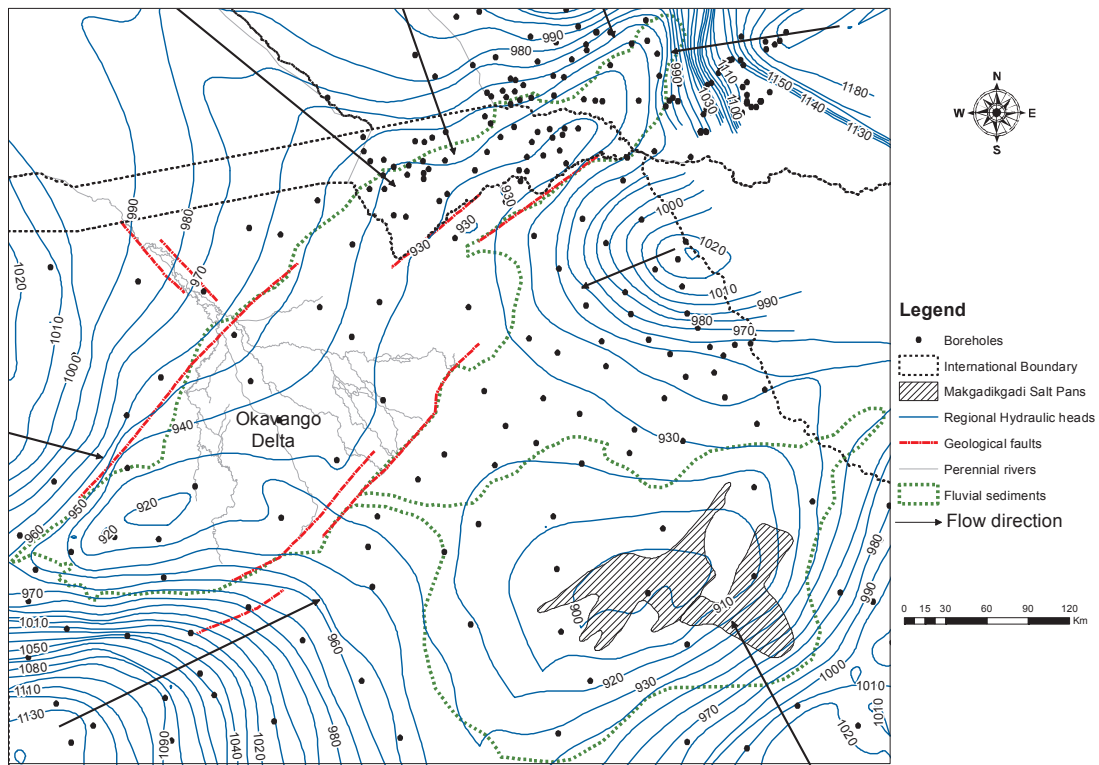
Fig. 5: Shows the groundwater flow regime over MOZB in which regional groundwater terminates at the MOZB. Groundwater is hosted within a closed basin system.

4.2 Recharge and stable isotopes

The occurrence of groundwater recharge from rainwater (direct recharge) through the Kalahari sediments has been a controversial issue (Obakeng, 2007). Some investigators concluded that no rainfall infiltration was occurring in the Kalahari due to seasonal moisture retention in the sands and com-

plete loss by subsequent evapotranspiration (Van Straten, 1955; Farr et al., 1981; Foster et al., 1982; De Vries & Von Hoyer, 1988). De Vries (1984) further substantiated this view point through a numerical study of declining regional groundwater level since the last pluvial period - palaeo recharge (12 Ka), and concluded that present day discharge was at the most 1 mm/yr thus more or less a stagnant groundwater system. However, evidence of substantial rain recharge through the Kalahari sands emerged from a variety of tracer studies including: Jennings (1974), Mazor et al. (1974), Verhagen et al. (1974), Mazor et al. (1977), Mazor (1982), Verhagen (1990), Verhagen (1992), Beekman et al. (1996), Beekman et al. (1997), Selaolo (1998), Beekman et al. (1999), De Vries et al. (2000), and Magombedze et al. (2004). In addition, Osenbrück et al. (2009), argues higher recharge during wet climatic periods (>30-20 ka and 8-4.5 ka) in the Kalahari sands in the past based on the atmospheric contamination of noble gas isotopes (^{20}Ne/^{22}Ne) in the groundwater around Serowe (see Fig. 2 for location). Other studies within the Kalahari Basin also support recharge during the glacial periods preserving low temperature groundwater up to 5 ºC lower than current temperature (Vogel, 1982; Stute & Talma, 1998; Kulongoski et al., 2004). Obakeng (2007) showed that the current substantial recharge is removed from the saturated zone through extraction by deep rooted trees as hypothesised by De Vries et al. (2000) and what is hosted in the aquifers is paleao water.

Given the primary role of evapotranspiration on both surface and groundwater within MOZB, stable isotopes (^{18}O and ^{2}H) studies (Dincer et al., 1978; Verhagen, 1995; Margane et al., 2005; McCarthy et al., 2012; Banda et al., submitted 2015b) are compiled to assess if stable isotope signature in groundwater would indicate palaeo or recent recharge and evaporation effects. Surface water from the Okavango Delta has ^{18}O, -5 to -3 ‰, and ^{2}H, -30 to -20 ‰ indicative of isotopic fractional effects. It has been shown that with increasing electrical conductivity (EC) of the Okavango surface water, the range of ^{18}O becomes narrower indicative of evapotranspiration effects resulting in increased accumulation of solutes (McCarthy et al., 1986; McCarthy & Metcalfe, 1990; McCarthy et al., 1991; McCarthy, 1992; McCarthy et al., 1993; McCarthy & Ellery, 1994; McCarthy & Ellery, 1998; McCarthy, 2006; Ramberg & Wolski, 2008; McCarthy et al., 2012). The groundwater has ^{18}O, -60 to 10 ‰, and ^{2}H, -9 to 10 ‰ of which some of the isotopes are on the global precipitation line ($\delta D = 8\delta^{18}O + 10$) and evaporation lines (slope approximately of 5) as shown in Fig. 6. Long term precipitation data from the nearest global monitoring stations in Windhoek, Namibia

and Harare, Zimbabwe indicate a weighted average of -5.03 ‰ and -6.14 ‰ for ^{18}O, -24.5 ‰ and -32.4 ‰, ^2H, respectively (IAEA, 1992). We suggest the groundwater isotopes on the precipitation line have undergone evaporation under varied humidity conditions, which influences precipitation variability. Gonfiantini (1986) suggests a gradient of 8 in a δ^2H-$\delta^{18}O$ plot, represents a high relative humidity, > 95 %, indicative of low potential evaporation effects. The evaporation slope (5) suggests a relative humidity of 75 % with higher evaporation. All the groundwater isotopes have thus sustained evaporation prior to infiltration.

Stable isotopic variability and mineralisation processes have also been accounted for by considering EC or total dissolved solids (TDS), consequently high EC but low fractionation within the Okavango Region (evapotranspiration effects (Dincer et al., 1978; McCarthy et al., 2012)), high EC and high fractionation especially in the fringe regions such as Boteti River (evaporation (Verhagen, 1995)) and high EC but relatively low fractionation such as within Lake Ngami, Caprivi Strip and Machile (mineral leaching/ dissolution (Verhagen, 1995; Margane et al., 2005; Banda et al., submitted 2015b)).

Stable isotopes (Fig. 6) has shown that it is not possible to categorise groundwater into a palaeo and recent recharge signature within MOZB as there seems to be some meteoric water influence that corroborate with recharge studies. Further, surface water contribution from the Okavango Delta does not interact with the regional groundwater and is predominantly lost to evapotranspiration; several studies have demonstrated these hydrological processes in the Okavango Delta (Such as McCarthy & Metcalfe, 1990; McCarthy et al., 1991; Bauer, 2004; Bauer et al., 2006a; Bauer et al., 2006b; Milzow et al., 2009; Kgotlhang, 2008; McCarthy et al., 2012).

Fig. 6: A synthesis of stable isotope of ^{18}O and ^{2}H (Dincer et al., 1978; Margane et al., 2005; Banda et al., submitted 2015b). Groundwater istopes in MOZB therefore represemt rapid infiltration

4.3 Groundwater ages

Groundwater ages are measured using ^{14}C with age ranges from 16-1.6 ka BP for Machile, Caprivi Strip, Okavango Pan Region and Drotskys' Cave. Groundwater modelling for the Okavango Delta and Boteti Region suggest ages of 36-8.6 ka and 12-7.5 ka, respectively (reference see Table 1). The oldest groundwater ages are from Orapa and Serowe and found to be between 40-0.5 ka BP (references as per Table 1). In general, sediment ages within MOZB from the studies reviewed indicate that sediment are much older (> 300 ka) compared to groundwater ages; this includes lake sediments as well as of rock out crops outside the MOZB. Calcretes (Table 1) are interpreted to have formed under salt-pan or playa conditions and are indicative of periods of low groundwater levels (Thomas & Shaw, 2002; Nash & McLaren, 2003). Drotskys' cave speleothems are inferred to have been sustained by groundwater (Cooke & Verhagen, 1977) and hence a proxy for paleaoclimatically induced recharge during humid conditions. Groundwater ages are between the

Late Pleistocene to Holocene (< 50 ka) within MOZB and the rim regions including Orapa and Serowe with Karoo sediments. The age difference between the sediments (>300 ka) and groundwater (< 50 ka) suggests the occurrence of groundwater salinity (discussed later in the paper) is therefore not due to burial of paleao-lake water but other processes such as sediment leaching, evaporation and evapotranspiration effects.

5 Groundwater Chemistry

5.1 Hydrogeophysics

Groundwater exploration and development in the MOZB region is restricted to geophysical techniques probably owing to the thick fluvio-lacustrine sediments with little or no outcrops and widespread occurrence of high salinity groundwater (Linn et al., 2003); the principal aim has been to locate fresh groundwater resources. Geophysical surveys have used ground and air-borne electrical methods to map both sediments and groundwater quality (fresh, brackish and saline); the groundwater classification ranks into three categories as fresh (Total Dissolved Solids (TDS) < 1, 000 mg/L), brackish (1,000 < TDS ≤ 10,000 mg/L) and saline (TDS > 10,000 mg/L) water (Freeze & Cherry, 1979).

Table 2 summarizes the lithologies, formation resistivities and methods used within MOZB. Air-borne Electro-Magnetic (AEM) and ground based Time Domain Electromagnetic surveying (TDEM) have essentially been used at a regional scale (references are shown in Table 2). These geo-electrical methods provide insights on aquifer variability and dimensions in the shallow and deeper levels. Geophysical resistivities within MOZB of clay is <3 Ωm, clayey sands and sand, 3-10 Ωm are typically saturated with saline and brackish water, respectively; fresh water resistivities typically occur in sands with values of 10-50 Ωm (Table 2 and Fig. 7). Fig. 7 outline the areas of geophysical mapping and cross sections from the various researchers (Sattel & Kgotlhang, 2004; Margane et al., 2005; Campbell et al., 2006; Podgorski et al., 2013; Chongo et al., 2014). Site 5, 6 and 7 shows a moderate resistivity (3-10 Ωm) occurring between a high resistivity (20-100 Ωm) below and a low resistivity (< 3 Ωm) formation above, which is a signature from the underlying Karoo Formation (Sattel & Kgotlhang, 2004) as shown in Fig. 7. This is probably attributed to tectonic disruptions that the basin has sustained. However, other authors, specifically within site 3 – Okavango Basin (Podgorski et al., 2013)

interpret the high resistivity formation (20-100 Ωm) to be remnants of the proto-Okavango Megafan (Fig. 7).

Table 2: Synthesis table of regional resistivities, methods and hydrogeological interpretations in the MOZB. Resistivities are generally homogenious and have been resolved to both sediments and water quality (<3 Ωm (saline/clay), 3-10 Ωm (brackish, clayey sands), 20-100 Ωm (fresh in Basement –fresh/weathered)).

Site (location number as shown in Fig.4)	Lithology	Formation Resistivity (ohm-meter)	Method	Reference
Machile Basin (1)	Upper Kalahari (surface sands) Middle Kalahari (sand, silt and clay) Stormberg Basalt	<3 Ωm (Saline/clay) 3-10 Ωm (Brackish) 20-40 Ωm (Dry Kalahari sands) 20-100 Ωm (Basement rocks)	AEM TDEM	Chongo et al. (2011) Chongo et al. (2014)
Caprivi Strip (2)	Upper Kalahari (surface sands) Middle Kalahari (sand, silt and clay)	<3 Ωm (Saline/clay) 5-10 Ωm (Brackish) 10-50 Ωm (Fresh)	TDEM	Margane et al. (2005)
Okavango Delta (3)	Upper Kalahari (surface sands) Middle Kalahari (sand, silt and clay)	<15 Ωm (Brackish-Saline), 15-40 Ωm (Fresh), >40 Ωm (Basement rocks)	AEM TDEM	Bauer (2004) Bauer et al. (2006c) Kgotlhang (2008) Podgorski et al. (2013) Meier et al. (2014)
Thamalakane Region (4)	Upper Kalahari (surface sands) Middle Kalahari (sand, silt and clay)	<3 Ωm (Saline/clays) 3-8 Ωm (Brackish) 9-30 Ωm (fresh)	TDEM, AEM	Campbell et al. (2006)
South of Thamalakane Region (5)	Upper Kalahari (surface sands) Middle Kalahari (sand, silt and clay)	<3 Ωm (Saline/clay) 3-10 Ωm (Brackish) 20-40 Ωm (Dry Kalahari sands) 40-100 Ωm (Basement rocks)	AEM	Sattel & Kgotlhang (2004)
South of Gidikwe (6)	Karoo Group	<3 Ωm (Saline/clay) 3-10 Ωm (Karoo mudstone) 20-40 Ωm (Dry Kalahari sands) 20-100 Ωm (Basement rocks)	AEM	Sattel & Kgotlhang (2004)

		<3 Ωm (Saline/clay)		
Rakops Region (7)	Middle Kalahari (sand, silt and clay) Karoo Group	3-10 Ωm (Karoo mudstone) 20-40 Ωm (Dry Kalahari sands) 20-100 Ωm (Basement rocks)	AEM	Sattel & Kgotlhang (2004)
Mopipi Region (8)	Upper Kalahari (surface sands) Middle Kalahari (sand, silt and clay)	<3 Ωm (Saline/clay) 3-10 Ωm (Brackish) 20-40 Ωm (Dry Kalahari sands) 20-100 Ωm (Basement rocks)	AEM	Sattel & Kgotlhang (2004)
Orapa Region (9)	Upper Kalahari (surface sands) Middle Kalahari (sand, silt and clay)	<3 Ωm (Saline/clay) 3-10 Ωm (Brackish) 20-40 Ωm (Dry Kalahari sands) 20-100 Ωm (Basement rocks)	AEM	Sattel & Kgotlhang (2004)

The Proto-Okavango Megafan is suggested to have been initiated during the period of the PLD (3-2.5 Ma) (Moore et al., 2012; McCarthy, 2013). The low resistivity unit (< 3 Ωm) hosting saline groundwater just below the modern day Okavango Delta covers (10-50 Ωm) is interpreted as an extension of saline sediments from the PLM (Podgorski et al., 2013) but mostly likely at higher level stage.
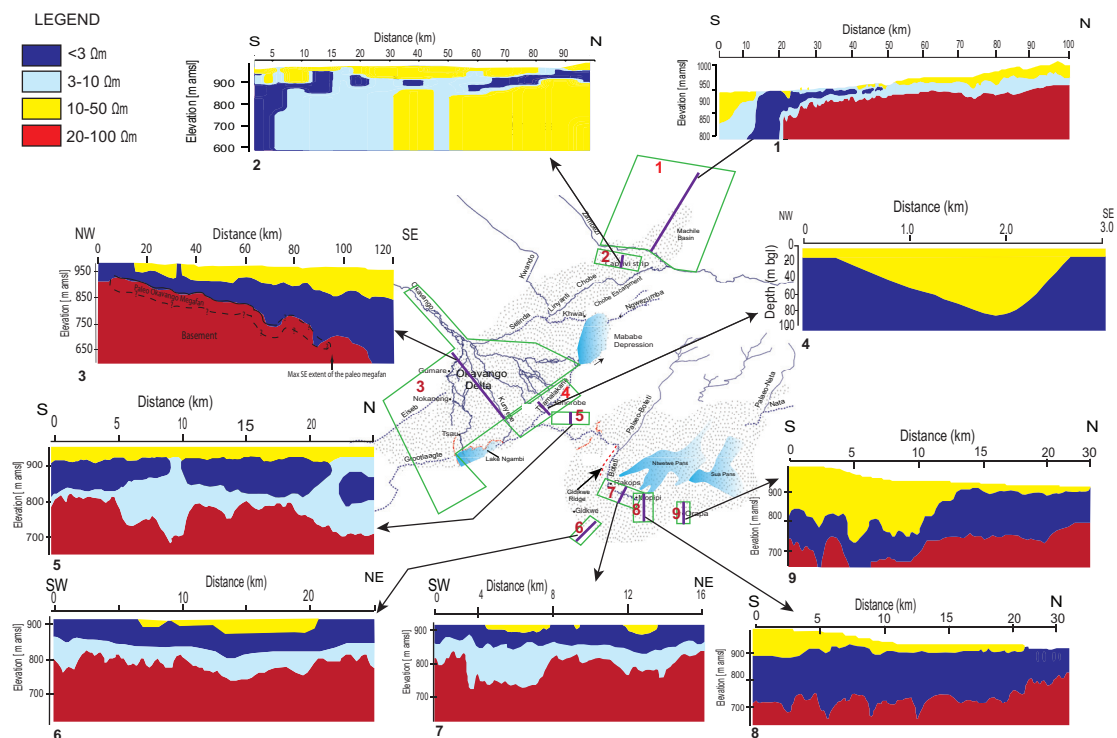
Fig. 7: A synthesis of the regional resistivity profiles within MOZB conducted using both ground and air based geophysics (Sattel & Kgotlhang, 2004; Margane et al., 2005; Campbell et al., 2006; Podgorski et al., 2013; Chongo et al., 2014). Geo-electrical methods (AEM and TDEM) are able to constrain and resolve PLM resistivities (<15 Ωm (near surface), 3-10 Ωm (intermediate depths), 20-100 Ωm (Basement depths).

The depth to the interface from low to high resistivities (saline to fresh groundwater), although well resolved, cannot be generalised and is rather specific to which part of MOZB is mapped but ranges from 10-80 m bgl (Fig. 7). Fresh groundwater potential exists in the near surface as perched aquifers (10-50 Ωm) linked to surficial drainages such as rivers, wetlands, alluvial deltaic features or palaeo-drainage, whereas brackish-saline groundwater is well spread throughout the basin predominately related to the Basement geology.

However, the geophysical model (site 6 and 7 (Sattel & Kgotlhang, 2004)), delineates resistivities of 3-10 Ωm just below an impervious saline layer (< 3 Ωm), this was interpreted as a sandstone formation within the Karoo Formation (Mosolotsane Formation, (Sattel & Kgotlhang, 2004)), that hosts fresh water. Conversely, high salinity formations, mapped within the Orapa Region (site 9, Fig. 7) were interpreted as deep sediments (mudstone, shales and

sandstones) of the Karoo Formation (Ecca Group, (Sattel & Kgotlhang, 2004)) and suggests an extension of high salinity groundwater beyond the MOZB. Ecca Group sediments are suggested to be the origin of high salinity water in salt-pans widespread in Southern Africa (Seaman et al., 1991; Day, 1993).

5.2 Hydrochemistry

Groundwater chemistry was compiled from various researchers (Mazor et al., 1980; McCarthy et al., 1991; Klock, 2001; Vogel et al., 2004; Margane et al., 2005; McCarthy, 2006; Bäumle et al., 2007; Eckardt et al., 2008; Stadler et al., 2008; Banda et al., submitted 2015b) with a background of PLD and PLM outlines (Fig. 8a); water quality types are carbonates (Ca-Mg-HCO$_3$/Na-Ca-HCO$_3$), sulphate (Na-Cl-SO$_4$) and chloride (Na-SO$_4$-Cl). Carbonate groundwater occurs within the Okavango Delta and the fringe region with active groundwater recharge; carbonate groundwater within the Okavango Delta has concentrations from 300-6,500 mg/L precipitating trona (NaHCO$_3$.Na2CO$_3$.2H$_2$O) on the surface as a result of evapotranspiration losses within the salt-pans/saline islands (McCarthy et al., 1986; McCarthy et al., 1991; McCarthy & Ellery, 1994; McCarthy & Ellery, 1998; McCarthy et al., 1998). In addition, chloride concentrations range from 5 to 6,500 mg/L and sulphate 5 to 2,000 mg/L within the Okavango Delta (McCarthy et al., 1986; McCarthy & Metcalfe, 1990; McCarthy et al., 1991; McCarthy & Ellery, 1994; McCarthy, 2006). In the northern margin of MOZB, Machile and Caprivi Strip, groundwater concentrations include: sulphate (280-10,600 mg/L), chloride (150-5,500 mg/L) and carbonate (290-2,300 mg/L) (Margane et al., 2005; Banda et al., submitted 2015b). In other parts, Mababe, Makalamadedi and Ngami Basin, groundwater concentrations include: sulphate (70-4,000 mg/L), carbonate (360-2,500 mg/L) and chloride (30-2,200 mg/L) (Mazor et al., 1980; Aquatec, 1982). The Makgadikgadi salt pans (Sua and Ntwetwe pans) have groundwater concentrations including: chloride (46,000-5,300,000 mg/L), sulphate (4400-1,550,000 mg/L) and carbonate (6,000-1,150,000 mg/L) with mineral precipitates of mirabilite (NaSO$_4$.10H$_2$O), halite (NaCl) and trona (NaHCO$_3$.Na$_2$CO$_3$.2H$_2$O) (Vogel et al., 2004; Eckardt et al., 2008; Wood et al., 2011).
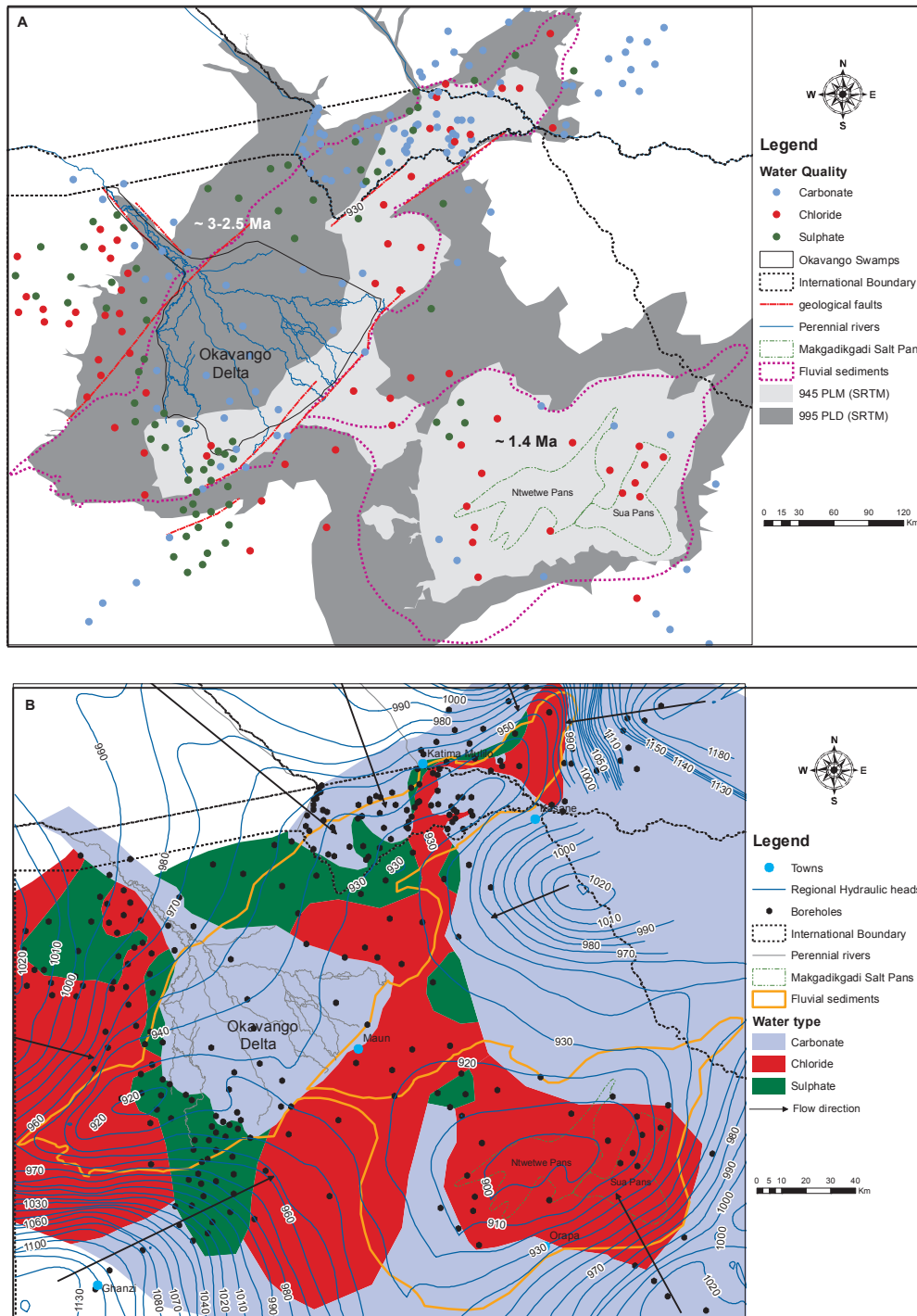
Fig. 8: (a) Water quality sampled points (Mazor et al., 1980; Vogel et al., 2004; Margane et al., 2005; Bäumle et al., 2007; McCarthy, 2013; Banda et al., submitted 2015b) over the MOZB with a background of lake stages at 995 and 945 m amsl with corresponding ages of 3-2.5 and 1.4 Ma, respectively. (b) Interpolated water quality (carbonates, chlorides and sulphates) with the groundwater flow regime. Chlorides are typically in the central region, sulphates in the fringes and carbonates in Okavango Delta and regional groundwater beyond MOZB.

The spatial variability of groundwater types is such that the chloride water is hosted in the central regions, where the palaeo-lake sediments are thickest, and shifts from sulphate to carbonate towards the fringes and the Okavango Region (Fig. 8b). Given that groundwater discharge is negligible and lost to evapotranspiration at the fringes of the MOZB, the net groundwater flow to the MOZB (Fig. 8b) does not change the hydrogeochemistry but rather represents probably a stagnant groundwater situation. A comparison of the two Fig.s (Fig. 8a & b), we suggest the chloride and sulphate water are a result of dissolution of evaporites, which had undergone differential levels of evapo-concentration (Eugster & Jones, 1979). The carbonate water type such as that of the Okavango Region and the fringes is from recent recharge by meteoric water (Stadler et al., 2008; McCarthy, 2013; Banda et al., submitted 2015b). However, the presence of chloride and sulphate ions in the fringes (south of the Okavango Delta) suggests leaching to the surrounding or underlying formation (Karoo) during the pluvial climatic period given that the Kalahari Group is thinner in this region (1-50 m).

6 Discussion

6.1 River water chemistry and formation of evaporites

PLM evolved through a series of five major lake stage changes (~995, 945, 936, 920 and 912 m asl) changing the drainage regime within Southern Africa driven primarily by tectonic disruptions and climatic variability (Moore & Larkin, 2001; Moore et al., 2012). The water budget of the system (Moore et al., 2012) with lake area change from 995 m amsl, 175,400 km^2 at a potential evaporation loss of ~ 1,000 mm/yr (Moore et al., 2012). The evaporation losses over the different lake phases were an important mechanism for accumulation of solutes within lake water. The contributing river water chemistry (Hall et al., 1977; Balon, 1978; Cronberg et al., 1995; Huntsman-Mapila et al., 2006) was probably not different at the time of formation compared to what we observe today; hydrochemistry is summarised in Table 3. River water interacts with rocks and minerals producing the anion alkalinity, almost exclusively HCO_3 (0.33-1.15 mmol/L), SO_4 (0.002-0.038 mmol/L) and Cl (0.011-0.0625 mmol/L) as shown in Table 3. River water chemistry of the Kafue (Table 3) has a very high sulphate concentration probably from anthropogenic activities and is not considered as potential contribution to the

palaeo-lake. Other solute constituents, including Ca (0.1-0.29 mmol/L), Mg (0.037-0.18 mmol/L), Na (0.087-0.367 mmol/L), are leached from alumino-silicate minerals such as plagioclase, biotite, muscovite and hornblende. The average river water chemistry (Table 3) has Ca, 0.162 mmol/L, Na, 0.237 mmol/L, Mg, 0.108 mmol/L, alkalinity, 0.798 mmol/L, Cl, 0.030 mmol/L and SO_4, 0.036 mmol/L.

Table 3: Outlines the river water chemistry of major rivers (Hall et al., 1977; Balon, 1978; Cronberg et al., 1995; Von Der Heyden & New, 2003; Huntsman-Mapila et al., 2006) that contributed to the palaeo-lake system during various stages of evaporation. The rivers are typically calcium carbonate dominated.

River	Site	Ca mmol/L	Mg mmol/L	Na mmol/L	Alkalinity as HCO_3) mmol/L	Cl mmol/L	SO_4 mmol/L
1. Okavango[a]	Pan-handle area	0.102	0.037	0.087	0.334	0.011	0.002
2. Luangwa[b]	At the confluence with Zambezi	0.294	0.181	0.293	0.778		0.094
3. Upper Zambezi[c]	Upper Zambezi before the Kariba Dam	0.129	0.151	0.367	1.15	0.063	0.108
4. Kwando[d]	James Camp	0.126	0.071	0.201	0.917	0.015	0.025
5. Kafue [e]	Before the Kafue	8.70	11.03	12.53	0.708		26.96
Average (1, 2, 3 ,4)		0.162	0.108	0.237	0.798	0.030	0.036

Sources: [a] Huntsman-Mapila et al. (2006), [b] Hall et al. (1977), [c] Balon (1978), [d] Cronberg et al. (1995), [e] Von der Heyden & New (2004)

To explore the probable mineral evolution in the evaporative basin as a function of the concentration factor, the geochemical software, PHREEQC 3 (Parkhurst & Appelo, 2013) , was used. We assume a situation where a finite volume of lake water evaporates (declining volume) and the sequence of minerals precipitated is calculated by assuming equilibrium for the most probable minerals based on the calculated saturation state of the water. The Pitzer database, included with PHREEQC 3, capable of handling the high ionic strength (Pitzer, 1973, 1975), was used in the calculation. A declining lake volume was assumed because no thick deposits of evaporites were observed within the Makgadikgadi Region. The initial model solution comprised 100 m^3, rather than the default volume of 1 litre, to avoid numerical

problems as the water is removed (evaporated). The initial model chemistry is the average river inflow water (Table 3). The saturation of evaporite minerals as equilibrium phases (allowed to dissolve and precipitate) is followed for calcite ($CaCO_3$), magnesite ($MgCO_3$), gypsum ($CaSO_4.2H_2O$), bassanite ($CaSO_4.\frac{1}{2}H_2O$), anhydrite ($CaSO_4$), mirabilite ($Na_2SO_4.10H_2O$), thenardite (Na_2SO_4), bischofite ($MgCl_2.6H_2O$), bloedite ($MgSO_4.Na_2SO_4.4H_2O$), burkeite ($Na_2CO_3.2Na_2S0_4$), carnallite ($KMgCl_3.6H2O$), epsomite ($MgS0_4\cdot7H_2O$), halite ($NaCl$), hexahydrite ($MgSO4.6H_2O$), kieserite $MgSO_4.H_2O$, sylvite (KCl), gaylussite ($Na_2CO_3.CaCO_3.5H_2O$), nahcolite ($NaHCO3$), thermonatrite ($Na_2CO_3.H_2O$), natron ($NaCO_3.l0H_2O$) and trona ($NaHCO3.Na_2CO_3.2H_2O$). In the geochemical modelling, the pH of lake water was buffered by equilibrium with atmospheric PCO_2 of 200 ppm corresponding to the CO_2 partial pressure in the atmosphere of about 1.4 Ma BP during formation. To calculate the concentration factor of the river water, Br was included in the inflow water with a concentration of 10^{-6} mmol/L.

The output from the PHREEQC 3 model (Fig. 9a & b) shows that the river precipites calcite and dolomite first after a 10 times concentration factor. With increased precipitation, solute accumulation increases through a gypsum saturation and precipiting halite after ~50,000 times of concentration. Simulation concentration show Ca, 1.48 mmol/L and alkalinity of 0.731 mmol/L at calcite and dolomite precipitation hence a ratio of 2 Ca:1 alkalinity. The evaporation sequence of the river water can be explained using the Hardie-Eugster Model (Hardie & Eugster, 1970). Fig. 10, shows a modified version of the Hardie-Eugster (Drever, 1997) of which we infer based on the 2 Ca:1 alkalinity ratio during calcite and dolomite precipitation, that the evolution of the palaeo-lake system followed path II. The sequence of mineral salts that precipitate follow a chemical divide proposed as shown in Fig. 10; typically during evapoconcentration, saturation of alkali earth carbonates is reached quickly (Hardie & Eugster, 1970; Eugster & Jones, 1979; Jankowski & Jacobson, 1989). Subsequent precipitation of silicates, carbonates, sulphates and chlorides are controlled by the relative concentration of magnesium, calcium, carbonate, sulphate and chloride (Jones et al., 1977; Eugster, 1980; Spencer et al., 1985b). The PHREEQC simulation results (Fig. 9 a & b) supports a carbonate river water evolution within the PLM, that endured evaporation, under closed basin coniditions, up to halite evaporites particularly in the deepest part of the lake – Makgadikgadi Basin.
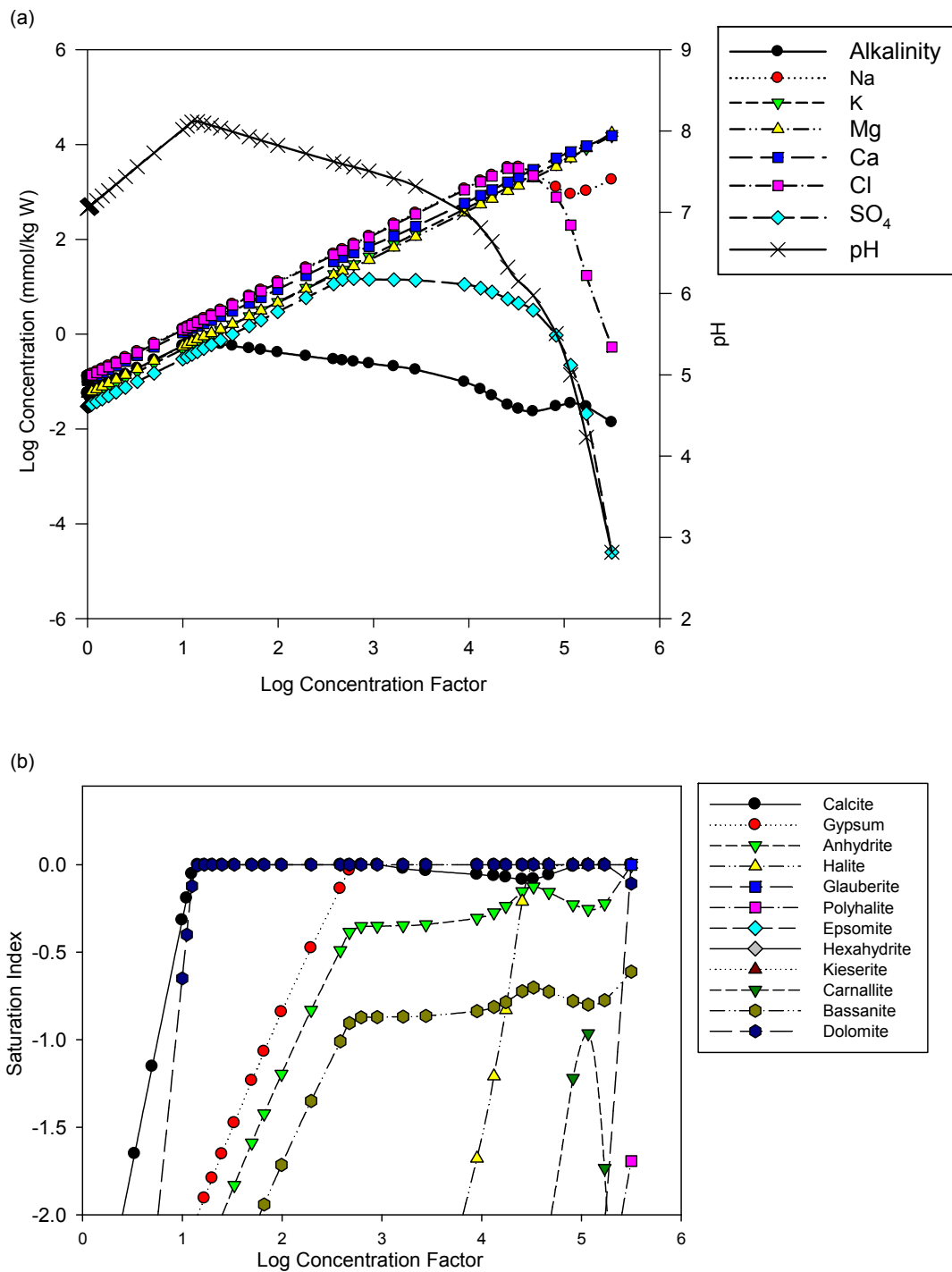
Fig. 9: (a) PHREEQC 3 simulation of evolving lake chemistry in the closed lake filled with fresh water (Zambezi Water) with evaporation and precipitation of minerals. Concentration factor represents the degree to which the remaining water is concentrated after water is evaporated. Carbonates are precipitated first followed by sulphates in accordance with Eugster's model under closed basin conditions (Hardie & Eugster, 1970). (b) Plot showing the mineral saturation against concentration
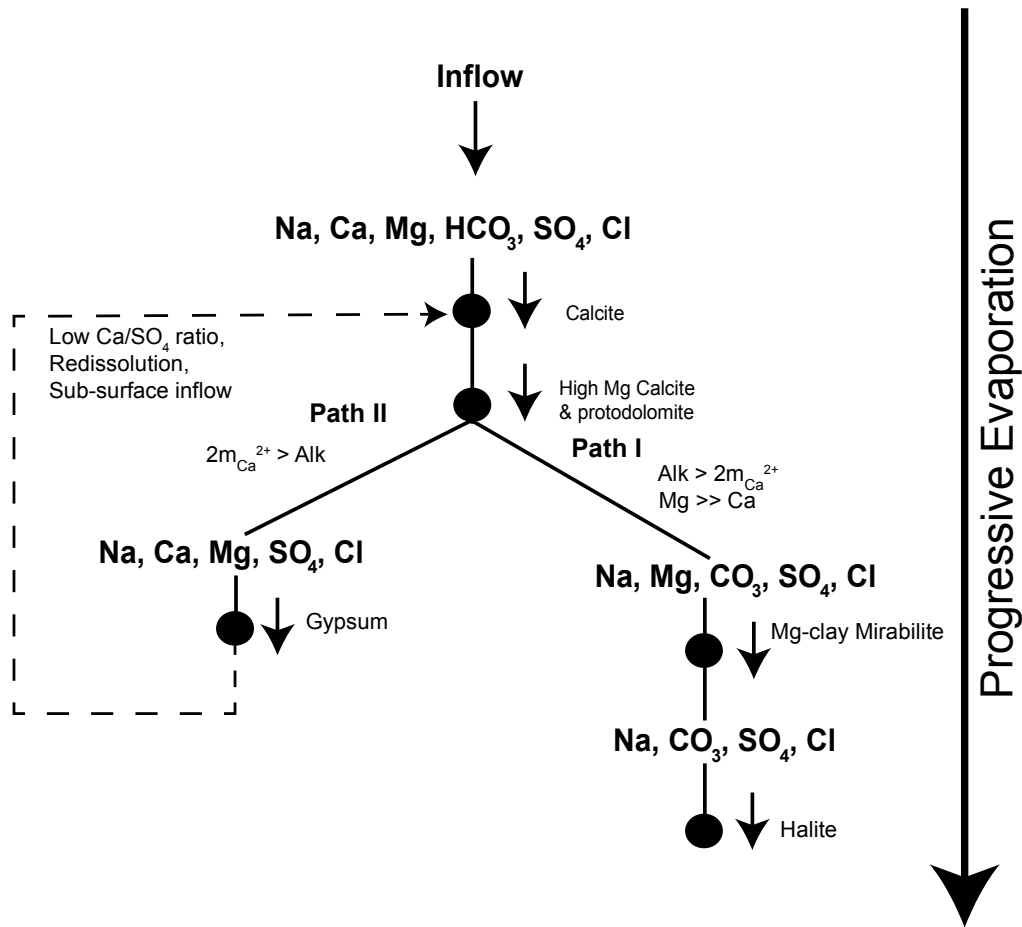
Fig. 10: Evaporation path of closed lake system of solutes with progressive evapo-concentration (adapted from Eugster & Hardie, 1978). Halite precipitation is typically the last to form, but the most soluble whereas, the least soluble, typically carbonates will form first.

It is probable that the precipitates within MOZB formed during deposition (syn-depositional). The notion is supported with core samples that are intimately intermixed with the detrital fraction as seen in the Machile Basin (Banda et al., submitted 2015a). Similar evaporite mineralogy in the stratigraphic column has been observed in the Sambhar Salt Lake (Sinha & Raymahashay, 2004), Searles Lake (Eugster & Smith, 1965), Great Salt lakes (Bowler, 1986), Ceylone (Last, 1989) and North Ingebrigt (Shang & Last, 1999). However, the PLM endured episodic tectonic activity, periodic flooding and overtopping of shorelines that raised and lowered the drainage divide to allow possible escape of solutes. Hence, chemical differentiation and thus mineral accumulation could have resulted from selective erosion of soluble salts and/or selective precipitation in the basin (Sinha & Raymahashay, 2004); progressive evaporation (Fig. 10) would thus not form some subse-

quent minerals. Consequently, this contributed to hydro-geochemical zoning (Fig. 8b) of the mega-lake resulting in a predominately sulphate saturation stage in the fringe zones (such as Caprivi depression and the Machile) and chloride saturation in the central region (Makgadikgadi Basin). Similarly, hydro-chemical zoning has been observed in closed basin salt lakes of Australia (such as Lake George), of which Bowler (1986), postulates that in the drying stages of any flat-floored basin, rapid transfer of salts from the surface to sub-surface occurs. Furthermore, high evaporative loss results in part of the upper waters exceeding sulphate saturation hence gypsum is precipitated interstitially. Finally, evaporative loss through the capillary fringe results in efflorescence of the more soluble salts, halite, in the central zone, provided groundwater evaporation/evapotranspiration at the margins (described as stage 4 of chemical accumulation, Bowler (1986)) takes place. In this regard, we suggest that the chloride probably is a result of groundwater discharge with progressive evaporation and sulphate is an imprint of evapo-centration in the initial phases of lake development desiccation.

6.2 Conceptual lake stage development and groundwater salinity

We suggest the development of groundwater salinity based on evidence from earlier sections (geochronology, groundwater ages, paleaoclimatics and recharge) is shown in the conceptual model of Fig. 11. The evolution steps indicate initially the formation of the PLD (3-2.5 Ma) within a closed basin sustained by surface water contribution, and later PLM (1.4 Ma) shown as stage 1 and 2, respectively, driven by tectonics and climatics. Reduced flow from 88-66 km^3/yr to the lake system after tectonic disruptions was balanced to evaporation of approximately from 946-395 mm/yr (Shahin, 2002; Moore et al., 2012); the main contributing river was the Zambezi, Okavango, Kwando and Kafue rivers (Moore & Larkin, 2001; Moore et al., 2007; Moore et al., 2012).

In stage 3, most of the PLM desiccated by 500 ka, during which groundwater influence probably was profound. Stage 4, progressive evapo-concentration led to rapid surface water-groundwater exchange precipitating carbonates (calcite and dolomite). Increased capillary fringe evaporation losses created a density flow at the discharge zone at the fringes hence precipitating gypsum. Increased evaporation and density flow continued forming halite following Hardie-Eugster's evaporation model in the central region.

1. **3-2.5 Ma**

Surface water runoff

Topographic surface

Mega-lake

Groundwater table

Groundwater inflow

Palaeo-Lake Deception formed at 995 m amsl approx. 3-2.5 Ma ago. The lake system comprised contributions from the Palaeo-Zambezi with a cummulative flow of 80 km³/ yr and evaporation of 946 mm/yr (Shahin, 2002 and Moore et al, 2012) in a closed basin. Input rivers transported products from the weathering of silicate minerals.

2. **1.4 Ma**

Evaporation

Due to tectonic disruptions and increasing aridity, the l ake stage level reduced to 945 m amsl by 1.4 Ma. River inputs were from the Okavango, Zambezi, Kwando and Kafue (66 km³/yr) balanced to an evaporation rate of 395 mm/yr (Moore et al, 2012).

3. **~500 ka**

Evaporation

Sediments

Tectonic disruptions and increasing aridity then desiccated most ofthe lake by 500 Ka.

4. **~500-100 ka**

Evaporation

Gypsum   Calcite/Dolomite   Halite

Progressive evapo-concentration then formed evaporates of carbonates (calcite, dolomite) within sediment and gypsum at the fringe (due to surface water-groundwater interaction, (Bowler J.M, 1986)). With continued desic--cation, capillary fringe losses increased and groundwater was increasly lost at the fringe zones concentrating the central zone to Halite. We assume this could have taken place between 500-100 ka just before the down throw of the Okavango Delta due to tectonic activities ~100 ka.

5. **<50 ka**

Precipitation

Pluvial climatic activites then followed between late-Pleistocence to Holocene (< 50 Ka) which partially leached the sediments hence releasing solutes of carbonates, sulphides and chlorides. The variation in water type is dependent on the amount of evaporation sustained as the lake system went through multiple lake water stages; chloride or chloride minerals were formed in the centre region as the highest accumulated concentrations.

Fig. 11: Summaried conceptual model of the evolution stages from the formation of the PLD to formation of evaporities that were partially leached contributing to salinity. The four stages represent salinity accumulation in the lake system and subsequent leaching to the groundwater.

Consequently, hydro-chemical zoning of chemical facies of chloride in the centre, and sulphate in the fringes was formed. We assume this process should have taken place ~ 500-100 ka before tectonic activities within the Okavango Delta Region. Formation of the Okavango Graben is estimated to be below 100 ka (Moore et al., 2012). Geophysical mapping has clearly shown a low resistivity layer below the Okavango Delta sediments probably as part of the PLM system (Podgorski et al., 2013). In stage 5, Pluvial climatic activities in the Pleistocence to Holocene (< 50 Ka), specifically, >30-20 ka and 8-4.5 ka, partially flushed or leached the evaporites that formed hence giving rise to younger groundwater ages than sediment ages.

The modern day groundwater salinity within MOZB, is a result of evapotranspiration effects, specifically in the Okavango Delta whereas in the other parts, evaporates form on the surface due to a near-surface evaporative loss. Near surface evaporation losses also occur especially in the Makgadikgadi Salt-pan Region. The current hydrogeological condition of the palaeo-lake basin is demonstrated in Fig. 12. Groundwater from the fringes is either forced out through the topographic depressions and drainages due to the hydraulic conductivity contrast between the lacustrine sediments and the regional groundwater contribution (Banda et al., submitted 2015b) or evapotranspiration facilitated by the root zone. Although, apparently stagnant, localised flow dynamics are evident through wetlands and rivers. Evaporites typically form on the surface due to near surface groundwater evaporation loss.
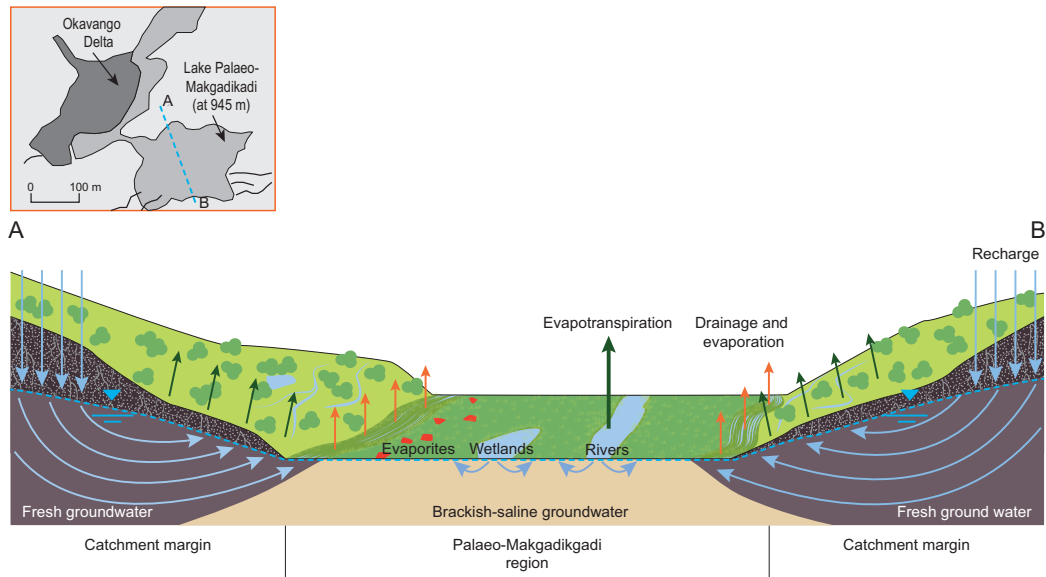
Fig. 12: A synthesis of hydrological processes within the PLM based on an extension of a local scale study by Banda et al. (submitted 2015b) in the Machile Basin. Groundwater is typically lost through topographic depressions (dambos) and drains facilitated by evapotranspiration; combined with the presence of lacustrine sediments (clays) groundwater flow is negligible with PLM although localised flow systems are present.

6.3 Future Research

Further research on the groundwater chemistry and hydrogeology should include: (1) deep borehole drilling through sediments of the Okavango Delta to establish the ages of both sediment and water to constrain the timing of down throw in relation to lake stages of the PLM as well as validate the conceptual model, specifically, if the sediments host palaeo-lake sediments and the nature of pore-water quality; (2) a model is required to link the five lake stages of lake evolution and the corresponding water quality that takes into account the tectonic events and evaporation over time; (3) The palaeo-lake modern day relics – the Makagardigardi Salt-pans, are prone to aeolian activity, which can be transport precipitates to fresh-water sediments hence causing groundwater contamination. Vulnerable aquifers need to be indentified and the potential geochemical salinisation controls; (4) the extent and depth of the saline-fresh water interface within the deeper Karoo sediments needs to be investigated; (5) MOZB has a limited number of drilled borehole and the few available lack hydro-chemical analysis at a regional scale and no geological stratigraphy. Increased data density would refine the chemical facies variation; and (6) a lot of studies have focussed on direct, diffuse recharge, how-

ever, the role of storm flood flows from ephemeral rivers and impacts on groundwater quality needs to be investigated.

7 Conclusions

This review paper sought to coherently explain the present day groundwater chemistry and hydrogeology of the Palaeo-Lake Makagardigardi based on existing state of knowledge. The following are the most important aspects:

- Regional groundwater flow terminates within the MOZB forming a closed groundwater drianage system. The thickness of the unsaturated zone is generally shallow (10-20 m bgl) in the basin and vulnerable to evapotranspiration losses via deep rooted savanna vegetation (10-70 m bgl as root depth) and near surface groundwater evaporation loss especially in the Makgadikgadi Salt-pan regions;

- Various studies investigated recharge mechanisms in MOZB, which suggest recharge occurs within the MOZB but is lost to the vegetation cover; regional studies support this assertion and further confirms that issolation of palaeo and recent recharge is not possible;

- Sediment ages within the MOZB are generally old (> 300 Ka) compared to groundwater ages, which are Late Pleistocene to Holocene (< 50 Ka). Saline groundwater observed today is not a result of connate lake water preserved in sediments but other processes including evapotranspiration and mineral dissolution processes;

- Hydrochemical facies within MOZB are generally a result of redissolution of evaporated minerals, composed of chloride (in the central zone), sulphate (in the fringes) and carbonates typically beyond the boundaries of MOZB or within the Okavango Delta. We suggest sulphate is a result of surface water – groundwater interaction in which evaporation from the surface water formed primary evaporites rapidly exchanged solutes to the groundwater; increased solute accumulated then formed evaporites of sulphates. Precipitation of halite is a result of progressive evaporation loss from the capillary fringe and groundwater discharge at the at the shoreline margins of the lake system. Carbonate groundwater is due to recent recharge water within the surrounding fresh groundwater input and surface water (particularly in the Okavango Delta Region);

- River chemistry water from present day river channels within the PLM (Zambezi, Okavango, Kwando/Linyanti are carbonate dominated. We demonstrate that under progressive evaporation, the river water under chemical evolution following Hardie-Eugster's model precipitate halite after 50,000 times concentration; and

- Sediments within the MOZB have been resolved using geophysics and typically are of resistivites < 3 Ωm (saline/clay), 3-10 Ωm (brackish, clayey sands), 20-100 Ωm (Kalahari sands and Basement rocks) using electrical based methods. Recent works within the Okavango Delta have mapped and resolved a high saline formation below the Okavango Delta probably hosting connate saline-brackish lake water from an earlier stage of the PLM.

8 References

Aquatec, 1982. Watering point survey: Ngamiland cattle trek route, Aqua Tec Grounfwater consultants 1982. 132 pp.

Balon, E.K., 1978. Reproductive guilds and the ultimate structure of fish taxocenes: amended contribution to the discussion presented at the mini-symposium. Environmental Biology of Fishes, 3, 149-152.

Banda, K., Jakobsen, R., Bauer-Gottwein, P., Murray, A.S., Nyambe, I. & Larsen, F., submitted 2015a. Palaeo-Lake Makgadikgadi: New perspectives and insights of its evolution from western Zambia. Submitted to Journal of African Earth Sciences.

Banda, K., Jakobsen, R., Bauer-Gottwein, P., Nyambe, I., Troels, L. & Larsen, F., submitted 2015b. Identification and evaluation of hydro-geochemical processes in the groundwater environment of Machile Basin, western Zambia. Submitted to Applied Geochemistry.

Bangert, B., Stollhofen, H., Lorenz, V. & Armstrong, R., 1999. The geochronology and significance of ash-fall tuffs in the glaciogenic Carboniferous-Permian Dwyka Group of Namibia and South Africa. Journal of African Earth Sciences, 29, 33-49.

Bauer, P. 2004. Flooding and salt transport in the Okavango Delta, Botswana: key issues for sustainable wetland management. PhD thesis, Swiss Federal Institute of Technology, Zurich, 177 pp.

Bauer, P., Gumbricht, T. & Kinzelbach, W., 2006a. A regional coupled surface water/groundwater model of the Okavango Delta, Botswana. Water Resources Research, 42, W04403.

Bauer, P., Held, R.J., Zimmermann, S., Linn, F. & Kinzelbach, W., 2006b. Coupled flow and salinity transport modelling in semi-arid environments: The Shashe River Valley, Botswana. Journal of Hydrology, 316, 163-183.

Bauer, P., Supper, R., Zimmermann, S. & Kinzelbach, W., 2006c. Geoelectrical imaging of groundwater salinization in the Okavango Delta, Botswana. Journal of Applied Geophysics, 60, 126-141.

Bäumle, R., Neukum, C., Nkhoma, J. & Silembo, O., 2007. The Groundwater Resources of Southern Province, Zambia (Phase 1). Vol 1, Technical Report.Ministry of Energy and Water Development, Department of Water Affairs, Zambia, and Federal Institute for Geosciences and Natural Resources (BGR: Bundesanstalt für Geowissenschafen und Rohstoffe, Hannover). 148pp.

Beekman, H., Gieske, A. & Selaolo, E., 1996. GRES: Groundwater recharge studies in Botswana 1987-1996. Botswana J. Earth Sci, 3, 1-17.

Beekman, H., Selaolo, E., Van Elswijk, R., Lenderink, N. & Obakeng, O. 1997. Groundwater recharge and resources assessment in the Botswana Kalahari–chloride and isotope profiling studies in the Letlhakeng-Botlhapatlou area and the Central Kalahari: GRES 11 Technical Report. Gaborone.

Beekman, H., Selaolo, E.T. & De Vries, J., 1999. Groundwater Recharge and Resources Assessment in the Botswana Kalahari: Executive Summary GRES II. Geological Survey Department.

Bowler, J.M., 1986. Spatial variability and hydrologic evolution of australian lake basins - analogue for pleistocene hydrologic change and evaporite formation. Palaeogeography Palaeoclimatology Palaeoecology, 54, 21-41.

Bufford, K.M., Atekwana, E.A., Abdelsalam, M.G., Shemang, E., Mickus, K., Moidaki, M., Modisi, M.P. & Molwalefhe, L., 2012. Geometry and faults tectonic activity of the Okavango Rift Zone, Botswana: Evidence from magnetotelluric and electrical resistivity tomography imaging. Journal of African Earth Sciences, 65, 61-71.

Burrough, S.L. & Thomas, D.S.G., 2008. Late quaternary lake-level fluctuations in the Mababe Depression: Middle Kalahari palaeolakes and the role of Zambezi inflows. Quaternary Research, 69, 388-403.

Burrough, S.L. & Thomas, D.S.G., 2009. Geomorphological contributions to palaeolimnology on the African continent. Geomorphology, 103, 285-298.

Burrough, S.L., Thomas, D.S.G. & Bailey, R.M., 2009a. Mega-lake in the Kalahari: A late pleistocene record of the Palaeolake Makgadikgadi system. Quaternary Science Reviews, 28, 1392-1411.

Burrough, S.L., Thomas, D.S.G. & Singarayer, J.S., 2009b. Late Quaternary hydrological dynamics in the Middle Kalahari: Forcing and feedbacks. Earth-Science Reviews, 96, 313-326.

Butzer, K.W., Stuckenrath, R., Bruzewicz, A.J. & Helgren, D.M., 1978. Late Cenozoic paleoclimates of the Gaap Escarpment, Kalahari margin, South-Africa. Quaternary Research, 10, 310-339.

Campbell, G., Johnson, S., Bakaya, T., Kumar, H. & Nsatsi, J., 2006. Airborne geophysical mapping of aquifer water quality and structural controls in the Lower Okavango Delta, Botswana. South African Journal of Geology, 109, 475-494.

Chongo, M., christiansen, A.V., Tembo, A., Nyambe, I., Larsen, F. & Bauer-Gottwein, P., 2014. Airborne and Ground based Transient Electromagnetic Mapping of Groundwater Salinity in the Machile-Zambezi Basin, South-western Zambia. . submitted to Hydrogeology Journal.

Chongo, M., Wibroe, J., Staal-Thomsen, K., Moses, M., Nyambe, I., Larsen, F. & Bauer-Gottwein, P., 2011. The use of Time Domain Electromagnetic method and Continuous Vertical Electrical Sounding to map groundwater salinity in the Barotse sub-basin, Zambia. Physics and Chemistry of the Earth, Parts A/B/C, 36, 798-805.

Cooke, H., 1975. The palaeoclimatic significance of caves and adjacent landforms in western Ngamiland, Botswana. Geographical Journal, 430-444.

Cooke, H., 1979. The origin of the Makgadikgadi Pans. Ministry of Mineral Resources and Water Affairs, Botswana notes and records No. 11, pp. 37-42.

Cooke, H., 1980. Landform evolution in the context of climatic change and neo-tectonism in the Middle Kalahari of north-central Botswana. Transactions of the Institute of British Geographers, 80-99.

Cooke, H. & Verhagen, B.T., 1977. The dating of cave development—an example from Botswana. Proceedings of the Seventh International Speleological Congress, Sheffield. pp. 122-124.

Cooke, H. & Verstappen, H.T., 1984. The landforms of the western Makgadikgadi basin in northern Botswana, with a consideration of the chronology of the evolution of Lake Palaeo-Makgadikgadi. Zeitschrift fur Geomorphologie, 1, 1-19.

Cooke, H.J., 1984. The evidence from northern Botswana of Late Quaternary climatic change. In: Vogel, J.C. (ed.) Late Cainozoic Palaeoclimates of the Southern Hemisphere. Balkema, Rotterdam. pp. 265-278.

Cordier, S., Harmand, D., Lauer, T., Voinchet, P., Bahain, J.-J. & Frechen, M., 2012. Geochronological reconstruction of the Pleistocene evolution of the Sarre valley (France and Germany) using OSL and ESR dating techniques. Geomorphology, 165, 91-106.

Cronberg, G., Gieske, A., Martins, E., Nengu, J.P. & Stenström, I.M., 1995. Hydrobiological Studies of the Okavango Delta and Kwando/Linyanti/Chobe River, Botswana; Surface Water Quality Analysis. Bostwana Society, Botswana notes and records No. 27, 151-226.

Day, J., 1993. The major ion chemistry of some southern African saline systems. Hydrobiologia, 267, 37-59.

De Vries, J.J., 1984. Holocene depletion and active recharge of the Kalahari groundwaters — A review and an indicative model. Journal of Hydrology, 70, 221-232.

De Vries, J.J., Selaolo, E.T. & Beekman, H.E., 2000. Groundwater recharge in the Kalahari, with reference to paleo-hydrologic conditions. Journal of Hydrology, 238, 110-123.

De Vries, J.J. & Von Hoyer, M., 1988. Groundwater Recharge Studies in Semi-Arid Botswana-A Review. In: Simmers, I. (ed.) Estimation of Natural Groundwater Recharge. 222. Springer, Netherlands. pp. 339-347.

Dincer, T., Hutton, L. & Kupee, B., 1978. Study, using stable isotopes, of flow distribution, surface-groundwater relations and evapotranspiration in the Okavango Swamp, Botswana. International Atomic Energy Agency, Proc. Ser. SM-228/52. pp. 3-25.

Dingle, R., Siesser, W.G. & Newton, A., 1983. Mesozoic and Tertiary geology of southern Africa. A.A. Balkema, Rotterdam.

Drever, J.I., 1997. The geochemistry of natural waters: surface and groundwater environments.

Du Toit, A., 1927. The Kalahari and some of its problems. South African Journal of Science, 24, 88-101.

Duncan, R.A., Hooper, P., Rehacek, J., Marsh, J. & Duncan, A., 1997. The timing and duration of the Karoo igneous event, southern Gondwana. Journal of Geophysical Research: Solid Earth (1978–2012), 102, 18127-18138.

Ebert, J.I. & Hitchcock, R.K., 1978. Ancient Lake Makgadikgadi, Botswana: mapping, measurement and palaeoclimatic significance. Palaeoecology of Africa, 10, 47-56.

Eckardt, F.D., Bryant, R.G., McCulloch, G., Spiro, B. & Wood, W.W., 2008. The hydrochemistry of a semi-arid pan basin case study: Sua Pan, Makgadikgadi, Botswana. Applied Geochemistry, 23, 1563-1580.

Edmunds, W., Fellman, E. & Goni, I., 1999. Lakes, groundwater and palaeohydrology in the Sahel of NE Nigeria: evidence from hydrogeochemistry. Journal of the Geological Society, 156, 345-355.

Edmunds, W., Fellman, E., Goni, I. & Prudhomme, C., 2002. Spatial and temporal distribution of groundwater recharge in northern Nigeria. Hydrogeology Journal, 10, 205-215.

Eugster, H.P., 1980. Geochemistry of evaporitic lacustrine deposits. Annual Review of Earth and Planetary Sciences, 8, 35-63.

Eugster, H.P. & Hardie, L.A., 1978. Saline Lakes. In: Lerman, A. (ed.) Lakes. Springer, New York. pp. 237-293.

Eugster, H.P. & Jones, B.F., 1979. Behavior of major solutes during closed-basin brine evolution. American journal of science, 279, 609-631.

Eugster, H.P. & Smith, G.I., 1965. Mineral equilibria in the Searles Lake evaporites, California. Journal of Petrology, 6, 473-522.

Farr, J., Cheney, C., Baron, J. & Peart, R., 1981. GS 10 Project: Evaluation of Underground Water Resources. 292 pp.

Foster, S.S.D., Bath, A.H., Farr, J.L. & Lewis, W.J., 1982. The likelihood of active groundwater recharge in the Botswana Kalahari. Journal of Hydrology, 55, 113-136.

Freeze, R.A. & Cherry, J., 1979. Groundwater. Prentice-Hall, Englewood Cliffs, NJ.

Gasse, F., 2000. Hydrological changes in the African tropics since the Last Glacial Maximum. Quaternary Science Reviews, 19, 189-211.

Gonfiantini, E., 1986. Environmental isotopes in lake studies. In: P.Fritz & J.-Ch.Fontes (eds.) Handbook of environmental isotope geochemistry. 2. Elsevier, Amsterdam, The Netherlands. pp. 113-168.

GRB - Government of the Republic Bostwana, 2006. Water accounts of Botswana (1992-2003). Department of Environmental Affairs and Centre for Applied Research. 66pp.

Grey, D. & Cooke, H., 1977. Some problems in the Quaternary evolution of the landforms of northern Botswana. Catena, 4, 123-133.

Grove, A.T., 1969. Landforms and climatic change in the Kalahari and Ngamiland. Geographical Journal, 191-212.

Haddon, I.G. & McCarthy, T.S., 2005. The Mesozoic-Cenozoic interior sag basins of Central Africa: The Late-Cretaceous-Cenozoic Kalahari and Okavango basins. Journal of African Earth Sciences, 43, 316-333.

Hall, A., Valente, I.M.C.B.S. & Davies, B.R., 1977. The Zambezi River in Moçambique. Freshwater Biology, 7, 187-206.

Hardie, L.A. & Eugster, H.P., 1970. The evolution of closed-basin brines. Mineral. Soc. Amer. Spec. Pap, 3, 273-290.

Heine, K., 1978. Radiocarbon chronology of late Quaternary lakes in the Kalahari, southern Africa. Catena, 5, 145-149.

Heine, K., 1982. The main stages of the late Quaternary evolution of the Kalahari region, southern Africa. Palaeoecology of Africa and the surrounding islands, 15, 53-76.

Heine, K., 1992. On the ages of humid Late Quaternary phases in southern African arid areas (Namibia, Botswana). In: Heine, K. (ed.) Palaeoecology of Africa and the surrounding islands. 23. Balkema A.A., Netherlands. pp. 149-164.

Huntsman-Mapila, P., Ringrose, S., Mackay, A.W., Downey, W.S., Modisi, M., Coetzee, S.H., Tiercelin, J.J., Kampunzu, A.B. & Vanderpost, C., 2006. Use of the geochemical and biological sedimentary record in establishing palaeo-environments and climate change in the Lake Ngami basin, NW Botswana. Quaternary International, 148, 51-64.

IAEA - International Atomic Energy Agency, 1992. Statistical treatment of data on environmental isotopes in precipitation. Technical Report No. 331. Vienna. 793 pp.

Jankowski, J. & Jacobson, G., 1989. Hydrochemical evolution of regional groundwaters to playa brines in central Australia. Journal of Hydrology, 108, 123-173.

Jennings, C.M.H. 1974. The hydrogeology of Botswana. PhD Thesis, University of Natal, Pietermaritzburg, 850 pp.

Johnson, T.C., Scholz, C.A., Talbot, M.R., Kelts, K., Ricketts, R., Ngobi, G., Beuning, K., Ssemmanda, I. & McGill, J., 1996. Late Pleistocene desiccation of Lake Victoria and rapid evolution of cichlid fishes. Science, 273, 1091-1093.

Jones, B.F., Eugster, H.P. & Rettig, S.L., 1977. Hydrochemistry of the Lake Magadi basin, Kenya. Geochimica et Cosmochimica Acta, 41, 53-72.

Jourdan, F., Féraud, G., Bertrand, H., Kampunzu, A.B., Tshoso, G., Le Gall, B., Tiercelin, J.J. & Capiez, P., 2004. The Karoo triple junction questioned: evidence from Jurassic and Proterozoic 40Ar/39Ar ages and geochemistry of the giant Okavango dyke swarm (Botswana). Earth and Planetary Science Letters, 222, 989-1006.

Jourdan, F., Féraud, G., Bertrand, H., Kampunzu, A.B., Tshoso, G., Watkeys, M.K. & Le Gall, B., 2005. Karoo large igneous province: Brevity, origin, and relation to mass extinction questioned by new 40Ar/39Ar age data. Geology, 33, 745-748.

Joyce, D.A., Lunt, D.H., Bills, R., Turner, G.F., Katongo, C., Duftner, N., Sturmbauer, C. & Seehausen, O., 2005. An extant cichlid fish radiation emerged in an extinct Pleistocene lake. Nature, 435, 90-95.

Kafri, U. & Yechieli, Y., 2010. Salinity, Salination and Freshening of the Different Base-Levels and Their Adjoining Groundwater Systems. Groundwater Base Level Changes and Adjoining Hydrological Systems. Springer Berlin Heidelberg. pp. 43-54.

Kgotlhang, L. 2008. Application of airborne geophysics in large scale integrated hydrological modelling. Case study: Okavango delta, Botswana. PhD thesis, ETH ZURICH, 138 pp.

Kinabo, B., Hogan, J., Atekwana, E., Abdelsalam, M. & Modisi, M., 2008. Fault growth and propagation during incipient continental rifting: Insights from a combined aeromagnetic and Shuttle Radar Topography Mission digital elevation model investigation of the Okavango Rift Zone, northwest Botswana. Tectonics, 27.

Kinabo, B.D., Atekwana, E.A., Hogan, J.P., Modisi, M.P., Wheaton, D.D. & Kampunzu, A.B., 2007. Early structural development of the Okavango rift zone, NW Botswana. Journal of African Earth Sciences, 48, 125-136.

Klock, H. 2001. Hydrogeology of the Kalahari in North-eastern Namibia: With Special Emphasis on Groundwater Recharge, Flow Modelling and Hydrochemistry. Selbstverlag Lehr-und Forschungsbereich Hydrogeologie, 350 pp.

Kulongoski, J.T., Hilton, D.R. & Selaolo, E.T., 2004. Climate variability in the Botswana Kalahari from the late Pleistocene to the present day. Geophysical Research Letters, 31.

Lancaster, I.N., 1979. Evidence for a widespread Late Pleistocene humid period in the Kalahari. Nature, 279, 145-146.

Lancaster, N., 1989. Late Quaternary paleoenvironments in the southwestern Kalahari. Palaeogeography, Palaeoclimatology, Palaeoecology, 70, 367-376.

Langer, T. & Heusser, D. 2004. Geochemical Groundwater Evolution and Age Estimations for Islands in the Okavango Delta. Department of Environmental Sciences. MSc Thesis, Swiss Federal Institute of Technology (ETH), Zürich, pp.

Last, W.M., 1989. Sedimentology of a saline playa in the northern Great Plains, Canada. Sedimentology, 36, 109-123.

Le Gall, B., Tshoso, G., Jourdan, F., Féraud, G., Bertrand, H., Tiercelin, J.J., Kampunzu, A.B., Modisi, M.P., Dyment, J. & Maia, M., 2002. 40Ar/39Ar geochronology and structural data from the giant Okavango and related mafic dyke swarms, Karoo igneous province, northern Botswana. Earth and Planetary Science Letters, 202, 595-606.

Linn, F., Masie, M. & Rana, A., 2003. The impacts on groundwater development on shallow aquifers in the lower Okavango Delta, northwestern Botswana. Environmental Geology, 44, 112-118.

Livingstone, D. A., 1857. Missionary travels and researches in South Africa. Salzwasser Verlag, Bremen, 2010 (reprint of original).

Magombedze, L.M., Frengstad, B. & Lubczynski, M.W., 2004. Spatial variation of groundwater recharge in a semi-arid environment: Serowe, Botswana. In: Stephenson, D., Shemang, E.M. & Chaoka, T.R. (eds.) Water resources of arid areas: proceedings of the international conference on water resources of arid and semi arid regions of Africa WRASRA, August 3-6th, 2004, Gaborone, Botswana. Balkema, Rotterdam. pp. 271-278.

Margane, A., Baeumle, R., Schildknecht, F. & Wierenga, A., 2005. Groundwater investigation in the Eastern Caprivi Region - Main Hydrogeological Report. Department of Water Affairs (Namibia) and Federal Institute of Geosciences and Natural Resources (Hannover). 164pp.

Mazor, E., 1982. Rain recharge in the Kalahari — A note on some approaches to the problem. Journal of Hydrology, 55, 137-144.

Mazor, E., Bielsky, M., Verhagen, B.T., Sellschop, J.P.F., Hutton, L. & Jones, M.T., 1980. Chemical composition of groundwaters in the vast Kalahari flatland. Journal of Hydrology, 48, 147-165.

Mazor, E., Verhagen, B.T. & Sellschop, J.P.F., 1974. Kalahari groundwaters: Their hydrogen, carbon and oxygen isotopes. Isotope techniques in groundwater hydrology, IAEA, Vienna. pp. 203-225.

Mazor, E., Verhagen, B.T., Sellschop, J.P.F., Jones, M.T., Robins, N.E., Hutton, L. & Jennings, C.M.H., 1977. Northern Kalahari groundwaters - hydrologic, isotopic and chemical studies at Orapa, Botswana. Journal of Hydrology, 34, 203-234.

McCarthy, T., 2006. Groundwater in the wetlands of the Okavango Delta, Botswana, and its contribution to the structure and function of the ecosystem. Journal of Hydrology, 320, 264-282.

McCarthy, T., 2013. The Okavango Delta and its place in the geomorphological evolution of southern africa. South African Journal of Geology, 116, 1-54.

McCarthy, T., Bloem, A. & Larkin, P., 1998. Observations on the hydrology and geohydrology of the Okavango Delta. South African Journal of Geology, 101, 101-117.

McCarthy, T. & Ellery, W., 1998. The Okavango Delta. Transactions of the Royal Society of South Africa, 53, 157-182.

McCarthy, T., Ellery, W. & Ellery, K., 1993. Vegetation-induced, subsurface precipitation of carbonate as an aggradational process in the permanent swamps of the Okavango (delta) fan, Botswana. Chemical Geology, 107, 111-131.

McCarthy, T.S., 1992. Physical and biological processes controlling the Okavango Delta : a review of recent research. Botswana Notes and Records 24, 57-86.

McCarthy, T.S. & Ellery, W.N., 1994. The effect of vegetation on soil and ground-water chemistry and hydrology of islands in the seasonal swamps of the Okavango-fan, Botswana. Journal of Hydrology, 154, 169-193.

McCarthy, T.S., Humphries, M.S., Mahomed, I., Le Roux, P. & Verhagen, B.T., 2012. Island forming processes in the Okavango Delta, Botswana. Geomorphology, 179, 249-257.

McCarthy, T.S., McIver, J.R. & Cairncross, B., 1986. Carbonate accumulation on islands in the Okavango Delta, Botswana. South African Journal of Science, 82, 588-591.

McCarthy, T.S., McIver, J.R. & Verhagen, B.T., 1991. Groundwater evolution, chemical sedimentation and carbonate brine formation on an island in the Okavango Delta swamp, Botswana. Applied Geochemistry, 6, 577-595.

McCarthy, T.S. & Metcalfe, J., 1990. Chemical sedimentation in the semi-arid environment of the Okavango Delta, Botswana. Chemical Geology, 89, 157-178.

McFarlane, M. & Eckardt, F., 2006. Lake Deception: a new Makgadikgadi palaeolake. Botswana notes and records, 195-201.

Meier, P., Kalscheuer, T., Podgorski, J.E., Kgotlhang, L., Green, A.G., Greenhalgh, S., Rabenstein, L., Doetsch, J., Kinzelbach, W. & Auken, E., 2014. Hydrogeophysical investigations in the western and north-central Okavango Delta (Botswana) based on helicopter and ground-based transient electromagnetic data and electrical resistance tomography. Geophysics, 79, B201-B211.

Mendelsohn, J. & El Obeid, S., 2004. Okavango River: The flow of a lifeline. Struik Publishers.

Milzow, C., Kgotlhang, L., Bauer-Gottwein, P., Meier, P. & Kinzelbach, W., 2009. Regional review: the hydrology of the Okavango Delta, Botswana—processes, data and modelling. Hydrogeology Journal, 17, 1297-1328.

Modisi, M., Atekwana, E., Kampunzu, A. & Ngwisanyi, T., 2000. Rift kinematics during the incipient stages of continental extension: Evidence from the nascent Okavango rift basin, northwest Botswana. Geology, 28, 939-942.

Moore, A., 1999. A reappraisal of epeirogenic flexure axes in southern Africa. South African Journal of Geology, 102, 363-376.

Moore, A., Blenkinsop, T. & Cotterill, F.W., 2009. Southern African topography and erosion history: plumes or plate tectonics? Terra Nova, 21, 310-315.

Moore, A.E., Cotterill, F., Main, M.P. & Williams, H.B., 2007. The Zambezi River. Large rivers: geomorphology and management, 311-332.

Moore, A.E., Cotterill, F.P.D. & Eckardt, F.D., 2012. The evolution and ages of Makgadikgadi palaeo-lakes: consilient evidence from Kalahari drainage evolution. South African Journal of Geology.

Moore, A.E. & Larkin, P.A., 2001. Drainage evolution in south-central Africa since the breakup of Gondwana. South African Journal of Geology, 104, 47-68.

Nash, D.J. & McLaren, S.J., 2003. Kalahari valley calcretes: their nature, origins, and environmental significance. Quaternary International, 111, 3-22.

Nash, D.J., Meadows, M.E., Shaw, P.A., Baxter, A.J. & Gieske, A., 1997. Late holocene sedimentation rates and geomorphological significance of the Ncamasere Valley, Okavango Delta, Botswana. South African Geographical Journal, 79, 93-100.

Nugent, C., 1990. The Zambezi River - Tectonism, climatic-change and drainage evolution. Palaeogeography Palaeoclimatology Palaeoecology, 78, 55-69.

Obakeng, O.T. 2007. Soil moisture dynamics and evapotranspiration at the fringe of the Botswana Kalahari, with emphasis on deep rooting vegetation. M.Sc, ITC International Institute for Geo-Information science and earth observation, 225 pp.

Ollier, C.D., 1985. Morphotectonics of continental margins with great escarpments. In: Morisawa, M. & Hack, J.T. (eds.) Tectonic geomorphology. George Allen & Unwin, London. pp. 3-25.

Osenbrück, K., Stadler, S., Sültenfuß, J., Suckow, A.O. & Weise, S.M., 2009. Impact of recharge variations on water quality as indicated by excess air in groundwater of the Kalahari, Botswana. Geochimica Et Cosmochimica Acta, 73, 911-922.

Parkhurst, D.L. & Appelo, C. 2013. Description of input and examples for PHREEQC version 3: a computer program for speciation, batch-reaction, one-dimensional transport, and inverse geochemical calculations. US Geological Survey.

Passarge, S., 1904. Die Kalahari. Dietrich Reimer (Ernst Vohsen), Berlin.

Pitzer, K.S., 1973. Thermodynamics of electrolytes. I. Theoretical basis and general equations. The Journal of Physical Chemistry, 77, 268-277.

Pitzer, K.S., 1975. Thermodynamics of electrolytes. V. Effects of higher-order electrostatic terms. Journal of Solution Chemistry, 4, 249-265.

Podgorski, J.E., Green, A.G., Kgotlhang, L., Kinzelbach, W.K., Kalscheuer, T., Auken, E. & Ngwisanyi, T., 2013. Paleo-megalake and paleo-megafan in southern Africa. Geology, 41, 1155-1158.

Purdy, E. & MacGregor, D., 2003. Map compilations and synthesis of Africa's petroleum basins and systems. Geological Society, London, Special Publications, 207, 1-8.

Ramberg, L. & Wolski, P., 2008. Growing islands and sinking solutes: processes maintaining the endorheic Okavango Delta as a freshwater system. Plant Ecology, 196, 215-231.

Riedel, F., Erhardt, S., Chauke, C., Kossler, A., Shemang, E. & Tarasov, P., 2012. Evidence for a permanent lake in Sua Pan (Kalahari, Botswana) during the early centuries of the last millennium indicated by distribution of Baobab trees (Adansonia digitata) on "Kubu Island". Quaternary International, 253, 67-73.

Riedel, F., Henderson, A.C., Heußner, K.-U., Kaufmann, G., Kossler, A., Leipe, C., Shemang, E. & Taft, L., 2014. Dynamics of a Kalahari long-lived mega-lake system: hydromorphological and limnological changes in the Makgadikgadi Basin (Botswana) during the terminal 50 ka. Hydrobiologia, 1-29.

Riedel, F., von Rintelen, T., Erhardt, S. & Kossler, A., 2009. A fossil Potadoma (Gastropoda: Pachychilidae) from Pleistocene central Kalahari fluvio-lacustrine sediments. Hydrobiologia, 636, 493-498.

Ringrose, S., Huntsman-Mapila, P., Kampunzu, A.B., Downey, W., Coetzee, S., Vink, B., Matheson, W. & Vanderpost, C., 2005. Sedimentological and geochemical evidence for palaeo-environmental change in the Makgadikgadi subbasin, in relation to the MOZ rift depression, Botswana. Palaeogeography Palaeoclimatology Palaeoecology, 217, 265-287.

Sattel, D. & Kgotlhang, L., 2004. Groundwater exploration with AEM in the Boteti area, Botswana. Exploration Geophysics, 35, 147-156.

Seaman, M.T., Ashton, P.J. & Williams, W.D., 1991. Inland salt waters of southern Africa. Hydrobiologia, 210, 75-91.

Selaolo, E.D. 1998. Tracer studies and groundwater recharge assessment in the Eastern Fringe of the Botswana Kalahari. The Lethlakeng – Botlhapatlou Area. . Ph.D. thesis, Vrije Universiteit te Amsterdam, 228 pp.

Shahin, M., 2002. Hydrology and water resources of Africa. Springer Science & Business Media.

Shang, Y. & Last, W.M., 1999. Mineralogy, lithostratigraphy, and inferred geochemical history of North Ingebrigt Lake, Saskatchewan. In: Lemmen, D.S. & Vance, R.E. (eds.) Holocene climate and environmental change in the Palliser Triangle: a geoscientific context for evaluating the impacts of climate change on the Southern Canadian Prairies. Geological Survey of Cananda Bulletin No. 534. pp. 99-110.

Shaw, P., 1985a. The desiccation of Lake Ngami - a historical-perspective. Geographical Journal, 151, 318-326.

Shaw, P., 1985b. Late Quaternary landforms and environmental change in northwest Botswana: the evidence of Lake Ngami and the Mababe Depression. Transactions of the Institute of British Geographers, 333-346.

Shaw, P. & Thomas, D., 1988. Lake Caprivi-A Late Quaternary Link Between the Zambezi and Middle Kalahari Drainage Systems. Zeitschrift fur Geomorphologie, 32, 329-337.

Shaw, P.A., Bateman, M.D., Thomas, D.S.G. & Davies, F., 2003. Holocene fluctuations of Lake Ngami, Middle Kalahari: chronology and responses to climatic change. Quaternary International, 111, 23-35.

Shaw, P.A. & Cooke, H.J., 1986. Geomorphic evidence for the late quaternary paleoclimates of the middle kalahari of Northern Botswana. Catena, 13, 349-359.

Shaw, P.A., Stokes, S., Thomas, D.S.G., Davies, F.B.M. & Holmgren, K., 1997. Palaeoecology and age of a Quaternary high lake level in the Makgadikgadi basin of the middle Kalahari, Botswana. South African Journal of Science, 93, 273-276.

Shaw, P.A., Thomas, D.S. & Nash, D.J., 1992. Late Quaternary fluvial activity in the dry valleys (mekgacha) of the Middle and Southern Kalahari, southern Africa. Journal of Quaternary Science, 7, 273-281.

Sinha, R. & Raymahashay, B.C., 2004. Evaporite mineralogy and geochemical evolution of the Sambhar Salt Lake, Rajasthan, India. Sedimentary Geology, 166, 59-71.

Spencer, R.J., Eugster, H.P. & Jones, B.F., 1985a. Geochemistry of great Salt Lake, Utah II: Pleistocene-Holocene evolution. Geochimica et Cosmochimica Acta, 49, 739-747.

Spencer, R.J., Eugster, H.P., Jones, B.F. & Rettig, S.L., 1985b. Geochemistry of Great Salt Lake, Utah I: Hydrochemistry since 1850. Geochimica Et Cosmochimica Acta, 49, 727-737.

Stadler, S. 2005. Investigation of natural processes leading to nitrate enrichment in aquifers of semi-arid regions. PhD thesis, Karlsruhe University, Germany, 262 pp.

Stadler, S., Osenbrück, K., Knöller, K., Suckow, A., Sültenfuß, J., Oster, H., Himmelsbach, T. & Hötzl, H., 2008. Understanding the origin and fate of nitrate in groundwater of semi-arid environments. Journal of Arid Environments, 72, 1830-1842.

Street, F.A. & Grove, A., 1976. Environmental and climatic implications of late Quaternary lake-level fluctuations in Africa. Nature, 261, 385-390.

Street, F.A. & Grove, A., 1979. Global maps of lake-level fluctuations since 30,000 yr BP. Quaternary Research, 12, 83-118.

Stute, M. & Talma, A.S., 1998. Glacial temperatures and moisture transport regimes reconstructed from noble gases and O-18, Stampriet aquifer, Namibia. -In: Isotope Techniques in the Study of Environmental Change. pp. 307–318.

Teter, K.L. 2007. Paleoenvironmental reconstruction of Paleolake Mababe, northwestern Botswana from sediment chemistry and biological productivity data. Msc Thesis Oklahoma State University, 78 pp.

Thomas, D. & Shaw, P., 1991a. The deposition and development of the Kalahari Group sediments, central southern Africa. Journal of African Earth Sciences (and the Middle East), 10, 187-197.

Thomas, D.S. & Shaw, P.A., 1991b. The Kalahari Environment. Cambridge University Press.

Thomas, D.S.G., Brook, G., Shaw, P., Bateman, M., Appleton, C., Nash, D., McLaren, S. & Davies, F., 2003. Late Pleistocene wetting and drying in the NW Kalahari: an integrated study from the Tsodilo Hills, Botswana. Quaternary International, 104, 53-67.

Thomas, D.S.G. & Shaw, P.A., 2002. Late Quaternary environmental change in central southern Africa: new data, synthesis, issues and prospects. Quaternary Science Reviews, 21, 783-797.

Van Straten, O.J., 1955. The geology and groundwater of Ghanzi cattle route. Bechuanaland Protectorate, Geological Survey, Annual report, pp. 28-39.

Verhagen, B.T., 1990. Isotope hydrology of the Kalahari: recharge or no recharge? In: Klausheine (ed.) Palaeoecology of Africa and the surrounding islands. Proc. ixth biennial conference at the University of Durban (South Africa), February 1989. pp. 143-158.

Verhagen, B.T., 1992. Detailed geohydrology with environmental isotopes. A case study at Serowe, Botswana. -in: Isotope Techniques in Water Resources Development. pp. 345-362.

Verhagen, B.T., 1995. Semiarid zone groundwater mineralization processes as revealed by environmental isotope studies. In: Adar, E.M. & Leibundgut, C. (eds.) Application of Tracers in Arid Zone Hydrology. International Association Hydrological Sciences, Volume 232, Wallingford. pp. 245-266.

Verhagen, B.T., Mazor, E. & Sellschop, J.P.F., 1974. Radiocarbon and tritium evidence for direct rain recharge to ground waters in the northern Kalahari. Nature, 249, 643-644.

Vogel, J., 1982. The age of the Kuiseb River silt terrace at Homeb. Palaeoecology of Africa, 15, 201-209.

Vogel, J., K, M. & T, S., 2004. Nitrate hotspots and salinity levels in groundwater in the Central District of Bostwana. Environmental Geology Division, Department of Geological Survey, Lobatse, Botswana.

Vogel, J.C. & Van Urk, H., 1975. Isotopic composition of groundwater in semi-arid regions of southern Africa. Journal of Hydrology, 25, 23-36.

Von Der Heyden, C.J. & New, M.G., 2003. The role of a dambo in the hydrology of a catchment and the river network downstream. Hydrology and Earth System Sciences Discussions, 7, 339-357.

Von der Heyden, C.J. & New, M.G., 2004. Sediment chemistry: a history of mine contaminant remediation and an assessment of processes and pollution potential. Journal of Geochemical Exploration, 82, 35-57.

White, K. & Eckardt, F., 2006. Geochemical mapping of carbonate sediments in the Makgadikgadi basin, Botswana using moderate resolution remote sensing data. Earth Surface Processes and Landforms, 31, 665-681.

Wood, W., Eckardt, F., Kraemer, T. & Eng, K., 2011. Quantitative Eolian Transport of Evaporite Salts from the Makgadikgadi Depression (Ntwetwe and Sua Pans) in Northeastern Botswana: Implications for Regional Ground-Water Quality. In: Öztürk, M., Böer, B., Barth, H.-J., Clüsener-Godt, M., Khan, M.A. & Breckle, S.-W. (eds.) Sabkha Ecosystems. 46. Springer Netherlands. pp. 27-37.

YEC (Yachiyo Engineering Company), 1995. The Study on the National Water Resources Master Plan in the Republic of Zambia. Japan International Cooperation Agency & Ministry of Energy and Water Development, Republic of Zambia. Final Report – Hydrogeology, 128 pp.

The Department of Environmental Engineering (DTU Environment) conducts science-based engineering research within four sections:
Water Resources Engineering, Urban Water Engineering,
Residual Resource Engineering and Environmental Chemistry & Microbiology.

The department dates back to 1865, when Ludvig August Colding, the founder of the department, gave the first lecture on sanitary engineering as response to the cholera epidemics in Copenhagen in the late 1800s.

DTU Environment
Department of Environmental Engineering
Technical University of Denmark

Miljoevej, building 113
2800 Kgs. Lyngby
Denmark

Phone: +45 4525 1600
Fax: +45 4593 2850
e-mail: reception@env.dtu.dk
www.env.dtu.dk